Reducing fuel consumption of Dynamic Positioning operations from Offshore Vessels:

A study on improved diesel generator load allocation for a Diving Support Vessel

MSc Thesis

M.J.C. Meeuwisse



TU Delft

Thesis for the degree of MSc in Marine Technology in the specialisation of *Marine Engineering*

Reducing fuel consumption of Dynamic Positioning operations from Offshore Vessels:

A study on improved diesel generator load allocation for a Diving Support Vessel

by

M.J.C. Meeuwisse

Performed at

Baggermaatschappij Boskalis bv

This thesis MT.23/24.035.M is classified as confidential in accordance with the general conditions for projects performed by the TUDelft.

Delft, Thursday 4th July, 2024

Company supervisors

Responsible supervisor:	H. Brejaart
Daily Supervisor(s):	G. Steentjes

Thesis exam committee

Chair/Responsible Professor:	Dr. ir. A. Coraddu
Staff Member:	Dr. ir. L. van Biert
Staff Member:	ir. N. Vasilikis
External Member:	Prof. L. Oneto (University of Genoa)
Company Member:	G. A. H. Steentjes (BSc)

Author Details

Student number:	4713001
E-mail:	2michielm@gmail.com

TU Delft

Boskalis

Preface

"Reducing fuel consumption of Dynamic Positioning operations from Offshore Vessels: A study on improved diesel generator load allocation for a Diving Support Vessel" is the title of my MSc Thesis for the degree of MSc in Marine Technology at Delft University of Technology.

More than a year ago, whilst in Trondheim for my exchange abroad, with 50 centimetres of snow around me and barely three hours of daylight, I had absolutely no clue about what or where to do my MSc Thesis. A very enthusiastic uncle and father convinced me to try my luck at Boskalis, and lucky I was.

I absolutely did not expect to do my MSc Thesis on Dynamic Positioning but was immediately intrigued by the proposal offered by Boskalis. Although the initial thesis proposal required some work, Boskalis offered me the confidence and freedom to put my own personal twist on it, which I always enjoy. In addition, I thoroughly enjoyed that this assignment consisted of a mix between theoretical scientific aspects and actual industry practices. All in all, it has been an invaluable learning experience that will take me further in my career, and I am grateful for the opportunities Boskalis has presented me.

First, I would like to thank my two daily supervisors, Gaby Steentjes from Boskalis and Andrea Coraddu from the TU Delft. Gaby, I truly appreciate the guidance and practical advice you gave me throughout my research. Andrea, thank you for the in-depth discussions and support you provided during my thesis. Additionally, I would like to express my gratitude to all people at Boskalis who made me feel welcome, showed interest in my MSc Thesis and helped me with their advice and experiences. I'm proud to have graduated from the university I highly value and at the company where I'm the third generation of my family (more or less, at least).

Strangely, writing the thesis itself wasn't the challenging part, as I had much more struggles with the many unexpected challenges I personally encountered last year. Eventually, I made it! But I couldn't have done it without the help and support of my friends and family. Special thanks to my parents, sister, close friends, and girlfriend for their unconditional love, support, and encouragement, which pulled me through my tough times last year.

Finally, I would like to thank everyone who helped and supported me throughout my studies. I didn't expect to be here at the end of my study. But then again, who knows what I will be doing in a few years, months or even days. No clue! So, I guess it's time to turn the last page and start a new chapter. Although unwritten, I am excited for the new adventures appearing on the horizon!

M.J.C. Meeuwisse
Delft, June 2024

Abstract

The demand for offshore marine contractor services is expected to increase in the coming years, whilst contractors, such as Boskalis, receive growing pressure to reduce greenhouse gas emissions from their offshore operations. Dynamic positioning (DP) is a crucial aspect of most offshore operations, but the high redundancy levels and frequent load variations present several problems and negatively impact fuel efficiency.

This MSc Thesis proposes improved diesel generator (DG) load allocation strategies as a method for reducing fuel consumption from DP operations of offshore vessels, considering existing ship designs and industry practices whilst maintaining high safety standards. The main principle of this solution is to improve the overall fuel consumption by allowing prime movers to operate at different loads. The main research objective of this report is to determine the fuel savings achieved through improved DG load allocation strategies for a selected case study, considering realistic operational constraints, standard industry practices, and a dynamic load profile which approximates real conditions.

A diving support vessel is selected as case study vessel based on its power system characteristics, operational profile, and expected load profile during DP operations.
Realistic vessel limits and practices are gathered from operational vessel documents, and constraints are established for different load allocation strategies. Instead of using evolutionary algorithms to create DG sequences that are optimised for fuel efficiency, DG sequences are manually created and correspond to ten different load allocation strategies in order to maintain a clear structure which operators are able to utilise in real life.
The best DG sequences of each load allocation strategy are selected and further analysed in a preliminary analysis, providing the hourly fuel consumption of each load allocation strategy, between 0% and 110% MCR w.r.t. the benchmark strategy.
In addition, a dynamic model is developed to simulate a 24-hour DP operation of the selected case study vessel, providing information on the resulting fuel consumption and potential savings of different improved DG loading strategies for a dynamic load profile. This load profile changes over time to approximate real-life conditions, including most frequent power levels and occasional load transients.

Results indicated that all improved DG load allocation strategies provide fuel savings for both load cases w.r.t. the benchmark strategy. Savings are maximally 5.5% for open bus-tie configurations and 11.3% for closed bus-tie configurations.
Additionally, the outcomes of the dynamic model are compared to those provided by the preliminary analysis, which represents current state-of-the-art methods. The frequently low power levels and occasional load transients are not well represented by an operational average load, whilst these significantly influence the prospected fuel savings of the proposed solutions. Therefore, the results emphasise the importance of considering realistic industry practices and determining fuel consumption for a dynamic load profile which approximates real DP operations.

Although similar fuel savings are expected for other conventional diesel-electric DP vessels, the extent greatly depends on aspects such as the operational profile in DP mode or the fuel consumption characteristics of the power system. Actual fuel savings are likely lower as the effects of load transients are not widely considered within this research. Nevertheless, significant fuel savings are expected, as methods could be devised to limit this.
Ultimately, fuel savings from improved diesel generator load allocation strategies have been provided for realistic operational constraints, presenting an alternative out-of-the-box solution for reducing fuel consumption of Dynamic Positioning operations from Offshore Vessels.

Contents

Preface ii
Summary iv
List of Figures viii
List of Tables ix
Nomenclature x
1 Introduction 1
1.1 Problem definition . . . 2
1.2 State-of-the-art . . . 5
1.3 Research gaps . . . 6
1.4 Research outline . . . 8
2 Case study selection 9
2.1 Vessel selection . . . 9
2.1.1 Technical . . . 9
2.1.2 Operational profile . . . 10
2.1.3 Dynamic positioning load profile . . . 10
2.2 Vessel description . . . 11
2.2.1 Case description . . . 12
3 Set-up load allocation strategies 13
3.1 Operational limits . . . 13
3.2 Strategies & constraints . . . 14
3.2.1 Load distribution method . . . 14
3.2.2 Number of engines operated . . . 15
3.2.3 Minimum diesel generator load limit . . . 15
3.2.4 Maximum diesel generator load limit . . . 15
3.2.5 First leading diesel generator size . . . 15
3.2.6 Open & Closed bus-tie configurations . . . 15
3.3 Diesel generator loading sequences . . . 16
4 Preliminary analysis 17
4.1 Methodology . . . 17
4.2 Results & analysis . . . 18
4.2.1 Loading sequence selection . . . 18
4.2.2 Preliminary analysis . . . 21
5 Dynamic Model 26
5.1 Model overview . . . 26
5.1.1 General assumptions . . . 27
5.2 Model description . . . 28
5.2.1 Environmental subsystem . . . 28
5.2.2 Vessel subsystem . . . 32
5.2.3 Controller subsystem . . . 34
5.2.4 Thruster subsystem . . . 35
5.2.5 Power subsystem . . . 37
6 Results & analysis 39
6.1 Validation & verification . . . 39
6.1.1 Environmental conditions . . . 39
6.1.2 Environmental forces . . . 41
6.1.3 Thrust allocation controller . . . 42

6.1.4 Load profile & fuel consumption . . . 42
6.2 Dynamic model results . . . 44
6.2.1 General analysis . . . 44
6.2.2 First leading diesel generator analysis . . . 46
6.2.3 Maximum diesel generator limit analysis . . . 48
6.2.4 Open & Closed bus-tie configurations . . . 50
7 Discussion & Recommendations **53**
7.1 Comparison preliminary & dynamic results . . . 53
7.2 Interpretation of results . . . 55
7.3 Comparison to state-of-the-art . . . 57
7.4 Recommendations . . . 57
8 Conclusion **59**
References **61**
A Appendix I - Literature study **66**
A.1 Introduction - Objective & report outline . . . 66
A.2 Academic state-of-the-art . . . 66
A.2.1 Equipment classification . . . 67
A.2.2 Power generation . . . 67
A.2.3 Power distribution . . . 71
A.2.4 Power management system . . . 73
A.2.5 Propulsion system . . . 75
A.3 Current best practices . . . 76
A.3.1 Operational practices . . . 76
A.3.2 Operational profile against vessel characteristics . . . 80
A.4 Reflection . . . 82
A.4.1 Assessment criteria . . . 82
A.4.2 Reflection on state-of-the-art solutions . . . 82
A.4.3 Conclusion . . . 87
A.5 Gap analysis . . . 89
A.5.1 Operational profile . . . 89
A.5.2 GHG emissions . . . 89
A.5.3 Real-time implementation . . . 90
A.6 Literature overview . . . 91
B Appendix II - Case study particulars **93**
B.1 Case vessel particulars . . . 93
B.2 Main particulars case conditions . . . 94
C Appendix III - Diesel generator loading sequence tables **95**
D Appendix IV - Preliminary analysis **98**
D.1 Specific fuel consumption curve lookup tables . . . 98
D.2 Preliminary results - loading sequences . . . 99
D.3 Preliminary results - selected cases . . . 101
E Appendix V - Dynamic Model **105**
E.1 Environmental conditions . . . 105
E.2 Environmental coefficients . . . 107
E.3 Thrust to shaft power lookup table . . . 109
F Appendix VI - Results **110**
F.1 Low load case results . . . 110
F.1.1 Vessel behaviour low load case . . . 110
F.1.2 DG load profiles low load case . . . 113
F.1.3 Fuel consumption results of low load case . . . 116
F.2 Higher load case results . . . 119
F.2.1 Vessel behaviour higher load case . . . 119
F.2.2 DG load profiles higher load case . . . 122
F.2.3 Fuel consumption results of higher load case . . . 125

List of Figures

1.1 Switchboard load profile during DP operations of an OSV, against sfc curves of the corresponding DGs installed [Malikouti, 2016] . . . 3
1.2 Port- and starboard power section load consumption during DP of a heavy lift crane vessel [Lyu, 2016] . . . 3

2.1 Schematic illustration of the machinery layout . . . 11
2.2 Histogram of the amount of 24-hour DP operations and corresponding average total vessel power . . . 12

3.1 Comparison of the benchmark loading sequence against the improved DG loading sequence . . . 16

4.1 Preliminary results of open bus DG sequences of strategies 1. and 1.2 . . . 19
4.2 Preliminary results of closed bus DG sequences of strategies 2., 2.1 and 2.2 . . . 20
4.3 Preliminary sfc-curve and fuel mass flow savings of all selected load allocation strategies 21
4.4 Comparison of preliminary results between first leading DG settings . . . 22
4.5 Comparison of preliminary results between maximum DG limit settings . . . 23
4.6 Comparison of preliminary results between open & closed bus-ties . . . 24

5.1 General overview of the Dynamic model in MATLAB-Simulink . . . 26
5.2 Schematic of the forbidden zones calculated through equation 5.28 [J. Dang, 2004] . . . 36

6.1 Current conditions of the low load case . . . 39
6.2 Wave conditions of the low load case . . . 40
6.3 Wind conditions of the higher load case . . . 40
6.4 Comparison between calculated and reported environmental forces . . . 41
6.5 Verification TA controller, error in thruster power . . . 42
6.6 Total DG load profile of the low load case . . . 42
6.7 Total DG load profile of the higher load case . . . 43
6.8 Total DG load profile of the low load case for a 4-hour interval . . . 45
6.9 Total DG load profile of the higher load case for a 4-hour interval . . . 45
6.10 Comparison fuel mass flow of open, 60% limit strategies . . . 46
6.11 Comparison fuel mass flow of closed, 60% limit strategies . . . 47
6.12 Comparison fuel mass flow of open, small DG sequence strategies . . . 48
6.13 Comparison fuel mass flow of closed, small DG sequence strategies . . . 49
6.14 Comparison fuel mass flow of benchmark strategies . . . 50
6.15 Comparison fuel mass flow of small DG sequence, 60% DG limit strategies . . . 51
6.16 Comparison fuel mass flow of small DG sequence, 70/75% DG limit strategies . . . 52

7.1 Histograms of total vessel load . . . 54

A.1 Example of a conventional power system, consisting of four DGs, two main thrusters and three bow thrusters [Swider and Pedersen, 2019] . . . 68
A.2 Load profiles with an ESD for peak shaving or load levelling [Chen et al., 2009] . . . 69
A.3 Structure of a supercapacitor energy storage device [Adeyemo et al., 2023] . . . 69
A.4 Structure of a flywheel energy storage device [Adeyemo et al., 2023] . . . 70
A.5 Estimated maturation timelines for energy converters, onboard CCS technologies, and corresponding safety regulations for onboard use [DNV, n.d.] . . . 71
A.6 Bus-tie configuration comparison from IMCA (2022a) . . . 72

A.7 The average sfc of a power system, affected by starting and stopping of DGs if loads sufficiently increase (blue) or decrease (red) [Radan et al., 2006] . . . 74
A.8 CAM outline (left) and example (right) for a basic two split configuration with shaft generators, for ROV operations[IMCA, 2022a, IMCA, 2021a] . . . 78
A.9 ASOG outline (left) and example (right) for a basic two split configuration with shaft generators, for ROV operations[IMCA, 2021a] . . . 79
A.10 Switchboard load profile during DP operations of an OSV, against sfc curves of corresponding DGs installed [Malikouti, 2016] . . . 80
A.11 Port- and starboard power section load consumption during DP of a heavy lift crane vessel [Lyu, 2016] . . . 81

C.1 DG loading sequences of benchmark strategies . . . 95
C.2 DG loading sequences of open bus configurations . . . 96
C.3 DG loading sequences of closed bus configurations . . . 97

D.1 Sfc-curve lookup tables of all DGs . . . 98
D.2 Preliminary results of open bus DG sequences of strategies 1., 1.2 and 1.4 . . . 99
D.3 Preliminary results of all closed bus strategy DG sequences . . . 100
D.4 All preliminary results of first leading DG strategies . . . 101
D.5 All preliminary results of maximum DG limit strategies . . . 102
D.6 All preliminary results of open and closed bus strategies comparisons . . . 103
D.7 Preliminary results of all selected load allocation strategies . . . 104

E.1 Generated wave conditions of both load cases . . . 105
E.2 Generated current conditions of both load cases . . . 106
E.3 Generated wind conditions of both load cases . . . 106
E.4 Wave coefficient lookup tables . . . 107
E.5 Current coefficient lookup tables . . . 108
E.6 Wind coefficient lookup tables . . . 108
E.7 Thrust to shaft power lookup tables of all propulsors . . . 109

F.1 Thruster characteristics for the low load case . . . 110
F.2 Environmental forces for the low load case . . . 111
F.3 Vessel dynamics for the low load case . . . 112
F.4 Total load profile for the low load case . . . 113
F.5 DG loads of benchmark strategies for the low load case . . . 113
F.6 DG loads of open bus strategies for the low load case . . . 114
F.7 DG loads of closed bus strategies for the low load case . . . 115
F.8 Hourly fuel-saving results of the dynamic model, w.r.t. the open bus benchmark strategy, for first leading DG strategies for the low load case . . . 116
F.9 Hourly fuel-saving results of the dynamic model, w.r.t. the open bus benchmark strategy, for max. DG limit strategies for the low load case . . . 117
F.10 Hourly fuel-saving results of the dynamic model, w.r.t. the open bus benchmark strategy, for open and closed strategies for the low load case . . . 118
F.11 Thruster characteristics for the higher load case . . . 119
F.12 Environmental forces for the higher load case . . . 120
F.13 Vessel dynamics for the higher load case . . . 121
F.14 Total load profile for the higher load case . . . 122
F.15 DG loads of benchmark strategies for the higher load case . . . 122
F.16 DG loads of open bus strategies for the higher load case . . . 123
F.17 DG loads of closed bus strategies for the higher load case . . . 124
F.18 Hourly fuel-saving results of the dynamic model, w.r.t. the open bus benchmark strategy, for first leading DG strategies for the higher load case . . . 125
F.19 Hourly fuel-saving results of the dynamic model, w.r.t. the open bus benchmark strategy, for max. DG limit strategies for the higher load case . . . 126
F.20 Hourly fuel-saving results of the dynamic model, w.r.t. the open bus benchmark strategy, for open and closed strategies for the higher load case . . . 127

List of Tables

2.1 Percentage of days and fuel spent in DP-mode during on-hire activities per Boskalis vessel type . . . 10

3.1 Combinations of load allocation strategies . . . 16

4.1 Calculated DG power, sfc and hourly mass flow errors of the sfc-polynomials w.r.t. manufacturer data . . . 17
4.2 Selected DG loading sequences for the static & dynamic model . . . 21

5.1 Controller settings . . . 35

6.1 Fuel consumption and respective savings for given time intervals for the low load case . 44
6.2 Fuel consumption and respective savings for given time intervals for the higher load case 44

7.1 Fuel consumption savings resulting from the preliminary analysis & the dynamic model 53

A.1 Summary solution assessments . . . 88
A.2 Overview of reviewed literature - Part 1 . . . 91
A.3 Overview of reviewed literature - Part 2 . . . 92

B.1 Main particulars of the selected case study vessel . . . 93
B.2 Main particulars of the low load test case . . . 94
B.3 Main particulars of the higher load test case . . . 94

Nomenclature

Abbreviations

Abbreviation	Definition
ABS	American Bureau of Shipping
AC	Alternating current
AHT	Anchor Handling Tug
ASOG	Activity Specific Operating Guidelines
CAM	Critical Activity Mode
CII	Carbon Intensity Indicator
CLV	Cable-laying Vessel
CoG	Centre of Gravity
CSV	Construction Support Vessel
DC	Direct current
DG	Diesel generator
DNV	Det Norske Veritas
DoF	Degrees of Freedom
DP	Dynamic positioning
DPO	Dynamic Positioning Operator
DPR	Daily Progress Report
DSV	Diving Support Vessel
EEDI	Energy Efficiency Design Index
EEOI	Energy Efficiency Operator Index
EES	Electrical Energy Storage
EHS-E	Enhanced electrical power management system
EMS	Energy Management System
EoM	Equations of Motions
ESD	Energy storage device
FMEA	Failure Modes and Effects Analysis
GA	Genetic algorithm
GHG	Greenhouse gas
HLV	Heavy Lift (Crane) Vessel
HTV	Semi-submersible Heavy Transport Vessel
IEA	International Energy Agency
IMCA	International Marine Contractors Association
IMO	International Maritime Organisation
ITTC	International Towing Tank Conference
MCR	Maximum Continuous Rating
NOx	Nitrogen oxides
OSV	Offshore Support Vessel
OTT	Ocean Towage Tug
PID	Proportional Integral Derivative
PM	Particulate matter
PMS	Power Management System
PSO	Particle Swam Optimization
ROV	Remotely Operated Vehicle
sfc	Specific fuel consumption
SQP	Sequential Quadratic Programming
SV	Seismic Survey Vessel

Abbreviation	Definition
TA	Thruster Allocation
TAM	Task Appropriate Mode
UNEP	UN Environment Programme
WCF	Worst-Case Failure
WCFDI	Worst-Case Failure Design Intent

Symbols

Symbol	Definition	Unit
A_{FA}	Effective frontal area in air	[m^2]
A_{FW}	Effective frontal area in water	[m^2]
A_{LA}	Effective lateral area in air	[m^2]
A_{LW}	Effective lateral area in water	[m^2]
B	Beam	[m]
$C(v)$	Coriolis–centripetal matrix	[t/s],[tm/s],[tm^2/s]
C_A	Hydrodynamic Coriolis and centripetal matrix	[t/s],[tm/s],[tm^2/s]
$C_{curr,i}$	Current coefficient in surge, sway or yaw, respectively for $i \in \{x, y, \psi\}$	[-]
C_f	Frictional resistance coefficient	[-]
C_R	Residual friction coefficient	[-]
C_{RB}	Rigid-body Coriolis and centripetal matrix	[t/s],[tm/s],[tm^2/s]
$C_{wave,i}$	Wave coefficient in surge, sway or yaw, respectively for $i \in \{x, y, \psi\}$	[-]
$C_{wind,i}$	Wind coefficient in surge, sway or yaw, respectively for $i \in \{x, y, \psi\}$	[-]
CD_l	Coefficient of longitudinal resistance	[-]
CD_t	Coefficient of lateral resistance	[-]
D	Thruster diameter	[m]
$D(v)$	Damping matrix	[t/s],[tm/s],[tm^2/s]
D_L	Linear damping matrix	[t/s],[tm/s],[tm^2/s]
D_{NL}	Nonlinear damping matrix	[t/s],[tm/s],[tm^2/s]
e_{pos}	Position error in respect of setpoint	[m],[rad]
e_{vel}	Velocity error in respect of setpoint	[m/s],[rad/s]
f_i	Total amount of force delivered by thruster i	[kN],[kNm]
g	Gravitational acceleration constant	[m/s^2]
H_s	Significant wave height	[m]
$\overline{H_s}$	Mean significant wave height	[m]
I_z	Rotational moment of inertia around the z-axis	[tm^2]
$k_{C_{wave,i}}$	Scale factor wave coefficients in surge, sway or yaw, respectively for $i \in \{x, y, \psi\}$	[-]
K_d	Derivative gain controller	[-]
K_i	Integral gain controller	[-]
K_p	Proportional gain controller	[-]
L_{lwl}	Length of waterline	[m]
L_{oa}	Overall length	[m]
L_{pp}	Length between perpendiculars	[m]
$Load_{PS}$	Load of port-side switchboard, in percentage of its maximum	[%]
M	System inertia matrix	[t],[tm],[tm^2]
M_A	Added mass matrix	[t],[tm],[tm^2]
M_{RB}	Rigid body system inertia matrix	[t],[tm],[tm^2]
m	Vessel displacement	[t]
m_f	Mass flow of fuel	[kg/h]

Symbol	Definition	Unit
n_{DG}	Number of DGs connected to the switchboard	[-]
P_b	Engine brake power	$[kW]$
P_{Lim_i}	Power limit i of the improved DG load allocation strategies	$[kW]$
P_{max_i}	Maximum available power of DG or switchboard i	$[kW]$
$P_{req_{PS}}$	Power required by port-side switchboard	$[kW]$
q	Dynamic pressure of the apparent wind	$[kN/m^2]$
R_{66}	Yaw radius of gyration	$[m]$
R_n	Reynolds number	[-]
S	Wetted hull surface area	$[m^2]$
s_L	Centroid of lateral wind area	$[m]$
sfc	Specific fuel consumption	$[g/kWh]$
T	Thrust of aft thruster	$[kN]$
T_0	Thrust of aft thruster in free open water	$[kN]$
T_i	Linear viscous damping time constants respectively for $i \in \{surge, sway, yaw\}$	$[s]$
T_m	Mean wave period	$[s]$
$T(\alpha)$	Thrust configuration matrix	$[m]$
TI	Turbulence Intensity	[-]
t	Thrust reduction ratio at zero steering angle	$[-]$
t_α	Thrust reduction ratio at steering angle α	$[-]$
u	Surge velocity	$[m/s]$
$u_{i,j}$	Force delivered by thruster i in surge and sway, for $j \in \{x, y\}$	$[kN]$,$[kNm]$
V_c	Current speed	$[m/s]$
V_w	Wind speed	$[m/s]$
$\overline{V_{wind}}$	Mean wind speed	$[m/s]$
v	Vessel velocity in surge, sway or yaw, respectively for $\{u, v, r\}$	$[m/s]$,$[rad/s]$
x	Distance between the two thrusters	$[m]$
x_g	Longitudinal location of CoG	$[m]$
x_i	x-position of thruster i	$[m]$
y_g	Transversal location of CoG	$[m]$
y_i	y-position of thruster i	$[m]$
α	Steering angle of aft thruster	$[deg]$
α_i	Angle of thruster i	$[rad]$
γ_c	Current angle of attack	$[deg]$
γ_{wave}	Wave angle of attack	$[deg]$
γ_{wind}	Wind angle of attack	$[deg]$
δ	Cross-force coefficient	[-]
ε	Angle of apparent wind	$[rad]$
ν	Kinematic viscosity	$[m^2/s]$
ρ_a	Density of air	$[t/m^3]$
ρ_{sw}	Density of seawater	$[t/m^3]$
σ_{H_s}	Shape factor Rayleigh distribution H_s	$[m]$
$\sigma_{V_{wind}}$	Standard deviation wind speed	$[m/s]$
$\tau_{env,i}$	Total environmental load in surge, sway or yaw, respectively for $i \in \{x, y, \psi\}$	$[kN]$
τ_{req}	Required force and moment of propulsion system	$[kN]$, $[kNm]$
τ_{thr}	Propulsion system forces in 3 DoF	$[kN]$

1

Introduction

In the year 1891, just before the revival of the Olympic Games or the invention of the diesel engine by Rudolf Diesel, the first submerged oil wells were drilled by platforms in the waters of Grand Lake St. Marys, Ohio [Navingo, 2010]. The oil industry continued to evolve until, in 1937, one of the first offshore platforms was developed for waters one mile offshore Louisiana, operating at depths of 4.3 metres. In June 2010, 620 mobile offshore drilling rigs were available for service, with the world's deepest platform being the Perdido Spar, operating in waters of 2,438 metres [Navingo, 2010]. This displays the remarkable advancements made within the offshore energy industry over the last century.

Today, this industry is crucial for meeting current and future global energy demands. Although well-recognised as the primary source of oil and gas, the renewables sector is developing rapidly. According to the International Energy Agency (IEA), annual offshore installations are projected to increase by 50% in 2027, driven by governmental policies [IEA, 2018]. As a result, the demand for offshore marine contractor services will increase even further in the coming years, combined with a trend of increasing wind turbine sizes [IEA, 2022].
These challenges are further aggravated due to the slow progress towards achieving the Paris Agreement's climate targets for 2030 [UNEP, 2022]. Major polluters will, therefore, face increasing pressure to reduce their greenhouse gas (GHG) emissions. Energy companies such as Vestas or Ørsted have introduced sustainability targets to reduce their scope-3 emissions, including those from offshore wind farm constructions, by 50% in 2030 and achieve net-zero in 2040 [Ørsted, 2023; Vestas, 2022]. Consequently, marine contractors such as Boskalis have to adopt measures to reduce their GHG emissions.

Since the 1960s, Dynamic Positioning (DP) has been a crucial aspect of most offshore operations [Sørensen, 2011]. It is of such importance that the International Marine Contractors Association (IMCA) organises annual conferences for sharing knowledge, improving safety and addressing current challenges associated with DP operations [IMCA DP Conference, 2023]. In this report, the definition provided by the International Maritime Organisation (IMO) is adopted for a DP vessel:

"Dynamically positioned vessels means a unit or a vessel which automatically maintains its position and/or heading (fixed location, relative location or predetermined track) by means of thruster force." [IMO, 2017]

Data from Boskalis showed that its entire offshore fleet spends 20 to 40% of its operational on-hire time in DP mode. DP-intensive vessels reach figures of above 70%. Therefore, Boskalis took the initiative to investigate GHG and fuel-reducing measures for DP operations from its offshore vessels, hence this MSc thesis.

1.1. Problem definition

An active, highly accurate, and flexible system is required to operate a vessel in DP mode due to the various activities and high risks involved with DP operations [Ihle et al., 2016]. Pivotal are the Power Management System (PMS) and Thruster Allocation (TA) controllers, as these control the vessel's prime movers and propulsors. Key performance indicators, such as position keeping, system reliability or power and fuel consumption, are therefore majorly influenced by these systems [Kalikatzarakis et al., 2022, Sørensen, 2018]. Both also significantly contribute to the system's overall complexity, given the many constraints and optimisation objectives involved [Ihle et al., 2016, Wu et al., 2016].
On top of that, high levels of redundancy and safety are required for DP vessel systems, originating from regulations, class rules and guidelines [ABS, 2021b,IMCA, 2022a,IMO, 2017]. The amount of redundancy is indicated by three equipment class notations, which are based on the worst-case failure design intent (WCFDI) of a vessel. Here, active components include diesel generators (DGs), thrusters, or switchboards:

"The specified minimum DP system capabilities to be maintained following the worst-case failure (WCF), which is the identified single fault in the DP system resulting in maximum detrimental effect on DP capability" [IMO, 2017].

- **Class 1 (DPS-1)**:
  A loss of position and/or heading may occur in the event of a single failure.
- **Class 2 (DPS-2)**:
  A loss of position and/or heading will not occur in the event of a single fault in any active component or system, excluding a loss of one or multiple compartments.
- **Class 3 (DPS-3)**:
  A loss of position and/or heading will not occur in the event of a single fault in any active or static component or system, including a complete loss of a compartment due to fire or flood.

In conclusion, DP class 2 and 3 systems should both be single fault-tolerant. The downside of this level of redundancy is that DGs are seldomly operated at their peak efficiency of around 80% maximum continuous rating (MCR) [Swider and Pedersen, 2019, Woud and Stapersma, 2017]. As no single-point failure should exceed the WCF, the maximum allowable load on the power system will generally be around 50% of total available power [IMCA, 2022a].
DP vessels are commonly operated with an open bus configuration, i.e. the power sections are disconnected from one another, which further aggravates this problem [ABS, 2021b]. Ultimately, due to the WCF requirement, at least two DGs have to be operated per switchboard. Considering a conventional power system of a DP vessel with four DGs and two switchboards, the result is that all four DGs would operate at very low loads. In such conditions, the DGs of a switchboard run at equal power levels [Chai, Reddy, et al., 2016, Chai, Sobrayen, et al., 2016].
Data analysis from literature shows that engines are often operated at 15% MCR on average during DP operations, generally within a load range of 5 to 25% MCR, which is well below their intended design and optimum fuel efficiency range [Kulkarni and Santoso, 2009, Lazarewicz and Rojas, 2017, Vásquez, 2016]. Figure 1.1 from Malikouti (2016) illustrates a distribution of power levels from an offshore support vessel (OSV) in DP mode and the corresponding high specific fuel consumption (sfc) for operating at such low loads.

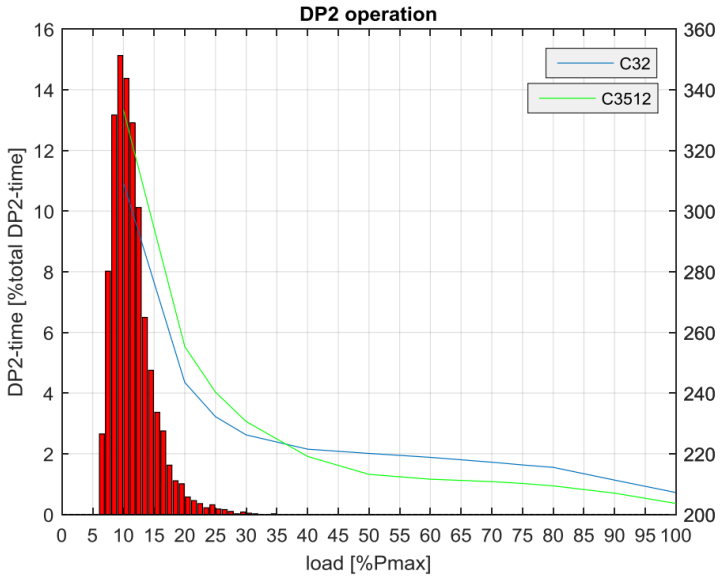


Figure 1.1: Switchboard load profile during DP operations of an OSV, against sfc curves of the corresponding DGs installed [Malikouti, 2016]

Disconnecting one DG from the power grid has significant consequences on the plant's efficiency because of the small number of prime movers [Bø et al., 2013]. Considering the average DG load of 15%, for example, remaining DGs would already operate at 30% MCR if one DG per switchboard is disconnected.
Nevertheless, operating DGs at such low loads has several negative consequences. Such as ignition problems, increased maintenance, decreased DG reactivity to load changes, and reduced system reliability [Tufte, 2014]. Furthermore, combustion conditions are less favourable, leading to a relatively higher increase in GHG emissions than just fuel consumption. Especially considering nitrogen oxides (NOx) and particulate matter (PM) [Lindstad et al., 2017, Lindstad and Sandaas, 2016].

Apart from the very low DG loading, DP vessels experience dynamically changing environmental loads. Figure 1.2 of Lyu (2016) illustrates both aspects. Prime movers are, as a result, subject to frequent load variations, which generally can be expressed as an oscillating load profile [Godjevac et al., 2017]. Over-actuated DP systems, which are considered to be more common, further aggravate this with higher load transients [Arditti et al., 2018, Kalikatzarakis et al., 2022, Wu et al., 2016].

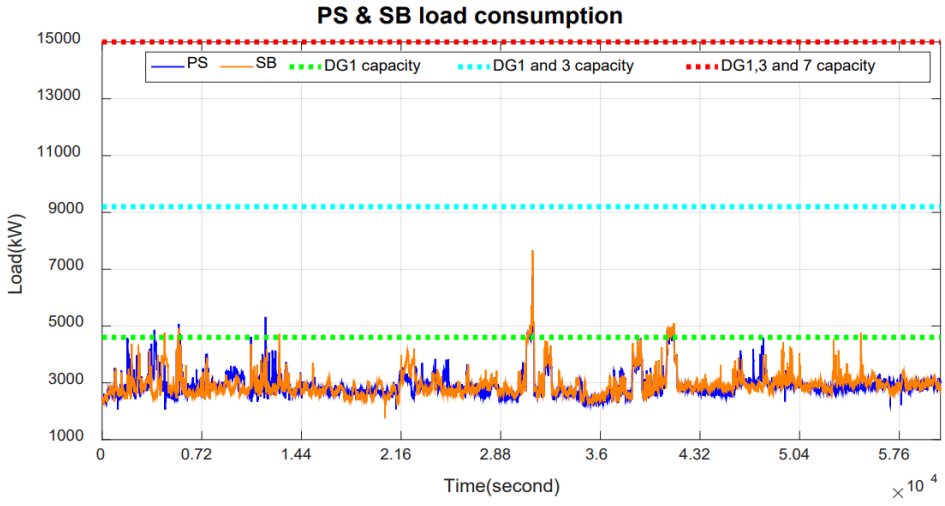


Figure 1.2: Port- and starboard power section load consumption during DP of a heavy lift crane vessel [Lyu, 2016]

Simultaneously, the dynamic response of a DG is limited and relatively poor, especially if operated at very low powers close to its limits [Montonen et al., 2022, Radan et al., 2008, Tufte, 2014]. Therefore, handling significant power demand surges could pose problems and result in a power system blackout if grid stability is not well maintained by the PMS [Chai, Sobrayen, et al., 2016]. As the power grid of a DP vessel has relatively small inertia, only minor frequency disturbances are allowed [Garg et al., 2011, Radan et al., 2008, Veksler et al., 2014]. Fuel efficiency and vessel emissions are besides negatively affected as both tend to increase during load transients [Radan et al., 2008, Veksler et al., 2014].

Given the presented problems, various research has been done to improve DP vessel systems. Such research mainly focuses on improving system reliability, fuel consumption, or accuracy. However, only a small amount of the by research proposed solutions have been adopted by the industry. Although technical challenges are often well-considered, current research appears to fall short in correctly considering operational and industry factors for DP vessels.

As elaborated, stringent safety factors implemented through guidelines and industry practices significantly reduce power system efficiency. An example of this is the use of closed bus-tie configurations, which could significantly reduce fuel consumption up to 10% if applied [Lindtjørn et al., 2014, Sørensen, 2018]. Fault propagation between switchboards can be prevented with current technology regarding bus-breakers and is even promoted by incentives from classification societies [ABS, 2021b]. Still, some clients obligate their contractors to operate with an open bus based on experiences with much older kinds of technology [IMCA DP Conference, 2023]. The actual added degree of safety of operating with an open bus is, on top of that, another topic of debate [Garg et al., 2011].
Regardless of the many regulations and guidelines involved, DP operations are primarily managed through self-regulation between contractors and clients [IMO, 2017]. As a result, various documents are involved with DP operations to facilitate clear communication between stakeholders. These documents define the actual vessel limitations and constraints that should be adhered to and are, therefore, essential for research on improving DP operations. If not appropriately considered, incorrect assumptions can be made on, for example, the benchmark conditions. Consequently, the calculated fuel savings of a proposed solution might be incorrect. This appears to be the case for several research papers with such an objective. The different documents involved regarding DP operations have already been investigated within the literature study presented in Appendix A.
Another consequence of self-regulation is that emissions and fuel consumption are much less important for clients compared to, for example, safety. Although this will likely change in the future, current regulations pressuring decarbonisation provide insufficient incentives as they fall short when applied to DP operations. This can be illustrated with the Energy Efficiency Design Index (EEDI), mandatory during the design and construction of a vessel, and the Energy Efficiency Operator Index (EEOI), which is so far still voluntary [Ihle et al., 2016]. The calculation scheme of these indices is not entirely applicable to DP vessels with diesel-electric propulsion [Ihle et al., 2016]. Secondly, almost none of the different DP operations require cargo to be transported from point A to B, as the sailing distance and speed over the ground are close to zero. The latter argument is also applicable to the recently implemented Carbon Intensity Indicator (CII) of the IMO as this index expresses an amount of CO2 emitted per cargo-carrying capacity and nautical mile [DNV, 2023, IMO, 2022].

Lastly, current research generally falls short in providing the industry with solutions that can be applied to existing DP vessels and their current operational DP profile. In the end, replacing the current offshore energy fleet with more sustainable new-build vessels containing the latest GHG-reducing measures is not viable. Especially given the rapid development in the offshore energy market, the demand for offshore DP vessel services will continue to climb [IEA, 2022, IMCA DP Conference, 2023].
Therefore, a literature study was conducted to identify and select effective solutions for reducing GHG emissions and fuel consumption of DP operations from offshore vessels, considering existing ship designs and industry practices whilst aiming to maintain current safety standards. Its main findings are presented in sections 1.2 and 1.3, and some chapters are given in Appendix A to provide readers the opportunity to review initial reasonings and associated literature. This literature study was conducted at an earlier stage and graded separately. Note that the research scope has slightly changed during the course of this MSc Thesis. As such, not all sections from the literature study are fully applicable, which is also indicated by additional notes throughout the literature study itself.

1.2. State-of-the-art

Section 1.2 presents the state-of-the-art research gathered in the literature study. DP 1 class vessels are not considered as these are not subject to restricting redundancy requirements. Additionally, differences between DP 2 and 3 class vessels are not accentuated, as there are no substantial operational differences. The power system of a conventional existing DP vessel is considered to be diesel-electric with DGs as prime movers and alternating current (AC) power distribution, operating with an open bus-tie configuration [IMCA, 2022a]. A similar scope is maintained in this report.

Within the literature study, ten solutions were proposed and analysed. These focused on reducing GHG emissions and fuel consumption or improving system reliability through modifications to power generation, power distribution, power management, or propulsion control systems. These solutions were subsequently assessed against several criteria, such as the degree of GHG emission reduction, proportionality between costs and savings, technical feasibility for existing vessels or the impact on current safety standards.
Some solutions, such as direct-current (DC) power distribution grids, significantly reduced GHG emissions. However, their applicability to existing vessels and the resulting cost-to-savings proportionality were considered to be very poor. Measures that modify the propulsion control systems for improved DP performance were considered to be more applicable for implementation to existing DP vessels. However, the actual savings were questionable, and due to the current research gaps, this would appear to become a trade-off between complexity or computational time and power.

Additionally, much research has been done on the application of energy storage devices (ESDs), especially lithium-ion batteries. Note that within the literature study itself, a clear distinction is made between spinning reserve replacement and peak shaving functions, which is adopted from state-of-the-art research. A combination between these two functions is not further considered, as ESDs fell out of the scope of this research.
Studies on batteries as spinning reserve replacement have shown significant fuel savings and good operational feasibility. However, the added degree of safety is currently a point of discussion within the industry. Spinning reserve batteries could increase safety by providing immediate backup for DG failures or reducing blackout risks. On the other hand, issues regarding thermal runaway events and increased risks for hidden failures are still debated [IMCA DP Conference, 2023]. Pure spinning reserve batteries are furthermore required to have a relatively large power capacity, even greater if vessel life cycle aspects are well considered [Adeyemo et al., 2023]. In the end, a spinning reserve battery should be able to provide powers which are equivalent to more than one DG for the duration required to start a new DG. Within the current literature, the cost-to-savings proportionality is questionable and currently not convincing yet for retrofits [Lindstad et al., 2017]. Do note that this could be different for very DP-intensive vessels, as research considered within the literature study did provide monetary results for retrofits of such vessels.
Pure peak shaving batteries would be more advantageous in that sense, as they are relatively smaller in size [Malikouti, 2016]. Furthermore, the risk of hidden failures is reduced as peak shaving batteries are regularly used during DP operations. Literature has argued that such batteries could also improve fuel efficiency and GHG emissions as DGs operate at a more constant load [Lindstad et al., 2017, Rekelhof, 2016]. However, due to current assumptions on electric transmission losses for (dis)charge processes of batteries, such significant fuel savings have not been widely provided by literature [Lyu, 2016]. Additionally, such a measure would not solve the problem of extremely low DG loads.
Although much research has been done on battery ESDs, and their potential is proven, the costs, efforts, and raw materials for their implementation are not ideal, at least so far. Therefore, a combination of solutions is chosen to directly address the current operational practices that pose problems for existing power systems during DP. Ultimately, such a fuel-reducing measure could also be implemented in combination with ESDs. However, this is left for future research.

The main problem is that DGs are operated equally at extremely low loads whilst having to manage load transients. These factors consequently affect fuel efficiency and system reliability negatively. Changing the operational practices of utilising conventional power systems could be a viable solution for addressing these main challenges directly and improving the system's fuel efficiency. Such a solution would also require fewer costs and raw materials, be technically feasible for a range of existing vessels, improve system reliability, and potentially be combined with other fuel-saving solutions such as ESDs. Based on these reasons, the best solution found during the literature study for the given scope is to improve the load allocation strategies of DGs for a conventional power system of a DP vessel. This solution consists of three measures found in literature: Unequal DG loading, Improved DG start-stop scheduling and Closed bus-tie configurations.
Typically, the total load requested from the power system is distributed equally across all running DGs. As a result, all DGs generate power at poor fuel efficiency levels [Chai, Reddy, et al., 2016, Chai, Sobrayen, et al., 2016]. Alternatively, with unequal DG loading (i.e. optimal DG scheduling), one DG generates a much higher load than the other online DGs. By doing so, the largest fraction of requested power is generated more efficiently with a lower sfc [Chauhan et al., 2016, Rao et al., 2015]. Consequently, GHG emissions, fuel consumption, and maintenance can be reduced whilst mainly a modification to the PMS is required [Chauhan et al., 2016, Rao et al., 2015].
The principles of unequal DG loading can be fully applied by adjusting the DG start-stop schedules. As the amount of prime movers is usually small, (dis)connecting DGs to the grid significantly influences efficiency [Bø et al., 2013]. The main criteria for initiating a new DG often is when another online DG reaches its limits, possibly during a short load transient [Radan et al., 2006]. This could result in unnecessary start procedures, which leads to excessive GHG emissions, especially in the event of cold start-ups [Radan et al., 2006]. Improving the DG start-stop schedules by considering these aspects could enhance system reliability and vessel performance during power surges, especially when combined with unequal DG loading. However, the ability to accept the WCF should still be maintained at all times.
With closed bus-tie configurations, the requested load can be shared across power sections. Consequently, fewer DGs are required during DP operations for sufficient power and for accepting the WCF criteria [Lindtjørn et al., 2014, Sørensen, 2018]. This is, however, not a common practice due to the potential dangers of fault propagation between sections, as presented in section 1.1. It does appear this is slowly changing within the industry, as sometimes marine contractors are allowed to operate with a closed bus. The reliability of protection systems has also improved greatly over the years and is being promoted by classification societies as DNV (2024). The American Bureau of Shipping (ABS), for example, introduced an enhanced electrical and power management systems (EHS-E) notation for DP vessels, which addresses additional requirements for safe operations with closed bus-tie configurations [ABS, 2021a, Wang et al., 2023].

1.3. Research gaps

During the literature study, several research gaps were identified regarding these topics. Especially, as it appears that a combination of the three proposed solutions has not been consciously investigated before. These research gaps will be presented throughout this section.
A major research gap on this subject is the absence of studies that consider realistic operational constraints and practices from the industry. A significant amount of research, for example, considers closed bus-tie configurations as a common operational practice. This isn't particularly the case as indicated in sections 1.1 and 1.2. In research by Chauhan et al. (2016), Chai, Sobrayen, et al. (2016), Chai, Reddy, et al. (2016) and Rao et al. (2015) on optimal DG scheduling, it isn't specified for which configuration type their proposed solution is tested. Results from Chauhan et al. (2016), Chai, Reddy, et al. (2016) and Rao et al. (2015) do, however, show this has only been tested for a closed bus-tie configuration. As a result, the saving potential of load allocation strategies for open bus-tie configurations would be worthwhile to investigate, especially considering that load demands between separated power sections differ. As such, realistic industry practices will be considered.

The same papers also provide little substantiation on the selected case study vessel and its corresponding DP operations. Research from Chauhan et al. (2016) and Rao et al. (2015), who consider an OSV, provide no explanation of the requirements, configurations and differences between a “Low DP” and “High DP” mode. Chai, Reddy, et al. (2016), who investigates the same for a Diving Support Vessel (DSV), similarly does not provide a clear explanation between “Dynamic Positioning” and “Dive Operation” modes. It is unknown what distinguishes these operating modes, apart from an unclear difference in average power consumption.
Furthermore, these papers have all chosen vessels with relatively simple power plant configurations, consisting of two switchboards with two DGs on either side. Different fuel savings could be found for other power system configurations with, for example, more DGs.

A distinctive and crucial characteristic of DP operations is that power systems are subject to extremely low loads with occasional load transients. Recreating such a load profile is very important as it tests whether solutions provide fuel savings over variable loads whilst maintaining system integrity during load transients. However, current research on improved DG loading has not tested its proposed solutions for such dynamic loads. Instead, calculating methods estimate the hourly fuel consumption for specific power levels. Subsequently, these results are extrapolated to an absolute amount of fuel saved per year.
As Figure 1.2 shows, such a method is relatively crude and does not represent the actual load profile of a DP operation, particularly considering the frequent load transients. This is especially true if provided hourly fuel savings start from loads of 25% of total system power, as is the case for Chai, Sobrayen, et al. (2016) and Chai, Reddy, et al. (2016). Such methods are, on top of that, susceptible to inaccuracies and local optima of the modelled sfc-curve [Chauhan et al., 2016, Rao et al., 2015]. The validity of the provided fuel savings for DP operations is therefore questionable and should instead be demonstrated with a DP model which is able to represent the actual load profile of a vessel on DP.

Similarly, the provided solutions and benchmark conditions of Chauhan et al. (2016), Chai, Reddy, et al. (2016) and Rao et al. (2015) appear to differ from current operational practices. The benchmark condition provided in Rao et al. (2015), for example, indicates that at 15% total system power, the vessel operates with just one DG at 60% MCR. This operating method does, however, not adhere to current IMO guidelines and the earlier described WCFDI [IMO, 2017].
Another unrealistic assumption is the adopted minimum loading limit constraint of a DG. Chauhan et al. (2016) assumes this to be minimally 30% and Chai, Reddy, et al. (2016) assumes 25%, which is very low considering an average DG loading of minimally 5 to 10% resulting from both Boskalis data and literature [Lyu, 2016, Malikouti, 2016].
On top of that, operating DGs above 50% is an uncommon practice as operational DP documents generally consider this as a “degraded status” where preparations should be taken to suspend operations IMCA, 2021a. Because of these reasons, it would be worthwhile to investigate the fuel savings of improved DG load allocation strategies for more realistic constraints and a genuine benchmark condition received from actual operational data.

A last aspect that receives little attention in current research is the importance of human factors on board during DP operations. The corresponding activities of a dynamic positioning operator (DPO) have been investigated and documented by Diggelen et al. (2018) and T.F. Hueting (2016). Both stress that although DP systems are automatically controlled computer systems, they heavily rely on human intervention from the bridge or engine control room. Furthermore, it is particularly interesting that human errors are amongst the highest triggers for failure events regarding DP incidents [IMCA DP Conference, 2023, Rokseth et al., 2016].
What can be deduced from this is that a DG load allocation strategy is required, which can be well understood and followed by vessel operators. Current research, however, uses evolutionary algorithms such as genetic algorithms (GA) to optimise the fuel consumption of DGs. As a result, the DG schedules with GA applied appear to be arbitrary as they are missing a clear underlying principle and structure [Chauhan et al., 2016, Chai, Reddy, et al., 2016 and Rao et al., 2015]. Therefore, it would be worthwhile to investigate a different method that delivers a DG loading strategy with a clear underlying structure that operators can follow with ease.

1.4. Research outline

The main objective is to investigate the applicability and real fuel savings of improved DG load allocation strategies through application to a chosen vessel as a case study. Considering state-of-the-art research, this MSc thesis will focus on utilising realistic operational constraints, such as a dynamic load profile, which are received from standard industry practices.
Based on this and the aforementioned research gaps of section 1.3, the main research question for this research is as stated below:

> ***What are the real fuel savings due to improved diesel generator load allocation strategies for an Offshore Vessel during Dynamic Positioning operations?***

Additional attention and substantiation will be provided on the selection process of the case study vessel. As presented in 1.3, a vessel should be chosen with applicable types of DP operations and preferably a more adaptable power system configuration. The first sub-question will focus on this and is used for the selection of the case study vessel and benchmark cases, only considering Boskalis vessels and operations. This sub-research question will be treated in Chapter 2 and is:

1. *Which types of Offshore Vessels and Dynamic Positioning operations would benefit from diesel generator load allocation improvements?*

Subsequently, a method is provided which selects different constraints in order to create several improved DG load allocation control strategies. Such is presented in Chapter 3. As indicated, this MSc Thesis will investigate the applicability of the proposed solution for both open and closed bus-tie configurations. Instead of using arbitrary algorithms, control strategies are manually self-created based on selected realistic vessel constraints. The second sub-research question becomes:

2. *What load allocation strategies can be created that are applicable to the selected case study vessel, considering realistic operational practices and constraints?*

Next, a preliminary analysis is executed in Chapter 4. The objective of this preliminary analysis is to test the hourly fuel consumption of different improved DG load allocation strategies between 0% and 110% MCR for a constant power level. This provides a preliminary analysis of the potential fuel savings and corresponding power levels. It is furthermore used for selecting the best DG loading sequences for the dynamic DP model. As such, the third sub-research question is:

3. *Based on a preliminary analysis with constant loads, what are the hourly fuel savings for improved DG load allocation strategies, and at which vessel load demands are these most significant?*

Chapter 5 will provide the methodology used for creating the dynamic model, and Chapter 6 will present its results with a corresponding analysis. The objective of this model is to simulate an entire 24-hour DP operation of the selected case study vessel and provide information on the resulting fuel consumption and potential savings for a dynamic load profile that is typical for DP operations. The corresponding last sub-research question is:

4. *What are the fuel savings of improved DG load allocation strategies for a dynamic load profile representing a Dynamic Positioning operation, compared to current research?*

A brief discussion will follow in Chapter 7, after which the research questions are answered in Chapter 8.

2

Case study selection

This chapter outlines the selection process for the chosen case study. First, in section 2.1, the process for selecting the vessel is presented. Section 2.2 will subsequently elaborate on the choice of vessel and case conditions.

2.1. Vessel selection

The vessel's operational profile and its current inefficiencies both significantly influence the prospected fuel savings of improved DG load allocation strategies. Therefore, the choice of a case study vessel should be well considered. The Boskalis offshore energy fleet database was consulted for this selection. The entire fleet can be categorised into ten different vessel types, of which eight have DP capabilities and are listed below, together with their corresponding abbreviations:

- Anchor Handling Tugs (AHTs)
- Cable-laying Vessels (CLVs)
- Construction Support and Offshore Construction Vessels (CSVs)
- Diving Support Vessels (DSVs)
- Heavy Lift (Crane) Vessels (HLVs)
- Ocean Towage Tugs (OTTs)
- Semi-submersible Heavy Transport Vessels (HTVs)
- Seismic Survey Vessels (SVs)

The selection of the case study vessel is based on three aspects, which will be further discussed throughout this section.

2.1.1. Technical

From a technical perspective, measures which improve DG load allocation, or other types of prime movers in a broader sense, are primarily intended for diesel-electric power system configurations. For such systems, the generated load is gathered at one point, a switchboard, from where it is distributed to the vessel's consumers. The method of load generation is, in that sense, not important as long as the generated power has the right amount and form. With that, operating one DG as close to its optimal fuel efficiency would be possible whilst operating other DGs at their minimum loads.

Such an operating method cannot be achieved for direct-drive vessels as the DGs directly power the propulsors for such a power system. Running DGs at unequal loads would ultimately cause vessel drift-offs and inefficient vessel manoeuvring. Therefore, the case vessel should have a diesel-electric power system with preferably conventional DGs as prime movers. It should also have at least two switchboards and DP class 2, as the presented problems do not apply to DP class 1 vessels. The use and modelling of ESDs is out of the scope of this research, given the added amount of complexity.
As most of the AHTs and OTTs have such a direct drive configuration, the majority of these vessels are excluded from the selection.

2.1.2. Operational profile

A vessel that spends the majority of its total operational profile in DP mode is preferred as it would result in the highest yearly savings. Therefore, data regarding the amount of time and fuel spent in DP mode during on-hire activities for different vessel types was analysed. The data used is from a 4-year period, which is gathered from Boskalis and presented in Table 2.1.

	No. of vessels	No. of vessels with (DP) data	Days in DP [%]			Fuel in DP [%]		
			min.	avg.	max.	min.	avg.	max.
AHTs	12	6	3.9	36.9	79.0	3.1	35.6	81.4
CLVs	4	3	45.5	60.3	72.8	45.3	57.6	68.4
CSVs	7	6	33.2	50.7	71.7	29.1	49.1	67.6
DSVs	5	5	59.8	68.6	82.1	54.5	68.7	83.2
HLVs	2	2	57.9	58.0	58.2	38.4	42.7	47.1
OTTs	5	0	…	…	…	…	…	…
HTVs	11	0	…	…	…	…	…	…
SVs	14	6	7.4	30.3	56.9	8.7	31.5	60.3

Table 2.1: Percentage of days and fuel spent in DP-mode during on-hire activities per Boskalis vessel type

Despite their DP capabilities, OTTs and HTVs showed an insignificant amount of time spent on DP, as this comprises only a small part of their total operational profile. HTVs, for example, spend most of their on-hire time instead in transit mode. Therefore, these vessel types are not considered further.
Significant variations in the operational profiles were visible for AHTs. Some of these vessels instead spent substantial amounts of fuel and time in other modes, such as bollard pull. On the other hand, AHTs that do spend significant amounts of time in DP mode have direct-drive configurations.
The five other vessel types have shown that they spend a significant amount of their activities operating in DP mode. Their operational profile in DP mode is therefore further considered in subsection 2.1.3.

2.1.3. Dynamic positioning load profile

The typical activities of a CLV consist of installation, burial, maintenance and repair activities for subsea cables [IMCA, 2022a]. Their DP operations often involve sailing a pre-determined track at low speeds while keeping sufficient cable tension. Additional thruster forces are therefore required to maintain the desired speed and cable tension. As such, the average load on the power system is higher, and less energy is wasted than in other DP operations. SVs have a similar operational DP profile as CLVs, although speeds can be higher and external equipment forces are likely lower. Nevertheless, both vessels are excluded from the case selection for these reasons.

Boskalis's HLVs are often used to transport and install large structures such as jackets or monopiles. DP is required for their lifting operations, which are regularly conducted near other offshore structures or vessels and, therefore, involve high risks. Lifting equipment and ballasting systems are crucial during such operations and have a relatively high power demand compared to the vessel's propulsion. The power plant has to be capable of responding to load transients, as heavy lift crane operations are sensitive to environmental forces such as wind gusts. Given the added complexity of such external factors, HLVs are removed from the scope.

Lastly, CSVs are removed from the scope despite the significant amount of time and fuel spent on DP activities. This is because CSVs execute a variety of different subsea construction and installation operations, from trenching work to maintenance work. As a result, there is an inconsistency between DP operations, as shown by the mixed data from these vessels.

Oppositely, DP operations of DSVs are consistent and more straightforward. Their operational role primarily consists of diving operations wherever manual intervention is required to complete subsea activities, which may either occur in open water or in close proximity to other structures [IMCA, 2022a]. As a result, DP operations consist of long periods of station-keeping during which safety is critical, as significant failures could be fatal for the divers working below. Diving operations are sensitive to water currents, given the diver's ability to work, and therefore, working in stronger water currents is usually prevented.
Boskalis data showed that all DSVs spend significant time and fuel in DP mode. This appears to be caused by the long periods of DP, which regularly go up to 3 days. Operations of and between DSVs are furthermore consistent and similar to each other. Inefficiencies are also present due to the high amounts of redundancy and the relatively lower external loads compared to, for example, HLVs. Therefore, DSVs are the chosen vessel type for the case study of this research.

2.2. Vessel description

The Boskalis fleet consists of five full-time DSVs. The Boka Atlantis and Boka Da Vinci, two identical vessels, are selected as case study vessels. In contrast to other research, the power system configuration of these vessels is more flexible as it consists of a larger amount of DGs and power sections. As presented in Figure 2.1, the power system consists of three sections, with two smaller-sized DGs (DG 2 and 6) and three medium-sized DGs (DG 3,4 and 5).

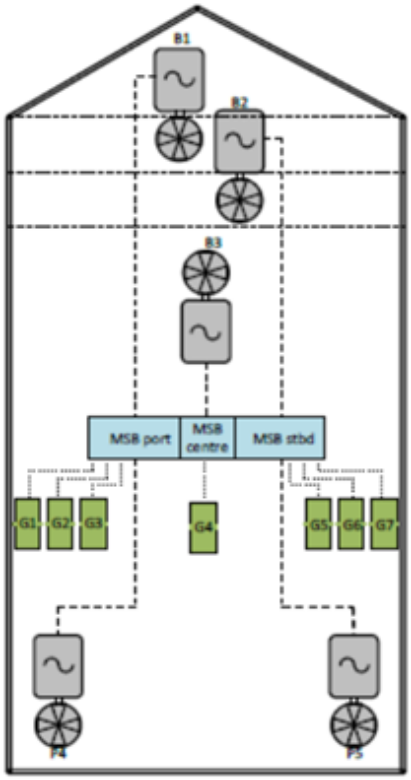


Figure 2.1: Schematic illustration of the machinery layout

Figure 2.1 also shows two auxiliary DGs (DG1 and DG7). However, these are never used during operations as it would result in even higher inefficiencies. Ultimately, average power levels are very low due to the relatively low external forces. A distribution of the average total vessel power during DP operations of the Boka Atlantis and Da Vinci is presented in Figure 2.2.

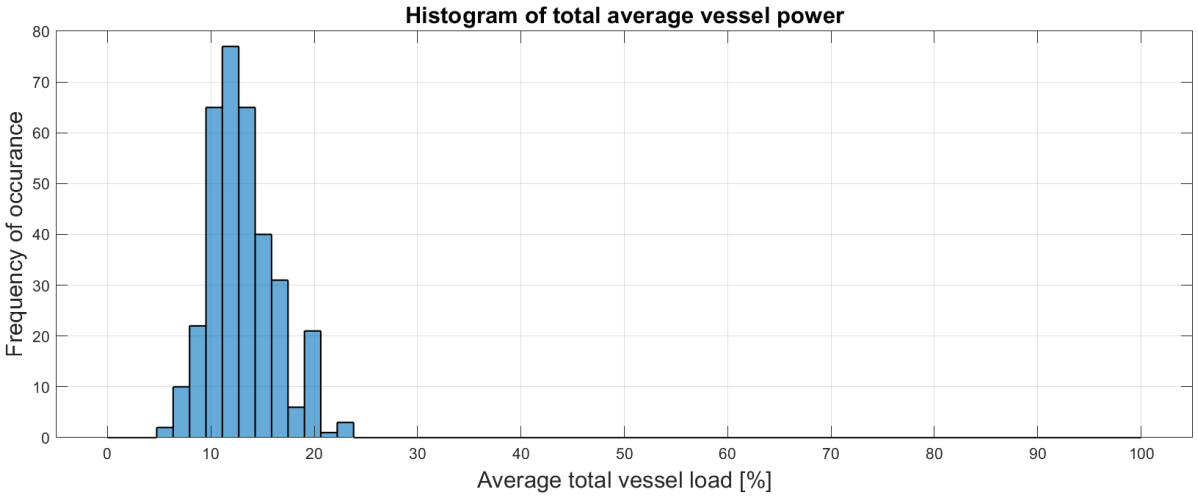


Figure 2.2: Histogram of the amount of 24-hour DP operations and corresponding average total vessel power

This data originated from the vessel's Daily Progress Reports (DPRs) and only accounts for DP operations that consist of an entire day of station-keeping events. Other vessel particulars of interest are presented in Table B.1 in section B.1 of Appendix B.
Later on during the research, after the selection process and during the development of the dynamic model, the case study vessels were fitted with one battery pack each. Their primary function is for spinning reserve, though peak shaving functions also appear to be executed by these ESDs. Given the added complexity, these are not taken into account in the dynamic model. However, as presented in the literature study, research of Godjevac et al. (2017) and Lyu (2016) indicates that the amount of fuel saved from peak shaving ESDs is not significant. Still, the potential effects of this deviation will be further considered throughout this research. Also note that the data used for Figure 2.2 is from before ESDs were added to the case study vessels.

2.2.1. Case description

Two DP operations of the Boka Atlantis have been selected for the case study. Both operations include diving and DP2 station-keeping activities, which have been carried out in the North Sea. One of these is at the lower end of the load spectrum of Figure 2.2, with an average load of 12.5% of total vessel power. The other DP operation is, on the other hand, at the higher end of the spectrum, with an average load of 17.5% of total vessel power. Another difference between these cases is that the higher load case will have more frequent and significant load transients. The environmental current conditions are low for both conditions compared to wind and waves. An essential difference between the two operations is the stronger sea state of the higher load condition and the shifting wind, which eventually did not align with the vessel's constant heading.

The information reported by the DPRs of these DP operations is presented in Tables B.2 and B.3, in section B.2 of Appendix B. The vessel is operated with a 2-way split bus configuration for both DP operations where DGs are equally loaded, which does not appear to deviate from the operational practices before ESDs were added to the case study vessels. The DG loading sequences of both benchmark cases will be portrayed in the next Chapter of 3.

3

Set-up load allocation strategies

Chapter 3 will present the considered vessel constraints and the method used for creating the different improved DG load allocation strategies. First, the operational limits of the case study vessels are presented in section 3.1. Subsequently, the strategies and constraints for the load allocation sequences are discussed in section 3.2. The different DG loading sequences are lastly presented in section 3.3.

3.1. Operational limits

Several sources have been consulted to picture the operational constraints. The IMO, IMCA and classification societies, such as ABS, give general guidelines and specifications. The most important guideline applicable to DP2 class vessels is that minimum DP system capabilities should be maintained after the WCF, i.e. the identified single fault in the DP system resulting in a maximum detrimental effect on DP capability as determined through the Failure Modes and Effects Analysis (FMEA) [IMO, 2017]. Compliance with these guidelines is achieved by operating the vessel with sufficient spinning reserve. This is defined as: *"The difference between the total power from immediately available sources (such as running generators, Energy Storage Systems, etc.) and the consumed power"* [ABS, 2021b].

In practice, DP vessel power systems are usually restricted to operating up to 50% of the total vessel power. Otherwise, there is insufficient spinning reserve available to accept the WCF.
IMO's guidelines also require power systems to be divisible into at least two or more power sections. Although power sections can run as one system during DP operations, bus-tie breakers should automatically separate switchboards upon failure to prevent fault propagation. Section 1.2 provides more information on the current state-of-the-art on this subject.
The IMCA also provides marine contractors and DP system practitioners with additional information from industry experiences, such as regarding step-loads of DGs. According to IMCA (2022a), the load response of modern DGs is influenced by emission legislations and such step load changes of 25% could result in under-frequency problems of the DGs.

The more specific operational limits of the case study vessels are, however, determined by operational documents drafted by Boskalis themselves, as DP operations are mainly self-regulated by contractors and their respective clients [IMO, 2017]. The Critical Activity Mode (CAM) defines the most fault-tolerant configuration of a vessel for critical DP operations [IMCA, 2022a]. The objective is to ensure that the vessel does not exceed the WCFDI at all times if a failure occurs [IMCA, 2021a]. Most importantly, this document states that the vessel should be operated with an open bus configuration for the benchmark DG load allocation strategy. Instead of the CAM, also the Task Appropriate Mode (TAM) could be used, which is an operational adjustment to CAM and often allows a more fuel-efficient power configuration. However, as this is not commonly used in practice, the procedures of the CAM are considered in this research.

The majority of the specific vessel limits and constraints result from the Activity Specific Operating Guidelines (ASOG), which defines the operational, environmental, and equipment performance limits for the specific activities a vessel could undertake [IMCA, 2022a]. The document has four columns, each defining a different limit and status. Here, the ”degraded” or ”yellow” status is of interest as it presents the maximum limits to which a vessel is allowed to operate during DP operations. The limits of interest are listed below.

- **Vessel performance**
  - **Vessel's Footprint**
    Position Alarm limit repeatedly exceeded; vessel's position-keeping unstable.
    Vessel's DP footprint exceeds 6 metres ($\pm$ 3 metres from setpoint)
  - **Heading excursion**
    Heading Alarm limit repeatedly exceeded; vessel's heading control unstable.
    Continued excursions > 3°
- **Vessel Moves and Heading Changes in Close Proximity to a Surface Structure or Hazard**
  - **Position Steps**
    Less than 60 metres: Steps $\leq$ 3 metres
  - **Heading Increments**
    Less than 60 metres: Steps $\leq$ 2°
  - **Vessel speed moving towards a fixed structure or a stationary vessel**
    From 30 to 10 metres: $\leq$ 0.3 knots
  - **Vessel speed moving away from a fixed structure or a stationary vessel**
    From 10 to 30 metres: $\leq$ 0.3 knots
  - **Rate of change of heading**
    From 60 to 10 metres: $\leq$ 5°per minute
- **Thrusters, Main Propulsion and Steering**
  In a 2-split configuration, if any individual bow thruster exceeds 33% thrust, or either stern thruster exceeds 45% thrust unless the vessel is manoeuvring.
- **Diesel Generator Configuration**
  - **2-Way Split 690V Bus**
    Minimum of four DGs running, two on either side of the open bus-tie, preferably with DG4 running on the mid section and DG5 or DG6 running on the starboard section.
    Remaining generators correctly configured for auto-start standby.
    DGs 1 & 7 to be on auto-start as six & seven in the auto-start sequence; for emergency back-up only, not for utilisation for DP operations.
  - **Diesel Generators**
    Loss of all generators on one bus section.
  - **Diesel Generator Loading**
    Any > 60% of maximum load with all generators running and on the board.
  - **Diesel Generators Auto Start Settings**
    Auto-start set at 65% and three seconds time delay. Minimum of two DGs per bus selected.
    DGs 1 & 7 to be on auto-start as six & seven in the auto-start sequence.

3.2. Strategies & constraints

Six constraints and settings were considered for the different load allocation strategies. Instead of using arbitrary optimisation GAs, the DG loading sequences have been created manually. This is done to maintain continuity between load allocation strategies and to ensure that operators are able to understand these, as discussed in section 1.3.

3.2.1. Load distribution method

The objective of improved DG load allocation strategies is to increase the fuel efficiency of the whole power system by generating the highest portion of power as efficiently as possible. As such, one DG operates as close to its optimal sfc point, which will be referred to as the ”leading” DG. The other DGs instead operate at minimal powers, which will be referred to as the ”supporting” DGs.

3.2.2. Number of engines operated
The amount of DGs should be as low as possible to maximise fuel efficiency. However, given the WCF, there is a minimum limit. According to the ASOG, a minimum of four running DGs is required for an open bus configuration, with two on either side. The main principle behind this is that as soon as one DG fails on a switchboard, another is able to compensate for the lost power. Based on this, operating three DGs is sufficient for a closed bus configuration, as either switchboard will have one backup DG in the event of a failure of the leading DGs.

3.2.3. Minimum diesel generator load limit
As discussed, the highest fuel savings should be reached if one leading DG is operated as high as possible while the supporting DGs are operated as low as possible. However, running a DG at very low loads is far from ideal and is bad for its health. Carbon deposits due to inefficient combustion can build up, resulting in engine damage and increased maintenance costs over time.
Despite this, the minimum DG load limit is chosen to be 5% MCR. This is based on data on the current practices of the case study vessels. Especially in the former years, the case study vessels commonly operated with a 3-way split open bus configuration. Consequently, DGs often operate at 5% MCR on average for 24 hours with such a configuration.
Another aspect considered is that the error of the estimated sfc for idle or near zero MCR loads is likely to be higher than the estimate at 5% MCR. Realistically, periodically changing the leading engine could prevent carbon deposit build-ups and, thus, the disadvantages of operating at such low loads.

3.2.4. Maximum diesel generator load limit
The maximum DG load limit is preferably as close to the optimum sfc point. The decision was made to investigate two maximum DG load limits.
First is the maximum operational limit of 60% MCR, in accordance with the ASOG of the case study vessels, and second is the optimal sfc point of the DGs. For the smaller DGs, this optimum is at 70% MCR. For the medium-sized DGs, this is 75% MCR.
Sequences with the lower maximum DG load limits will be regarded as ”60%-sequences”, whilst the others will be considered as ”70/75%-sequences”.

3.2.5. First leading diesel generator size
The case vessel’s power system consists of both smaller and medium-sized DGs. Although all kinds of different load sequences are possible with this power system configuration, a separate setting is made for the first leading DG. As a DP vessel’s average operational power is very low, the first leading DG will significantly influence the overall fuel efficiency. Still, all possible loading sequences will be tested in Chapter 4, after which the best are selected and used for the dynamic model in Chapter 5. Sequences starting with smaller DGs will be regarded as ”small DG sequences”, whilst those starting with medium DGs will be considered as ”medium DG sequences”.

3.2.6. Open & Closed bus-tie configurations
As proposed in section 1.2, both open and closed bus configurations will be tested for each load allocation strategy, given the potential fuel savings that have been indicated. Therefore, each load allocation strategy will be configured for both an open and a closed bus-tie configuration.

3.3. Diesel generator loading sequences

Based on the outcomes of section 3.2, different combinations can be created using the two defined settings for both the first leading DG size, maximum DG load limit, and the bus-tie configuration. Also, a closed bus-tie configuration version of the benchmark strategy will be created and tested. With that, ten possible combinations are possible, as shown in Table 3.1.

Open bus		Closed bus	
1.	Benchmark condition	2.	Benchmark condition, Closed
1.1	Open, 5% - 60%, S>M	2.1	Closed, 5% - 60%, S>M
1.2	Open, 5% - 60%, M>S	2.2	Closed, 5% - 60%, M>S
1.3	Open, 5% - 70/75%, S>M	2.3	Closed, 5% - 70/75%, S>M
1.4	Open, 5% - 70/75%, M>S	2.4	Closed, 5% - 70/75%, M>S

Table 3.1: Combinations of load allocation strategies

Do note that for each combination, different DG loading sequences are possible. Both a small and a medium DG can, for example, be used as the second leading DG. As such, thirty-one cases are possible, which are all tested in Chapter 4. Those that have been selected after the preliminary analysis and are used for the dynamic model, are presented in Appendix C and two examples are illustrated in Figure 3.1.

The main difference of the improved DG load allocation strategies is visualised in Figure 3.1. For the benchmark conditions, DGs are equally loaded, and the load is increased until they all reach the upper limit. Alternatively, for the improved DG load allocation strategies, only one loading DG is loaded until it reaches its limit. After that, the second leading DG is loaded until its limit and so on.

1. Benchmark condition – Open bus						
		Swb. Port		Swb. Stbd.		
P_tot	%_Load	DG2	DG3	DG4	DG5	DG6
0	0%	0.0%	0.0%	0.0%	0.0%	0.0%
565	5%	5.0%	5.0%	0.0%	7.9%	7.9%
1129	10%	10.0%	10.0%	0.0%	15.7%	15.7%
1694	15%	15.0%	15.0%	0.0%	23.6%	23.6%
2258	20%	20.0%	20.0%	0.0%	31.4%	31.4%
2823	25%	25.0%	25.0%	0.0%	39.3%	39.3%
3387	30%	30.0%	30.0%	0.0%	47.2%	47.2%
3952	35%	35.0%	35.0%	0.0%	55.0%	55.0%
4310	**38.2%**	**38.2%**	**38.2%**	**0.0%**	**60.0%**	**60.0%**
4516	40%	40.0%	40.0%	40.0%	40.0%	40.0%
5081	45%	45.0%	45.0%	45.0%	45.0%	45.0%
5645	50%	50.0%	50.0%	50.0%	50.0%	50.0%
6210	55%	55.0%	55.0%	55.0%	55.0%	55.0%
6774	**60%**	**60.0%**	**60.0%**	**60.0%**	**60.0%**	**60.0%**
7339	65%	65.0%	65.0%	65.0%	65.0%	65.0%
7903	70%	70.0%	70.0%	70.0%	70.0%	70.0%
8468	75%	75.0%	75.0%	75.0%	75.0%	75.0%
9032	80%	80.0%	80.0%	80.0%	80.0%	80.0%
9597	85%	85.0%	85.0%	85.0%	85.0%	85.0%
10161	90%	90.0%	90.0%	90.0%	90.0%	90.0%
10726	95%	95.0%	95.0%	95.0%	95.0%	95.0%
11290	100%	100.0%	100.0%	100.0%	100.0%	100.0%
11855	105%	105.0%	105.0%	105.0%	105.0%	105.0%
12419	110%	110.0%	110.0%	110.0%	110.0%	110.0%

(a) DG loading sequence of strategy 1. Benchmark condition

1.1 Open, 5% - 60%, S>M						
		Swb. Port		Swb. Stbd.		
P_tot	%_Load	DG2	DG3	DG4	DG5	DG6
0	0%	0.0%	0.0%	0.0%	0.0%	0.0%
565	5%	5.0%	5.0%	0.0%	5.0%	11.7%
1129	10%	16.7%	5.0%	0.0%	5.0%	30.0%
1694	15%	28.4%	5.0%	0.0%	5.0%	48.4%
2051	**18.2%**	**35.7%**	**5.0%**	**0.0%**	**5.0%**	**60.0%**
2258	20%	40.0%	5.0%	0.0%	10.0%	60.0%
2823	25%	51.7%	5.0%	0.0%	23.8%	60.0%
3224	**28.6%**	**60.0%**	**5.0%**	**0.0%**	**33.6%**	**60.0%**
3387	30%	60.0%	7.5%	0.0%	37.5%	60.0%
3952	35%	60.0%	16.3%	0.0%	51.3%	60.0%
4310	**38.2%**	**60.0%**	**21.8%**	**0.0%**	**60.0%**	**60.0%**
4516	40%	60.0%	25.0%	5.0%	60.0%	60.0%
5081	45%	60.0%	33.8%	18.8%	60.0%	60.0%
5645	50%	60.0%	42.5%	32.5%	60.0%	60.0%
6210	55%	60.0%	51.3%	46.3%	60.0%	60.0%
6774	**60%**	**60.0%**	**60.0%**	**60.0%**	**60.0%**	**60.0%**
7339	65%	65.0%	65.0%	65.0%	65.0%	65.0%
7903	70%	70.0%	70.0%	70.0%	70.0%	70.0%
8468	75%	75.0%	75.0%	75.0%	75.0%	75.0%
9032	80%	80.0%	80.0%	80.0%	80.0%	80.0%
9597	85%	85.0%	85.0%	85.0%	85.0%	85.0%
10161	90%	90.0%	90.0%	90.0%	90.0%	90.0%
10726	95%	95.0%	95.0%	95.0%	95.0%	95.0%
11290	100%	100.0%	100.0%	100.0%	100.0%	100.0%
11855	105%	105.0%	105.0%	105.0%	105.0%	105.0%
12419	110%	110.0%	110.0%	110.0%	110.0%	110.0%

(b) DG loading sequence of strategy 1.1. Open, 5% - 60%, S>M

Figure 3.1: Comparison of the benchmark loading sequence against the improved DG loading sequence

4

Preliminary analysis

The preliminary analysis of the improved load allocation strategies created in Chapter 3 will be presented in Chapter 4. The objective of the preliminary analysis is to provide the hourly fuel consumption of the different load allocation strategies across all possible power levels (i.e. from 0% to 110% total vessel power). As such, results can be compared to each other to select the best loading sequences and to analyse initial fuel savings w.r.t. the benchmark strategy.
First, in section 4.1, the methodology of the preliminary analysis is presented. Section 4.2 will elaborate on the preliminary results.

4.1. Methodology

For the preliminary analysis, the engine brake power, sfc and hourly fuel consumption are calculated based on specified DG powers as input. DG powers are implemented through time-based lookup tables to provide a quick, applicable method for testing all combinations. In total, thirty-six DG loading sequences have been tested, including benchmark conditions and stand-alone switchboard configurations.

The lookup tables used as input are drafted such that power increases by 5% of the total per second. Values listed in the lookup tables consist of MCR percentages, which are first multiplied by their respective maximum DG power. These are subsequently divided by DG efficiency to obtain engine brake power. This value is used to determine the sfc of each engine, which is modelled through sfc-curve lookup tables for each engine and based on manufacturer specifications.
The sfc at lower loads is determined through linear extrapolation beyond the minimum data points given, using the latter slope. A polynomial fit was consequently used to draft the lookup tables for the sfc. A brief error analysis was executed to check the credibility of the drafted sfc curves. The errors are given in Table 4.1.

	Lowest	**Highest**	**Average**
P_{gen}	-0.48%	1.36%	0.67%
sfc & m_f	-1.6%	1.9%	0.01%

Table 4.1: Calculated DG power, sfc and hourly mass flow errors of the sfc-polynomials w.r.t. manufacturer data

As DG power is converted to engine power for the preliminary analysis, the error results of DG power should be interpreted oppositely, i.e., negative values are positive and vice versa. As can be concluded from the error analysis, engine brake powers are generally overestimated at lower powers and typically underestimated at higher powers.

For the sfc, the error fluctuates over different power levels, resulting in an average near zero. The modelled sfc-curves likely overestimate the sfc at loads of 25%, 75% and 110% MCR whilst underestimating values around 50% and 100% MCR.
The most extreme error values are all from diesel generator 4. Analysing the characteristics of its sfc-curve and the results presented in its specification report show that the measurements executed on this engine might diverge somewhat. Nevertheless, the errors on the sfc-curves are considered within margins and are therefore acceptable. The lookup tables of the sfc-curves of each DG are presented in section D.1 of Appendix D.
Subsequently, the hourly fuel consumption of each DG is calculated using equation 4.1 and summed to obtain the total hourly fuel consumption per configuration [Woud and Stapersma, 2017].

$$m_f = sfc\frac{P_b}{1000} \tag{4.1}$$

with:
m_f	$[kg/h]$	–	Mass flow of fuel
P_b	$[kW]$	–	Engine brake power
sfc	$[g/kWh]$	–	Specific fuel consumption

Internal research from Boskalis showed that there could be a significant difference between reported sfc values from manufacturer reports compared to actual measured sfc values. Sfc differences can go up to 20 to 30%. This is the reason why actual sfc data from manufacturer reports is used rather than corrected values for ISO conditions, especially as DG conditions during DP operations are unknown. In that sense, the ”worst-case” is used. Because there are additional modelling errors for sfc-curves, the results of both the preliminary model and the dynamic model will focus on relative fuel savings with respect to the benchmark conditions rather than absolute overall savings.

4.2. Results & analysis

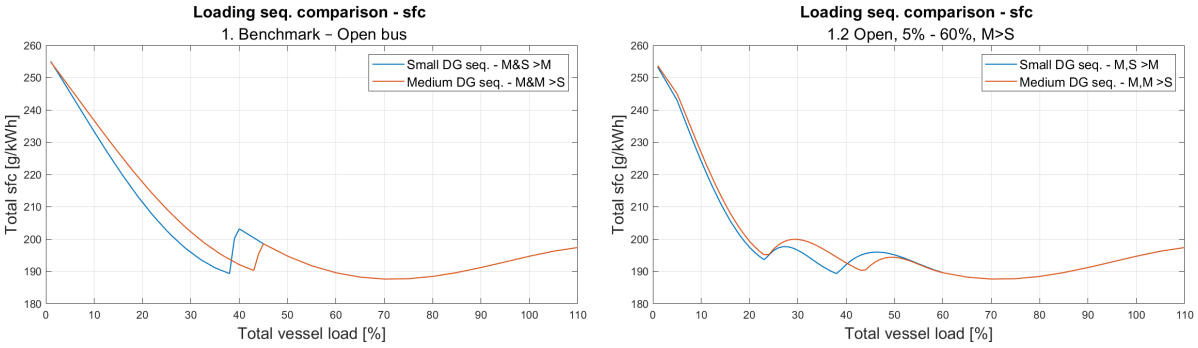
The improved DG load allocation strategies used for the preliminary analysis are formulated in Chapter 3 and given in Appendix C. Corresponding results and graphs will be presented throughout this section. However, all graphs can be found in Appendix D, sections D.2 and D.3.
Although all improved strategies show positive results in regard to fuel savings, the best DG loading sequences of each load allocation strategy are selected first in section 4.2.1 to reduce the number of combinations to ten. Next, a preliminary analysis will be executed to differences between load allocation settings in section 4.2.2.

4.2.1. Loading sequence selection

As discussed, the loading sequence selection will only focus on the size of the second leading DG onwards, considering the separate setting for the first leading DG.
Furthermore, loading strategies for open-bus configurations are applied individually to the separated switchboards. The amount of possible loading sequences depends on the number of different DGs. The two-DG-switchboard of open bus strategies, for example, has just one possible sequence, whilst some closed-bus strategies have six possible loading sequences.

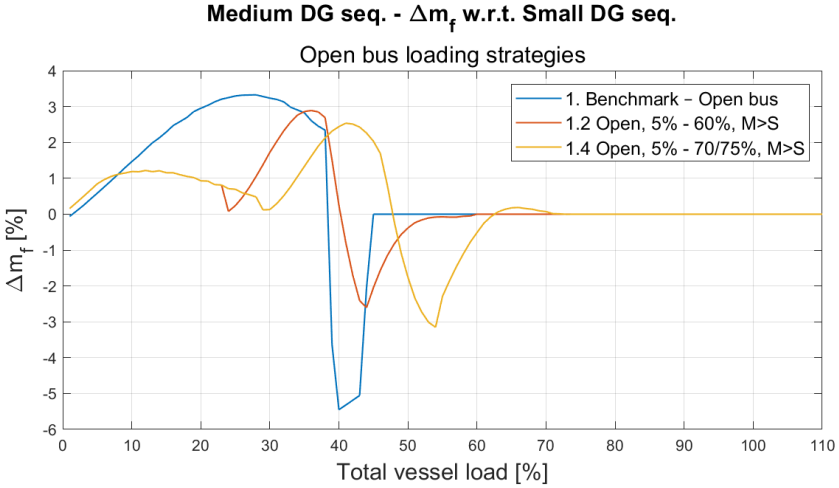
Open bus configurations

A comparison of the system sfc-curves of a 3-DG-switchboard is shown in Subfigures 4.1a and 4.1b. The blue lines in this figure depict small DG sequences, and the orange lines are medium DG sequences. Subfigure 4.1a depicts the sequences of the benchmark conditions, and Subfigure 4.1b the sequences of open bus loading strategy 1.2, as is illustrated in both graphs. Results of open bus load allocation strategies with small DG sequences as the first leading DG are not given as there is only one possible sequence for these.
Subfigure 4.1c illustrates the percentage difference in hourly fuel consumption of medium DG sequences w.r.t. small DG sequences. Here, a positive difference signifies a higher fuel consumption compared to its benchmark.



(a) Switchboard sfc-curve of loading strategy 1. sequences

(b) Switchboard sfc-curve of loading strategy 1.2 sequences



(c) Hourly fuel consumption difference between open bus medium DG sequences w.r.t. small DG sequences

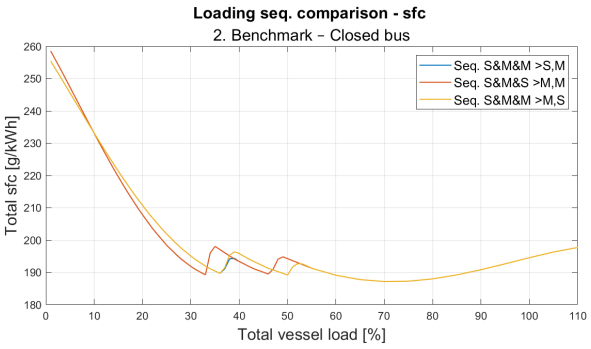
Figure 4.1: Preliminary results of open bus DG sequences of strategies 1. and 1.2

As discussed in section 2.2 and depicted in Figure 2.2, the average total vessel load of the case study vessels generally ranges from 10 to 17.5% total vessel power. Considering such a load profile, the sequences that start with small DGs appear to be generally more favourable than those with medium DGs. This is because smaller DGs are able to run closer to their optimal sfc at lower loads.

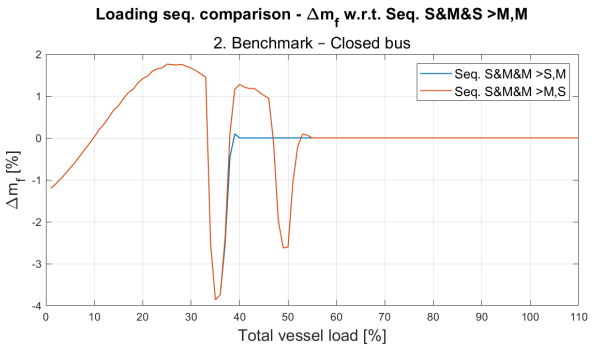
For the benchmark conditions, the advantage of the small DG sequence increases up to loads of 37.5%. At this stage, the advantage disappears as the smaller DGs reach their upper limit, and a third DG has to be started while the other configuration can still run on 2 DGs. After the medium DG sequence also reaches its limits, the sfc-curves of both loading sequences become equal.
A different picture is visible for the two improved DG load allocation strategies. Here, up to loads of 20%, the small DG sequences are slightly better with fuel saving differences of about 1%. This difference consequently decreases and significantly increases after the first leading DG reaches its limits. After this, it again shows that the small DGs are able to run closer to their optimum, resulting in hourly fuel consumption differences of 2.5%, near 35 and 45% load. The small DGs do, however, reach their limits more quickly, and thus, at 45% and 55% loads, the medium DG sequences are more advantageous.

Closed bus configurations

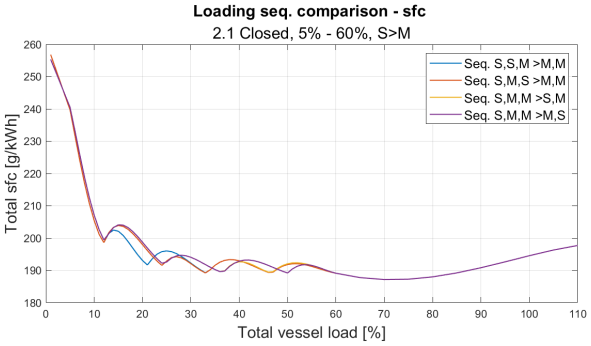
Similar graphs are made for the closed bus loading sequences, as shown in Figure 4.2. Note that the results of all loading sequences are depicted in Appendix D, section D.2.



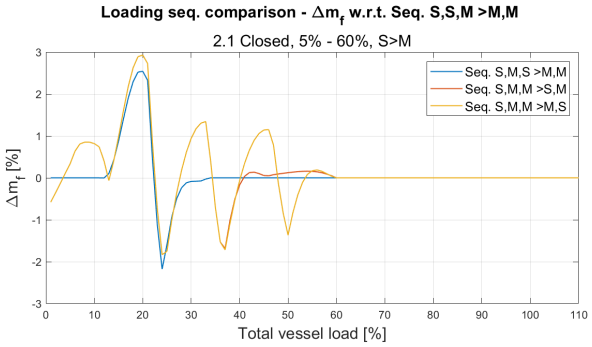
(a) Total system sfc-curves of loading strategy 2. sequences



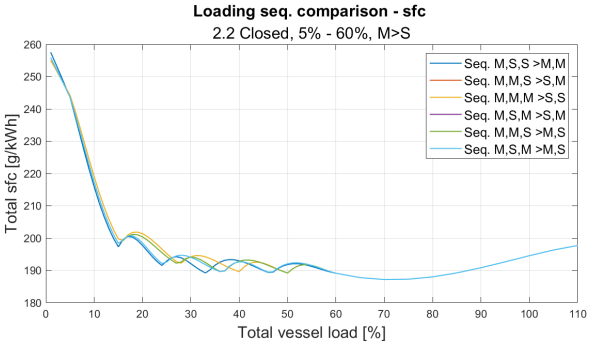
(b) Hourly fuel consumption differences between strategy 2. sequences



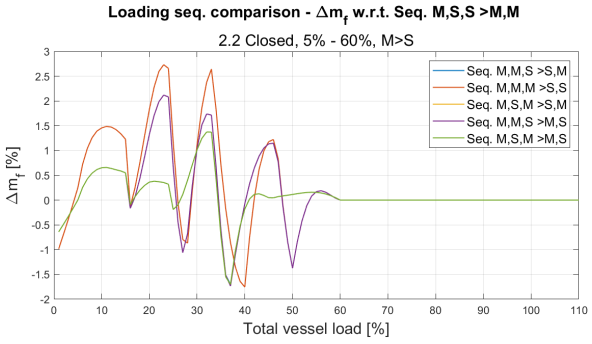
(c) Total system sfc-curves of loading strategy 2.1 sequences



(d) Hourly fuel consumption differences between strategy 2.1 sequences



(e) Total system sfc-curves of loading strategy 2.2 sequences



(f) Hourly fuel consumption differences between strategy 2.2 sequences

Figure 4.2: Preliminary results of closed bus DG sequences of strategies 2., 2.1 and 2.2

A similar trend can be seen for the closed bus-tie configurations. Generally, sequences that start with initiating small DGs show better fuel consumption results than medium DG sequences.
At very low powers, the medium DG sequences appear to perform slightly better. However, relative differences are small, and therefore, the absolute differences in fuel mass flow are especially small.
For sequences 2.1 and 2.3, small DG sequences obtain better fuel savings of close to 3% for powers near 12.5 to 27.5% total load. Also, here, fuel savings become relatively lower compared to other sequences as the smaller-sized DGs reach their corresponding maximum limit earlier than others, requiring a third DG to ramp up.
Notably, for sequences 2.2 and 2.4, small DG sequences are more favourable to higher powers as the first leading DG is of medium size. As such, sequences with smaller-sized DGs stay more advantageous for higher amounts of powers up to 35 to 45%, given the higher power limit of the first leading DG.

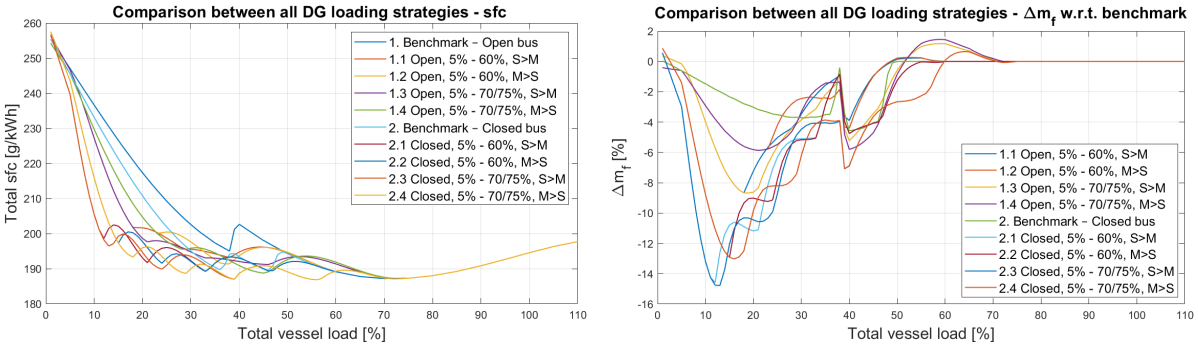
The preliminary analysis shows that DG loading sequences that start with initiating smaller-sized DGs have clear advantages for lower powers. Given the data presented in Figure 2.2 of section 2.2, this corresponds with the operational DP profile of the case study vessels. As a result, only sequences which initiate with small DGs first will further be considered in the analysis of section 4.2.2. Table 4.2 presents the different load allocation strategies and their respective loading sequences as an overview.

No.	Settings	DG loading sequence
1.	Benchmark condition - Open bus	| 2 & 3 > 4 | 5 & 6 |
1.1.	Open, 5%-60%, S>M	| 2, 3 > 4 | 6, 5 |
1.2.	Open, 5%-60%, M>S	| 3, 2 > 4 | 5, 6 |
1.3.	Open, 5%-70/75%, S>M	| 2, 3 > 4 | 6, 5 |
1.4.	Open, 5%-70/75%, M>S	| 3, 2 > 4 | 5, 6 |
2.	Benchmark condition - Closed bus	| 2 & 4 & 6 > 5 > 3 |
2.1.	Closed, 5%-60%, S>M	| 2, 6, 4 > 3 > 5 |
2.2.	Closed, 5%-60%, M>S	| 2, 6, 4 > 3 > 5 |
2.3.	Closed, 5%-70/75%, S>M	| 4, 2, 6 > 3 > 5 |
2.4.	Closed, 5%-70/75%, M>S	| 4, 2, 6 > 3 > 5 |

Table 4.2: Selected DG loading sequences for the static & dynamic model

4.2.2. Preliminary analysis

The total sfc and fuel mass flow results of all improved DG load allocation strategies are all provided in Figure 4.3. Note that the fuel mass flow results of Subfigure 4.3b are percentage differences w.r.t. the benchmark strategy.



(a) Total system sfc-curves of all selected load allocation strategies

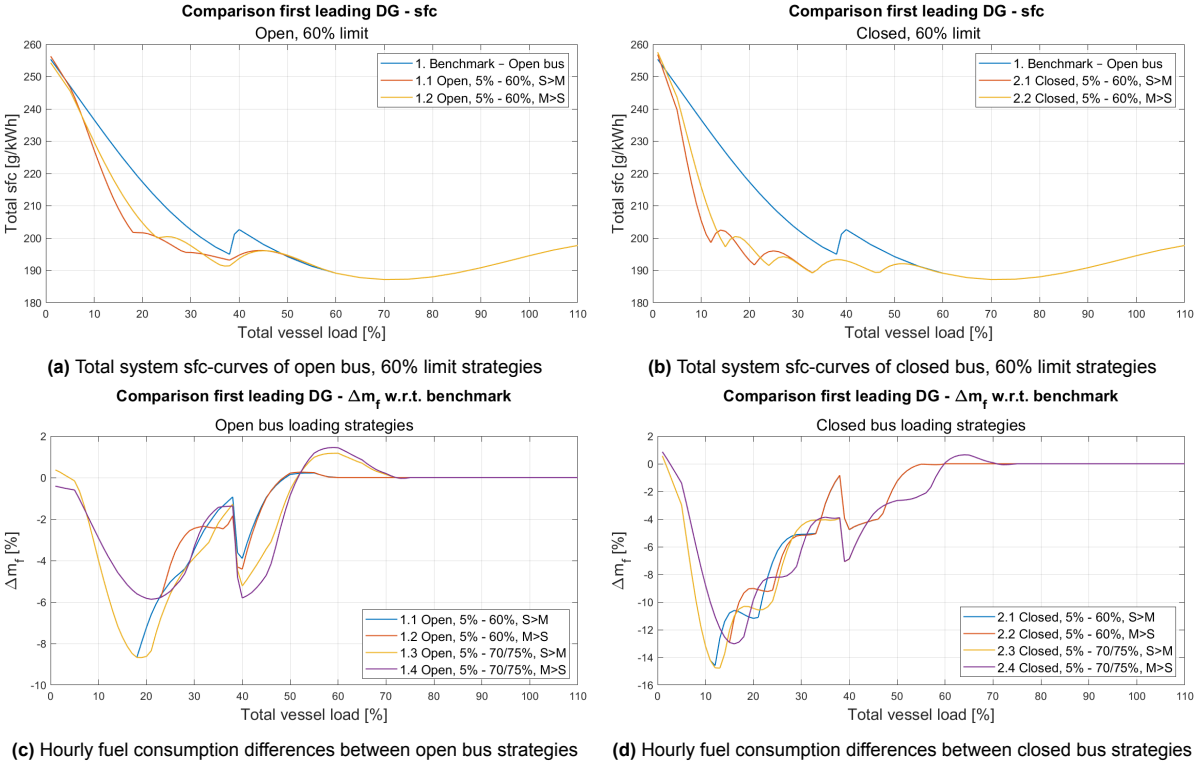
(b) Fuel mass flow savings of all selected load allocation strategies

Figure 4.3: Preliminary sfc-curve and fuel mass flow savings of all selected load allocation strategies

Without identifying differences between the improved DG load allocation strategies, Figure 4.3 illustrates that all strategies result in fuel consumption improvements up to loads of 50% of total vessel power.
A positive outlook is that the highest fuel savings are reached between loads of 10 to 20%, corresponding to the case vessel's average operational loads. There are also fuel savings visible for higher loads, which correspond to power reached during load transients.
The upcoming sections will discuss the variations in results based on different load allocation settings. Note that all figures of the preliminary results are depicted in section D.3 of Appendix D.

First leading DG analysis

Preliminary results between first leading DG settings are depicted in Figure 4.4. Here, fuel mass flow results are given as fuel-saving percentages relative to the benchmark strategy. The benchmark strategy is further depicted in every sfc-curve graph as a blue line.



(a) Total system sfc-curves of open bus, 60% limit strategies

(b) Total system sfc-curves of closed bus, 60% limit strategies

(c) Hourly fuel consumption differences between open bus strategies

(d) Hourly fuel consumption differences between closed bus strategies

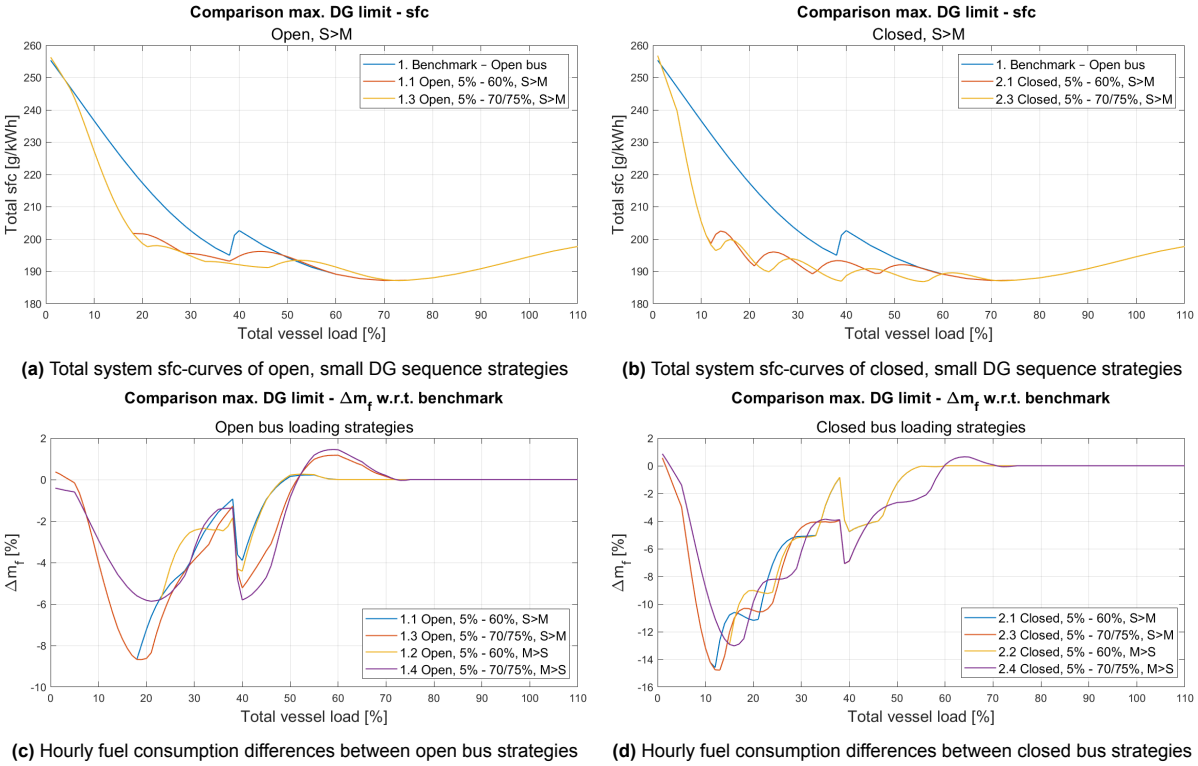
Figure 4.4: Comparison of preliminary results between first leading DG settings

Comparing results shows that sequences starting with small DGs are more advantageous at lower vessel powers. For the open bus-tie strategies, differences in hourly fuel consumption savings go up to 4%. Again, this is because smaller DGs are able to run closer to their optimum and are, therefore, more fuel-efficient than the medium DG sequences. Similarly, this difference diminishes at higher powers. At loads of 40 to 50%, the medium DG sequences are slightly better.

Such differences are, however, much less noticeable for the closed bus-tie strategies. Small DG sequences are still significantly more advantageous at lower powers, though differences also diminish earlier. This is likely because of the lower number of DGs operated with a closed bus-tie configuration. As DGs reach their limits more quickly, fuel, so do differences between first leading DG settings diminish earlier.

Maximum DG limits analysis

As discussed in Chapter 3, there are two maximum DG limits. One is at 60% MCR, which corresponds with the current operational limit as given in the ASOG. The other is at the optimum sfc operating point of the DGs, which is 70% for the small DGs and 75% for the medium DGs.
In theory, the 70/75% limit should yield higher fuel savings. This is not just because DGs operate more efficiently at later stages; start-up sequences also occur at higher vessel powers. Preliminary results between the maximum DG limits settings are presented in Figure 4.5.



(a) Total system sfc-curves of open, small DG sequence strategies

(b) Total system sfc-curves of closed, small DG sequence strategies

(c) Hourly fuel consumption differences between open bus strategies

(d) Hourly fuel consumption differences between closed bus strategies

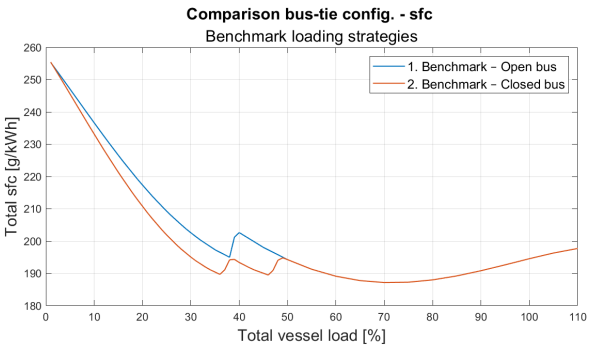
Figure 4.5: Comparison of preliminary results between maximum DG limit settings

As with all strategies, fuel savings of the different DG limit settings are identical, up to approximately 10 to 17.5%, since DG limits are not reached at such loads.
As expected, 60%-sequences reach their limits earlier and become, therefore, relatively worse at higher loads compared to 70/75%-sequences. Ultimately, it seems as if fuel-saving characteristics are drawn out across a wider load range due to increased DG limits. This results in a wave-like sfc-curve pattern, which is especially visible from the results of the closed bus loading strategies depicted in Subfigures 4.5b and 4.5d.

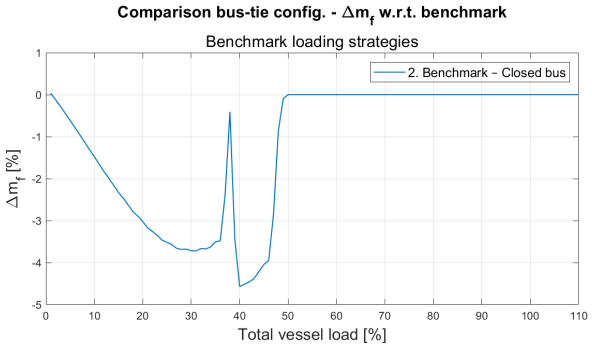
Interestingly, for the open bus loading strategies, 70/75%-sequences appear less efficient for higher powers, near 60% load, compared to the benchmark strategy. The main difference is that for both the benchmark strategy as the 60%-sequences, all DGs operate equally at 60% MCR. The 70/75%-sequences, however, operate with three DGs near their optimum and two at lower powers of around 40% MCR. It appears that in such an instance, this combination of DG loading is just less efficient. Still, considering the operational profile of the DSV, this will likely not influence the overall fuel savings significantly. Such power levels would only be reached during extreme power transients and would raise emergency alert levels, according to the ASOG.
Differences between the results of both settings are less notable for the closed bus strategies. This again appears to be influenced by the smaller amount of DGs operated. Still, for both open and closed bus tie strategies, the 70/75%-sequences appear to be generally more beneficial considering the vessel's operational profile. On the other hand, a combination between a medium DG and 70/75%-sequence could be more advantageous if DG powers are on the high side of the power spectrum.

Open & Closed bus analysis

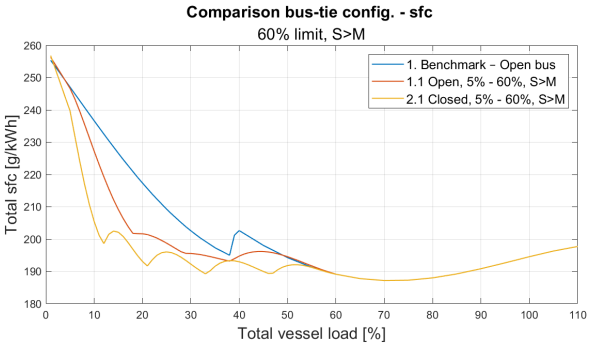
The preliminary results between open and closed bus strategies are presented in Figure 4.6. Additionally, the results of the closed bus-tie benchmark strategy are presented in Subfigures 4.6a and 4.6b.



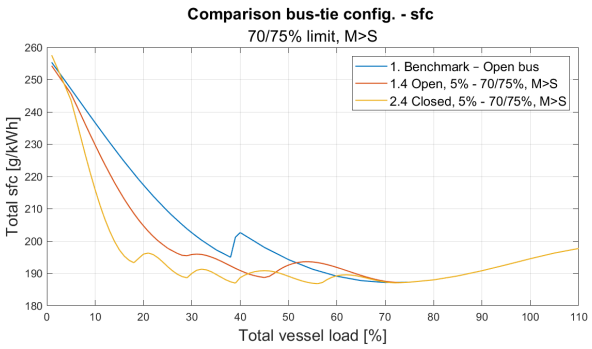
(a) Total system sfc-curves of both benchmark strategies



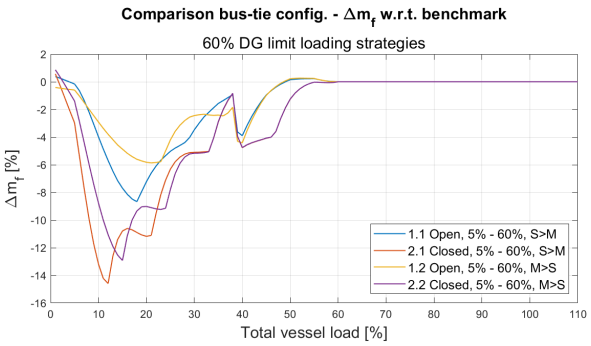
(b) Hourly fuel consumption differences between both benchmark strategies



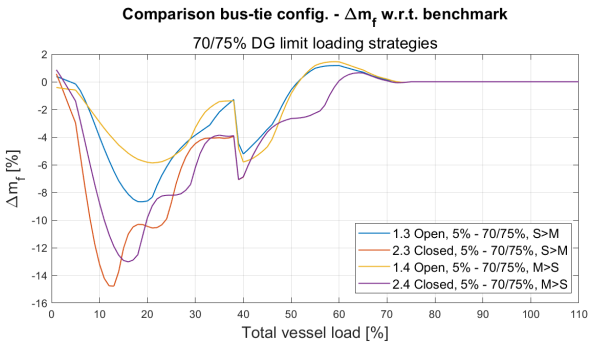
(c) Total system sfc-curves of 60% limit, small DG sequence strategies



(d) Total system sfc-curves of 70/75% limit, medium DG sequence strategies



(e) Hourly fuel consumption differences between 60% limit strategies



(f) Hourly fuel consumption differences between 70/75% limit strategies

Figure 4.6: Comparison of preliminary results between open & closed bus-ties

The closed bus benchmark strategy shows fuel savings throughout in Subfigures 4.6a and 4.6b. In contrast to the other load allocation strategies, fuel savings increase with higher vessel powers until DG limits are reached. This shows the fuel-saving potential of operating with one less DG.

Combining closed bus-ties with other load allocation strategies causes significant fuel savings and appears to have a leveraging effect.
Such differences are, however, only for lower vessel powers. Although still significant fuel savings are achieved at higher vessel powers, these are of a lesser degree given that limits are reached sooner.

Conclusion

Overall, it appears that the improved DG load allocation strategies will provide the vessel with significant fuel savings during DP operations. Fuel savings are apparent throughout the operational profile of the case vessel. The highest fuel savings are around the low average operational powers, though savings are also depicted for load transients.

For the dynamic model, open bus-tie sequences starting with smaller leading DGs will likely result in higher savings than those starting with medium-sized DGs. However, it is questionable whether such significant differences will also be the case for closed bus-tie configurations as relative savings diminish more quickly. Another aspect that should be accounted for in the dynamic model is frequent load transients. As a consequence, the configurations with smaller first-leading DGs are likely to reach their limits earlier.

Furthermore, 70/75%-sequences should provide somewhat higher fuel savings compared to 60%-sequences, though the difference will likely depend on the significance of load transients. This is because relative fuel savings are generally the same at lower power levels and only appear for higher loads which occur during transients.
Another aspect to be examined with the dynamic model is whether there are higher risks involved with 70/75%-sequences. On one hand, DGs operate closer to their maximum, and therefore, there is less DG power available as spinning reserve. On the other hand, DGs reach their limit later on, and the chances of exceeding their limits are lower during load transients.

For the dynamic model, the closed bus-tie strategies are expected to result in the most significant fuel savings, as combining these with other improvements appears to have a leveraging effect. However, as closed bus-tie strategies operate on fewer DGs, their ability to handle large load transients is likely worse than those of open bus-tie strategies.

Load transients will, in the end, likely be the main cause of differences between the preliminary results and those of the dynamic model. Despite the presented results throughout this section, the actual fuel savings are questionable, given that DP vessels rarely operate at constant average power levels. For this, a dynamic model is drafted to simulate such a load profile more realistically.
Also note that for open bus configurations, actual power levels between switchboards will deviate as these operate separately from each other and have to provide power to different consumers.
As the exact fuel savings for accounting for such aspects remains unknown, a dynamic model and its respective results will be presented in Chapters 5 and 6.

5

Dynamic Model

This chapter will present the methodology used to make the dynamic model. This model aims to simulate an entire 24-hour DP operation for the two selected cases of the Boka Atlantis and provide fuel consumption results for the improved DG load allocation strategies based on a realistic dynamic load profile.
First, in section 5.1, an overview of the model will be presented. Subsequently, in section 5.2, the different subsystems of the model will be described in detail.

5.1. Model overview

Figure 5.1 presents a general overview of the Dynamic Model, which is made using MATLAB-Simulink. Its working principle can be seen as a digital twin, which simulates the vessel's behaviour and power consumption based on specified sea state conditions as input.

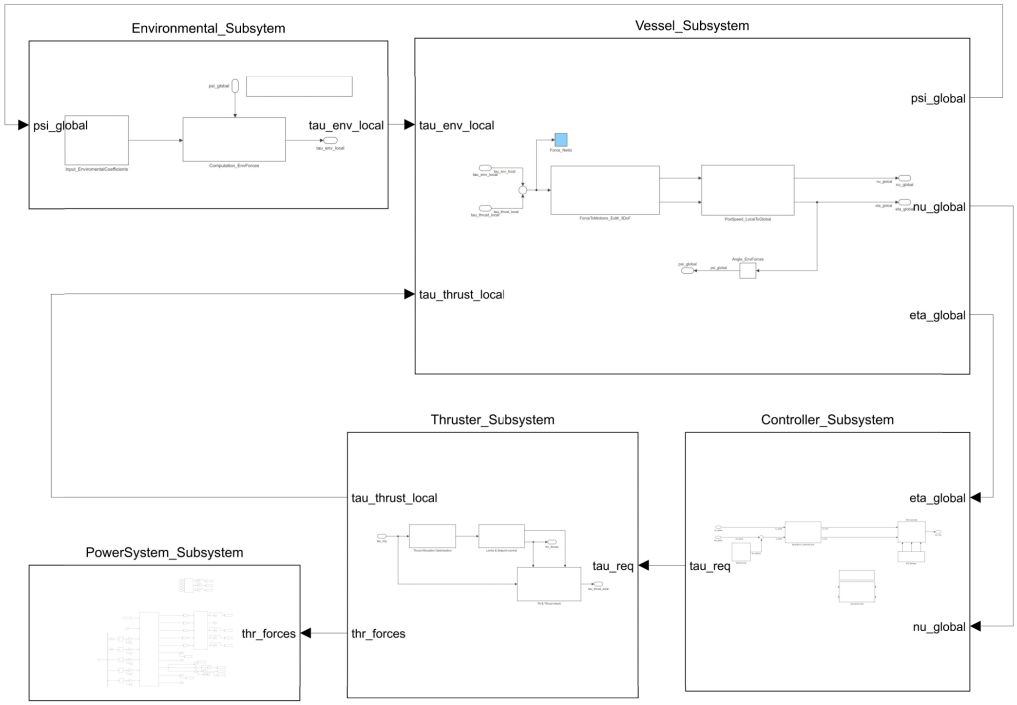


Figure 5.1: General overview of the Dynamic model in MATLAB-Simulink

The input of the dynamic model is the perceived environmental conditions reported in the Daily Progress Report (DPR) of the selected DP operations. As discussed, this is presented in section B.2 of Appendix B. The environmental subsystem transforms these conditions into forces acting on the vessel, which are added to the thruster forces.
The vessel subsystem transforms the sum into a resulting vessel velocity and position through a three degrees of freedom (DoF) equations of motions (EoM). The subsequent velocity and position errors are determined through the set reference values and are used by a proportional integral derivative (PID) controller. Using the error, the controller determines the amount and direction of thrust required by the thruster subsystem.
Based on the algorithm used by de Boer (2023), a quadratic optimisation algorithm is used for the thrust allocation (TA) controller. This subsystem determines the setpoint and absolute amount of thrust required by each propulsor. The resulting sum of thruster forces loops back to the vessel subsystem.
The individual thrust of each propulsor is passed to the power generation system, where it is converted to a specific shaft power per propulsor. The power system consequently determines the amount of power required by the vessel. A PMS algorithm allocates the required load to the corresponding DGs in accordance with the different DG load allocation strategies. The individual DG powers are subsequently converted to a corresponding amount of fuel and accumulated over time.

5.1.1. General assumptions

Due to differences in data reporting frequencies, an entire day of a DP operation was simulated. Some data, such as vessel heading, is measured and reported every ten minutes. Data on environmental conditions is reported every six hours, whilst data on the average DG load or overall fuel consumption is reported every 24 hours. Although some of this data is measured more frequently, Boskalis has not processed this, and therefore, it couldn't be used. As a result, the entire 24 hours were taken to have some form of validation for the average power and total fuel consumption. Because of that, the model runtime is 86400 seconds, with fixed step sizes of 0.5 seconds. This is to guarantee a desirable controller response time and prevent unrealistic transients in the model.
The DP model is made in the horizontal plane with three DoF in surge, sway and yaw. As mentioned by Fossen (2011), such is a frequently used simplification and good approximation for most conventional ships. Low speeds below two metres per second are assumed, making the model suitable for simulating station-keeping operations. Dynamics associated with heave, roll and pitch motions are neglected, as are the restoring forces from gravity and buoyancy.
Two coordinate systems are used within the dynamic model. A global coordinate system and a local, body-fixed coordinate system. The local coordinate system's origin is in the vessel's centre of gravity to simplify some of the calculations. The main difference between these coordinate systems is that the global coordinate system is fixed at 0,0,0, which is the setpoint of the vessel during the DP operation. The vessel's heading is constant for both selected benchmark cases and, therefore, fixed within the model. As the vessel's heading is not necessarily north, such as for the low load case, the directions of the environmental conditions are rotated accordingly and transformed into corresponding angles of attack. Rotational matrices 5.1 and 5.2 are used for the transformation between coordinate systems:

For Global to Local transformations:

$$\begin{bmatrix} cos(\psi) & sin(\psi) & 0 \\ -sin(\psi) & cos(\psi) & 0 \\ 0 & 0 & 1 \end{bmatrix} \tag{5.1}$$

and for Local to Global transformations:

$$\begin{bmatrix} cos(\psi) & -sin(\psi) & 0 \\ sin(\psi) & cos(\psi) & 0 \\ 0 & 0 & 1 \end{bmatrix} \tag{5.2}$$

Limits and constraints for DP operations, as described by Chapter 3, have not been implemented in the model itself. However, results have been verified whether such limits have been exceeded. Most of the computations and formulas used in the dynamic model are from Fossen (2011). Other assumptions made will be mentioned throughout the rest of this chapter.

5.2. Model description

Section 5.2 will present the different subsystems of the dynamic model in greater detail. Section 5.2.1 will describe the environmental subsystem, and section 5.2.2 the vessel subsystem. Next, the controller subsystem is elaborated in section 5.2.3, and section 5.2.4 will focus on the thruster subsystem. Lastly, the power system is covered in section 5.2.5.

5.2.1. Environmental subsystem

The environmental loads considered to be acting on the vessel consist of current, wave, and wind forces. As can be observed from section B.2 of Appendix B, the environmental conditions are reported every six hours in the DPRs of the chosen case conditions.
To approximate the changing sea state conditions and create a realistic dynamic load profile, the reported mean environmental values are transformed into randomised signals, which vary over time. These randomised signals are implemented in the dynamic model using lookup tables. Within Simulink, a cubic spline interpolation is used to create a smooth signal, avoiding excessive and unrealistic transients.

Environmental input

A separate MATLAB script is made to generate the randomised signals. If the characteristics of such a signal were satisfactory, these were saved as the environmental conditions of specific benchmark cases. Although only two benchmark cases have been selected and tested, the purpose of this working method is to select and test the results of other benchmark cases quickly.

The water current is characterised by a certain speed and direction. A specific distribution and randomised signal are not necessary for approximation as variations in velocity and direction are very slow [J.M.J. Journée, 2008]. Given the operational profile of DSVs, current conditions are often not significant. Therefore, the water current is considered a steady phenomenon and is instead modelled with the five data points given in the DPRs.

The wave conditions are described by a significant height, period, and direction. The wave height is approximated with a Rayleigh distribution [J.M.J. Journée, 2008, Mackay, 2012]. The shape factor of the distribution is computed by using the mean wave height for the given interval and formulations 5.3 and 5.4 for Rayleigh distributions [Aldo Vieira da Rosa, 2022, Burton et al., 2011]:

$$\overline{H_s} = \sigma_{H_s}\sqrt{\frac{\pi}{2}} \tag{5.3}$$

Rewriting and substitution gives:

$$\sigma_{H_s} = \frac{\overline{H_s}}{\sqrt{\frac{\pi}{2}}} \tag{5.4}$$

With:
$\overline{H_s}$ $[m]$ – Mean significant wave height
σ_{H_s} $[m]$ – Shape factor Rayleigh distribution H_s

To ensure that the wave height and period are conform to each other, the Brettschneider formulation of equation 5.5 is used to compute the mean wave period [ITTC, 1987, J.M.J. Journée, 2008].

$$T_m = 3.86\sqrt{H_s} \tag{5.5}$$

with:
H_s $[m]$ – Significant wave height
T_m $[s]$ – Mean wave period

The wave direction is computed using a normal distribution, as this would provide a better representation [J.M.J. Journée, 2008]. The standard deviation is determined to be five degrees, based on trial and error.

The wind conditions are modelled by wind speed and direction, which are described by normal distributions. Although some sources, such as E. Kavak Akpinar (2005), state that Rayleigh distributions can be used to model wind speeds, normal distributions provided better-randomised signals without unrealistically high occasional values.
Relatively large fluctuations over time characterise both wind velocity and direction. This was achieved using data on standard deviations of wind characteristics at the North Sea [Burton et al., 2011, Caires et al., 2019]. The standard deviation of wind velocity was gathered through data on wind turbulence intensity, depicted by equation 5.6:

$$TI = \frac{\sigma_{V_{wind}}}{\overline{V_{wind}}} \tag{5.6}$$

	TI	[-]	–	Turbulence Intensity
With:	$\overline{V_{wind}}$	$[m/s]$	–	Mean wind speed
	$\sigma_{V_{wind}}$	$[m/s]$	–	Standard deviation wind speed

Turbulence intensity is approximated at 10% based on North Sea Turbulence Data [Caires et al., 2019]. The standard deviation for wind direction was also based on North Sea data and set at ten degrees [Burton et al., 2011].

With these presented methods, a randomised signal is created which approximates the varying load profile of a vessel during DP operations. The created environmental conditions are illustrated in section E.1 of Appendix E. Do note that as the vessel heading is recorded for the whole DP operation, the environmental directions are corrected relative to the vessel's heading. Therefore, the graphs of environmental directions depict the incoming angle of attack.

Environmental forces

As discussed, the environmental forces consist of current, wind and waves in three DoF. The total force exerted on the vessel by environmental loads is given by equation 5.7.

$$\tau_{env} = \begin{bmatrix} \tau_{env,x} \\ \tau_{env,y} \\ \tau_{env,\psi} \end{bmatrix} = \begin{bmatrix} F_{curr,x} + F_{wave,x} + F_{wind,x} \\ F_{curr,y} + F_{wave,y} + F_{wind,y} \\ M_{curr,\psi} + M_{wave,\psi} + M_{wind,\psi} \end{bmatrix} \tag{5.7}$$

With: $\tau_{env,i}$ $[kN]$ – Total environmental load in surge, sway or yaw, respectively for $i \in \{x, y, \psi\}$

The current forces are modelled using area-based current coefficients, which depend on the incoming current angle, which is depicted in equation 5.8 [Fossen, 2011].

$$\begin{aligned} F_{curr,x} &= \frac{1}{2}\rho_{sw} A_{FW} C_{curr,x}(\gamma_c) V_c^2 \\ F_{curr,y} &= \frac{1}{2}\rho_{sw} A_{LW} C_{curr,y}(\gamma_c) V_c^2 \\ M_{curr,\psi} &= \frac{1}{2}\rho_{sw} A_{LW} L_{lwl} C_{curr,\psi}(\gamma_c) V_c^2 \end{aligned} \tag{5.8}$$

	A_{FW}	$[m^2]$	–	Effective frontal area in water
	A_{LW}	$[m^2]$	–	Effective lateral area in water
	$C_{curr,i}$	[-]	–	Current coefficient in surge, sway or yaw, respectively for $i \in \{x, y, \psi\}$
With:	L_{lwl}	$[m]$	–	Length of waterline
	V_c	$[m/s]$	–	Current speed
	γ_c	$[deg]$	–	Current angle of attack
	ρ_{sw}	$[t/m^3]$	–	Density of seawater

As vessel velocities are near zero during station-keeping operations, current forces only depend on the current speed.

The current coefficients have been scaled from a similar vessel of Boskalis. Initially, these were given in ton-force units and have, therefore, first been converted to newtons and made non-dimensional. Equation 5.9 is used for scaling the current coefficient in surge [Fossen, 2011].

$$C_{curr,x} = \frac{S}{A_{FW}} C_f \tag{5.9}$$

With:

C_f	[-]	–	Frictional resistance coefficient
S	$[m^2]$	–	Wetted hull surface area

As the reference vessel has a shorter length, the frictional resistance coefficient will be different. The frictional resistance coefficient depends on the Reynolds number, which cannot be directly calculated given the near-zero speeds. Both variables are depicted by equations 5.10 and 5.11 [Fossen, 2011].

$$C_f(u) = \frac{0.075}{(log_{10} R_n - 2)^2} + C_R \tag{5.10}$$

$$R_n = \frac{u L_{pp}}{\nu} \tag{5.11}$$

With:

C_R	[-]	–	Residual friction coefficient
L_{pp}	$[m]$	–	Length between perpendiculars
R_n	[-]	–	Reynolds number
u	$[m/s]$	–	Surge velocity
ν	$[m^2/s]$	–	Kinematic viscosity

Therefore, scaling is done up to the Reynolds number, using the difference in length, and is consequently scaled back to the current coefficient in surge. This is achieved using the formulations of equation 5.12. Note that the residual friction coefficient is neglected for making the computation possible.

$$\begin{aligned} C_{f,ref} &= C_{curr,x,ref} \frac{A_{FW,ref}}{S_{ref}} \\ R^*_{n,ref} &= 10^{\sqrt{\frac{0.075}{C_{f,ref}}}+2} \\ R^*_n &= \frac{L_{pp}}{L_{pp,ref} R^*_{n,ref}} \\ C_f &= \frac{0.075}{(log_{10} R^*_n - 2)^2} \\ C_{curr,x} &= \frac{S}{A_{FW}} C_f \end{aligned} \tag{5.12}$$

Scaling of the current coefficient in sway and yaw is done by analysing the formulations of Faltinsen (1990). As is argued by Fossen (2011), the current coefficients in sway and yaw depend on the draft of the vessel and the 2D drag coefficients, C_{2D_d}. As these are a function of $\frac{B}{2T}$, the difference in C_{2D_d} is negligible between vessels as their beam and draft are almost equal to each other. As such, the current coefficients in sway and yaw are regarded as equal for both vessels.
The current coefficients are implemented in the model through lookup tables that depend on the incoming current velocity. These are depicted in section E.2 of Appendix E.

As described by Fossen (2011) and J.M.J. Journée (2008), wave-induced forces can be separated into first-order and second-order. First-order wave loads are observed as zero-mean oscillatory motions, whilst second-order wave loads are nonzero and slowly varying components. Therefore, only the second-order wave-induced forces are taken into account.
These are computed using the square of the significant wave height, which is multiplied by the wave coefficient, as is shown in equation 5.13. Note that the wave coefficients depend on the incoming angle of attack and the mean wave period.

$$\begin{aligned} F_{wave,x} &= C_{wave,x}(\gamma_{wave}, T_m)H_s^2 \\ F_{wave,y} &= C_{wave,y}(\gamma_{wave}, T_m)H_s^2 \\ M_{wave,\psi} &= C_{wave,\psi}(\gamma_{wave}, T_m)H_s^2 \end{aligned} \tag{5.13}$$

With:

$C_{wave,i}$	[-]	–	Wave coefficient in surge, sway or yaw, respectively for $i \in \{x, y, \psi\}$
H_s	$[m]$	–	Significant wave height
T_m	$[s]$	–	Mean wave period
γ_{wave}	$[deg]$	–	Wave angle of attack

The formulations and scaling methods of the wave coefficients are based on information provided by the reference vessel's DP capability report. Coefficients in surge and sway are scaled using the vessel beam and length and in yaw only with the vessel's beam.
As such, the scaling factors for the wave coefficients are depicted by equation 5.14. Note that the gravitational constant is implemented in the equation to transform the ton-force units into newtons.

$$\begin{aligned} k_{C_{wave,x}} &= k_{C_{wave,y}} = g\frac{B^2/L_{pp}}{B_{ref}^2/L_{pp_{ref}}} \\ k_{C_{wave,\psi}} &= g\frac{B^2}{B_{ref}^2} \end{aligned} \tag{5.14}$$

With:

B	$[m]$	–	Beam
g	$[m/s^2]$	–	Gravitational acceleration constant
$k_{C_{wave,i}}$	[-]	–	Scale factor wave coefficients in surge, sway or yaw, respectively, for $i \in \{x, y, \psi\}$

The lookup tables of the wave coefficients, both in 2D and 3D, are presented in section 5.14 of Appendix E.

The wind forces are calculated similarly to the current forces using equation 5.15 [Fossen, 2011].

$$\begin{aligned} q &= \frac{1}{2}\rho_a V_w^2 \\ F_{wind,x} &= qA_{FA}C_{wind,x}(\gamma_w) \\ F_{wind,y} &= qA_{LA}C_{wind,y}(\gamma_w) \\ M_{wind,\psi} &= qA_{LA}L_{oa}C_{wind,\psi}(\gamma_w) \end{aligned} \tag{5.15}$$

With:

A_{FA}	$[m^2]$	–	Effective frontal area in air
A_{LA}	$[m^2]$	–	Effective lateral area in air
$C_{wind,i}$	[-]	–	Wind coefficient in surge, sway or yaw, respectively for $i \in \{x, y, \psi\}$
L_{oa}	$[m]$	–	Overall length
q	$[kN/m^2]$	–	Dynamic pressure of the apparent wind
V_w	$[m/s]$	–	Wind speed
γ_{wind}	$[deg]$	–	Wind angle of attack
ρ_a	$[t/m^3]$	–	Density of air

Again, the resulting wind force solely depends on the incoming wind speed, given the low vessel speeds that are typical for station-keeping operations.

Wind coefficients are scaled from the reference vessel, using the formulation of Blendermann (1994) depicted in equation 5.16.

$$
\begin{aligned}
C_{wind,x} &= -CD_l \frac{A_{LA}}{A_{FA}} \frac{cos(\varepsilon)}{1 - \frac{\delta}{2}\left(1 - \frac{CD_l}{CD_t}\right) sin^2(2\varepsilon)} \\
C_{wind,y} &= CD_t \frac{sin(\varepsilon)}{1 - \frac{\delta}{2}\left(1 - \frac{CD_l}{CD_t}\right) sin^2(2\varepsilon)} \\
C_{wind,\psi} &= \left[\frac{s_L}{L_{oa}} - 0.18\left(\varepsilon - \frac{\pi}{2}\right)\right] * C_{wind,y}
\end{aligned}
\tag{5.16}
$$

With:

CD_l	[-]	–	Coefficient of longitudinal resistance
CD_t	[-]	–	Coefficient of lateral resistance
s_L	$[m]$	–	Centroid of lateral wind area
δ	[-]	–	Cross-force coefficient
ε	$[rad]$	–	Angle of apparent wind

As both vessels have similar properties and primarily differ in length, the non-dimensional coefficients are the same for both vessels. As a result, the wind coefficients in surge and sway are considered equal. However, the wind coefficient in yaw requires scaling, given the difference in length. This is done by rewriting and solving the formulations of equation 5.16.
Also, these lookup tables have been presented in section E.2 of Appendix E. The overall environmental forces from the dynamic results are presented in sections F.1.1 and F.2.1 of Appendix F, for both load cases.

5.2.2. Vessel subsystem

Considering the three DoF in surge, sway and yaw, the resulting EoM is presented in equation 5.17, which is deduced from Fossen (2011) and Sørensen (2018).

$$
M\dot{v} + C(v)v + D(v)v = \tau_{env} + \tau_{thr} \tag{5.17}
$$

with:

$C(v)$	$[t/s]$, $[tm/s]$, $[tm^2/s]$	–	Coriolis–centripetal matrix
$D(v)$	$[t/s]$, $[tm/s]$, $[tm^2/s]$	–	Damping matrix
M	$[t]$, $[tm]$, $[tm^2]$	–	System inertia matrix
v	$[m/s]$, $[rad/s]$	–	Vessel velocity in surge, sway or yaw, respectively, for $\{u, v, r\}$
τ_{thr}	$[kN]$	–	Propulsion system forces in 3 DoF

Restoring forces resulting from gravity and buoyancy have been neglected. It is also assumed that the centre of gravity coincides with the origin of the ship's coordinate system. As such, it is assumed that the vessel is symmetrical in the xz-plane and is placed in an ideal fluid with mass uniformly distributed. Equation 5.17 is rewritten to equation 5.18 to solve for acceleration and allow the EoM to be solved.

$$
\begin{aligned}
\dot{v} &= M^{-1}\left(\tau_{total} - C(v)v - D(v)v\right) \\
&\text{where :} \\
M &= M_{RB} + M_A \\
C(v) &= C_{RB}(v) + C_A(v) \\
D(v) &= D_L + D_{NL}(v)
\end{aligned}
\tag{5.18}
$$

with:

C_A	$[t/s]$, $[tm/s]$, $[tm^2/s]$	–	Hydrodynamic Coriolis and centripetal matrix
C_{RB}	$[t/s]$, $[tm/s]$, $[tm^2/s]$	–	Rigid-body Coriolis and centripetal matrix
D_L	$[t/s]$, $[tm/s]$, $[tm^2/s]$	–	Linear damping matrix
D_{NL}	$[t/s]$, $[tm/s]$, $[tm^2/s]$	–	Nonlinear damping matrix
M_A	$[t]$, $[tm]$, $[tm^2]$	–	Added mass matrix
M_{RB}	$[t]$, $[tm]$, $[tm^2]$	–	Rigid body system inertia matrix

The rigid body mass matrix is determined through equation 5.19 [Fossen, 2011].

$$M_{RB} = \begin{bmatrix} m & 0 & -my_g \\ 0 & m & mx_g \\ -my_g & mx_g & I_z \end{bmatrix} = \begin{bmatrix} m & 0 & 0 \\ 0 & m & 0 \\ 0 & 0 & I_z \end{bmatrix} \tag{5.19}$$

where :

$$I_z = m * R_{66}^2$$
$$R_{66} \approx 0.25 L_{pp}$$

with:

I_z	$[tm^2]$	–	Rotational moment of inertia around the z-axis
m	$[t]$	–	Vessel displacement
R_{66}	$[m]$	–	Yaw radius of gyration
x_g	$[m]$	–	Longitudinal location of CoG
y_g	$[m]$	–	Transversal location of CoG

Here, the radius of gyration in yaw is determined from Fossen (2011) and DP capability report calculations. As the vessel's centre of gravity coincides with the origin of the local coordinate system, the off-diagonal terms are zero.

The added mass matrix is given by equation 5.20 [Fossen, 2011].

$$M_A = -\begin{bmatrix} X_{\dot{u}} & X_{\dot{v}} & X_{\dot{r}} \\ Y_{\dot{u}} & Y_{\dot{v}} & Y_{\dot{r}} \\ N_{\dot{u}} & N_{\dot{v}} & N_{\dot{r}} \end{bmatrix} = -\begin{bmatrix} X_{\dot{u}} & 0 & 0 \\ 0 & Y_{\dot{v}} & Y_{\dot{r}} \\ 0 & Y_{\dot{r}} & N_{\dot{r}} \end{bmatrix} \tag{5.20}$$

Some of the off-diagonal terms become zero due to the choice of the origin point. Also, coefficients $Y_{\dot{r}}$ and $N_{\dot{v}}$ are equal to each other because of this [Berge and Fossen, 2000]. Furthermore, as the assumption for low-speed applications is made, the added mass components of the matrix are selected for zero frequency.

The added mass components are scaled from a known added mass matrix from an offshore supply vessel presented by Fossen (2011). Scaling is based on the method presented by Bertram (2012) and Fossen (2011) by normalising the mass components as given by equation 5.21.

$$\begin{Bmatrix} X_i' \\ Y_i' \\ N_i' \end{Bmatrix} = \frac{1}{qL^2} \begin{Bmatrix} X_i \\ Y_i \\ N_i/L \end{Bmatrix} \tag{5.21}$$

where :

$$q = \rho \frac{u^2}{2}$$

Assuming both vessels have an equal speed and are in a body of water with equal density, only the length terms remain. Similarly, the normalisation variables used for the added mass components are given by Fossen (2011) and presented by equation 5.22, yielding the elements of the added mass matrix.

$$\begin{aligned} \text{Mass terms} &: X_{\dot{u}}, Y_{\dot{v}} : \frac{1}{2}\rho L^3 \\ \text{Mass} \cdot \text{length terms} &: Y_{\dot{r}} : \frac{1}{2}\rho L^3 \cdot L \\ \text{Inertia moment terms} &: N_{\dot{r}} : \frac{1}{2}\rho L^5 \end{aligned} \tag{5.22}$$

The rigid body Coriolis-centripetal matrix is computed using equation 5.23, which depends on the linear and rotational vessel speed.

$$C_{RB}(v) = \begin{bmatrix} 0 & 0 & -m\left(x_g r + v\right) \\ 0 & 0 & -m\left(y_g r - u\right) \\ m\left(x_g r + v\right) & m\left(y_g r - u\right) & 0 \end{bmatrix} = \begin{bmatrix} 0 & 0 & -mv \\ 0 & 0 & mu \\ mv & -mu & 0 \end{bmatrix} \tag{5.23}$$

The added mass components of the Centripetal Matrix are defined by equation 5.24, using the added mass components that are described earlier.

$$C_A(v) = \begin{bmatrix} 0 & 0 & Y_{\dot{v}} v + Y_{\dot{r}} r \\ 0 & 0 & -X_{\dot{u}} u \\ -Y_{\dot{v}} v - Y_{\dot{r}} r & X_{\dot{u}} u & 0 \end{bmatrix} \tag{5.24}$$

The damping terms can lastly be divided into a linear part, consisting of potential damping and skin friction, and a non-linear part, consisting of wave drift damping, vortex shedding and possible lifting forces [Berge and Fossen, 2000]. According to Berge and Fossen (2000), the non-linear damping term is negligible for this model as vessel speeds are low. As such, the overall damping terms only consist of linear damping, which is depicted by equation 5.25 [Fossen, 2011].

$$D_L = -\begin{bmatrix} X_u & 0 & 0 \\ 0 & Y_v & Y_r \\ 0 & N_v & N_r \end{bmatrix} \approx \begin{bmatrix} B_{11v} & 0 & 0 \\ 0 & B_{22v} & 0 \\ 0 & 0 & B_{66v} \end{bmatrix}$$

where :

$$\begin{aligned} B_{11v} &= \frac{m + X_{\dot{u}}}{T_{surge}} \\ B_{22v} &= \frac{m + Y_{\dot{v}}}{T_{sway}} \\ B_{66v} &= \frac{I_z + N_{\dot{r}}}{T_{yaw}} \end{aligned} \tag{5.25}$$

with: T_i [s] – Linear viscous damping time constants respectively for $i \in \{surge, sway, yaw\}$

The subsequent vessel velocity and position are consequently transformed from a local coordinate system to a global coordinate system. The vessel heading is used further to calculate the resulting environmental forces. The overall velocity and position components are used as input for the controller subsystem. The corresponding vessel dynamic results of these computations are depicted in sections F.1.1 and F.2.1 of Appendix F, for both load cases.

5.2.3. Controller subsystem

The objective of the controller subsystem is to determine the required amount of thrust in three DoFs to compensate for the environmental disturbances.

Controller model

First, the position and velocity errors in the local coordinate system are determined. The subsequent errors are used by the PID controller, which can be represented by equation 5.26 [Sørensen, 2018].

$$\tau_{req} = K_p e_{pos} + K_i \int_0^t e_{pos}(\tau) \mathrm{d}\tau + K_d e_{vel} \tag{5.26}$$

with:

K_d	[-]	–	Derivative gain controller
K_i	[-]	–	Integral gain controller
K_p	[-]	–	Proportional gain controller
e_{pos}	[m], [rad]	–	Position error in respect of setpoint
e_{vel}	[m/s], [rad/s]	–	Velocity error in respect of setpoint
τ_{req}	[kN], [kNm]	–	Required force and moment of propulsion system

Based on similar PID-controllers of Fossen (2011) and Sørensen (2018), the derivative gains are coupled to the velocity errors in order to minimise vessel velocity and prevent unrealistic load transients, given the lack of inertia within the model. The proportional and integral gains are both coupled to the position errors.

Controller tuning

As there is a PID controller for every DoF, nine different gains are manually tuned to obtain the desired vessel behaviour and, with that, a realistic power system load profile. Therefore, the following requirements for the desired vessel behaviour were drafted and used:

- Settling time should be around 10 to 20 minutes for the vessel
- DP footprint within 4 to 6 metres, so 2 to 3 metres from the setpoint
- DP heading limit at 3 degrees from setpoint
- Position steps below 3 metres
- Heading increment steps below 2 degrees
- Vessel speed, close to the structure below 0.3 knots
- Rate of change of heading below 5 degrees per minute

The first requirement is gathered from Bray et al. (2020) and personal communications at Boskalis and the IMCA DP Conference (2023). The other requirements are from the ASOG of the Boka Atlantis for a 2-way split bus.

The model is first tuned for constant forces obtained from the DP capability report. After receiving a desired response, the controller is tested for all environmental conditions of the DP Capability report and the two selected benchmark conditions. The corresponding vessel dynamic results used to check whether the provided limits were achieved are presented in sections F.1.1 and F.2.1 of Appendix F, for both load cases.

First, all proportional gains were set to one and all others to zero. Then, the proportional gains were tuned for each DoF until the desired magnitude for the thruster forces was reached. Subsequently, the integral gains were increased until the desired settling time was obtained and iteratively adjusted with the derivative gains, which decreased system overshoots and the vessel's settling time. The resulting PID-controller gains are depicted in Table 5.1.

	x	y	ψ
P-gains	300	450	300,000
I-gains	0.075	0.1	150
D-gains	70	150	100,000

Table 5.1: Controller settings

5.2.4. Thruster subsystem

The TA controller and underlying optimisation algorithm are derived from the MSc Thesis of de Boer (2023) and research of Yushi et al. (2013). This algorithm can mathematically be represented by equation 5.27 [MathWorks, 2024, Yushi et al., 2013].

$$\min_{u} \left(\frac{1}{2} u^T W u\right) \text{ such } \begin{cases} A_{eq} \cdot u = \tau_{eq}, \\ A \cdot u \leq \tau_{max} \end{cases} \quad \text{where } \begin{cases} u_i = [u_{i,x}, u_{i,y}]^T, \\ u_{i,x} = f_i cos(\alpha_i), u_{i,y} = f_i sin(\alpha_i) \end{cases} \tag{5.27}$$

with:

f_i	$[kN]$, $[kNm]$	–	Total amount of force delivered by thruster i
$u_{i,j}$	$[kN]$, $[kNm]$	–	Force delivered by thruster i in surge and sway, for $j \in \{x, y\}$
α_i	$[rad]$	–	Angle of thruster i

As represented in equation 5.27, the quadratic programming algorithm consists of a quadratic objective function, equality constraints and non-equality constraints.
The objective function solves the equation for u, which represents the amount of force in the x and y direction for each thruster. Its objective is to minimise the absolute total force delivered by all thrusters, as is denoted by the first part of equation 5.27. Here, W is a diagonal weight matrix.
The purpose of the equality constraints is to ensure that the total force delivered by the thrusters is equal to the required thruster force from the PID controller. The non-equality constraints ensure that the thrusters remain within their given thrust boundaries.
Note that the input of this solver is the required amount of force in three DoF, determined by the controller subsystem. In this case, the quadratic objective function is solvable. However, increasing the amount of DoF would result in the system becoming indefinite, causing the solution to become infinite and difficult to solve [Yushi et al., 2013].

Furthermore, a linearisation is applied to the azimuth thrusters as these have two DoFs that are coupled together. As a result, the azimuth's thruster region is approximated by an N-sided regular polygon as defined by [Yushi et al., 2013]. Additionally, forbidden zones have been determined using equation 5.28 presented by J. Dang (2004).

$$t = \frac{T}{T_0} = 1 - 0.75^{\frac{x}{D}^{\frac{2}{3}}}$$
$$t_\alpha = t + (1-t)\frac{\alpha^3}{\frac{130}{t^3} + \alpha^3} \tag{5.28}$$

	D	$[m]$	–	Thruster diameter
	t	$[-]$	–	Thrust reduction ratio at zero steering angle
	t_α	$[-]$	–	Thrust reduction ratio at steering angle α
with:	T	$[kN]$	–	Thrust of aft thruster
	T_0	$[kN]$	–	Thrust of aft thruster in free open water
	x	$[m]$	–	Distance between the two thrusters
	α	$[deg]$	–	Steering angle of aft thruster

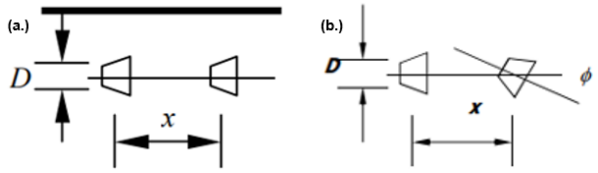


Figure 5.2: Schematic of the forbidden zones calculated through equation 5.28 [J. Dang, 2004]

The first part of equation 5.28 calculates the thrust ratio for thrusters placed in tandem under a flat bottom, as is visualised by figure 5.2. The second part of equation 5.28 subsequently determines the thruster losses for certain steering angles [J. Dang, 2004].
It is assumed that a thruster loss of below 5% is negligible. Calculations showed that the thruster losses between retractable thruster 3 at the bow and thrusters 4 and 5 at the stern, are low enough to be negligible. However, the thruster losses between azimuths 4 and 5 posed to be 48% if directly placed in tandem.
Steering angles of 20 degrees are considered sufficient for thruster losses to be neglected. As a result, both azimuth 4 and 5 have a forbidden zone of 40 degrees. The algorithm defines forbidden zones by taking these out of the feasible set of solutions the solver uses to search for its solutions [Yushi et al., 2013].

The resulting variable from the TA controller is a certain amount of thrust in two directions. This value is converted into an absolute thrust and a designated setpoint angle for the three rotatable thrusters. A saturation limiter is applied to prevent thrusters from exceeding their maximum capacity. The subsequent thruster forces are multiplied with a TA matrix to calculate the total thrust generated, which is depicted in equation 5.29.

$$\begin{aligned} &\tau_{thr} = T(\alpha) f_i \\ &\text{where :} \\ &T(\alpha) = \begin{bmatrix} 0 & 0 & cos(\alpha_3) & cos(\alpha_4) & cos(\alpha_5) \\ 1 & 1 & sin(\alpha_3) & sin(\alpha_4) & sin(\alpha_5) \\ x_1 & x_2 & x_3 sin(\alpha_3) & x_4 sin(\alpha_4) + y_4 cos(\alpha_4) & x_5 sin(\alpha_5) + y_5 cos(\alpha_5) \end{bmatrix} \end{aligned} \tag{5.29}$$

with:

$T(\alpha)$	[m]	–	Thrust configuration matrix
x_i	[m]	–	x-position of thruster i
y_i	[m]	–	y-position of thruster i

As a result, the total force exerted by the thruster system is forwarded to the vessel system. The required amount of thrust for each propulsor is transferred to the power system model.

5.2.5. Power subsystem

The conversion of thrust to shaft power is executed by lookup tables, which are created from DP capability reports of the case study vessels. These are depicted in section E.3 of Appendix E.
A transmission efficiency of 95% is used, based on thruster manufacturer specifications. The resulting variable is the power required from the DGs and is, therefore, the input for the PMS algorithm.
Auxiliary power is furthermore taken into account as a constant value of 700 kW, based on DP operational manuals of the case study vessels. A total of 400 kW is supplied from the port-side switchboard, 10 kW from the centre switchboard, and 290 kW from the starboard-side switchboard.

The PMS algorithms for the benchmark cases have been constructed such that all DGs run at an equal load. This algorithm is depicted by equation 5.30. Since all DGs per switchboard run at equal loads, dividing the required amount of power by the maximum available amount yields the required MCR that has to be delivered by the DGs.

$$\begin{aligned} P_{req_{PS}} &= Load_{PS} \cdot P_{max_{PS}} \\ &= \sum_{i=1}^{n_{DG}} (Load_{PS} \cdot P_{max_{DG2}} + Load_{PS} \cdot P_{max_{DG3}}) \end{aligned} \tag{5.30}$$

with:

$Load_{PS}$	[%]	–	Load of port-side switchboard, in percentage of its maximum
n_{DG}	[-]	–	Number of DGs connected to the switchboard
P_{max_i}	[kW]	–	Maximum available power of DG or switchboard i
$P_{req_{PS}}$	[kW]	–	Power required by port-side switchboard

The PMS algorithms of the improved DG load allocation strategies are constructed differently using if-else statements and defined power limits. A general example is presented by equation 5.31.

$$
\begin{aligned}
1. for\,(P_{req_{PS}} \leq P_{Lim_1}) &\begin{cases} P_{DG2} = P_{req_{PS}} - P_{DG3} \\ P_{DG3} = Load_{min} \cdot P_{max_{DG3}} \end{cases} \\
2. for\,(P_{Lim_1} \leq P_{req_{PS}} \leq P_{Lim_2}) &\begin{cases} P_{DG2} = Load_{max} \cdot P_{max_{DG2}} \\ P_{DG3} = P_{req_{PS}} - P_{DG2} \end{cases} \\
3. for\,(P_{Lim_2} \leq P_{req_{PS}}) &\begin{cases} P_{DG2} = P_{max_{DG2}} \cdot (P_{req_{PS}}/P_{max_{PS}}) \\ P_{DG3} = P_{max_{DG3}} \cdot (P_{req_{PS}}/P_{max_{PS}}) \end{cases}
\end{aligned}
\tag{5.31}
$$

with: P_{Lim_i} $[kW]$ – Power limit i of the improved DG load allocation strategies

If the required switchboard power is below the first power limit, DG3 is operated at its minimum of 5% MCR. As such, the variable amount of power is delivered by DG2. As the first power limit is reached, DG2 will constantly run at its defined maximum power, and instead, DG3 will compensate for the variable remaining power. Exceeding the second power limit will require both DGs to operate at their respective maximum. Therefore, both DGs are equally loaded above their maximum, at least until a new DG is initiated, if possible. As such, the required spinning reserve limits are considered for the different load allocation strategies.

A slightly different maximum DG limit of around 65% MCR is used for the benchmark strategy sequences. This is because the depicted 60% MCR limit is not exactly the same limit given in the ASOG for initiating a new DG. Although this limit is manually set to operator preferences which they consider ”safe”, the reported MCR limit for initiating a new DG is reported to be 65% MCR, with a three-second time delay. As such, the DG sequences used by the dynamic model are slightly different than those of the preliminary analysis of section 4.2. Resulting fuel savings will not be significantly affected due to this change, as such limits are rarely reached during load transients.
The resulting different DG load profiles are depicted in sections F.1.2 and F.2.2 of Appendix F, for both load cases and all tested load allocation strategies.

With this method, the PMS algorithm determines the individual DG powers based on the improved DG load allocation strategy used. The method used for converting individual DG powers to fuel consumption values is described in section 4.1 of Chapter 4. Using integrator blocks within the Simulink model, the total amount of fuel is determined for 24 hours of a DP operation.

6

Results & analysis

Chapter 6 will present the results of the model described in Chapter 5. The validation and verification steps that have been undertaken are given in section 6.1. The results of the dynamic model are analysed in section 6.2.

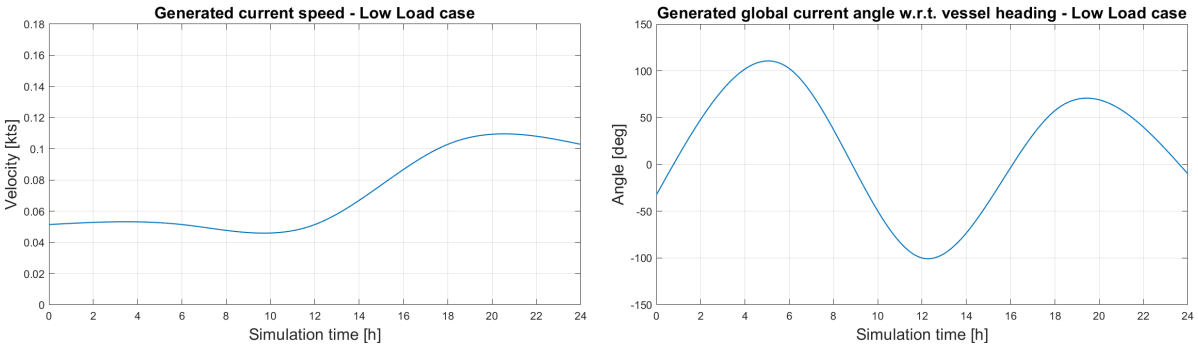
6.1. Validation & verification

Throughout the development of the model, several validation and verification steps have been conducted to ensure the credibility of the dynamic model. All graphs and figures on vessel behaviour, environmental forces or conditions are presented in Appendix F.

6.1.1. Environmental conditions

The randomised environmental conditions are presented in section E.1 of Appendix E.
The correctness of these environmental input conditions could not be validated with Boskalis data due to the limited reporting frequency. As such, the environmental conditions are, to some extent, verified using literature. All environmental conditions have been implemented through time-based lookup tables. Simulink's option for cubic spline interpolation is used to ensure a relatively smooth signal to prevent unrealistic transients.

According to J.M.J. Journée (2008), current conditions can be considered a steady phenomenon and are therefore not further verified using literature. As an example, Figure 6.1 illustrates the current conditions for the low-load case.

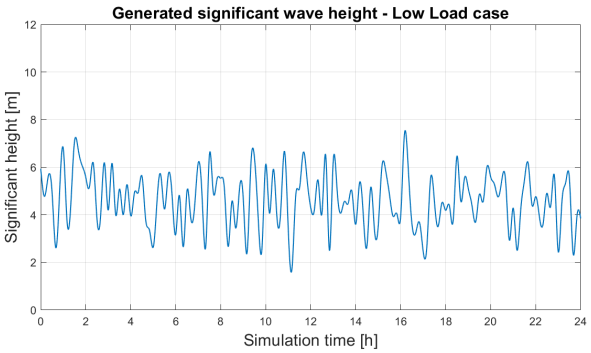


(a) Current speed conditions of the low load case

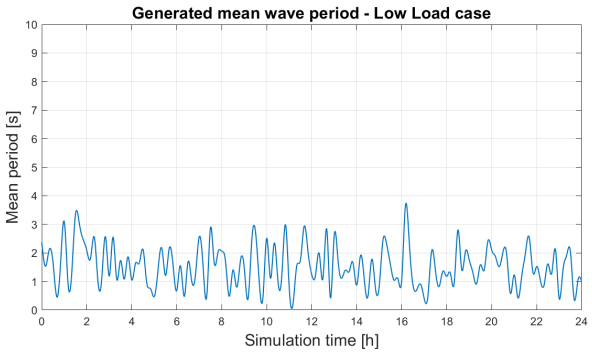
(b) Current angle of attack of the low load case

Figure 6.1: Current conditions of the low load case

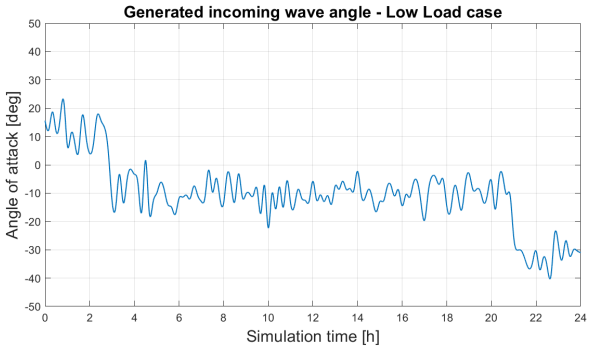
Wind and wave conditions are instead updated every ten minutes to represent their erratic nature. The shape of the wave period and wave height graphs are identical, as these are directly related to one another due to the use of the Brettschneider formulation of equation 5.5. An example of the wave conditions for the low load case is illustrated in Figure 6.2. Compared to the source material of Caires et al. (2019) and J.M.J. Journée (2008), the randomised wave conditions are considered acceptable.



(a) Wave height conditions of the low load case



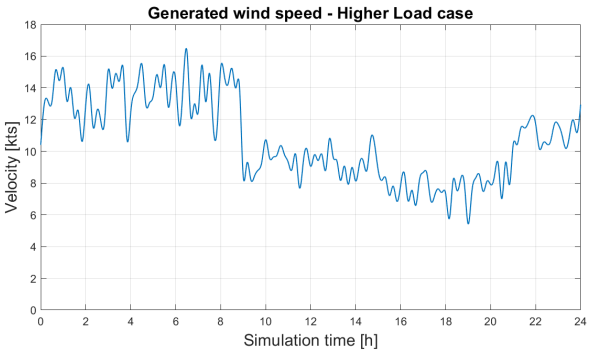
(b) Wave period conditions of the low load case



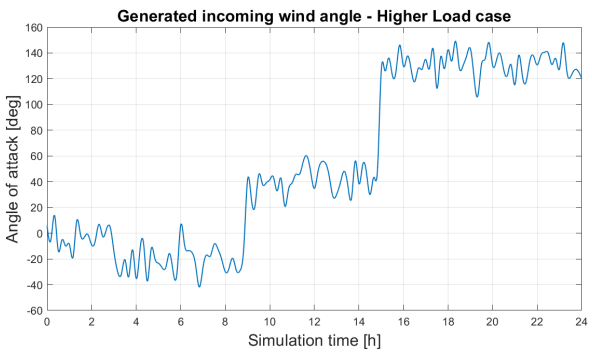
(c) Wave angle of attack of the low load case

Figure 6.2: Wave conditions of the low load case

The modelled wind conditions are depicted in Figure 6.3 for the higher load case. Changes in wind direction and speeds might seem very significant between time intervals. However, as these have little influence on overall vessel performance, such changes are accepted. Using the material provided by Caires et al. (2019) or Burton et al. (2011), the characteristics of the randomised wind conditions were also verified using literature.



(a) Wind speed conditions of the higher load case

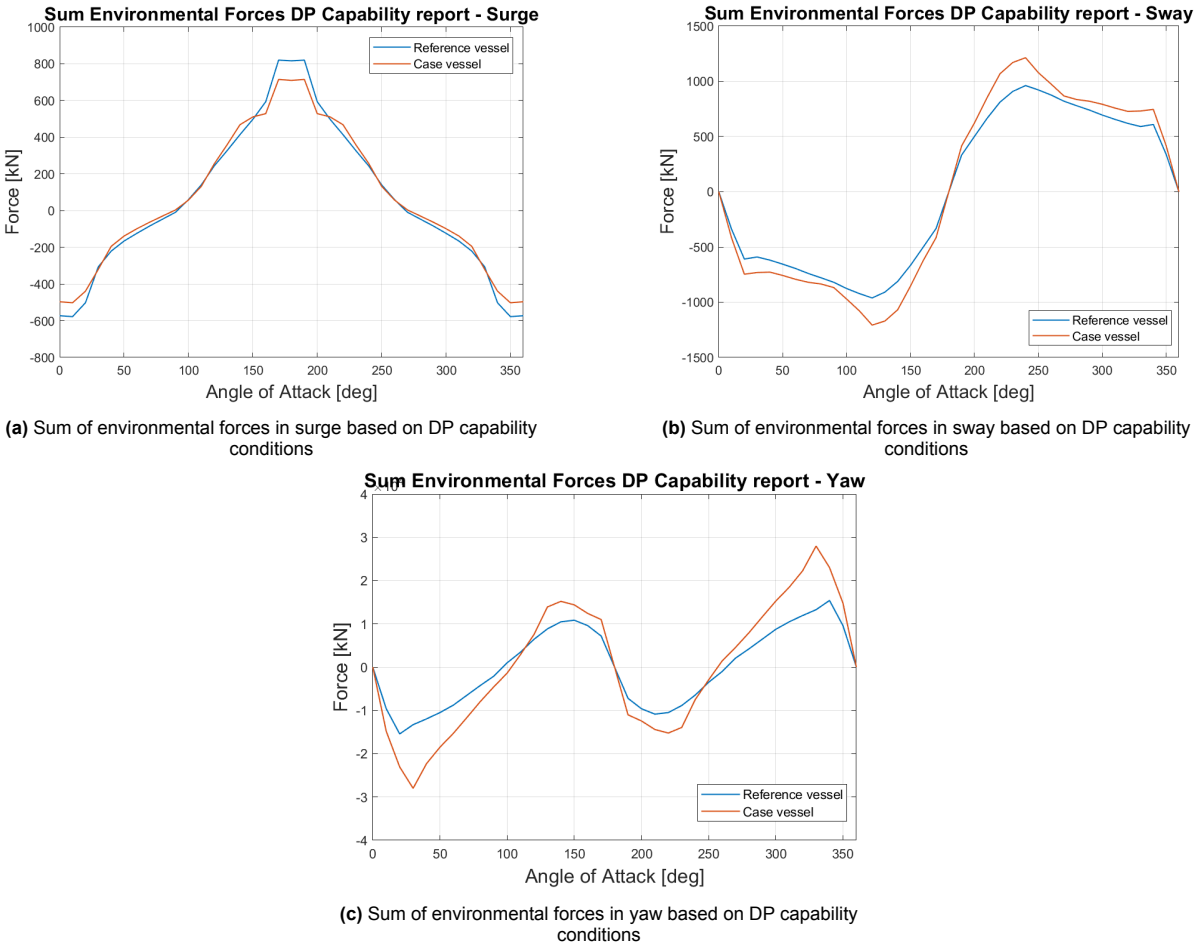


(b) Wind angle of attack of the higher load case

Figure 6.3: Wind conditions of the higher load case

6.1.2. Environmental forces

The environmental forces are computed using the randomised environmental conditions and the coefficients scaled from a reference vessel. For the latter, the characteristics of the environmental coefficients have been verified using Fossen (2011).
Calculations regarding the environmental forces have been verified with the DP capability reports of the case vessels. For this, equal environmental conditions were used as input. A comparison between these results is depicted in Figure 6.4.



(a) Sum of environmental forces in surge based on DP capability conditions

(b) Sum of environmental forces in sway based on DP capability conditions

(c) Sum of environmental forces in yaw based on DP capability conditions

Figure 6.4: Comparison between calculated and reported environmental forces

Only a small fraction of the overall forces presented in Figure 6.4 consist of current forces. Wind and wave conditions exert a similar amount of force in the DP capability analysis.
The results show that the environmental forces exerted on the vessel are well represented by the environmental subsystem of the model, as shape characteristics are alike. Differences between absolute values can be substantiated through the different vessel dimensions. As the reference vessel has a smaller length, sway forces and yaw moments are likely smaller. Surge forces for the reference vessel are, however, a bit larger, given the slightly smaller draft of the case vessel.
All environmental forces are presented in section F.1.1 and F.2.1 of Appendix F for both load cases. Analysing these shows that the wave forces, especially the resulting moment in yaw, are quite significant compared to the other environmental forces. In hindsight, this is because the reported wave height values were assumed to be significant wave height. Although results do not appear to be far off from reality, especially given the resulting vessel dynamics, thruster powers and fuel consumption, it is considered important to point out this potential small error.

6.1.3. Thrust allocation controller

Further verification is done by using the reported input values of the DP capability analysis report of the case vessel and comparing the resulting thruster forces and directions. As such, the environmental subsystem, vessel subsystem, controller subsystem and thruster subsystem can be verified. Most importantly, this is done to check the resulting value from the TA controller, which is illustrated in Figure 6.5.

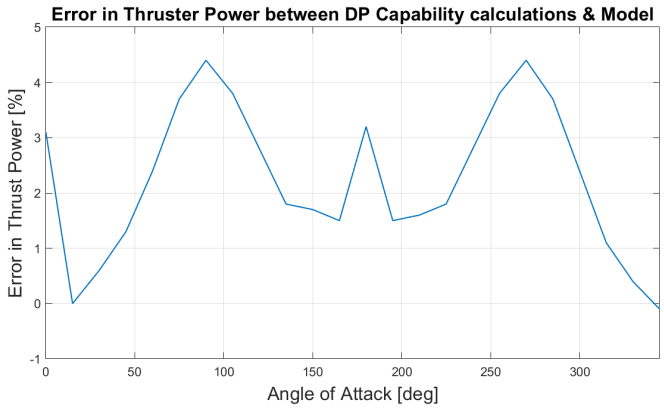


Figure 6.5: Verification TA controller, error in thruster power

The main error of the TA controller is that the amount of thrust required from azimuth 3 is often overestimated and much higher than for the DP capability analysis. It appears that azimuth 3 is treated similarly to the stern azimuths, while its power capacity is lower by a factor of two. Although attempts have been made to fix this error by adjusting the weight matrices, as elaborated in equation 5.27, an error in the input model prevented this from working accordingly.

Ultimately, this error is accepted as the difference in the total amount of required thrust is still within acceptable margins. Thrust is generated a bit less efficiently, resulting in slightly higher powers. The highest absolute error is 229 kW, which is a relative increase of 4% and, therefore, considered negligible. The defined forbidden angles could also cause such differences as the actual values are unknown. Nevertheless, as the loads for the DP capability analysis are much higher than for the selected case conditions, deviations and errors are likely lower for the dynamic model.

6.1.4. Load profile & fuel consumption

The resulting load profiles of the selected case conditions are presented in Figures 6.6 and 6.7. The average operational power and MCR of the DGs are also depicted within these figures, similar to Figure 1.2 of section 1.1.

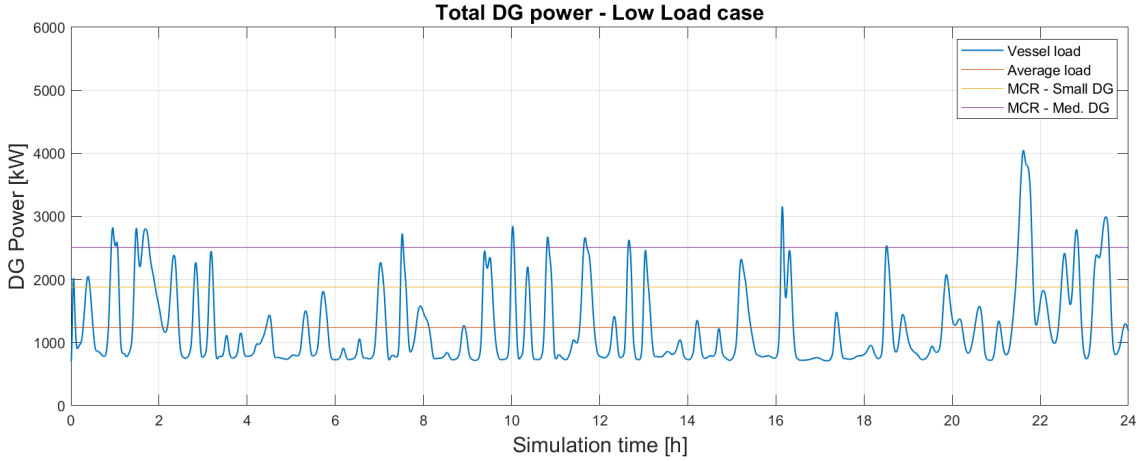


Figure 6.6: Total DG load profile of the low load case

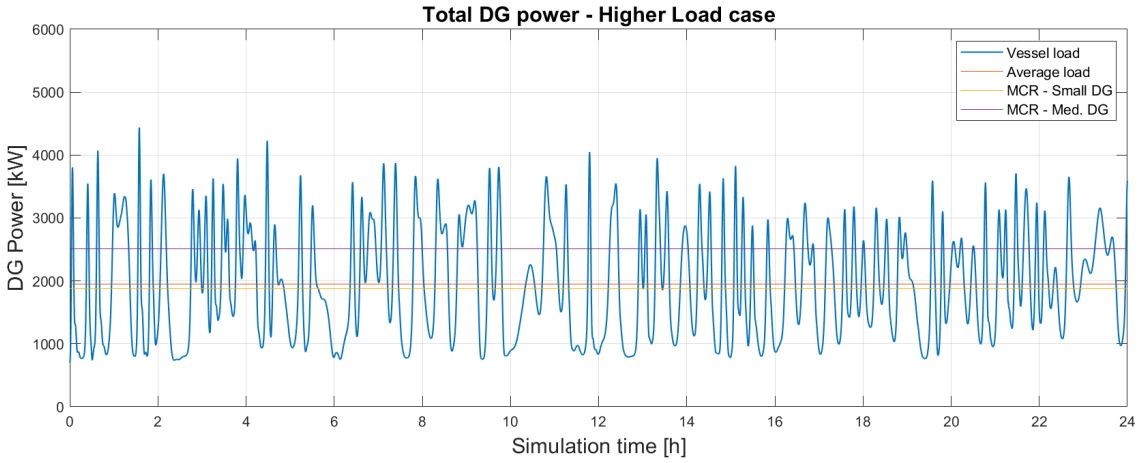


Figure 6.7: Total DG load profile of the higher load case

From both figures, it is clear that the DGs are continuously operated at extremely low loads, which are below the average given the occasional load transients. As discussed, such load transients are likely to affect the actual fuel savings. It is expected that the fuel savings will be relatively higher for the low-load case, given the results of the preliminary analysis in Chapter 4 and the more frequent and severe load transients of the higher-load case.
The MCR powers of the DGs depicted in Figures 6.6 and 6.7 visualise how inefficient DP power systems are actually loaded compared to their maximum. Ultimately, the load profiles resulting from the dynamic profile are considered to represent realistic load profiles, considering source material of other research, such as from Lyu (2016) as presented in figure 1.2.

The fuel consumption calculated by the dynamic model for the higher load case comes close to the reported values with a difference of 25 kW in power and 0.09 % in total fuel consumption. Although average power differences are marginal, the power distribution across switchboards is slightly different, with average differences of 3% in total power. This difference is likely caused by not considering the battery pack of the case study vessel or a difference in assumed auxiliary powers.

Calculations for the low load case deviate more significantly, with an error of 170kW less for the average power and 12% less for the total fuel consumption. This difference is likely caused by the environmental conditions simulated due to, for example, a lower amount of occurring power transients. However, also less beneficial DG conditions could have occurred during the actual DP operation, resulting in a higher sfc. Such deviations from reality will, however, not affect the relative fuel savings between load allocation strategies, as all of these results will contain the same error. The neglected battery pack of the case study vessel likely does not cause this difference, as it would cause power and fuel consumption results to be overestimated.
Also, as pointed out in section 4.1, internal research from Boskalis clarified that there could be significant differences between reported sfc values from manufacturers compared to actual measured sfc values. Results will, therefore, focus on relative fuel savings with respect to the benchmark conditions rather than absolute overall savings.

6.2. Dynamic model results

Throughout section 6.2, the results of the dynamic model are analysed. First, a general analysis is executed in section 6.2.1. In section 6.2.2, results between the first leading DG settings are analysed. Section 6.2.3 will subsequently compare the results between maximum DG limit settings. Section 6.2.4 will elaborate on the results of open bus strategies against closed bus strategies. Chapter 7 will subsequently provide a discussion on the results and the overall research methodology.

6.2.1. General analysis

Tables 6.1 and 6.2 present the fuel consumption results of load allocation strategies and their respective savings w.r.t. the benchmark strategy. Results of six hour time intervals are given, as well as total fuel consumption results.

Time interval	**0h-6h**		**6h-12h**		**12h-18h**		**18h-24h**		**Total**	
Fuel cons. & Savings	[ton]	[%]	[ton]	[%]	[ton]	[%]	[ton]	[%]	[ton]	[%]
1. Benchmark - Open	1.88	…	1.75	…	1.56	…	2.10	…	7.28	…
1.1 Open, 5-60%, S>M	1.77	-5.6	1.66	-5.0	1.49	-4.1	1.98	-5.8	6.91	-5.2
1.2 Open, 5-60%, M>S	1.79	-4.5	1.68	-4.1	1.50	-3.4	2.00	-4.6	6.98	-4.2
1.3 Open, 5-70/75%, S>M	1.77	-5.9	1.66	-5.3	1.49	-4.2	2.0	-6.1	6.89	-5.5
1.4 Open, 5-70/75%, M>S	1.79	-4.5	1.68	-4.2	1.50	-3.5	2.00	-4.7	6.97	-4.3
2. Benchmark - Closed	1.82	-3.1	1.70	-3.0	1.52	-2.6	2.03	-3.5	7.06	-3.1
2.1 Closed, 5-60%, S>M	1.67	-11.3	1.56	-10.9	1.40	-10.3	1.87	-11.2	6.49	-11.0
2.2 Closed, 5-60%, M>S	1.70	-9.3	1.60	-8.6	1.44	-7.7	1.90	-9.5	6.64	-8.9
2.3 Closed, 5-70/75%, S>M	1.66	-11.8	1.56	-11.1	1.39	-10.5	1.86	-11.6	6.46	-11.3
2.4 Closed, 5-70/75%, M>S	1.70	-9.6	1.59	-8.9	1.43	-8.0	1.90	-9.8	6.62	-9.2

Table 6.1: Fuel consumption and respective savings for given time intervals for the low load case

Time interval	**0h-6h**		**6h-12h**		**12h-18h**		**18h-24h**		**Total**	
Fuel cons. & Savings	[ton]	[%]	[ton]	[%]	[ton]	[%]	[ton]	[%]	[ton]	[%]
1. Benchmark - Open	2.62	…	2.71	…	2.58	…	2.78	…	10.69	…
1.1 Open, 5-60%, S>M	2.45	-4.7	2.59	-4.6	2.46	-4.9	2.62	-5.7	10.16	-5.0
1.2 Open, 5-60%, M>S	2.53	-3.4	2.62	-3.5	2.49	-3.8	2.66	-4.3	10.29	-3.7
1.3 Open, 5-70/75%, S>M	2.49	-4.9	2.58	-4.8	2.45	-5.3	2.61	-6.0	10.13	-5.2
1.4 Open, 5-70/75%, M>S	2.52	-3.9	2.60	-4.1	2.47	-4.3	2.65	-4.6	10.24	-4.2
2. Benchmark - Closed	2.53	-3.4	2.61	-3.7	2.49	-3.6	2.67	-3.9	10.30	-3.7
2.1 Closed, 5-60%, S>M	2.40	-8.3	2.49	-8.1	2.35	-8.9	2.52	-9.4	9.76	-8.7
2.2 Closed, 5-60%, M>S	2.42	-7.6	2.51	-7.5	2.37	-8.2	2.54	-8.7	9.84	-8.0
2.3 Closed, 5-70/75%, S>M	2.39	-8.8	2.48	-8.6	2.34	-9.6	2.50	-10.0	9.67	-9.3
2.4 Closed, 5-70/75%, M>S	2.40	-8.3	2.49	-8.2	2.36	-8.8	2.52	-9.4	9.76	-8.7

Table 6.2: Fuel consumption and respective savings for given time intervals for the higher load case

The results of Tables 6.1 and 6.2 show that all improved DG load allocation strategies provide fuel savings for both case conditions. Apart from the closed bus benchmark sequence, all improved loading strategies provide higher fuel savings for low-load conditions. This is expected, given that fuel savings are mainly significant for low loads, around 10 to 20% of total vessel power.
Oppositely, fuel savings reached by the closed bus benchmark condition become more significant for higher powers, which is also depicted by the results.

Strategies 2.1 and 2.3 appear to perform best better for lower operational loads, given the relative difference in fuel savings compared to other loading strategies. As can be substantiated by the preliminary results, these strategies also provide the most significant savings at extremely low loads of 5% to 10% total vessel power.

The analyses provided in the upcoming sections will not contain all graphs generated by the dynamic model, given the large quantity. Furthermore, only graphs depicting results for four-hour time intervals are presented and analysed, given the long run-time of the dynamic model and for better visualisation purposes. The load profiles of these intervals are depicted in Figures 6.8 and 6.9 for both case conditions. Still, all results, for both the time intervals as the total 24 hours, are depicted in sections F.1.3 and F.2.3 for Appendix F. Further note that the DG load profiles of each DG loading strategy are depicted in sections F.1.2 and F.2.2.

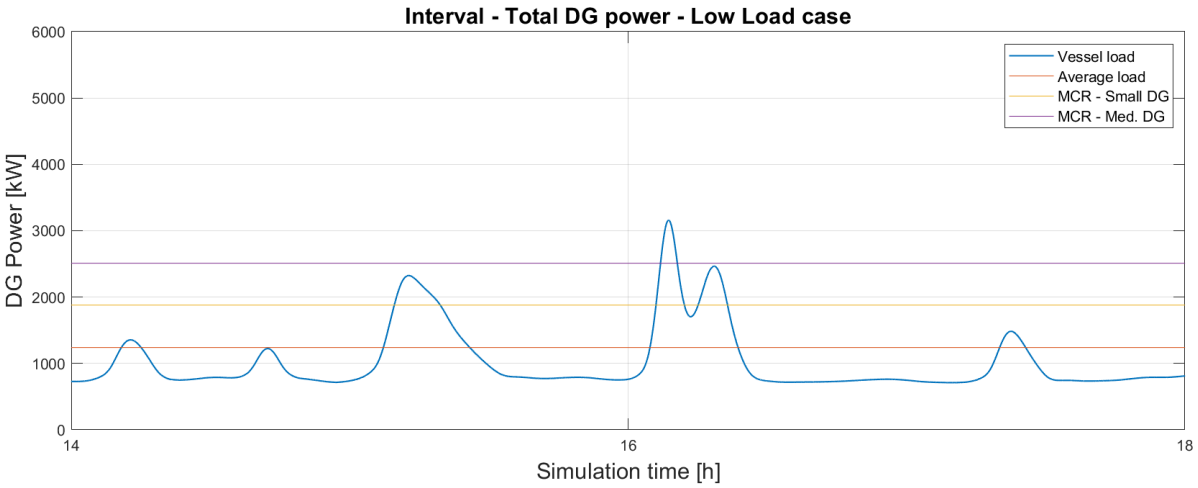


Figure 6.8: Total DG load profile of the low load case for a 4-hour interval

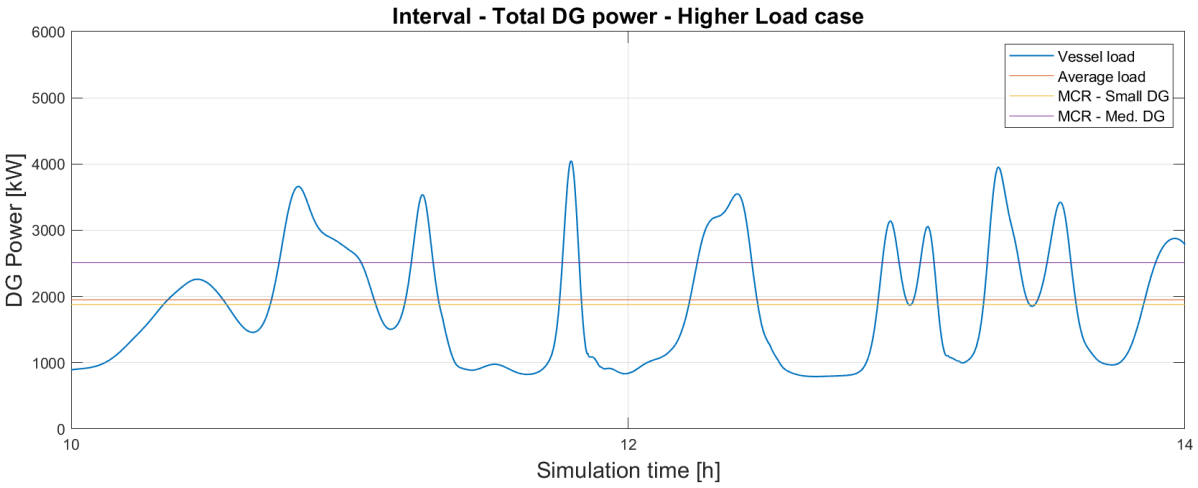
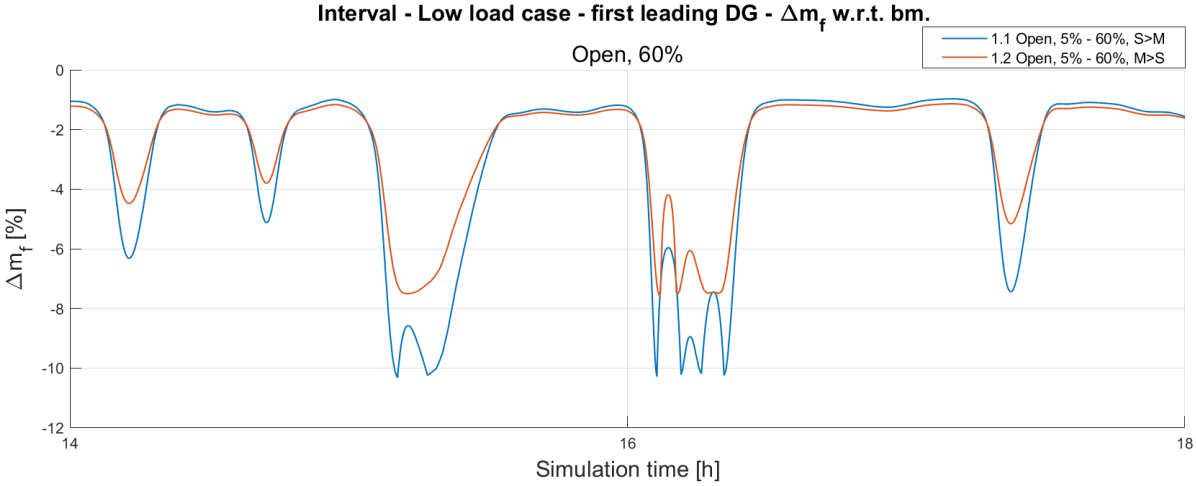


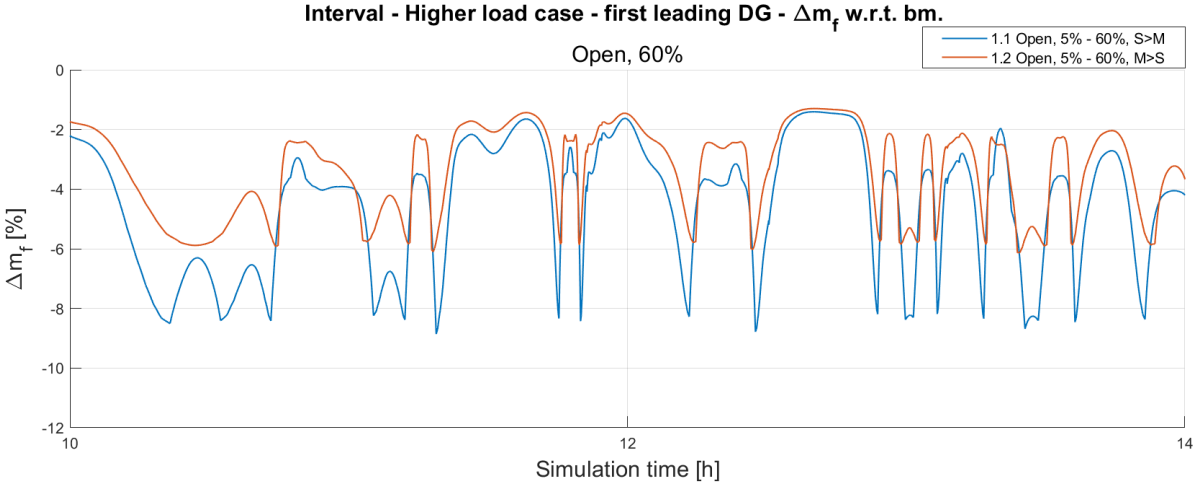
Figure 6.9: Total DG load profile of the higher load case for a 4-hour interval

6.2.2. First leading diesel generator analysis

Figure 6.10 can be used to analyse the difference between small DG sequences and medium DG sequences, showing the fuel mass flow savings of two DG load allocation strategies for both case conditions.



(a) Comparison fuel mass flow of 1.1 against 1.2 - low load case interval



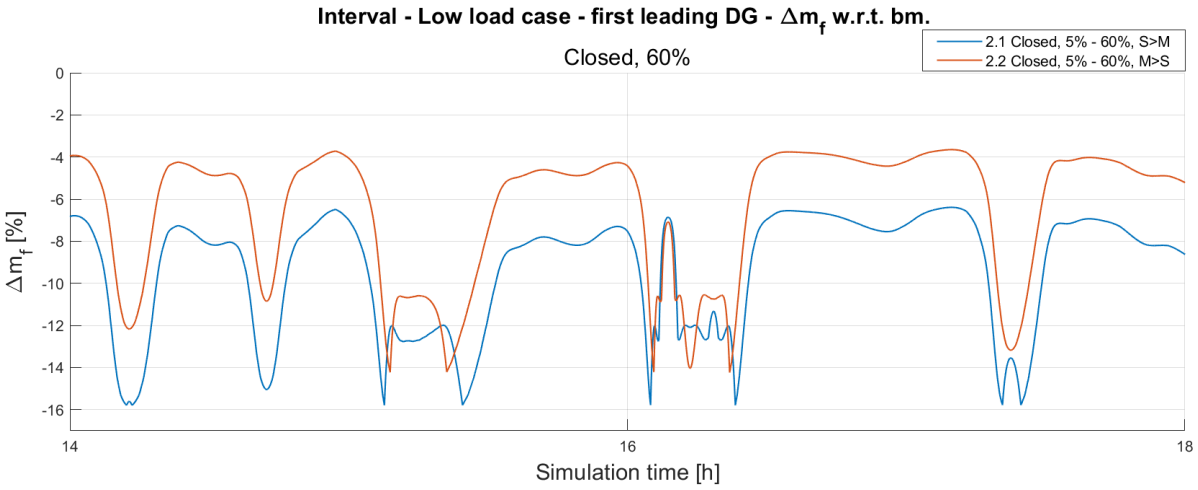
(b) Comparison fuel mass flow of 1.1 against 1.2 - higher load case interval

Figure 6.10: Comparison fuel mass flow of open, 60% limit strategies

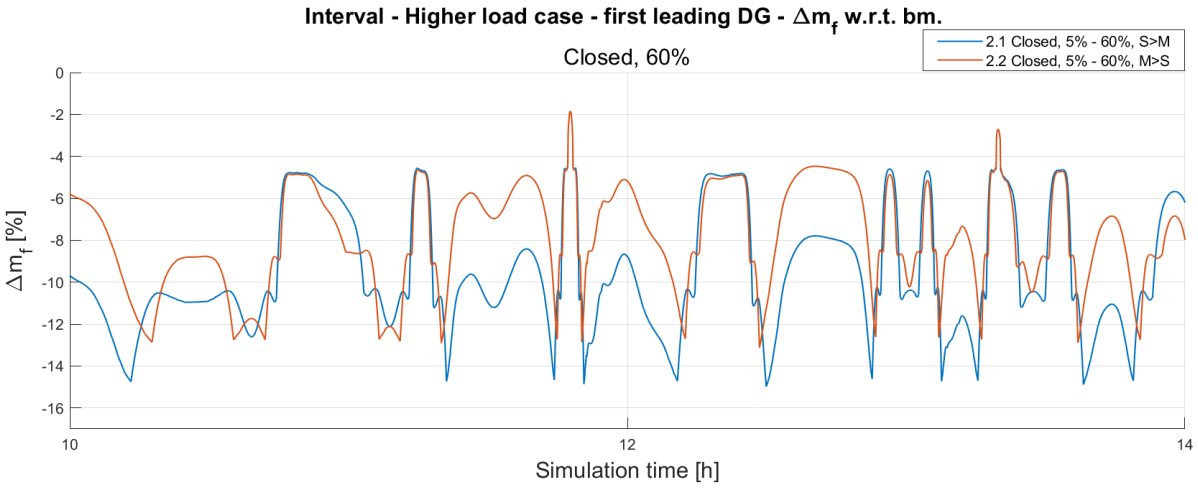
Considering Tables 6.1 and 6.2, small DG sequences provide better overall fuel savings than medium DG sequences. As discussed, this is because the smaller DGs operate more efficiently at lower loads as they are able to operate closer to their optimum sfc compared to the medium-sized DGs. This is not just because of the lower maximum power but also because the optimum sfc for small-sized DGs is at 70% MCR compared to 75% MCR for medium-sized DGs.

Interestingly, as can be seen in Figure 6.10a, the medium DG sequences provide better fuel savings at the absolute minimum loads. Differences are nevertheless around 0.1% in hourly fuel savings with respect to the benchmark condition. These are, therefore, diminishable compared to the rest of the operational profile and could also be caused by errors in the estimation of the sfc of the DGs.
There are also other specific power levels at which medium DG sequences perform slightly better, as limits of small DG sequences are reached more quickly. These instances can be seen in Subfigures 6.10b or 6.11b. Still, these overlaps are also very power-specific and negligible.

As a result, small DG sequences also perform better at higher operational loads, and relative differences go up to 3% in higher fuel flow savings for open bus-tie configurations, which is much more substantial than the instances where medium DG sequences are more advantageous. This matches the analysis of the preliminary results. These also showed that the advantage for small DG sequences is less for closed bus-tie configurations, which are depicted in Figure 6.11.



(a) Comparison fuel mass flow of 2.1 against 2.2 - low load case interval



(b) Comparison fuel mass flow of 2.1 against 2.2 - higher load case interval

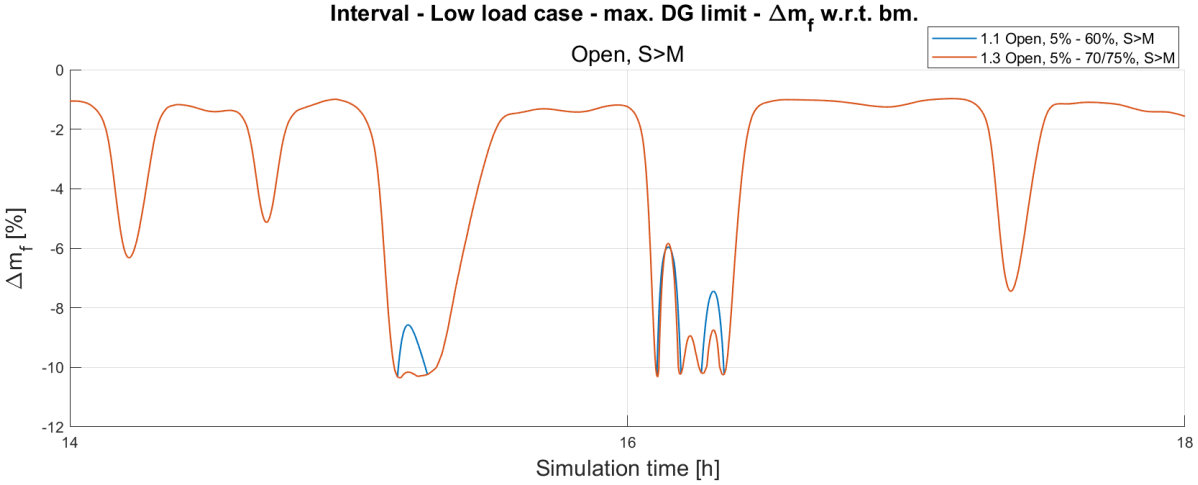
Figure 6.11: Comparison fuel mass flow of closed, 60% limit strategies

As can be gathered from the results depicted in Figure 6.11b, small DG sequences with closed bus configurations appear to be relatively less advantageous for higher operational powers. As fewer DGs are operated for closed bus configurations, the increased slack of medium DG sequences becomes more noticeable. As a result, the overlaps at which medium DG sequences are more advantageous increase and differences occasionally can go up to 2% in higher savings.

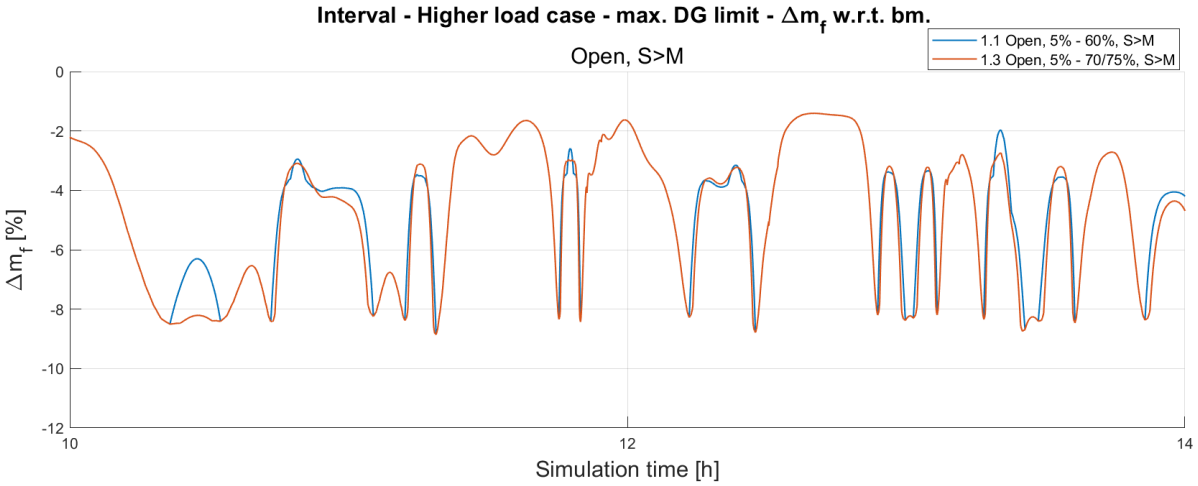
For lower operational powers, however, the opposite is true. Relative differences DG sequences become twice as high compared to open bus configurations. Such can be seen in Figure 6.11, especially between the 16h-18h interval. Differences between both sequences are generally higher for lower loads and are typically around 3%. Also, here, for some load transients, the small DG sequences still perform better despite the event where a second leading DG is initiated. This again shows that regardless of the overlaps where medium DG sequences are better, the load range and savings are more substantial for small DG sequences.

6.2.3. Maximum diesel generator limit analysis

Differences between 60%-sequences and 70/75%-sequences fuel mass flow results are presented in Figure 6.12 for both case conditions. Again, note that all other graphs, both for fuel mass flows and for the specific power consumption, are listed in sections F.1 and F.2 of Appendix F.



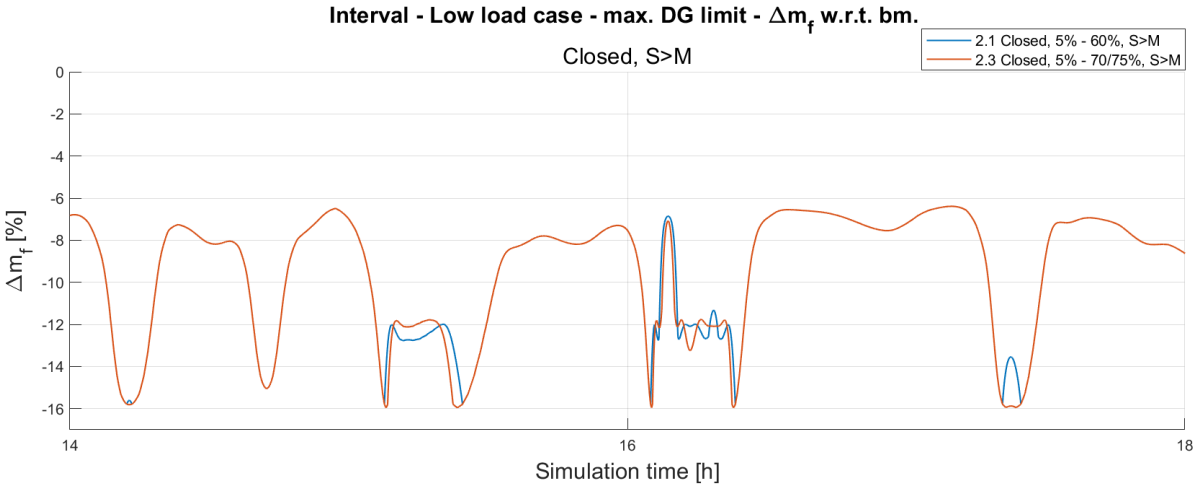
(a) Comparison fuel mass flow of 1.1 against 1.3 - low load case interval



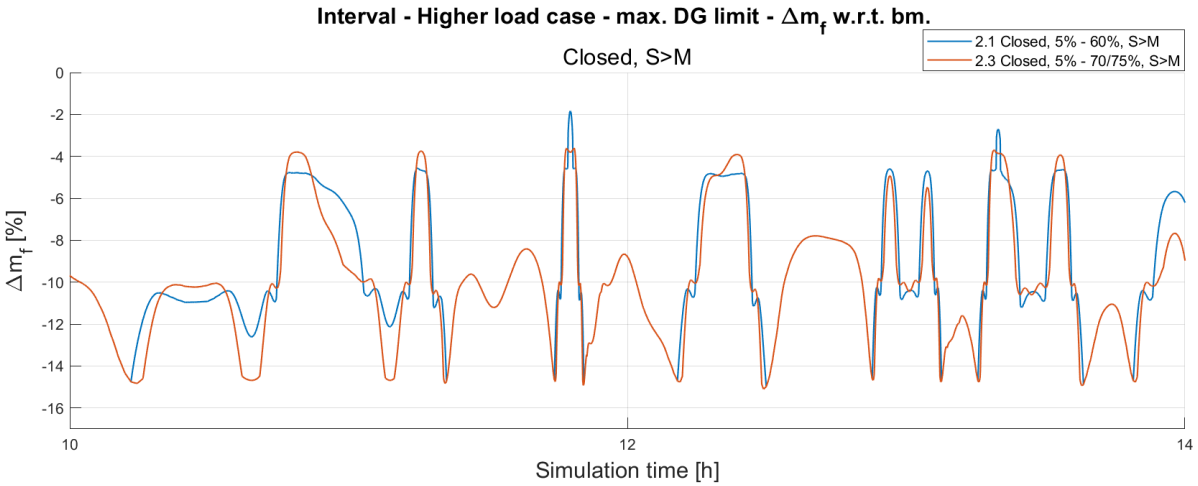
(b) Comparison fuel mass flow of 1.1 against 1.3 - higher load case interval

Figure 6.12: Comparison fuel mass flow of open, small DG sequence strategies

As discussed, the main difference between the 60%-sequences and the 70/75%-sequences is noticeable at higher powers where DG limits are reached. Subfigure 6.12a clearly demonstrates this as it shows that the fuel mass flow savings are identical, except for three instances during which a load transient occurs.
Such is also the case for the closed bus-tie configurations depicted in Figure 6.13. However, for such configurations load, transients have a more significant effect due to the lower amount of DGs, causing DGs to reach their limits sooner.



(a) Comparison fuel mass flow of 2.1 against 2.3 - low load case interval



(b) Comparison fuel mass flow of 2.1 against 2.3 - higher load case interval

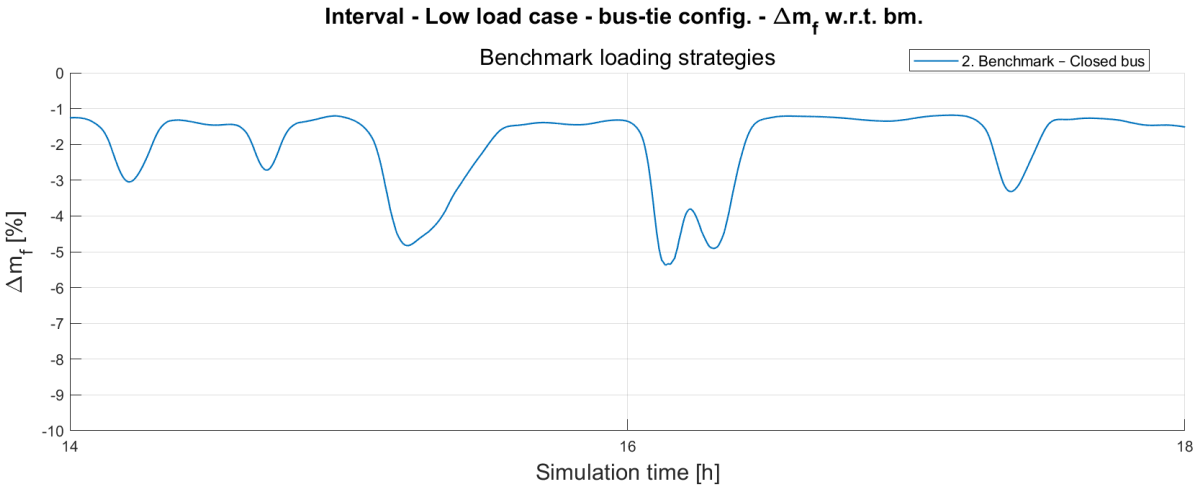
Figure 6.13: Comparison fuel mass flow of closed, small DG sequence strategies

As expected, 70/75%-sequences generally perform better during lower load transients, reaching differences of 2% to 3% in higher hourly fuel savings. This is not just because limits are reached later on for higher operational powers but also because DGs are able to operate at their most optimal sfc, which is, for example, demonstrated by Subfigure 6.13b.
However, at some particular power levels, the 60%-sequences are more beneficial during load transients. Such is especially apparent for the higher load condition Subfigures of 6.12b and 6.13b. These appear to be local optima where the load combination is coincidentally better for the 60%-sequences. Still, this is only at specific power levels with differences that are not over 1% in fuel savings.

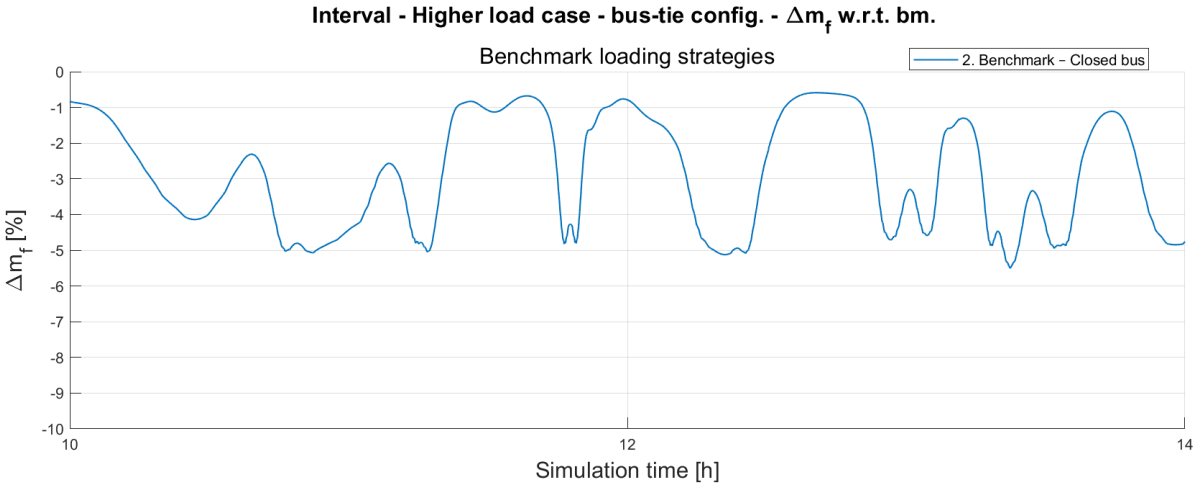
In the end, closed bus-ties configurations seem to benefit more from the higher and optimal DG limits due to the lower amount of DGs operated. Limits of a leading DG are therefore reached more quickly, resulting in a leveraging effect with higher fuel savings. Such can also be concluded from the relative fuel differences between maximum DG limit settings in Tables 6.1 and 6.2, which is especially apparent for the higher load case.

6.2.4. Open & Closed bus-tie configurations

As elaborated during the preliminary analysis of section 4.2, a combination of closed bus configurations with improved DG load allocation settings is expected to deliver high fuel savings when compared to other load allocation strategies. Figure 6.14 depicts the fuel savings of the benchmark strategy with a closed bus.



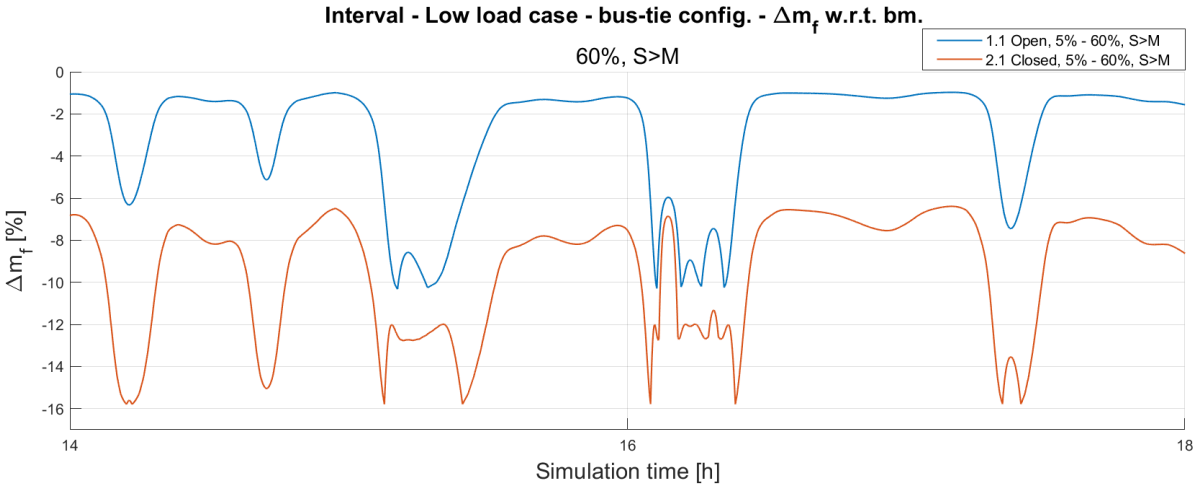
(a) Comparison fuel mass flow of 1. against 2 - low load case interval



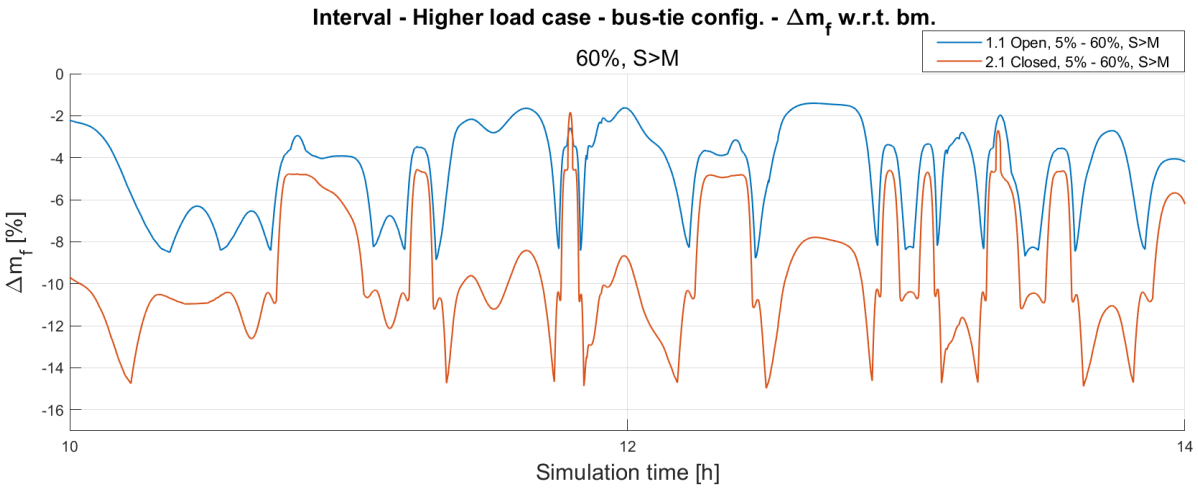
(b) Comparison fuel mass flow of 1. against 2. - higher load case interval

Figure 6.14: Comparison fuel mass flow of benchmark strategies

As discussed in the preliminary results of section 4, the closed bus configuration of the benchmark strategy showed higher fuel savings at higher operational powers. A similar trend can be seen in Figure 6.14 as fuel savings increase during load transients. For lower average powers, hourly fuel savings are around 1 to 1.5%, and during load transients, these increase up to 5%.
Compared to other load allocation strategies, the savings reached by solely closed bus configuration are the lowest. This shows the importance of a solution that provides fuel savings at lower average loads. Nevertheless, the closed bus configuration of the benchmark strategy is also the only improved load allocation strategy which provides higher fuel savings for higher operational loads. As such, a leveraging effect is created if combined with the other load allocation strategies, as is depicted in Figure 6.15.



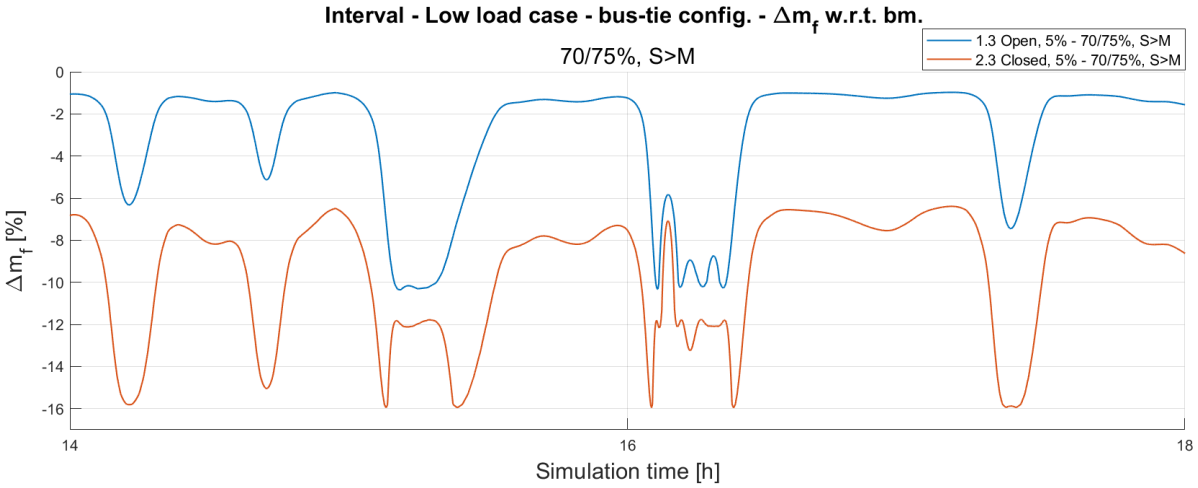
(a) Comparison fuel mass flow of 1.1 against 2.1 - low load case interval



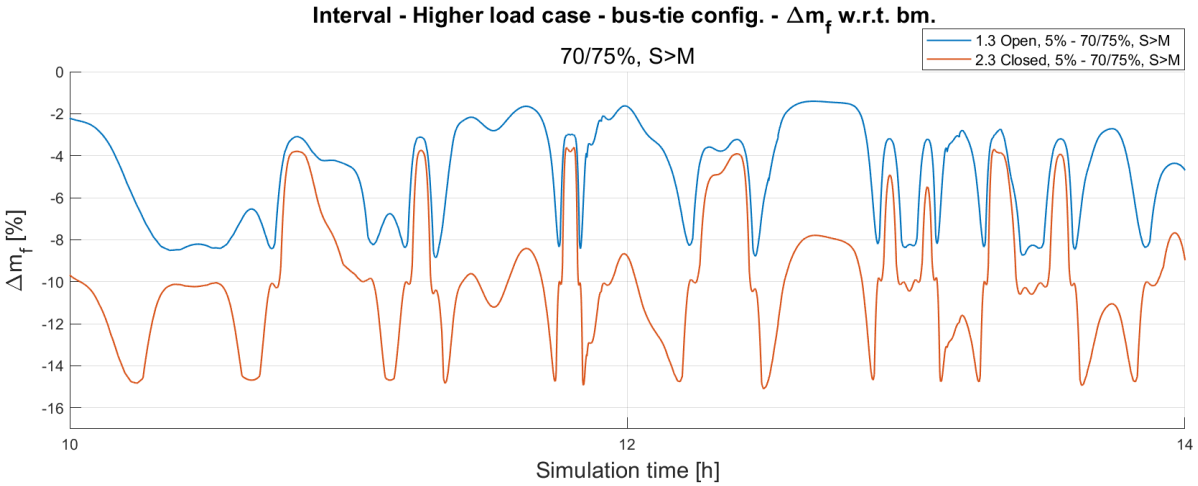
(b) Comparison fuel mass flow of 1.1 against 2.1 - higher load case interval

Figure 6.15: Comparison fuel mass flow of small DG sequence, 60% DG limit strategies

The leveraging effect can be explained by the principle behind unequal DG loading, where the idea is to increase fuel efficiency by having the largest amount of power generated most efficiently. As the number of operated DGs decreases for a closed bus, DGs operate more often at higher powers, near their optimum fuel efficiency. As a result, higher fuel savings are reached, especially for lower powers. For example, in Subfigure 6.15a, fuel savings are especially high compared to their open bus counterparts at lower loads. Only one DG can be operated at 30% and another at 5% for these instances, instead of 2DGs operating at 15%. The result is that differences between open and closed bus configurations easily reach up to 7 to 9% in higher fuel savings. Increased DG limits further increase these differences with 1 to 2 %, as depicted in Figure 6.16.



(a) Comparison fuel mass flow of 1.3 against 2.3 - low load case interval



(b) Comparison fuel mass flow of 1.3 against 2.3 - higher load case interval

Figure 6.16: Comparison fuel mass flow of small DG sequence, 70/75% DG limit strategies

For medium DG sequences, these differences are slightly less at lower powers, given their lower efficiency as discussed in section 6.2.2. Still, significantly higher fuel savings of 6 to 9% are reached compared to their respective open bus counterparts, and their performance is relatively better at higher load transients. Closed bus configurations with medium DG sequences could, therefore, be more efficient for DP operations where frequently high transient loads are expected.
Still, the highest fuel savings are reached with a small DG sequence, a 70/75%-sequence and a closed bus configuration.

7

Discussion & Recommendations

Chapter 7 will provide a discussion on the results and several recommendations for future research. Section 7.1 will first compare the preliminary results with those of the dynamic model, and section 7.2 will present the overall interpretations of the results. Section 7.3 will subsequently compare the used methodology with other state-of-the-art research and substantiate the resulting differences. Lastly, section 7.4 will elaborate on aspects left for future research.

7.1. Comparison preliminary & dynamic results

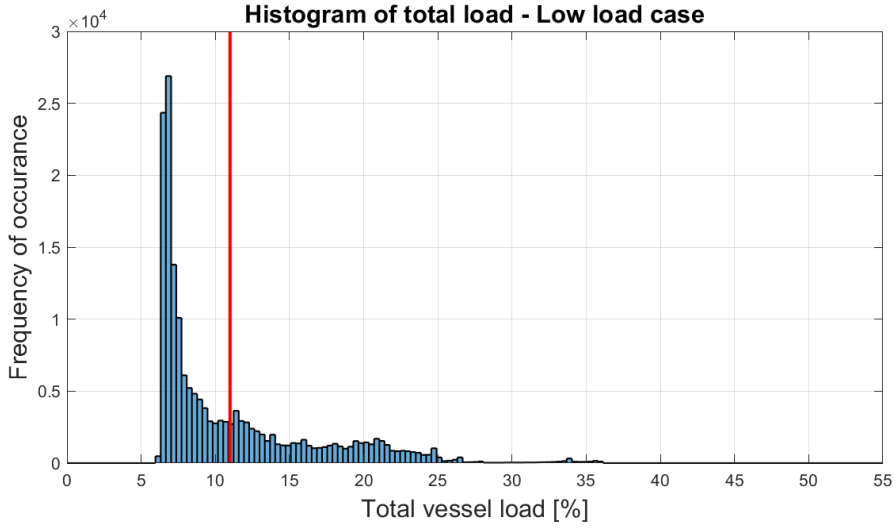
The total fuel savings calculated by the dynamic model can be compared with results determined from the preliminary analysis in Table 7.1. The same method described in section 4.1 is used, and the preliminary results are calculated using the average powers of the created load profiles. As discussed in section 1.2, this method corresponds with the current state-of-the-art as is done in the research of Chauhan et al. (2016) for example. Note that differences are not significant enough given the sfc-curve errors presented in Table 4.1. Claims and conclusions can, therefore, not be fully supported with the errors presented in Table 7.1. Still, differences visible from this comparison will be explained throughout this section.

	Low load case			**High load case**		
	Prelim.	Model	Diff.	Prelim.	Model	Diff.
1.1 Open, 5-60%, S>M	5.0%	5.2%	-0.2%	7.4%	5.0%	2.4%
1.2 Open, 5-60%, M>S	3.4%	4.2%	-0.8%	5.4%	3.7%	1.7%
1.3 Open, 5-70/75%, S>M	5.0%	5.5%	-0.5%	8.2%	5.2%	3.0%
1.4 Open, 5-70/75%, M>S	3.4%	4.3%	-0.9%	5.4%	4.2%	1.2%
2. Benchmark - Closed	1.7%	3.1%	-1.4%	2.7%	3.6%	-0.9%
2.1 Closed, 5-60%, S>M	12.6%	11.0%	1.6%	11.0%	8.7%	2.3%
2.2 Closed, 5-60%, M>S	9.9%	8.9%	1.0%	10.9%	8.0%	2.9%
2.3 Closed, 5-70/75%, S>M	12.9%	11.3%	1.6%	11.2%	9.3%	1.9%
2.4 Closed, 5-70/75%, M>S	9.9%	9.2%	0.7%	11.3%	8.7%	2.6%

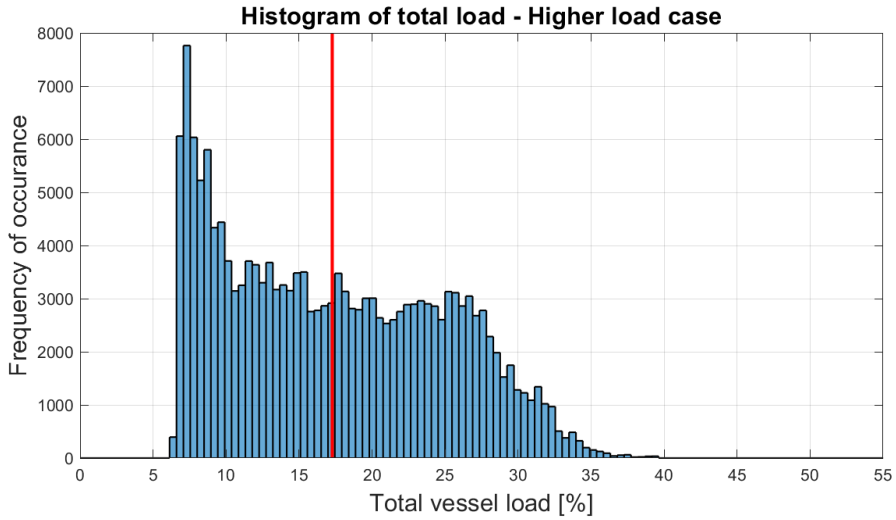
Table 7.1: Fuel consumption savings resulting from the preliminary analysis & the dynamic model

As is visible from the results presented in Table 7.1, the method used for determining the preliminary results, both under and overestimates the fuel savings reached by improved DG load allocation strategies. Such deviations can be explained through fundamental differences between the used inputs. As discussed, the preliminary results are calculated for a total average power whilst the dynamic results are calculated for a load profile created to approximate reality, as presented in Figures 6.6 and 6.7.

The average operational power of a case condition is not necessarily the most frequent power level provided by the vessel's power system. This is depicted in the histograms in Figure 7.1, showing the frequency of occurrence of vessel loads for both load cases. Here, the red line illustrates the average vessel power of these load conditions.



(a) Histogram of total vessel load - low load case



(b) Histogram of total vessel load - higher load case

Figure 7.1: Histograms of total vessel load

Subfigure 7.1a illustrates that the most frequent power level provided by the power system, is well below the overall average with approximately 400 kW. For the high load case, depicted in subfigure 7.1b, this difference is higher with 1000 kW due to the more frequent and higher load transients. Still, the frequency of occurrence of the average power is similar for both load cases.
As a result, the preliminary analysis method overestimates fuel savings provided by the open bus configurations for higher load cases and closed bus configurations for both load cases. For most improved load allocation strategies, fuel savings become relatively less during load transients. As a consequence, the overall fuel savings are negatively impacted. Such is illustrated in Figure 4.3 of section 4.2.2, providing the preliminary total sfc and fuel mass flow results of all improved DG load allocation strategies.
This is similar to the closed bus strategies, however, these are subject to higher load transients. Instead of two DGs, only one DG has to account for load transients, and as such, the effects of load transients appear to be more significant for the results of the medium DG sequences for the higher load case.

On the other hand, the fuel savings of open bus-tie configurations at lower operational powers appear to be slightly underestimated by the preliminary analysis method. Although the vessel's power levels are often below the average for the low load case, deviations also appear to be caused by load transients. Considering the preliminary results depicted in Figure 4.6 of section 4.2.2, the highest fuel savings are reached for total vessel loads between 15% to 20%. Compared to the average, absolute fuel savings differ by 30 kilograms per hour, whilst the absolute fuel savings between the average and most frequent power levels differ by 10 kilograms per hour. As such, due to the low load transients depicted in the low load case, fuel savings are underestimated by the preliminary analysis method. This might seem to be in contrast with the explanations given for the closed bus-tie configurations. However, for the closed bus sequences, the highest fuel savings are reached at relatively lower loads, with the optimum closer to the average load of the lower load case.
Similarly, the preliminary results of the closed bus benchmark strategy also appear to be underestimated, though, for both case conditions. As illustrated in Figure 4.6a, fuel savings provided for this load allocation strategy increase for higher powers. The closed bus benchmark strategy especially benefits from load transients, and therefore, the fuel savings provided by the preliminary results are underestimated.

Although claims made in this section cannot be fully supported given the sfc-curve errors presented in Table 7.1, a clear trend is visible and can be further substantiated. The main conclusion of this section is that load transients have a significant influence on the calculated savings of improved DG load allocation strategies. Fuel savings can both be underestimated and overestimated with current state-of-the-art methods that only use operational averages, as relative fuel savings can be very power-specific for both lower and higher powers. As such, it is worthwhile to consider both the most frequently occurring power levels and the occasional load transients a DP vessel experiences during DP operations.

7.2. Interpretation of results

The results of the dynamic model showed that fuel savings can be achieved by all improved DG load allocation strategies for both case conditions. This was expected given the results presented by the preliminary analysis, in section 4.2, as fuel savings over the whole operational profile were apparent. As discussed in section 7.1, the savings achieved for higher but less frequent powers showed to have a considerable effect on the resulting savings. Combining the improved load allocation strategies with closed bus configurations furthermore showed considerable fuel savings through a leveraging effect. All in all, this also indicates that improving the load allocated to DGs is a good operational solution for reducing fuel consumption of DP operations. Especially as fuel savings are provided for the frequently low operational vessel loads whilst the power system is still able to withstand load transient safely.

The results analysed in section 6.2 showed that small DG sequences provide higher fuel savings than medium DG sequences. Small DG sequences are, therefore, generally advised for DP operations, especially for operating with an open bus configuration. Medium DG sequences could be more beneficial for DP operations where significant load transients are more encountered frequently. However, only closed bus configurations would benefit from this, which is especially uncommon for stormy sea states, given the risks and WCF aspects involved. In that sense, this could be determined through a risk analysis and implemented in a CAM or TAM.

The dynamic results have further shown the effects of increasing the maximum limit of DGs to their respective fuel efficiency optimum. Although fuel savings for lower powers are not affected, especially for closed bus configurations, the fuel savings reached at higher loads benefit from this increase. Although there is less spinning reserve available from the leading, increasing the upper limit of DGs does not necessarily affect safety. Ultimately, the case vessel's operational limit of 60% is based on the current load allocation strategy used by the vessel, which is that all DGs are loaded equally.
To illustrate this, imagine the case vessel is operated with four DGs, all at 40% MCR. As such, 60% of the vessel's total power is left as spinning reserve. The vessel could also be operated with two DGs at 70% MCR and the other two at 10% MCR, also leaving 60% of the vessel's total power as spinning reserve.

In the end, this different method of allocating loads to DGs gives the ability to change the currently used individual DG limits. Instead, documentation could increase DG limits to their respective optimum and provide a different limit that is constrained to the amount of spinning reserve left that is minimally required for accepting the WCF. This would be a necessary step for implementing the provided solution in current industry practices.

Although fuel savings of closed bus configurations have been indicated before by other papers, this research has also shown that its respective savings can significantly be increased through a combination with improved load allocation strategies.
Savings of the closed bus benchmark strategy were arguably less than was in literature. For example, Lindtjørn et al. (2014) presented fuel savings of 9%. However, these are results for a drilling vessel that usually operates on 6 DGs. In this research, operating with a closed bus-tie configuration would reduce this amount to 4 DGs. Realistically, the fuel savings provided in this research for closed bus-ties solely are not far off.

Similar fuel savings can likely be expected for other conventional diesel-electric DP vessels. Although both case study vessels have five DGs, the benchmark strategies still showed that, generally, the vessel uses four DGs, which operate at very low loads. Therefore, similar fuel savings are also expected for other conventional DP vessels with such power systems. As discussed, however, the degree of fuel savings will be highly dependent on the operational profile of the vessel and the sfc characteristics of their engines.

Still, the effect of load transients on the power system is not widely considered throughout this research. A critical yet unexplored practical aspect is how load transients should be compensated without requiring interventions of the PMS through, for example, load shedding. Ultimately, all four DGs would be used for the benchmark strategy to manage load transients. For the improved DG load allocation strategies, this would likely only be one or two DGs if the presented method is used. As a result, load transients managed per DG would be twice to four times as high. In this case, a reasonable solution would be to consider the peak shaving function of the battery pack on board of the case study vessel, which was not considered in this research.
Another motivation for considering load transients is because of their effect on the resulting fuel savings. It can be argued that (higher) load transients will affect the overall fuel consumption as fuel efficiency tends to decrease during those [Veksler et al., 2014, Radan et al., 2008]. As such, it can be argued that the actual fuel savings are lower, although the degree to which this is yet unknown,

Actual fuel savings are likely also affected by considering that the battery packs of the case study vessels are not considered in the dynamic model. The histograms of Figure 7.1, will likely consist of less load transients that are rather managed by the peak shaving function of the ESD. Arguably, relative fuel savings could actually be higher, considering that the highest relative fuel savings are reached at very low DG powers and that the effects of load transients are less for the selected case vessels. Given that, considering the proposed solutions in combination with ESDs is recommended for future research.

Absolute fuel savings could, however, be more significant than indicated, given the internal research from Boskalis on actual sfc values as discussed before in section 4.1. Currently, the depicted absolute savings range from 0.3 to 0.82 ton fuel for the low case and savings from the higher load case range from 0.4 to 1.02 ton fuel, which are daily savings for a 24h DP operation of the considered DSV. Considering a sfc difference of 20 to 30%, absolute fuel differences could actually be higher.

7.3. Comparison to state-of-the-art

Comparing the results to the other research that has investigated similar solutions indicates some differences [Chai, Sobrayen, et al., 2016, Chai, Reddy, et al., 2016, Chauhan et al., 2016, Rao et al., 2015].
A first general difference in the method utilised is that no genetic algorithms have been applied to create the improved DG load allocation strategies and corresponding DG loading sequences. As argued in section 1.2, this is done to keep continuity in DG loading sequences. As such, the captain or DPO could understand and work with these schedules, as they will have to check and interfere manually when limits are exceeded or failures occur.
Secondly, realistic constraints and limits have been applied to the selected problem, such as considering open bus-tie configurations, considering IMO and IMCA guidelines regarding the WCF, or adhering to DG limits that are based on DPRs of actual DP operations.

The resulting fuel savings between this research and others appear to be more positive as there are higher fuel savings in general. Do note that this comparison is somewhat tricky, as other research mainly provides absolute fuel savings and not relative fuel savings. A first argument is that the papers' selected benchmark conditions do not appear to be realistic, given current industry practices. The indicated benchmark condition of, e.g. Chai, Reddy, et al. (2016), argues that at 25% total vessel power, only two DGs are operated at 50%. This operating method is used up to vessel powers of 45%, where both DGs are operated at 90% MCR. As discussed, such a configuration would not be allowed and is in direct violation of the IMO guidelines.
As a result, the benchmark conditions used by this research have an unrealistically low fuel consumption. Relative fuel savings provided by the paper are, therefore, lower than what they actually would be for a realistic benchmark condition.
Another argument is that other research has generally considered vessels with a higher average operational load. As also indicated in the results of this research, the consequent fuel saving will be lower, therefore further substantiating differences with other research on this topic.

7.4. Recommendations

Several aspects of this research and the dynamic model used can be improved. For example, the dynamic model created for this thesis might be a bit too accurate and complex for the purpose it's used for. However, initial plans for the structure and use of this model were a bit different and more elaborate at the start of this thesis.

In advance, the higher amounts of load transients on the power system were already considered, and plans were made to include transient effects on the power system. Several ideas were drafted, such as modelling increased fuel consumption due to significant load transients by adding sort of "fuel consumption penalties" depending on absolute values. Moreover, transient limits of the power systems could be added by implementing a feedback loop back from the power system to the thruster or vessel system. If such a limit is exceeded for a DG, the maximum amount of power would be reduced to simulate load shedding. The actual thruster force, and perhaps the respective system inertia, would consequently be recalculated and forwarded to the vessel system. However, as very limited research and information was found on this subject, these aspects are further regarded for future work.

Furthermore, the frequency of data reporting for DP operations was much lower than anticipated, especially regarding aspects such as fuel consumption or average DG power. If such data had been reported more frequently, the resulting fuel consumption of the model could have been validated more extensively. Another method that could have been used for more extensive validation of the model would be to perform multiple tests for other 24-hour operations. However, as creating the different randomised environmental conditions and load allocation strategies is time-consuming, this is also left for future research. Also, other ideas for validation, such as real-life tests with an actual DP vessel or with an in-house DP simulator of Boskalis, were considered for investigating human factors. However, these ideas would also be too time-consuming for an MSc Thesis.

The purpose of the model was to create a realistic load profile based on environmental conditions. Ultimately, all load allocation strategies are tested for the same load profiles, and therefore, fuel savings are indicated as relative values instead of absolute, allowing results to be compared and giving the possibility to provide conclusions.

A higher data frequency of the environmental conditions could also improve the correctness of the load profile. Such data was available for the wind conditions and could have been used to create the wave conditions using environmental tables applicable to the North Sea. However, data reported in the DPRs also showed that the intensity and directions of wind and wave conditions are sometimes unrelated. This is, for example, visible for the higher loading case where a change in wind direction does not result in a change in wave direction. Therefore, the choice was made to create a randomised signal based on normal and Rayleigh distributions based on the five reported environmental conditions during the day. Still, future research would benefit from such data as it could be easily implemented in such a model and create a more realistic load profile.

Lastly, the improving DG load allocation strategies can also be applied in addition to other fuel-saving measures, especially ESDs. Although both case study vessels are fitted with one battery pack, these are not taken into account, given the added complexity. However, as load transients appear to affect actual fuel savings, ESDs could reduce the effects and severity of load transients on DGs. Besides, batteries would also create the possibility of adding other types of energy sources to the grid, such as fuel cells. As such, it would be worthwhile to consider the fuel savings results and effects of combining improving DG load allocation strategies with ESDs.

8

Conclusion

The main objective of this MSc Thesis is to investigate methods for reducing greenhouse gas emissions from the Dynamic Positioning (DP) operations of offshore vessels. A literature study proposed a combination of three solutions, consisting of unequal diesel generator (DG) loading, improved DG start-stop scheduling, and closed bus-tie configurations.
The current research gaps in this area are primarily related to incorporating realistic operational constraints and industry practices. Therefore, the main goal of this report is to determine the fuel savings achieved through improved DG load allocation strategies for a selected case study, considering realistic operational constraints, standard industry practices, and a dynamic load profile approximating reality.

Section 1.4 formulated four sub-research questions and one overall main research question. Chapter 8 will present the answers to these research questions in chronological order.

1. *Which types of Offshore Vessels and Dynamic Positioning operations would benefit from diesel generator load allocation improvements?*

The proposed solution aims to improve the overall fuel consumption by allowing prime movers to operate at different loads. Considering conventional offshore DP vessels, this approach is only relevant to diesel-electric power systems of DP class 2 or higher.
Improved DG load allocation strategies are most suitable for ships with a DP-intensive operational profile, such as cable-laying vessels, heavy lift vessels, construction support vessels, or diving support vessels.
Most significant fuel savings are likely reached for DP operations that are characterised by long station-keeping events, minor current conditions, relatively low external forces and very high redundancy levels that cause fuel inefficiencies. This highly relates to diving support vessels, which is the selected case study vessel type.

2. *What load allocation strategies can be created that are applicable to the selected case study vessel, considering realistic operational practices and constraints?*

The realistic operational constraints concerned are mainly defined by the Activity Specific Operating Guidelines, from which six constraints can be considered for the different loading strategies.
One method is considered for the load distribution method and the number of operated DGs, as these are the most optimal that adhere to redundancy guidelines. One minimum DG load limit is chosen as a compromise between fuel efficiency, system reliability, and modelling errors. Two settings are selected for maximum DG load limits, the first leading DG sizes and types of bus-tie configurations.
As a result, this report provides ten different loading strategies for the selected case study vessel. Ultimately, this amount depends on the case study vessel's power characteristics, such as different DG sizes, and depends on the set research objectives.

3. *Based on a preliminary analysis with constant loads, what are the hourly fuel savings for improved DG load allocation strategies, and at which vessel load demands are these most significant?*

Initial analysis shows that DG sequences, which start with smaller-sized DGs, provide higher fuel savings for low powers near the operational average. Only these are selected for the preliminary analysis, which indicates that all improved DG load allocation strategies provide fuel savings across the operational profile of the case vessel. Savings are most significant at low operational powers of 10 to 20% total vessel load, but also occur for load transients of 40 to 50%.
Sequences starting with small DGs provide higher fuel savings of 5.0 and 7.4%, compared to the 3.4 and 5.4% savings of medium DG sequences, respectively, for the low and higher load cases. The advantages of increased DG limits at the sfc optimum appear if DG limits are reached, which is only for the higher load case of the small DG sequences, increasing hourly fuel savings to 8.2%. Combining the improved loading strategies with closed bus-tie configurations yields significantly higher fuel savings, with the highest at 12.9% from the small DG sequence with a sfc optimum DG limit and a closed bus for the low load cases.

4. *What are the real fuel savings of improved DG load allocation strategies for a dynamic load profile representing a Dynamic Positioning operation, compared to current research?*

The average operational power used for the preliminary analysis does not accurately represent the main characteristics of an actual DP load profile, such as the occasional load transients. Consequently, the preliminary analysis overestimates the savings of open bus configurations for higher load cases and closed bus configurations for both load cases. For these loading strategies, fuel savings are relatively low during load transients, and as such, total fuel savings should actually be less.
The preliminary analysis underestimates the fuel savings of open bus strategies at lower powers, which is also caused by the effects of load transients. For open bus strategies, the highest fuel savings are reached for vessel loads between 15% to 20%, which is higher than the operational average of 11% for the low load case, therefore causing total savings to be underestimated. This is similar to the results of the closed bus benchmark strategy, which provides the highest fuel savings near loads of 37.5%.

What are the real fuel savings due to improved diesel generator load allocation strategies for an Offshore Vessel during Dynamic Positioning operations?

Ultimately, the operational constraints and modelled load transients significantly influence the determined savings and should, therefore, be considered. All improved DG load allocation strategies provided fuel savings for both load cases w.r.t. realistic benchmark conditions.
Regarding open bus strategies, small DG sequences provide higher fuel savings of 5.2% and 5% compared to medium DG sequences with fuel savings of 4.2% to 3.7%, respectively, for the low and higher load cases. Increasing the maximum DG limit to the sfc optimum of a DG provides higher fuel savings if DG limits are frequently approached during operations due to load transients. For the open bus, small DG sequences, total fuel savings slightly increase from 5.2 and 5% to 5.5 and 5.2%, respectively, for the low and higher load cases. Its implementation would require a change in the current operational practices, with a new limit regarding a minimum to the total amount of spinning reserve left.
Fuel savings provided by the closed bus variation of the benchmark strategy provided fuel savings of 3.1 to 3.6%. Combining closed bus configurations with the other defined strategies shows a leveraging effect that approximately doubles the fuel-saving reached by the open bus strategies. From these, the lowest fuel savings are reached by the medium DG sequence with a 60% limit, providing fuel savings of 8.9% and 8%. The highest savings are reached with the small DG sequences with optimum sfc limits, providing total fuel savings of 11.3% and 9.3%.

Similar fuel savings are expected for other conventional diesel-electric DP vessels. However, the extent of fuel savings depends on factors such as the operational profile during DP or the fuel consumption characteristics of the power system. Actual fuel savings could be lower as the effects of load transient have not been widely considered within this research. Nevertheless, significant fuel savings are expected, as methods could be devised to limit this decrease.
Ultimately, fuel savings from improved diesel generator load allocation strategies have been provided for realistic operational constraints, presenting an alternative out-of-the-box solution for reducing fuel consumption of Dynamic Positioning operations from Offshore Vessels.

References

ABS. (2021a). *Cut sheet: Abs dynamic positioning systems*. https://ww2.eagle.org/content/dam/eagle/publications/cutsheets/abs-dynamic-positioning-systems-cutsheet.pdf

ABS. (2021b). Guide for dynamic positioning systems.

Accetta, A., & Pucci, M. (2019). Energy management system in dc micro-grids of smart ships: Main gen-set fuel consumption minimization and fault compensation. *IEEE Transactions on Industry Applications*, *55*, 3097–3113. https://doi.org/10.1109/TIA.2019.2896532

Adeyemo, A. A., Alves, E., Marra, F., Brandao, D., & Tedeschi, E. (2023). Suitability assessment of high-power energy storage technologies for offshore oil and gas platforms: A life cycle cost perspective. *Journal of Energy Storage*, *61*. https://doi.org/10.1016/j.est.2023.106643

Aldo Vieira da Rosa, J. C. O. (2022). Chapter 15 - wind energy (A. V. da Rosa & J. C. Ordóñez, Eds.; Fourth Edition), 721–794. https://doi.org/https://doi.org/10.1016/B978-0-12-816036-7.00028-2

Arditti, F., Souza, F., Martins, T., & Tannuri, E. (2015). Thrust allocation algorithm with efficiency function dependent on the azimuth angle of the actuators. *Ocean Engineering*, *105*, 206–216. https://doi.org/10.1016/j.oceaneng.2015.06.021

Arditti, F., Cozijn, H., Daalen, E. F. V., & Tannuri, E. A. (2018). Dynamic positioning simulations of a thrust allocation algorithm considering hydrodynamic interactions. *IFAC-PapersOnLine*, *51*, 122–127. https://doi.org/10.1016/j.ifacol.2018.09.480

Berge, S., & Fossen, T. (2000). On the properties of the nonlinear ship equations of motion. *Mathematical and Computer Modelling of Dynamical Systems*, *6*(4), 365–381. https://doi.org/10.1076/mcmd.6.4.365.3660

Bergman, J. (2023, January). *Predictions for the marine fuels market in 2023*. https://gcaptain.com/opinion-predictions-for-the-marine-fuels-market-in-2023/

Bertram, V. (2012). *Chapter 6 - ship maneuvering* (V. Bertram, Ed.; Second Edition). Butterworth-Heinemann. https://doi.org/https://doi.org/10.1016/B978-0-08-097150-6.10006-5

Blendermann, W. (1994). Parameter identification of wind loads on ships. *Journal of Wind Engineering and Industrial Aerodynamics*, *51*(3), 339–351. https://doi.org/https://doi.org/10.1016/0167-6105(94)90067-1

Bø, T. I., Johansen, T. A., & Mathiesen, E. (2013). Unit commitment of generator sets during dynamic positioning operation based on consequence simulation. *IFAC Proceedings Volumes (IFAC-PapersOnline)*, *9*, 156–160. https://doi.org/10.3182/20130918-4-JP-3022.00009

Bray, D., Daniels, J., Fiander, G., & Foster, D. (2020). *Dp operator's handbook* (S. Spark, Ed.; 3th). The Nautical Institute. https://www.nautinst.org/uploads/assets/8a5d1e69-27b3-4323-acdd08f4e7cb94e5/DP-Operators-handbook-extract.pdf

Bui, T. M., Dinh, T. Q., Marco, J., & Watts, C. (2021). Development and real-time performance evaluation of energy management strategy for a dynamic positioning hybrid electric marine vessel. *Electronics (Switzerland)*, *10*. https://doi.org/10.3390/electronics10111280

Burton, T., Jenkins, N., Sharpe, D., & Bossanyi, E. (2011). *Wind energy handbook*. John Wiley & Sons, Ltd. https://doi.org/https://doi.org/10.1002/9781119992714

Caires, S., Schouten, J.-J., Lønseth, L., Neshaug, V., Pathirana, I., & Storas, O. (2019). *Uncertainties in offshore wind turbulence intensity*. https://www.sintef.no/globalassets/project/eera-deepwind-2019/presentations/c1_caires_deltaresfugro.pdf

Chai, M., Reddy, B. D., Sobrayen, L., Panda, S. K., Die, W., & Xiaoqing, C. (2016). Improvement in efficiency and reliability for diesel- electric propulsion based marine vessels using genetic algorithm. *2016 IEEE Transportation Electrification Conference and Expo, Asia-Pacific (ITEC Asia-Pacific)*, 180–184. https://doi.org/10.1109/ITEC-AP.2016.7512944

Chai, M., Sobrayen, L., Reddy, B. D., Yelaverthi, D. B., Panda, S. K., Die, W., & Xiaoqing, C. (2016). Fuel-efficient low-voltage dc architecture for diesel-electric diving support vessels. *IECON Proceedings (Industrial Electronics Conference)*, 4413–4418. https://doi.org/10.1109/IECON.2016.7793299

Chauhan, P. J., Rao, K. S., Panda, S. K., Wilson, G., Liu, X., & Gupta, A. K. (2016). Fuel efficiency improvement by optimal scheduling of diesel generators using pso in offshore support vessel with dc power system architecture. *Asia-Pacific Power and Energy Engineering Conference, APPEEC*, *2016-January*. https://doi.org/10.1109/APPEEC.2015.7380963

Chen, H., Cong, T. N., Yang, W., Tan, C., Li, Y., & Ding, Y. (2009). Progress in electrical energy storage system: A critical review. *Progress in Natural Science*, *19*, 291–312. https://doi.org/10.1016/j.pnsc.2008.07.014

Clarksons. (2023). *World fleet register*. https://www.clarksons.net/wfr/

de Boer, J. (2023). Multi-horizon prediction of power consumption during dynamic positioning operations: Physical, data-driven and hybrid model approaches.

Diggelen, J. V., Broek, H. V. D., Schraagen, J. M., & Waa, J. V. D. (2018). *An intelligent operator support system for dynamic positioning*. TNO.

Dinh, T. Q., Bui, T. M., Marco, J., Watts, C., & Yoon, J. I. (2018). Optimal energy management for hybrid electric dynamic positioning vessels. *International Federation of Automatic Control*, *51*, 98–103. https://doi.org/10.1016/j.ifacol.2018.09.476

DNV. (2023). https://www.dnv.com/maritime/insights/topics/CII-carbon-intensity-indicator/answers-to-frequent-questions.html#:~:text=CII%20apply%20to%3F-,Answer%3A,passenger%20vessels%20and%20cruise%20ships.

DNV. (2024). *Promoting more robust dp power systems with closed bus-ties*. https://www.dnv.com/expert-story/maritime-impact/promoting-more-robust-DP-power-systems-with-closed-bus-ties/

DNV. (n.d.). *Future fuels*. https://www.dnv.com/maritime/hub/decarbonize-shipping/fuels/future-fuels.html

E. Kavak Akpinar, S. A. (2005). An assessment on seasonal analysis of wind energy characteristics and wind turbine characteristics. *Energy Conversion and Management*, *46*(11), 1848–1867. https://doi.org/https://doi.org/10.1016/j.enconman.2004.08.012

Faltinsen, O. (1990). *Sea loads on ships and offshore structures*. Cambridge University Press.

Fossen, T. I. (2011). *Handbook of marine craft hydrodynamics and motion control*. John Wiley & Sons, Ltd. https://doi.org/https://doi.org/10.1002/9781119994138

Garg, K., Weingarth, L., & Shah, S. (2011). Dynamic positioning power plant system reliability and design. *Petroleum and Chemical Industry Conference Europe Electrical and Instrumentation Applications*.

Godjevac, M., Visser, K., Boonen, E., Malikouti, C., Mestemaker, B., Lyu, Z., & van der Veen, F. (2017). Electrical energy storage for dynamic positiong operations - investigation of three application case.

Hansen, J. F., Lindtjørn, J. O., & Vanska, K. (2011). Onboard dc grid for enhanced dp operation in ships. *MTS Dynamic Positioning Conference*.

Hein, K., Xu, Y., Senthilkumar, Y., Gary, W., & Gupta, A. K. (2020). Rule-based operation task-aware energy management for ship power systems. *IET Generation, Transmission and Distribution*, *14*, 6348–6358. https://doi.org/10.1049/iet-gtd.2020.0668

HellenicShippingNews. (2023, January). *Shipbuilding review 2022: Record orders for alternative fuel orders*. https://www.hellenicshippingnews.com/shipbuilding-review-2022-record-orders-for-alternative-fuel-orders/#:~:text=Across%202022%2C%2061%25%20of%20tonnage,and%201.2%25%20included%20battery%20hybrid.

IEA. (2018). Offshore energy outlook. https://www.iea.org/reports/offshore-energy-outlook-2018

IEA. (2022). Renewables 2022 - analysis and forecast to 2027. https://www.iea.org/reports/renewables-2022

Ihle, I., Alme, J., & Block, F. (2016). Approaches to a greener dp vessel. *MTS DP Conference - Houston*.

IMCA. (2019). Guidance on failure modes and effects analysis (fmea) - m166 rev.2.

IMCA. (2020). A guide to dp-related documentation for dp vessels - m109 rev.3.1.

IMCA. (2021a). Guidance on operational activity planning - m220 rev.2.

IMCA. (2021b). Recommended code of practice on enviromental sustainability - es 001.

IMCA. (2022a). Guidelines for the design and operation of dynamically positioned vessels - m103 rev.5.1.

IMCA. (2022b). International guidelines for the safe operation of dynamically positioned offshore supply vessels - m182 rev.4.

IMCA DP Conference. (2023). Proceedings and personal communication during the imca dp conference 2023.

IMO. (2017). International maritime organization guidelines for vessels and units with dynamic positioning (dp) systems - maritime safety committee (msc) circular 1580 - 245 imo.

IMO. (2022, November). *Rules on ship carbon intensity and rating system enter into force*. https://www.imo.org/en/MediaCentre/PressBriefings/pages/CII-and-EEXI-entry-into-force.aspx

ITTC. (1987). *Report of the seakeeping committee*. https://ittc.info/media/2562/report-of-seakeeping-committee.pdf

J. Dang, H. L. (2004). Hydrodynamic aspects of steerable thrusters. *Marine Technology Society - Dynamic Positioning Conference*.

J.M.J. Journée, W. M. (2008). *Offshore hydromechanics* (2nd). Delft University of Technology.

Kalikatzarakis, M., Coraddu, A., Oneto, L., & Anguita, D. (2022). Optimizing fuel consumption in thrust allocation for marine dynamic positioning systems. *IEEE Transactions on Automation Science and Engineering*, *19*, 122–142. https://doi.org/10.1109/TASE.2021.3069779

Kambrath, J. K., Wang, Y., Yoon, Y. J., Alexander, A. A., Liu, X., Wilson, G., Gajanayake, C. J., & Gupta, A. K. (2017). Modeling and control of marine diesel generator system with active protection. *IEEE Transactions on Transportation Electrification*, *4*, 249–271. https://doi.org/10.1109/TTE.2017.2764324

Kulkarni, S., & Santoso, S. (2009). Impact of pulse loads on electric ship power system: With and without flywheel energy storage systems. *2009 IEEE Electric Ship Technologies Symposium*, 568–573. https://doi.org/10.1109/ESTS.2009.4906568

Lazarewicz, M., & Rojas, A. (2017). Grid frequency regulation by recycling electrical energy in flywheels. *Proceedings of the 9th International Scientific Symposium on Electrical Power Engineering, ELEKTROENERGETIKA 2017*, 159–164. https://doi.org/10.1109/pes.2004.1373235

Lindstad, H. E., & Sandaas, I. (2016). Emission and fuel reduction for offshore support vessels through hybrid technology. *Journal of Ship Production and Design*, *32*, 195–205. https://doi.org/10.5957/JSPD.32.4.150006

Lindstad, H. E., Eskeland, G. S., & Rialland, A. (2017). Batteries in offshore support vessels – pollution, climate impact and economics. *Transportation Research Part D: Transport and Environment*, *50*, 409–417. https://doi.org/10.1016/j.trd.2016.11.023

Lindtjørn, J. O., Wendt, F., Gundersen, B., & Hansen, J. F. (2014). Demonstrating the benefits of advanced power systems and energy storage for dp vessels.

Lyu, Z. (2016). Concept design of hybrid crane vessel - feasibility study of utilizing electric energy storage technology.

Mackay, E. (2012). 8.03 - resource assessment for wave energy (A. Sayigh, Ed.), 11–77. https://doi.org/https://doi.org/10.1016/B978-0-08-087872-0.00803-9

Malikouti, C. (2016). Energy storage for dp.

MathWorks. (2024). *Quadprog - quadratic programming*. https://nl.mathworks.com/help/optim/ug/quadprog.html

Montonen, J. H., Lindh, T., Lana, A., Peltoniemi, P., Pinomaa, A., Tikkanen, K., & Pyrhonen, O. (2022). Comparison of different power balance control methods for battery energy storage systems on hybrid marine vessels. *IEEE Access*, *10*, 58578–58588. https://doi.org/10.1109/ACCESS.2022.3179716

Navingo. (2010). *Offshore drilling: History and overview*. https://www.offshore-energy.biz/offshore-drilling-history-and-overview/

Nebb, O. C., Zahedi, B., Lindtjorn, J. O., & Norum, L. (2012). Increased fuel efficiency in ship lvdc power distribution systems. *2012 IEEE Vehicle Power and Propulsion Conference*, 564–568. https://doi.org/10.1109/VPPC.2012.6422695

Oomen, F. H. A. (2016). Improving the energy efficiency, emissions and maintenance costs of a deep-water dp-3 drillship by implementing an energy storage system in the energy distribution system.

Ørsted. (2023). Green energy to power lasting positive impact - sustainability report 2022. https://orstedcdn.azureedge.net/-/media/2022-annual-report/orsted-sustainability-report-2022.ashx?rev=eda5465ba5784866b6cea99e58088f94&hash=90B3E835AD1E32D033AD31CE49FA865C

Osen, O. L. (2016). Optimizing electric energy production on-board offshore vessels: Vessel power consumption profile and production strategies using genetic algorithms. *OCEANS 2016 - Shanghai*. https://doi.org/10.1109/OCEANSAP.2016.7485614

Pestana, H. (2014). Future trends of electrical propulsion and implications to ship design.

Probst, J.-O. (2022, December). *Methanol as an alternative fuel for container vessels*. https://www.dnv.com/expert-story/maritime-impact/methanol-as-an-alternative-fuel-for-container-vessels.html

Radan, D., Johansen, T. A., Sørensen, A. J., & Adnanes, A. K. (2005). Optimization of load dependent start tables in marine power management systems with blackout prevention.

Radan, D., Sørensen, A. J., Ådnanes, A. K., & Johansen, T. A. (2008). Reducing power load fluctuations on ships using power redistribution control. *Marine Technology*, *45*, 162–174.

Radan, D., Sørensen, A. J., Johansen, T. A., & Adnanes, A. K. (2006). Probability based generator commitment optimization in ship power system design.

Rao, K. S., Chauhan, P. J., Panda, S. K., Wilson, G., Liu, X., & Gupta, A. K. (2015). Optimal scheduling of diesel generators in offshore support vessels to minimize fuel consumption. *IECON 2015 - 41st Annual Conference of the IEEE Industrial Electronics Society*, 4726–4731. https://doi.org/10.1109/IECON.2015.7392838

Rekelhof, B. M. (2016). Optimisation of the power generation system of a dp2 class pipelay vessel.

Ribeiro, P., Johnson, B., Crow, M., Arsoy, A., & Liu, Y. (2001). Energy storage systems for advanced power applications. *Proceedings of the IEEE*, *89*, 1744–1756. https://doi.org/10.1109/5.975900

Rokseth, B., Utne, I., & Vinnem, J. (2016). A systems approach to risk analysis of maritime operations. *Proceedings of the Institution of Mechanical Engineers Part O Journal of Risk and Reliability*. https://doi.org/10.1177/1748006X16682606

Rozendaal, J. M. (2021). Methanol hybrid offshore working vessels - a technical, environmental and economic assessment.

Sørensen, A. J. (2011). A survey of dynamic positioning control systems. *Annual Reviews in Control*, *35*, 123–136. https://doi.org/10.1016/j.arcontrol.2011.03.008

Sørensen, A. J. (2018). Marine cybernetics - towards autonomous marine operations and systems - lecture notes.

Stapersma, D. (2010, April). *Emissions and heat transfer* (Vol. 4).

Swider, A., & Pedersen, E. (2019). Data-driven methodology for the analysis of operational profile and the quantification of electrical power variability on marine vessels. *IEEE Transactions on Power Systems*, *34*, 1598–1609. https://doi.org/10.1109/TPWRS.2018.2876252

T.F. Hueting, J. R. (2016). *Task analysis and decision support requirements for dynamic positioning operators*. https://publications.tno.nl/publication/34623326/PZPpyp/TNO-2016-R11583.pdf

Tufte, E. D. (2014). Impacts of low load operation of modern four-stroke diesel engines in generator configuration.

UNEP. (2022). Emissions gap report 2022: The closing window - climate crisis calls for rapid transformation of societies. https://www.unep.org/emissions-gap-report-2022

Vásquez, C. A. M. (2016). Evaluation of medium speed diesel generator sets and energy storage technologies as alternatives for reducing fuel consumption and exhaust emissions in electric propulsion systems for psvs. *Ship Science & Technology*, *9*, 49–62.

Veksler, A., Johansen, T. A., & Skjetne, R. (2012). Thrust allocation with power management functionality on dynamically positioned vessels. *Proceedings of the American Control Conference*, 1468–1475. https://doi.org/10.1109/acc.2012.6315084

Veksler, A., Johansen, T. A., Skjetne, R., & Mathiesen, E. (2014). Reducing power transients in diesel-electric dynamically positioned ships using repositioning. *IECON Proceedings (Industrial Electronics Conference)*, 268–273. https://doi.org/10.1109/IECON.2014.7048510

Veksler, A., Johansen, T. A., Skjetne, R., & Mathiesen, E. (2016). Thrust allocation with dynamic power consumption modulation for diesel-electric ships. *IEEE Transactions on Control Systems Technology*, *24*, 578–593. https://doi.org/10.1109/TCST.2015.2446940

Vestas. (2022). Scaling-up sustainably with strategic partners - sustainability report 2022. https://www.vestas.com/content/dam/vestas-com/global/en/sustainability/reports-and-ratings/sustainability-reports/sustainability-report-2022.pdf.coredownload.inline.pdf

Wang, F., Zhao, L., & Bai, Y. (2023). Survey on reliability analysis of dynamic positioning systems. *Ships and Offshore Structures*, 1–11. https://doi.org/10.1080/17445302.2023.2225959

Wit, C. D. (2009). Optimal thrust allocation methods for dynamic positioning of ships.

Woud, H. K., & Stapersma, D. (2017). *Design of propulsion and electric power generation systems*. IMarEST.

Wu, D., Ren, F., & Zhang, W. (2016). An energy optimal thrust allocation method for the marine dynamic positioning system based on adaptive hybrid artificial bee colony algorithm. *Ocean Engineering*, *118*, 216–226. https://doi.org/10.1016/j.oceaneng.2016.04.004

Xia, G., Sun, X., Zhao, B., & Yang, Y. (2019). Thrust allocation for dynamic positioning vessels with switchboard power limit and diving forbidden sectors. *Chinese Automation Congress*.

Yushi, W., Fu, M., Ning, J., & Sun, X. (2013). Quadratic programming thrust allocation and management for dynamic positioning ships. *TELKOMNIKA Indonesian Journal of Electrical Engineering*, *11*. https://doi.org/10.11591/telkomnika.v11i3.2318

Zahedi, B., Norum, L. E., & Ludvigsen, K. B. (2013). Optimization of fuel consumption in shipboard power systems. *IECON Proceedings (Industrial Electronics Conference)*, 1124–1129. https://doi.org/10.1109/IECON.2013.6699290

Zahedi, B., Norum, L. E., & Ludvigsen, K. B. (2014). Optimized efficiency of all-electric ships by dc hybrid power systems. *Journal of Power Sources*, *255*, 341–354. https://doi.org/10.1016/j.jpowsour.2014.01.031

Zhao, D.-w., Ding, F.-g., Tan, J.-f., & Bian, X.-q. (2010). Optimal thrust allocation based ga for dynamic positioning ship [https://ieeexplore.ieee.org/document/5589933]. *2010 IEEE International Conference on Mechatronics and Automation*, 1254–1258. https://doi.org/10.1109/ICMA.2010.5589933

A

Appendix I - Literature study

The three solutions and corresponding research gaps that are considered in this report resulted from a literature study. As such, Appendix A presents some of the chapters and sections written for the literature study to provide readers with the opportunity to review initial reasonings and associated literature. Not all sections and chapters have been provided, as portions of the literature review have been implemented into the Thesis report. Note that this literature review is written at an earlier stage during the research. As such, certain parts of the scope may deviate from this report and may contain some contradictions. However, these aspects are changed at a later stage during the research, conducted after the literature study.

A.1. Introduction - Objective & report outline

This literature study aims to identify solutions for reducing GHG emissions of DP operations from offshore vessels and to determine which of these would be most effective given the set scope. In the end, a solution is sought for an existing ship design, taking current best practices into account and without compromising on safety standards.

Based on these objectives, the report contains the following structure. Chapter A.2 will present state-of-the-art research on improving DP operations, mapping several solutions which could reduce GHG emissions. Chapter A.3 will elaborate on current best practices of DP operations within the industry, identifying current problems and limiting factors. Next, Chapter A.4 will reflect the presented solutions against the current best practices and determine which solutions would be most effective. Consequently, Chapter A.5 presents research gaps found in the state-of-the-art research of the further considered solution(s).

A.2. Academic state-of-the-art

Chapter A.2 will introduce state-of-the-art research on improving DP operations, identifying solutions which potentially reduce GHG emissions. First, the different equipment classes applicable to the systems of a DP vessel are highlighted in section A.2.1. Next, measures which apply to the power generation, power distribution, power management and propulsion system are presented in sections A.2.2, A.2.3, A.2.4 and A.2.5 respectively.
Research focusing on controller algorithm improvements, such as model predictive controllers, will not be taken into account as such research primarily examines controller robustness rather than GHG minimisation.

A.2.1. Equipment classification

Before different solutions are identified, attention is paid to the equipment classification of a DP vessel's system, as this illustrates the level of redundancy embedded in a DP vessel's systems. Redundancy in this sense is understood as:

"The ability of a component or system to maintain or restore its function when a single failure has occurred" [IMO, 2017].

The level of redundancy of a DP system is categorised into three equipment classes based on the Worst-Case Failure Design Intent (WCFDI):

"The specified minimum DP system capabilities to be maintained following the Worst-Case Failure (WCF), which is the identified single fault in the DP system resulting in maximum detrimental effect on DP capability" [IMO, 2017].

As defined by IMO (2017) and ABS (2021b), the three equipment classification notations for DP systems are:

- **Class 1 (DPS-1)**:
  A loss of position and/or heading may occur in the event of a single failure.
- **Class 2 (DPS-2)**:
  A loss of position and/or heading will not occur in the event of a single fault in any active component or system, excluding a loss of one or multiple compartments.
- **Class 3 (DPS-3)**:
  A loss of position and/or heading will not occur in the event of a single fault in any active or static component or system, including a complete loss of a compartment due to fire or flood.

Active components are such as DGs, thrusters or switchboards, and static components are such as cables or pipes that could immediately affect DP performance upon failure. Both class 2 and 3 systems should be single fault tolerant. However, the difference between these is that class 3 systems require a physical separation as protection against, for example, fire.
DP1 vessels will not be taken into account in this literature study as they are not subject to the relevant restricting requirements. Additionally, differences between DP2 and DP3 vessels will not further be emphasised as these are no operational differences.

A.2.2. Power generation

The equipment classification of section A.2.1 has a direct impact on the design of a DP vessel's power system, as it requires the system to be divided into two or more sections. In the event that a failure occurs in either one of the power sections, which is the WCF, the remaining section(s) are still able to provide the vessel with sufficient power [IMO, 2017]. As elaborated in section A.1, this causes DGs to operate at much lower loads than designed for. Additionally, flexible power demands during DP operations can generally be poorly absorbed by the somewhat static power delivery from the DGs, which will further be explained in section A.3.2. Additionally, this is further aggravated as power sections are commonly disconnected from one to another during operations, which can be referred to as open bus-tie operations [ABS, 2021b].
This section will identify solutions for the power generation system. Throughout, vessels with diesel-electric power systems, DGs as the prime mover and an alternating current (AC) distribution system, are considered conventional for DP offshore vessels [IMCA, 2022a].

Power generation redesign

DGs are ideally operated at their peak efficiency of around 80% MCR [Woud and Stapersma, 2017]. However, as already elaborated, this rarely occurs, which will further be explained in chapter A.3.
The power generation system of a DP vessel consists of minimally two switchboards, each containing at least two DGs, as is presented in figure A.1. Such a system is designed with the objective of minimising capital expenditures and ensuring sufficient redundancy [Swider and Pedersen, 2019]. As a result, however, there is little flexibility in operating such a system.

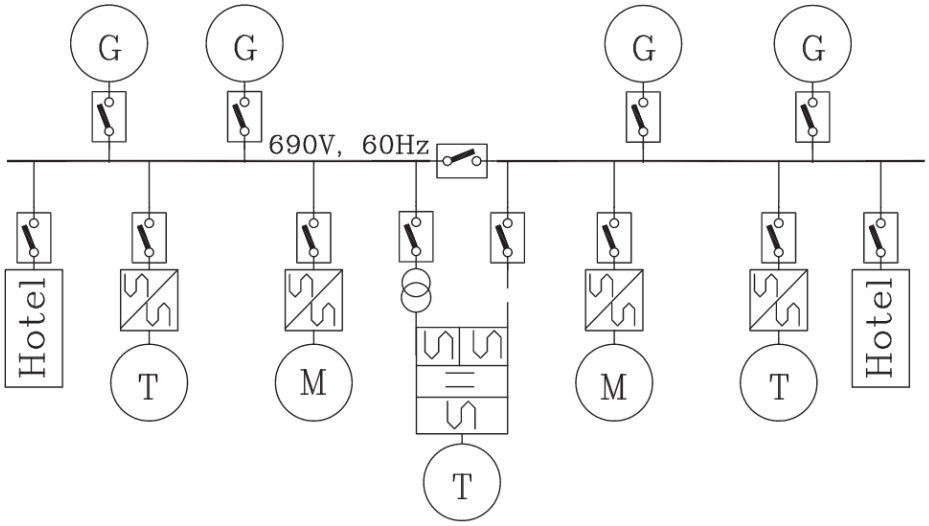


Figure A.1: Example of a conventional power system, consisting of four DGs, two main thrusters and three bow thrusters [Swider and Pedersen, 2019]

Redesigning such a conventional power generation system could offer significant benefits. Altering the system to have differently sized DGs could allow prime movers to operate closer to their peak efficiency as they can be operated more flexibly [Rekelhof, 2016].

Swider and Pedersen (2019) discuss how this can be achieved, emphasising how crucial assumptions are regarding the vessel's operational profile and actual load range. Data from real-time measurements are used in this research to determine the complete load profile, including the mean and extreme loads, by applying stochastic load analysis. Based on this, aspects such as the size and configuration of the power generation system can be selected. Similar problems and objectives are addressed in the thesis of Rekelhof (2016). He proposed five alternative power generation configurations for a DP2 class flex-lay vessel, focusing on increased flexibility and considering battery implementation.
Osen (2016), on the other hand, proposes to perform a power generation redesign through the use of a Genetic Algorithm (GA), optimising for maximum energy efficiency. Contrarily to the other two, Osen (2016) focuses on high DG utilisation and discusses the technical aspects in greater detail.
Redundancy aspects are, however, still applicable for adjusted power generation designs. As such, Bø et al. (2013) studied how WCF simulations can be used for assessing whether such systems are sufficiently redundant.

Implementation of energy storage devices

The implementation of Energy Storage Devices (ESDs) on board ships is a widely investigated topic. Also, for DP vessels, different ESD types and functions offer a variety of improvements.
Note that throughout the whole literature study, a clear distinction is made between ESDs for spinning reserve replacement and alternatively for peak shaving. Although a combination of these two could be possible, a similar distinction was visible and adopted from current research. Later on, other functions, combinations and practical aspects were discovered. Therefore, some of the statements made regarding ESDs might not be fully applicable. However, these have not all been adopted in the main report, as ESDs fell out of the scope of this research.

Using ESDs as spinning reserve replacement of DGs is the first well-investigated function [Lindstad et al., 2017]. For this, the ESD is connected to the grid but is only involved in the event of a power loss. If this occurs, the ESD provides sufficient power until another DG is fully started and operating [Godjevac et al., 2017]. The advantage is that fewer DGs are required online as the ESD maintains redundancy. Additionally, the online DGs are capable of running closer to their peak efficiency [Lyu, 2016, Vásquez, 2016].

Peak shaving is a second widely considered function for ESDs. Generally, DP operations have an oscillating load profile [Godjevac et al., 2017]. Peak loads, especially, require immediate action from the prime movers. The dynamic response of a DG is, however, limited and relatively poor [IMCA, 2022a, Montonen et al., 2022]. As a result, under-frequency can occur, or if the response is too slow, this could result in system disturbances. With peak shaving, however, the ESD accommodates short-term power peaks as is shown in figure A.2. Consequently, This allows DGs to run at a more constant load and prevents failures which could cause system blackouts [Lindstad et al., 2017, Rekelhof, 2016].

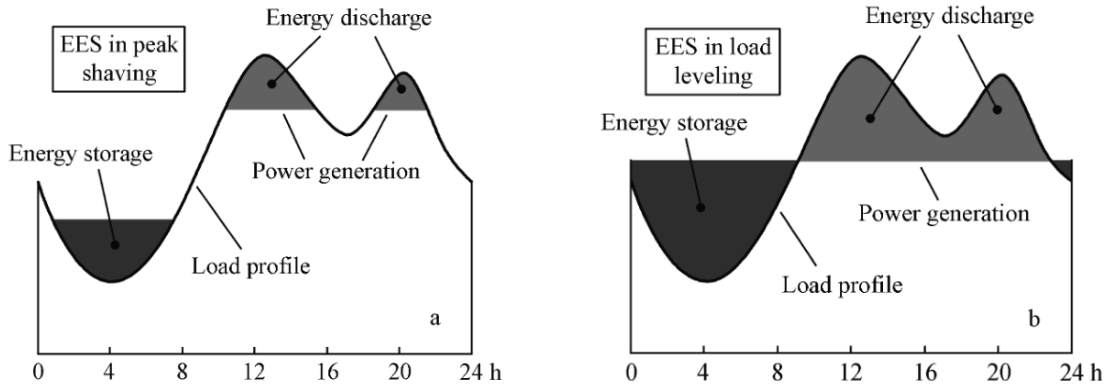


Figure A.2: Load profiles with an ESD for peak shaving or load levelling [Chen et al., 2009]

A third suggested function for ESDs is enhanced dynamic performance, or load levelling, as presented in figure A.2. This method is similar to peak shaving; however, it focuses on ramping the changeover to slower types of prime movers [Godjevac et al., 2017]. Such an application would be particularly useful for new types of technologies with a slower dynamic response, such as LNG engines or fuel cells [Lyu, 2016].

Within the literature, typically, three different types of ESDs are generally considered. These are Lithium-ion batteries, flywheels and supercapacitors. The energy storage of supercapacitors is based on storing excess energy by accumulating positive and negative charges between two electrodes, as is shown in figure A.3 [Lyu, 2016, Ribeiro et al., 2001].

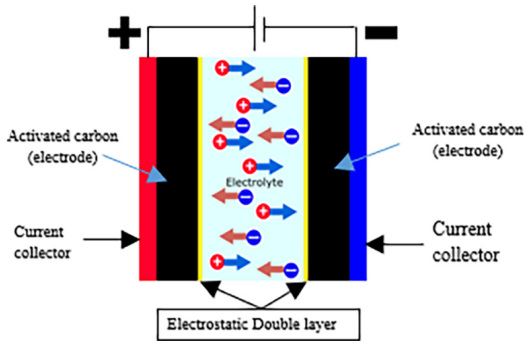


Figure A.3: Structure of a supercapacitor energy storage device [Adeyemo et al., 2023]

Supercapacitors have a high self-discharge rate, require little maintenance and are inherently safe [Adeyemo et al., 2023, Malikouti, 2016]. Most operational experience with supercapacitors is within the transportation sector for regenerative braking of trains and electric vehicles [Adeyemo et al., 2023]. However, in 2013, supercapacitors have also been implemented on board the full electric catamaran ferry, STX France Lorient [Lyu, 2016]. As the energy dissipates, however, supercapacitors have only been considered for applications with a short operational duration. Additionally, supercapacitors are primarily applicable for delivering lower amounts of power [Adeyemo et al., 2023]. Therefore, this type of ESD is only applicable to peak shaving applications.

Flywheels are mechanical ESDs which store rotational energy through the angular momentum of a spinning mass, which is shown in figure A.4 [Lyu, 2016, Chen et al., 2009].

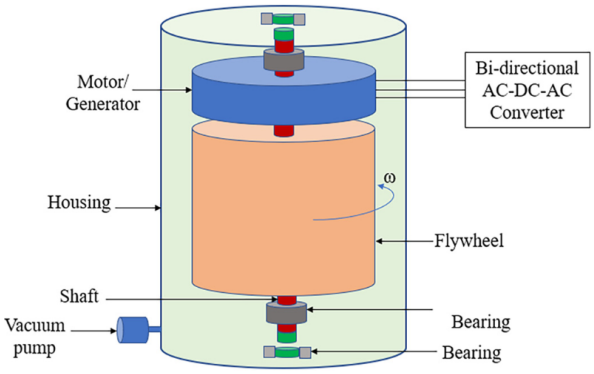


Figure A.4: Structure of a flywheel energy storage device [Adeyemo et al., 2023]

Flywheels are generally considered to be highly efficient, with efficiencies up to 95%, and are capable of providing high amounts of power with fast time responses [Lazarewicz and Rojas, 2017, Chen et al., 2009]. On top of that, flywheels can operate for a high amount of life cycles under a wide temperature range and are therefore considered to be reliable and safe. However, flywheels are not capable of storing energy over long periods of time as they suffer from significant standby losses [Malikouti, 2016, Adeyemo et al., 2023]. Flywheels are therefore only applicable for peak shaving applications or for preventing voltage blackouts during pulse load operations as was investigated by Kulkarni and Santoso (2009). Generally, research on its application for offshore vessels has mostly considered flywheels for grid voltage and frequency stabilisation [Adeyemo et al., 2023].

Batteries are the most widely investigated ESDs for DP, partially because of their commonality in all sorts of other applications. On top of that, they appear to be suitable for marine applications due to their relatively good life-cycle performance, beneficial current handling characteristics for (dis)charging, and their versatile application range [Malikouti, 2016]. Although different types of batteries exist, only lithium-ion batteries will be considered throughout this study as they are generally considered to be most suitable for marine applications [Lyu, 2016, Adeyemo et al., 2023]
Research of Lyu (2016), Godjevac et al. (2017) and Vásquez (2016) present significant fuel savings if batteries are applied as spinning reserve, showing reductions of around 15 to 20%. Fuel savings are also reported by Lindstad et al. (2017) and Lindstad and Sandaas (2016), who indicate that the impact of emission reductions is more significant than that of the decrease in fuel consumption alone.
Such fuel savings have, however, not been reported for peak shaving battery applications, based on results of Lyu (2016) and Godjevac et al. (2017). On the other hand, Montonen et al. (2022) states that one DG would often be sufficient for providing enough power during DP DP operation. The limiting factor, however, is the insufficient dynamic response of the DG to handle load variations. As such, peak-shaving batteries could still aid in preventing power system blackouts.

Alternative fuels

For the application of alternative fuels, relatively significant system conversions are required. Still, it is deemed an interesting measure due to its considerable potential in reducing GHG emissions. Throughout the maritime industry, much research has been done on the application of alternative fuels. However, little research has considered its implementation on board offshore DP vessels. Therefore, only alternative fuels are considered with matured technologies and corresponding safety regulations, as is depicted in figure A.5.

LNG is currently the most applied alternative fuel within the marine sector as a whole, covering approximately three-quarters of all vessels ordered with alternative fuels in 2022 [Bergman, 2023, HellenicShippingNews, 2023]
Methanol would be an alternative as both its technology and regulations for its onboard usage have considerably matured over the last couple of years [DNV, n.d., Probst, 2022]. Such is indicated in figure A.5, compared to other fuels such as ammonia or hydrogen. Its implementation on board an offshore working vessel has been investigated in the thesis of Rozendaal (2021).

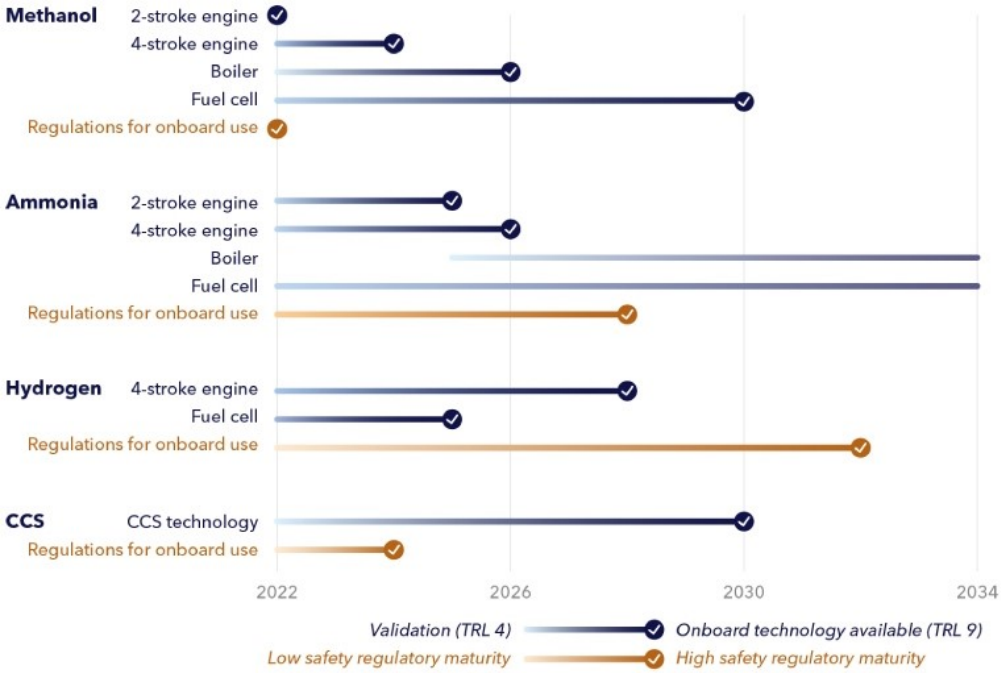


Figure A.5: Estimated maturation timelines for energy converters, onboard CCS technologies, and corresponding safety regulations for onboard use [DNV, n.d.]

A.2.3. Power distribution

As elaborated in section A.2.2, power distribution systems with AC operating with an open bus are considered conventional. This section will identify solutions altering both of these aspects.

Closed bus-tie configuration

With closed bus-tie operations, the usually separated power sections are connected. As this allows power to be shared across sections, not all DGs are required to be operated to provide the ship with sufficient power, improving energy efficiency [Lindtjørn et al., 2014, Sørensen, 2018].
The resulting fuel savings can be illustrated with the following example. Assume a conventional power system as shown in figure A.1. An open bus-tie configuration would require all four DGs to be operated. However, with a closed bus-tie configuration, it would be possible to operate with three DGs. Closed bus configurations solely could reduce fuel consumption by 5 to 7% based on self-made calculations. Additional advantages can be gathered from figure A.6.

	Open bus tie	Closed bus tie
Continuity of vessel DP operations	Good	Good
Station keeping integrity	Good	Good provided no critical failure modes occur
Flexibility for maintenance	Poor if all generators need to be connected at all times	Good
Fuel efficiency	Poor if all generators need to be connected at all times	Good
Emissions	Poor if all generators need to be connected at all times	Better than open bus tie systems

Figure A.6: Bus-tie configuration comparison from IMCA (2022a)

To date, there is no research investigating the saving potential of closed bus-tie operations as it is already often adopted within research to other solutions. Though, as will be further elaborated in chapter A.3, closed bus-tie operations are not considered standard practice as there is a greater chance a complete power system blackout occurs.
As discussed by Garg et al. (2011), power systems of a DP vessel have a relatively small inertia. Short system disturbances could, therefore, result in system instabilities. When operating with a closed bus-tie configuration, a failure in one of the power sections could propagate to the other(s), resulting in a complete vessel blackout. Research from Garg et al. (2011) therefore investigates designs which could provide sufficient reliability for operating with closed bus-ties.

Direct current grid

For AC architectures, the voltage and frequency outputs from DGs have to be synchronised to the power grid. If not done correctly, this could cause a blackout of the power system [Chai, Sobrayen, et al., 2016]. As a result, DGs have to be operated at constant speeds. However, for such cases, the specific fuel consumption (sfc) of the DGs is only minimum at a small operating window, typically around 85% MCR [Kambrath et al., 2017, Hansen et al., 2011].
Synchronisation is, however, not required for Direct Current (DC) architectures, allowing DGs to be operated independently at a variable speed. This enhances the optimum sfc window from 50 to 100% MCR, significantly improving efficiency [Chauhan et al., 2016, Hansen et al., 2011]. The absence of DG synchronisation on top of that allows faster system recovery as DG start-ups can be executed more quickly [Hansen et al., 2011, Oomen, 2016]. DC grids furthermore require less space as transformers or thruster rectifiers are not necessary [Chai, Sobrayen, et al., 2016, Nebb et al., 2012]. Lastly, it accommodates more straightforward implementation of ESDs or newer types of technologies such as fuel cells [Nebb et al., 2012, Zahedi et al., 2013].

Research investigating the fuel savings of applying DC architectures shows a variety of fuel savings. Chai, Sobrayen, et al. (2016) and Zahedi et al. (2013) argue that DC architectures could lead to fuel savings of 8 to 9% compared to AC architectures. Chauhan et al. (2016) on the other hand discusses fuel savings of 5%, but only at loads around 15 to 30%. Alternatively, papers as Hansen et al. (2011), Zahedi et al. (2014) and Zahedi et al. (2013) discuss fuel savings can go up to 15 to 20% in case an ESD is implemented in addition.
However, according to Nebb et al. (2012) and Kambrath et al. (2017), DGs operating at variable speeds are more susceptible to load variation disturbances due to their poor dynamic behaviours exacerbated by the fuel pump. The dynamic response of a DG operating in a DC architecture is therefore investigated by Kambrath et al. (2017). This aspect is also taken into account in the research of Nebb et al. (2012), investigating the optimal control strategy of DGs and ESDs on the DC grid.

A.2.4. Power management system

The Power Management System (PMS) ensures continuity of power supply to all consumers under all operating conditions [IMO, 2017, Sørensen, 2018]. Three primary functions of this system can be illustrated.
First, it controls all prime movers and their configurations. DGs are often operated in voltage droop mode, which means that their frequency levels are controlled by varying their voltage output, allowing the system to handle load transients and prevent system failures [IMCA, 2022a].
Secondly, the system executes power limitation functions to prevent blackouts. Load shedding, deliberately removing the electrical load from a power system in order to balance the power supply and demand, for example, illustrates this, which is particularly important in the event of sudden power losses [Sørensen, 2018, ABS, 2021b]. Lastly, the system manages the distribution of power, controlling the power system's configuration [ABS, 2021b].
If the PMS has extended abilities where it monitors and controls energy flows, it is regarded as an Energy Management System [Sørensen, 2018]. This is required for hybrid vessel systems as the EMS additionally regulates the (dis)charge of ESDs while optimising fuel consumption, considering historical and future energy demand [Bui et al., 2021]. Such a system is widely addressed and investigated in papers as Bui et al. (2021), Dinh et al. (2018) and Hein et al. (2020), though is not considered conventional given its limited applicability to date [IMCA, 2022a].

Unequal generator loading

As elaborated at the start of section A.2.2, DGs commonly operate at low loads during DP operations with an open bus bar. Commonly, the total load requested from the power system is shared equally across all running DGs [Chai, Reddy, et al., 2016, Chai, Sobrayen, et al., 2016]. However, instead, the PMS could distribute the requested load such that one DG delivers more power than the others. In that case, the most significant portion of the load is generated more efficiently with a lower sfc [Chauhan et al., 2016, Rao et al., 2015]. On top of that, this could also significantly improve the emission characteristics of the DG as it is operated at a higher load [Lindstad et al., 2017, Lindstad and Sandaas, 2016]. Such a measure would only require a change in the PMS' algorithm and could applied to a wide variety of DP vessels and power system configurations [Chai, Reddy, et al., 2016, Chauhan et al., 2016].

Current research on this concept so far has investigated its application to relatively simple power system configurations of Offshore Support Vessels (OSVs) and Diving Support Vessels (DSVs). Research of Chai, Reddy, et al. (2016) and Rao et al. (2015) investigates the use of GAs for determining the most optimal load distribution to achieve minimal fuel consumption. Chai, Reddy, et al. (2016) on top of that argues that unequal generator loading could also lead to increased power system reliability. Chai, Sobrayen, et al. (2016) further investigates the concept of using GAs by taking minimum DG loading and redundancy aspects into account. Chauhan et al. (2016), on the other hand, uses Particle Swam Optimisation (PSO) for determining the most optimal loading distribution across DGs.

Fuel savings resulting from unequal generator loading are not clearly presented and given as absolute values, such as 152 or 307 ton fuel per year for Chauhan et al. (2016), discussing that there are only fuel savings when operating at loads below 35%. however Rao et al. (2015) adversely argues fuel savings are around 3%. Chai, Reddy, et al. (2016) discusses fuel savings of 1.8% while Chai, Sobrayen, et al. (2016) argues savings are minimum and close to 0%.
All in all, actual relative fuel savings are unclear from the state-of-the-art research. However, several aspects, such as the specified benchmark conditions, do not appear to be correct or conform to actual operational industry practices. Especially as results between state-of-the-art research diverge or appear to be calculated for one average power, actual results are unclear so far.

Load dependent start-stop optimisation

As elaborated in the introduction of section A.2.4, the PMS manages the amount and which DGs are required online, amongst other matters. Usually, this is done according to a predetermined load-dependent start-stop table [Radan et al., 2005]. In the event of a sufficient load increase, DGs are started and connected to the grid gradually one at a time, according to the sequence within the start-stop table [Radan et al., 2006, Bø et al., 2013].

Connecting and disconnecting DGs to the power system of a DP vessel has, however, significant consequences for the plant's efficiency as the amount of prime movers is usually small [Bø et al., 2013]. This can be illustrated with an example where, initially, the vessel is operated with two DGs, both operating at 55% MCR. If one DG fails, the other has to compensate for the missing power and consequently has to ramp up to a much higher load of 110% MCR. Alternatively, if the system deems it necessary to start a third DG, the load on all DGs will significantly drop to 36.7% MCR. The effect this has on the average sfc of a power system is illustrated in figure A.7.

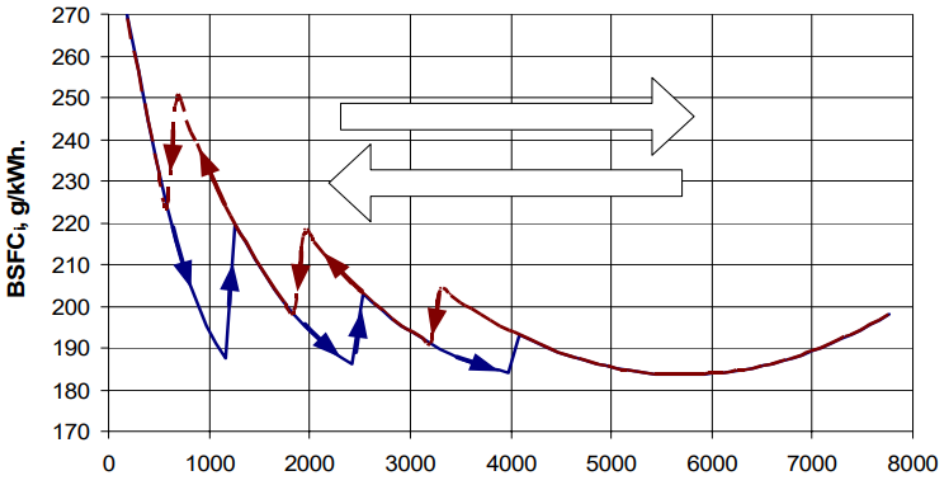


Figure A.7: The average sfc of a power system, affected by starting and stopping of DGs if loads sufficiently increase (blue) or decrease (red) [Radan et al., 2006]

Radan et al. (2006) argues that there is no clear definition of when DGs should be started or stopped despite it having such a significant impact on the system's performance. Often, the only criterion is that the stop tables should not coincide with the start tables. In practice, gathered from personal communications, criteria are set at a desired spinning reserve level, at which operators "feel safe". Such criteria are, therefore, more so aimed at feeling and not at system efficiencies. As a result, this could lead to unnecessary DG switching. Especially in the event of cold start-up procedures, this could lead to excessive GHG emissions [Radan et al., 2006].

Radan et al. (2005) comes with an improvement by proposing a method where the load-dependent start tables are optimised in order to minimise fuel consumption. Alternatively, Bø et al. (2013) defines it as a unit commitment problem where operational costs are minimised given a predicted load, determining the amount of DGs which should be committed accordingly.
Both papers also aim to prevent unnecessary generator starting as this could lower fuel consumption, decrease maintenance costs and reduce risks of blackout occurring [Radan et al., 2005, Bø et al., 2013].
Radan et al. (2006) is a continuation, presenting a more general optimisation method which includes a more detailed operational profile based on a probabilistic approach.
Fuel saving results from these papers vary, ranging from 2 to 3% according to Radan et al. (2005) and 2 to 8% from Bø et al. (2013).

A.2.5. Propulsion system

Typically, the main propulsion of DP offshore vessels is located aft with several tunnel thrusters and perhaps an additional retractable thruster at the bow. Also, the propulsion system is subject to the equipment classification presented in section A.2.1 and is therefore divided across the power sections [ABS, 2021b]. This literature study will focus on diesel-electric DP vessels with azimuth and azipull thrusters for main propulsion, as this is considered conventional for offshore DP vessels. Other types of propulsors or configurations are left out of scope.

The amount of thrust and direction required from each propulsion is managed by the thrust allocation (TA) controller and calculated through a TA algorithm. The force each thruster delivers cannot be measured directly and is therefore estimated using aspects such as its revolution speed [Sørensen, 2018]. This module also links the positioning system with the PMS, receiving continuous updates on the power availability with the intention of preventing power blackouts and undesired load shedding [Sørensen, 2018].

Thruster allocation algorithm improvements

The difficulty in TA algorithms lies in the fact that they need to address a multi-objective optimisation problem with certain constraints [Wu et al., 2016, Kalikatzarakis et al., 2022]. Besides being programmed to maintain the vessel's position and prevent blackouts, a TA algorithm ideally also aims to minimise fuel consumption, system wear and tear, or load fluctuations [Sørensen, 2018, Kalikatzarakis et al., 2022]. However, in the meantime, constraints such as system limitations and failures should also be accounted for within the algorithm [Wu et al., 2016]. Especially considering a vessel equipped with azimuths, the TA problem can become a non-convex nonlinear optimisation problem [Wu et al., 2016]. As discussed by Kalikatzarakis et al. (2022), state-of-the-art approaches to TA optimisation, therefore, often simplify the problem in order to make them convex, enabling automatic computer systems to solve them.

Many papers, therefore, have investigated overall approaches to improve conventional TA algorithms. Wit (2009), for example, discusses the shortcomings of the Lagrange multiplier method and instead proposes Sequential Quadratic Programming (SQP). The advantages of SQP are that it is regarded as a robust optimisation algorithm with a strong local optimisation ability and its real-time implementation applicability [Wu et al., 2016, Wit, 2009, Arditti et al., 2018]. Though as Zhao et al. (2010) and Wu et al. (2016) discuss, the global optimisation of SQP is weak, and when the initially selected value is inappropriate, optimisation takes longer. Both Zhao et al. (2010) and Wu et al. (2016) therefore, either propose the use of a GA or an improved Artificial Bee Colony Algorithm. As is also discussed by Arditti et al. (2015), these two methods can achieve the global optimal solution by escaping from local minimums. However, they also tend to have high computational costs compared to SQP. In the end, however, these papers unfortunately do not offer insight into the fuel savings such an alteration of the TA algorithm can deliver.

The TA algorithm can also be improved by representing the system with higher fidelity. Kalikatzarakis et al. (2022) discusses general weaknesses of state-of-the-art approaches in the physical modelling of the transmission subsystems. The results here show fuel savings of 5% with respect to conventional approaches. Alternatively, Xia et al. (2019) considers constraints regarding the switchboard power limit.
Furthermore, both Kalikatzarakis et al. (2022) and Xia et al. (2019) avoid hydrodynamic effects and interactions between thrusters by specifying forbidden zones as thruster constraints. Arditti et al. (2015) recognises this from state-of-the-art approaches and proposes to take hydrodynamic interaction effects of thrusters into account by using thruster efficiency functions in the formulation of the optimisation problem, showing power reductions of 2 to 5%. Later on, this work was further improved by Arditti et al. (2018).

Load levelling thruster allocation controller

As elaborated in section A.2.2, the dynamic response of a DG can prove to be insufficient in sustaining load fluctuations. Peak shaving applications of ESDs have, therefore, already been proposed. Alternatively, the TA controller could also play a role in stabilising the load demanded from the power plant.

Radan et al. (2008), for example, proposes a power redistribution controller where the controller redistributes power from consumers, which generates load fluctuations. This power is then redirected to the thruster, which is then capable of compensating for the load fluctuations. Although this will result in quick thruster load fluctuations, the author discusses this will not significantly affect a vessel's response due to its large inertia.

Veksler et al. (2012) proposes a somewhat different TA controller where the algorithm allows deviations between the commanded and actually generated thrust, up to a certain extent. The TA algorithm is then able to compensate for load variations from other (heavy consumers) and improve the frequency stability of the grid. Veksler et al. (2014) continues on this by improving aspects such as allowing more significant velocity deviations in directions where a higher safety margin is present. Lastly, Veksler et al. (2016) expands on the contributions of these two papers. Additional arguments mentioned for load levelling TA algorithms are that emissions can be reduced as they tend to increase during (upward) load transients. In addition, this form of load levelling could prevent excessive starting and stopping of DGs, which create additional pollution and wear and tear during their start procedures [Veksler et al., 2016].

A.3. Current best practices

Chapter A.3 will elaborate on the current best practices within the industry. By doing so, factors and consequences posing difficulty in improving DP operations are revealed. The first section A.3.1 will discuss operational practices, elaborating on the safety incentive during operations and how this is implemented in operational guidance. Subsequently, section A.3.2 presents how this influences the operational DP profile of a vessel compared to its system characteristics.

A.3.1. Operational practices

The real-time implementation of GHG emission-reducing measures for DP operations has been limited so far. This appears to be caused by current practices that are generally not well reflected within existing research. In particular, safety, which is highly prioritised in the offshore industry, seems to play a crucial role. Section A.3.1 will therefore expand on the impact this has on DP operations. Subsequently, section A.3.1 will elaborate on how this safety incentive is represented within operational guidance. Section A.3.1 will lastly discuss the shortcomings of current GHG-reducing guidelines and regulations regarding DP operations.

Safety incentive

Many of the current requirements and guidelines for DP operations have been established to ensure high safety standards. Section A.2.1 already explained how this affects the system design by discussing the different equipment classification notations. Moreover, the incentive for maintaining high safety standards also influences how a vessel is operated during DP. This became particularly clear from presentations and personal conversations at the IMCA DP Conference (2023). Here, most of the discussed topics focused on securing safety during DP operations. Though, as current practices are strictly focused on safety, efficiency is negatively affected.

During one of the discussion rounds of the IMCA DP Conference (2023), attention was paid to improving vessel efficiency through hybridisation, primarily through hybridisation with the implementation of batteries. Particularly here, under-trust in the safety of such new types of technologies was visible. Throughout the round, stakeholders raised concerns regarding the lack of large amounts of testing, insufficient battery health indicators, the current inadequate training of crew or the burden of proof that comes with the implementation of batteries. This illustrates how, from a contractor's side, safety concerns limit the progression of implementing GHG emission-reducing measures for DP operations.

The same is also the case for clients who hire marine contractors for their offshore services. Any failures during DP operations could have severe consequences for them, e.g., financial losses. Because of this, some clients obligate their contractors to operate with an open bus-tie configuration despite the fact that procedures on board are solely aimed at closed bus-tie configurations.
As elaborated in section A.2.3, closed bus-ties could significantly decrease fuel consumption up to 10 to 15%. Nevertheless, this shows how clients value safety more than the extra fuel costs and GHG emissions the client has to compensate for. Besides, the added degree of safety of operating with an open bus-tie configuration is another topic of debate.

Also, from an operator's side, the safety incentive reduces efficiency. Data analysis showed cases where vessels with four DGs operate on all of these with an equal load of 15% MCR. Alternatively, the ship could be operated within limits if only two DGs on 30% MCR are operated, as it would significantly improve efficiency and fuel consumption. It appears that such cases exist as operators want to ensure maximum safety while having slight under-trust in the system's capabilities [Diggelen et al., 2018]. However, it can be argued that there are also other human factors which play a role in this, like company pressure [IMCA DP Conference, 2023].
Nevertheless, these examples illustrate how the prioritisation of prioritisation of contractors and clients as operators significantly reduces operational efficiency. As gathered from personal communications at Boskalis, humans have a false sense of safety in the end. Considering that the amount of risk can be quantified by a certain likelihood and impact severity, consequences will, in the end, remain the same, though the likelihood can be reduced.

Operational guidance

Although there are several regulations and guidelines established, DP operations are primarily managed by the self-regulation of contractors [IMCA, 2022a]. A variety of documents are therefore used as operational guidance for operators. Its purpose is to facilitate clear communication between stakeholders involved, predetermine the risks involved in the operation, and act as a decision support tool. Nevertheless, it is crucial to understand the structure and contents of these documents as they determine the limits to which a vessel is allowed to operate during DP. During the remainder of section A.3.1, the three significant documents are discussed.

Failure modes and effects analysis
Failure modes and effects analysis (FMEA) is defined as a systematic process executed to identify potential failures. Its purpose is to eliminate these or minimise the associated risk [IMCA, 2019]. Through this, the WCF of a vessel is determined, making operators aware of the vessel's limitation and providing guidance in the event a failure occurs.

Operational Manuals
Two different operational manuals are established for DP. First, the DP operations manual contains information only necessary for operating the vessel under DP system control [IMCA, 2020]. Such documents provide an overview of, e.g. the established organisational responsibilities, DP system descriptions, the vessel's FMEA and capability plots during DP.
Alternatively, the vessel's operational manual describes all vessel systems external to the DP system. This document will still contain information relevant to DP operations, depending on the specific vessel type [IMCA, 2020].

The documents mentioned above solely depend on the specific vessel and the systems on board, reporting its corresponding limitations. Therefore, these documents are set and cannot be altered to improve DP operations, at least not without changing the vessel's design. These documents are, however, direct input for the subsequent documents.

Critical Activity Mode

The Critical Activity Mode (CAM) defines the most fault-tolerant configuration of a vessel for critical DP operations [IMCA, 2022a]. This ensures that DP2 or 3 class vessels do not exceed their WCFDI during operations in the event a failure occurs [IMCA, 2021a].

If it is permissible to operate with a lesser standard of fault tolerance, the CAM can be replaced by the Task Appropriate Mode (TAM). Risk assessment should then have demonstrated that the consequences of exceeding the WCFDI are within acceptable margins [IMCA, 2021a].

The difference between these can be illustrated with a DSV as an example. If the operation involves human divers in the water, a CAM is likely to be used, which will require the vessel to operate with an open bus-tie configuration. Alternatively, if the operation only involves a remotely operated vehicle (ROV), a TAM could be used to allow the vessel to operate more efficiently with a closed bus-tie configuration. As is shown in the example presented in figure A.8, this type of document uses a tabular layout with two columns. The first column defines the normal operational conditions, and the second column outlines which conditions require the conduction of a risk assessment.

	Green	Blue
Definition	Normal operations – all systems and equipment fully operational, DP verification processes completed, and DP set up confirmed	Advisory status – where any of the GREEN conditions are not met
Response	For DP operations to commence and continue the conditions in the GREEN column must be met	Conduct risk assessment to determine whether to continue, change position or cease operations

Action	Continue normal operations	Informative/consultative status (risk assess)
Switchboard configuration	All bus ties open	Any other configuration
SG1, SG2, DA1 and DA2 (testing)	Tested at 100% on field arrival or within last 6 months	Not tested to 100% within 6 months or problems present
SG1, SG2, DA1 and DA2 configuration	SG1 and SG2 online, DA1 and DA2 stand-by	Any other configuration or problems present
Emergency generator	Auto-start selected and available for use. Auto start/connect tested prior to arrival on field	Any other configuration or know problems that reduce redundancy
Blackout drill (single fuel system)	Blackout drill conducted for all DPOs and engineers. Procedures in place	Any DPOs or engineers not performed blackout drill within the last 6 months
DP power supply	All UPS functional and load tested for 30 mins 24 hours prior to field arrival. Note: Batteries to be at optimum charge before entering 500 m zone	Any other configuration or known problems that reduce redundancy. Not tested for 30 mins prior to field arrival
24 Vdc power systems (load test)	All fully functional with crossover breakers DC 10 and DC 20 open. 30 min battery tests performed and at optimum charge before entering 500 m zone	Any other configuration or known problems that reduce redundancy. Not tested for 30 mins prior to field arrival
Main engines (drive)	Operational and tested to 100% prior to field arrival	Engines not capable of 100% output or problems present
Propellers and rudders (configuration)	One pump running on each with stand-by pumps ready	Any other setup or loss of any rudder
Bow thrusters 1 and 2	Thrusters tested to 100% in both directions on manual and DP at field arrival	Thrusters not capable of 100% command or problems present
Stern thrusters 1 and 2	Thrusters tested to 100% in both directions on manual and DP at field arrival	Thrusters not capable of 100% command or problems present

Figure A.8: CAM outline (left) and example (right) for a basic two split configuration with shaft generators, for ROV operations[IMCA, 2022a, IMCA, 2021a]

DP vessels often have just one CAM and one TAM. Several cases have, however, been observed where only a CAM is used. As a result, the ship will continuously operate in its most redundant, typically least efficient, configuration.

Such documents are furthermore unique per vessel, as these depend on vessel characteristics and the FMEA [IMCA, 2022b]. However, the operational characteristics of some vessels, such as OSVs or Anchor Handling Tugs (AHTs), vary a lot. As DP vessels often have one CAM and TAM, there is a risk that their operational characteristics are not well defined in these documents. Especially considering some offshore vessels have switched from the oil & gas industry to offshore wind.

Lastly, an ambiguity in the CAM's main objectives can be discussed. As defined by [IMCA, 2022a], the purpose of this document is to ensure the vessel is able to accept the WCF. However, as a result, this document defines the most redundant configuration. It can be discussed that a less redundant but more efficient configuration could prevent a vessel from exceeding its WCDFI. As DP operations are primarily managed through self-regulation, contractors themselves would have the ability to make such changes if these comply with regulatory and client restrictions.

Activity Specific Operating Guidelines The Activity Specific Operating Guidelines (ASOG) define the operational, environmental, and equipment performance limits for the specific activities a vessel could undertake [IMCA, 2022a]. If a ship is likely to perform different types of DP activities, multiple ASOGs should be drafted for each of these activities. The limits of each ASOG are based on the defined levels of risk for each activity and location. The ASOG furthermore provide guidance if limits are being exceeded.
This document has a tabular format containing four columns, as is shown in figure A.9. Each column defines the conditions if operations have a normal, advisory, degraded or emergency status. Specific limits for DG loading, vessel excursions or thruster loading levels are covered in each of the columns.

Activity Specific Operating Guidelines – Outline				
	Green	Blue	Yellow	Red
Definition	Normal operations – operational, environmental and equipment performance criteria are all categorised as normal.	Advisory status – operational, environmental or equipment performance limits are being approached. An event or failure has occurred that does not compromise single-fault tolerance of the DP system.	Degraded status – approaching operational, environmental or equipment performance limits have been reached. A condition exists which may require a suspension of operations.	Emergency status – operational, environmental or equipment performance limits have been exceeded. A condition exists which requires an immediate termination of operations.
Response	For DP operations to commence and continue the conditions in the **green** column must be met.	Operations can continue whilst risks are being assessed. Conduct dynamic risk assessment to determine whether to continue, change position or cease operations.	Preparations should be made to suspend operations in a controlled manner. Contingency procedures should be initiated with a view to reducing the time to terminate. The operation should not be resumed before the vessel has regained redundancy or before all risks have been fully assessed to determine whether it is acceptable to resume operations with compromised redundancy.	Abandon operations. Take immediate action, to ensure the safety of people, the vessel, the environment and the operation. The vessel should be moved to a safe position. No DP operation is to be recommenced until a full investigation has been implemented with the failure resolved and full normal capacity verified by testing.

Action	Continue normal operations	Informative/consultative status (risk assess)	Prepare to suspend operations and initiate contingency plan (be ready to move off)	Stop operations Disconnect/bell recovery/DP reliant operation to stop
Shaft generators SG1-2	SG1 and SG2 online, DA1 and DA2 stand-by. No alarms	Any other setup or alarms	Any generator failure	
Shaft generator loading	SG1 and SG2 <45%	Any SG approaching 50%	Either >50% or failure of a generator	
DP UPSs	No UPS in bypass, no alarms	Any UPS in bypass or alarm	Loss of one DP UPS	
24 Vdc system	All 24 Vdc active and fully charged. No alarms	Any alarms	Loss of 24 Vdc system or charger failure	
Main propulsion (engines and rudders)	Both enabled, no alarms	Any other setup, any alarms or poor control	Loss or either port or starboard engine or rudder	
Bow thrusters available	Both enabled, no alarms	Any other setup, any alarms or poor control	Loss of any bow thruster	
Stern thrusters available	Both enabled, no alarms	Any other setup, any alarms or poor control	Loss of any stern thruster	
Fuel systems	No alarms	Any sign or potential threat of fuel oil contamination, supply line blockage, or any other supply failure	Loss of any generator due to fuel oil contamination, line blockage, or any other supply failure	

Figure A.9: ASOG outline (left) and example (right) for a basic two split configuration with shaft generators, for ROV operations[IMCA, 2021a]

A common problem, which is also discussed by [IMCA, 2021b], is that ASOG is developed to ensure a vessel is operated with an appropriate level of safety for a specific activity at a particular location. As a consequence, redundancy requirements pile up and may often lead to inefficient vessel operations.
Secondly, it appears that for projects with multiple scopes of work, commonly just one ASOG is drafted. Considering this document is drafted for the worst-case scenario, such an ASOG will contain the most stringent criteria to be applied throughout the whole project [IMCA, 2022b].
Lastly, ASOGs are the responsibility of contractors. They should make these documents themselves based on their level of risk and experience with their vessel. Client opinions are, however, also considered when drafting such documents. As established, they consider safety of much higher importance than aspects such as fuel consumption. As a result, this could result in ASOG with very high, though unnecessary, amounts of redundancy.

GHG reducing guidelines and regulations

While safety regulations are highly valued and generally followed by offshore contractors, regulations pressuring decarbonisation seem to come up short for DP.
Two examples are the Energy Efficiency Design Index (EEDI), which is mandatory during the design and construction of a vessel, and the Energy Efficiency Operator Index (EEOI), which is voluntary [Ihle et al., 2016]. Firstly, the calculation scheme of these indices is not entirely applicable to ships with diesel-electric propulsion [Ihle et al., 2016]. Secondly, nearly none of DP operations require cargo to be transported from point A to B. Sailing distance, or vessel speeds are on top of that, either low or close to zero.
The latter two arguments also apply to the recently implemented Carbon Intensity Indicator (CII) of the IMO [DNV, 2023]; this is again an index which is expressed as the amount of CO2 emitted per cargo-carrying capacity and nautical mile [IMO, 2022].

A.3.2. Operational profile against vessel characteristics

The contents discussed in section A.3 have shown how safety is embedded in current practices. Section A.3.2 will further elaborate on how efficiency is affected by illustrating the mismatch between the operational profile during DP and the vessel's system characteristics. The first section A.3.2 will discuss the causes and consequences of operating DGs at very low loads. Section A.3.2 will subsequently discuss the load variabilities DGs have to endure. A conventional power system of a DP offshore vessel, presented in section A.2.2, will be used to illustrate this. Such a system is assumed to consist of two power sections, each side containing two DGs of equal size.

Low engine load utilisation

The peak efficiency of a DG is typically around 80 to 90 % of its MCR [Woud and Stapersma, 2017]. However, it quite rarely occurs that DGs have to operate at such loads during DP [Swider and Pedersen, 2019].
The equipment classification presented in section A.2.1 is the first reason for this. The purpose of the class 2 and 3 notations is to ensure that no single-point failure should exceed the WCF. As a result, the maximum allowable load per power section will already be near 50%. Considering at least one DG has to be used per power section, a DG should not be operated above 50% of its MCR with current operational practices.

Additionally, it should be considered that also the propulsion system is affected by the equipment classification as thrusters have to be evenly divided across the two power sections [IMO, 2017, ABS, 2021b]. However, in the event of a power blackout, half of the propulsion will not only have to compensate for the missing amount of thrust but also the decreased thrust allocation efficiency. As a result, the remaining power section likely has to compensate for more than 50% of the missing power. Consequently, most CAM and ASOG consider a maximum power limit of 45% MCR per DG [IMCA, 2021a].

Lastly, it appears that it is not common practice to operate with only one DG per switchboard. As was already established in section A.3, this has to do with the safety incentive from an operator perspective. Furthermore, it can be argued that vessels operating with more spinning reserve are more capable of accommodating sudden load increases [Montonen et al., 2022, IMCA, 2021a]. As result, DG are often operated around 15% MCR on average, with general load ranges between 10 to 25% MCR per DG [Vásquez, 2016, Lazarewicz and Rojas, 2017, Kulkarni and Santoso, 2009]. Figure A.10 illustrates such a load profile of DP operations from an OSV and the corresponding high sfc.

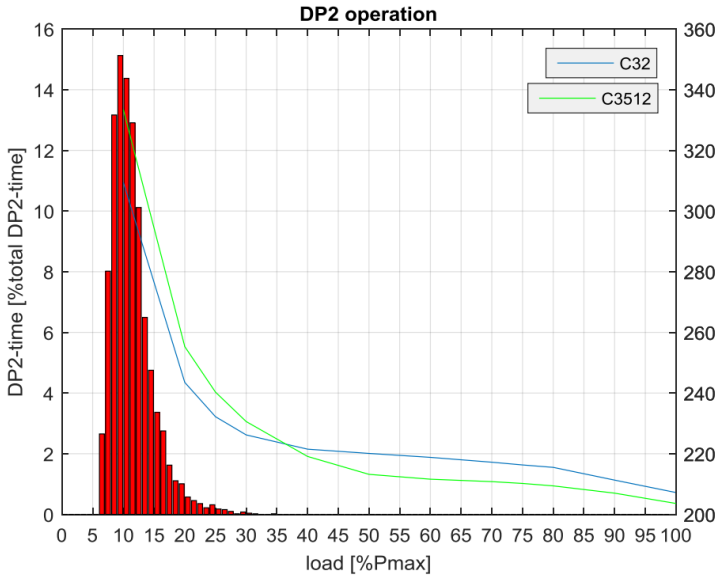


Figure A.10: Switchboard load profile during DP operations of an OSV, against sfc curves of corresponding DGs installed [Malikouti, 2016]

Operating DGs at such low loads has several negative consequences. Such as ignition problems, increased maintenance, decreased DG reactivity to load changes, reduced system reliability or increasingly pollutive GHG emissions [Tufte, 2014].
Besides, as combustion conditions are less favourable, they lead to relatively higher amounts of GHG emissions than just the increased amount of fuel consumption. This will especially be the case for the nitrogen oxides (NOx) and Particulate Matter (PM) [Lindstad et al., 2017, Lindstad and Sandaas, 2016].

Load variability

Additionally to the low loading, DGs are also subject to load variations during DP operations, illustrated by figure A.11 [Godjevac et al., 2017]. On top of that, several papers have indicated that over-actuated DP vessels are more common, which would further aggravate this problem [Arditti et al., 2018, Wu et al., 2016, Kalikatzarakis et al., 2022].

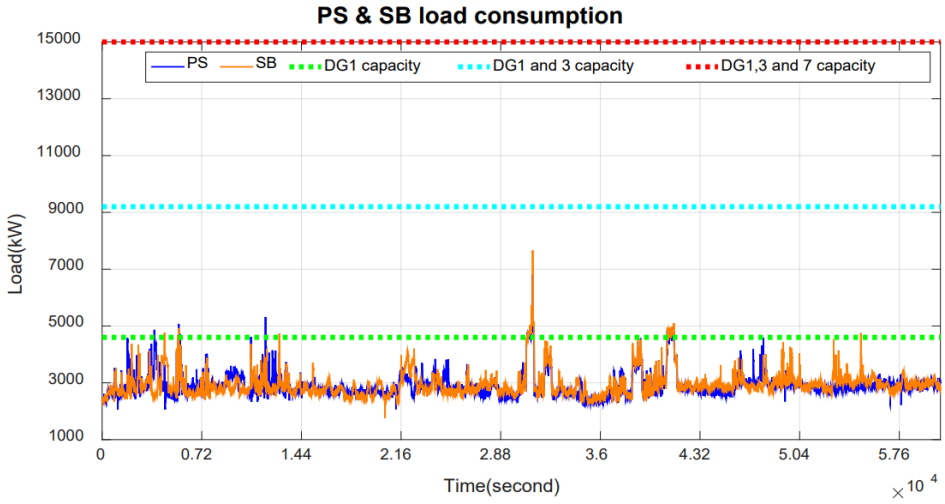


Figure A.11: Port- and starboard power section load consumption during DP of a heavy lift crane vessel [Lyu, 2016]

Furthermore, it should be considered that DGs have one of the slowest response times within the marine power systems, according to Radan et al. (2008). Because of this, the PMS should have power limitation functions, such as load shedding, to prevent the occurrence of power blackouts from such fluctuations [Sørensen, 2018].

Still, the poor response of DGs increases the risks of power section blackouts through possible frequency or voltage disturbances on the power grid [Radan et al., 2008, Veksler et al., 2014]. Additionally, system reliability is reduced due to the increased wear-and-tear on machinery, and emissions tend to increase during load transients. This is further aggravated if such load transients cause unnecessary start procedures of DGs [Veksler et al., 2014].

As was established in section A.3.2, operating on multiple DGs per power section is one of the factors causing DGs to have to operate at low powers. Another drawback of this is that the responsiveness of DGs is particularly poor if operated close to its limits [Tufte, 2014, Radan et al., 2008]. According to Montonen et al. (2022), however, operating on a single DG could still pose problems for handling load transient.
Alternatively, load transients can be distributed among multiple DGs in operation. As a result, the power system would have a higher degree of resilience against such variations in power [IMCA, 2022a]. In that sense, it could be argued that operating with a closed bus-tie configuration could also increase system reliability. This would enable power fluctuations to be distributed across three to four DGs compared to only two DGs when operating with an open bus tie.

A.4. Reflection

Based on the improving measures presented in chapter A.2 and the current best practice elaborated in chapter A.3, chapter A.4 will reflect the contents of these chapters against each other in order to determine which solutions would be most effective given the scope of this literature study.
First, section A.4.1 will discuss the different assessment criteria. Subsequently, each of the DP improving measures is evaluated in section A.4.2 on which a conclusion will be given in section A.4.3.

A.4.1. Assessment criteria

The objective of this literature study is to identify and select GHG emission-reducing solutions for DP operations. The degree to which harmful emissions can be reduced is, therefore, a first assessment criterion. Fuel consumption and efficiency are still taken into account when considering whether the expenditures of a solution would be proportional to the savings achieved.
As elaborated in chapter A.1, the demand for offshore services requiring DP will only increase in the upcoming years. The technical feasibility of implementing solutions on existing vessel designs will, therefore, be considered. In addition, it will be assessed whether solutions are either effective for a variety of different DP vessels or only for a limited amount of cases.
Whether solutions are operationally feasible, given the current operational practices, will furthermore be assessed using the contents of A.3.1. The impact of solutions on safety standards will lastly be taken into account.

A.4.2. Reflection on state-of-the-art solutions

Section A.4.2 will reflect on the GHG-improving solutions of chapter A.2, using the assessment criteria presented in section A.4.1. The order in which solutions are given is in respect to that of chapter A.2. In hindsight, GHG-reducing methods throughout this literature study can be categorised into three different directions. These are operational adjustments, technical adjustments or major overhauls. As will be discussed later in this chapter, a combination of solutions was selected, which mainly focused on adjusting operational aspects. Ultimately, this corresponds best to the scope of the overall research.

Power generation redesign

Redesigning the power generation system could enhance configuration flexibility and allow DGs to operate closer to their optimum. To achieve this, it is vital to prioritise the analysis of the vessel's operational profile and to consider efficiency during the design processes, as opposed to focusing on redundancy.

Fuel and emission savings depend, however, on the degree of inefficiency of the existing power generation system. Therefore, this approach would only be viable for specific ships which have an inefficient system combined with enough space for changes to be implemented.
Fuel savings still might not weigh up against the cost and effort required. Research of Rekelhof (2016) and Bø et al. (2013), present fuel savings of 2 to 8%. Such savings would be significant for newly built vessels, though they are likely not cost-effective for retrofits.
In addition, aiming to operate with high power utilisation poses a challenge. The newly designed system should still adhere to redundancy aspects, such as accepting the WCF or being able to handle sudden load variations [Osen, 2016]. These aspects do not seem to be entirely taken into account in Rekelhof (2016) and Bø et al. (2013), raising doubts on the feasibility of achieving such fuel saving.
Another critical remark made by Osen (2016) is that the power generation system with the highest efficiency will have the least amount of installed power possible. The minimum required is determined by the most extreme conditions the vessel has to withstand. As a result, reducing the standards of such assumptions will improve efficiency but negatively affect safety levels.

Considering the limited applicability range, very poor applicability to retrofits and likely insufficient fuel savings, this solution is not entirely suitable in accordance with the presented scope.

Implementation of energy storage devices

Extensive research has already been conducted on the implementation of ESDs. Potential types considered are lithium-ion batteries, supercapacitors, and flywheels. Spinning reserve and peak shaving applications have primarily been investigated. Spinning reserve ESDs are typically larger as they have to provide higher amounts of power.
As pointed out earlier as a later added note, throughout the literature study, a clear distinction is made between the characteristics and performance of ESDs for spinning reserve replacement and ESDs for peak shaving. Although a combination of these two could be possible, a similar distinction was visible and adopted from current research. Only later on during the research other functions, combinations and practical aspects were discovered. Therefore, note that some of the statements initially made within the section about ESDs, or the whole literature study in that sense, may not be applicable given the current knowledge. However, these have not all been adopted in the main report, as ESDs are out of the scope of the main research.

As is discussed in section A.2.2, supercapacitors are only applicable for peak shaving applications. On top of that, Adeyemo et al. (2023) discusses that they are usually not considered ships due to their high capital costs and relatively short life span. Since operational experiences for offshore applications are additionally very limited, supercapacitors are not further considered.
This is similar to flywheel applications, which are also limited to peak shaving and require high capital costs. Additionally, flywheels would require constant charging if their power is not used, are voluminous and heavy [Lyu, 2016, Adeyemo et al., 2023]. Given current research has mostly focused on its application for improving frequency and voltage stability, flywheels will also not further be considered as ESD.
Batteries are, in that sense, the most suitable ESD option for DP. Especially due to their variety in many marine applications and their operational flexibility [Malikouti, 2016, Adeyemo et al., 2023].

Nonetheless, the GHG and fuel savings of battery applications highly depend on their given functions and the ship they are applied to [Godjevac et al., 2017, Lyu, 2016]. Papers on spinning reserve applications have presented fuel savings of around 15 to 20% [Lyu, 2016, Godjevac et al., 2017, Vásquez, 2016]. Research of Lindstad and Sandaas (2016) and Lindstad et al. (2017) on top of that discusses these savings will have an even higher impact on the reduction in GHG emissions.
However, similar research has not reported fuel savings for peak shaving applications. Montonen et al. (2022) discusses this is due to transmission losses between the charging and discharging processes of the battery. It appears, however, that these papers have not considered that with peak shaving, fewer DGs are necessary for handling quick load transients. Theoretically, only one DG would be required to deliver sufficient power whilst the battery handles load fluctuations.

Still, the proportionality between expenditures and savings of both applications is questionable. As spinning reserve batteries will have a similar power capacity of one DG, these will be larger and more expensive than peak shaving batteries. As is also presented by Lindstad et al. (2017), the payback period for a retrofit with spinning reserve batteries is not convincing. Especially if it is considered that batteries should be oversized for their applications in order to prevent a relatively short life cycle Adeyemo et al., 2023. Results could, however, be different for vessels that spent significant amounts of time in DP mode. Still, in that sense, peak shaving applications are interesting as they are generally less expensive and as some aspects appear to be omitted from current research.

Technically, implementing batteries on existing vessels still poses some challenges. First, for both applications, the PMS should be upgraded to an EMS [Lyu, 2016]. Secondly, adding batteries to an existing grid will result in higher short-circuit currents, which the existing system might not be able to withstand [Vásquez, 2016]. Thirdly, space should be reserved for battery compartments which contain several safety features in the event of a thermal runaway or battery fire [Adeyemo et al., 2023, IMCA DP Conference, 2023]. The latter two aspects will be more challenging for spinning reserve batteries, given their higher capacity and size.

Lastly, safety regarding battery applications is still a major concern for some of the primary industry players, as was highlighted during the IMCA DP Conference (2023). Thermal runaway events or battery fires are, however, not expected to be an issue, given the already existing battery compartments. Even more, it could be discussed that both battery applications would enhance safety given their ability to either provide immediate backup for DG failures or reduce blackout risk by ensuring grid stability. Nevertheless, the operations themselves could be endangered after a battery failure. For spinning reserve applications, this would be more severe, as these are only used if a failure to a DG has already occurred. Also, as spinning reserve batteries are backup systems, the risk of hidden failures is greater. Peak shaving batteries are, in that sense, operationally safer, as the vessel will not be entirely dependent on these during an operation. Moreover, the risks of hidden failures are smaller as peak shaving batteries are constantly used during an operation.

Although research has indicated significant fuel savings from spinning reserve batteries, their implementation is somewhat challenging given the proportionality between costs and savings, their technical feasibility for implementation on board existing vessels and operational safety concerns from the industry. Given this literature study, spinning reserve applications of batteries will not be further considered as this research mainly aims to improve DP operations through operational measures rather than major technical overhauls.
For smaller peak shaving batteries, however, the technical feasibility and operational safety aspects seem to be more achievable for existing vessels and current operational practices. On top of that, state-of-the-art research appears to have overlooked aspects which could lead to more significant fuel savings. However, because of the slow response of DGs, combined with safety criteria which order DGs to operate far below their optimum, there are so-to-say fewer peaks to shave. Still, peak shaving applications of batteries are further considered.

Alternative fuels

Alternative fuels are widely considered a promising solution for reducing GHG emissions within the maritime industry. Fuel conversion of an existing vessel certainly comes with a set of technical challenges, such as power system modifications or adjustments to the fuel tanks. Despite these challenges, alternative fuels are still considered in this study due to their potential to reduce GHG emissions significantly.

Capital expenditures are a well-known problem that serves as a disincentive for contractors to implement such large conversions. This problem could be tackled by subsidising such conversions and if converted vessels are selected more quickly by clients. However, the latter is currently not applicable because of the large demand for offshore DP vessel service.

Additionally, it remains unclear whether alternative fuels are feasible for this application. As elaborated in section A.3.2, DGs are operated at very low loads during DP. This can pose difficulties for alternative fuels, such as LNG or methanol, as this could cause incomplete combustion. As a consequence, methane or methanol slip can occur, which are both highly polluting GHGs [Stapersma, 2010]. Similarly, load transients can also pose challenges for both alternative fuels as dual-fuel engines given that their dynamic response is often worse than conventional fuelled engines [Lindstad et al., 2017, Pestana, 2014]. This suggests that alternative fuels are only feasible for DP operations if ESDs are added to compensate for their poor dynamic behaviour.

The current implementation of alternative fuels is, therefore, quite limited for offshore DP vessels. So far, the Orion of Deme and the Sleipnir of Heerema are the only offshore DP vessels which have implemented alternative fuels through a duel-fuel LNG system [Clarksons, 2023]. The implementation of fully fuelled LNG or methanol power systems still has to be realised for offshore DP vessels [Rozendaal, 2021].

Although they have a significant GHG emission-saving potential, their technical challenges, high capital costs, and the uncertainty regarding their feasibility for DP operations are the reasons why alternative fuels will not be further considered.

Closed bus-tie configuration

During closed bus-tie operations, the usually separated power sections are connected. As a result, the power sections cooperate, and the number of DGs online can be reduced whilst still fulfilling the WCFDI [Lindtjørn et al., 2014, Sørensen, 2018].

Significant fuel savings of up to 10 to 15% have been observed for a case vessel of Boskalis, with a conventional power system as described in section A.3.2. Similarly, Lindtjørn et al., 2014 has shown fuel savings of 9% for drilling vessels.
Implementation costs are additionally relatively low, as in theory, only an improved bus-tie breaker is required, which is able to prevent fault propagation between power sections [Garg et al., 2011].
Given that all DP2 and 3 vessels are required to have a split power system, such a measure would, on top of that, be applicable to the majority of diesel-electric offshore DP vessels [IMO, 2017, ABS, 2021b].
Closed bus-tie configurations are even proposed in guidelines of the IMCA (2022a) or ABS (2021b)
However, some clients especially pose against closed bus-tie breakers as it increases the chances of a complete vessel blackout due to possible hidden failures [Garg et al., 2011]. Contractors are, therefore, sometimes obliged by clients to operate with an open bus-tie configuration.
It can be discussed, however, that sufficiently reliable closed bus-tie breakers have already been developed for preventing power section blackout proportions [Garg et al., 2011]. In some cases, contractors have already been allowed to operate with a closed bus-tie configuration without seemingly significant differences in event reports [IMCA DP Conference, 2023].

Given the significant advantages, closed bus-tie configurations will further be considered throughout this study. However, open bus-tie configurations will also be taken into account, given the current industry practices.

Direct current grid

Converting a vessel's power system from AC to DC would enable DGs to operate at variable speeds. As a result, efficiency increases and new hybrid technologies can be implemented more easily [Chai, Sobrayen, et al., 2016, Nebb et al., 2012].

Although results between Chauhan et al. (2016), Chai, Sobrayen, et al. (2016)] and Zahedi et al. (2013) do not completely align, significant fuel savings of 5 to 9% have been reported respectively. Implementing an ESD additionally, could even yield fuel savings of 15 to 20% according to Hansen et al. (2011), Zahedi et al. (2014) and Zahedi et al. (2013).

Despite these significant fuel savings, the applicability of DC grids to existing DP vessels is questionable. Although DC grids require fewer electrical components, a complete redesign of the power distribution system is needed, which is very costly. Typically, DC grids are therefore often more viable for retrofits of small vessels or new build projects [Vásquez, 2016, Oomen, 2016].

DC grids do offer several safety enhancements, such as improved grid stability through the absence of frequency synchronisation or quicker DG recovery after a power loss [Hansen et al., 2011, Oomen, 2016]. However, as there is no slack within a DC system, there is little room for error in voltage regulation [IMCA DP Conference, 2023, Accetta and Pucci, 2019]. DGs are, on top of that, more prone to suffer from load variations, given their dynamic behaviour decreases when operating at variable speed [Nebb et al., 2012, Kambrath et al., 2017]. Short-circuit currents are additionally developed in a much shorter time [Vásquez, 2016, Hansen et al., 2011]. The combination of these aspects makes voltage regulation of a DC system much more difficult, therefore requiring a more complex and costlier protection system. Although adding an ESD could mitigate some of these problems, it would introduce even higher costs.
Therefore, despite the significant potential savings, DC grid conversion will not be further considered.

Unequal generator loading

The objective of unequal generator loading is to have one DG operating at a higher load than the others. By doing so, the majority of the requested load is generated more efficiently with a lower sfc. This results in reduced GHG emissions, fuel consumption, and maintenance [Chauhan et al., 2016, Rao et al., 2015].

While significant fuel savings have not been indicated so far, with these, on average, being 3%, some aspects of current research could be improved. Firstly, accurate sfc curve modelling of DGs significantly affects the fuel-saving outcomes, particularly given DGs are operated at very low loads [Chauhan et al., 2016, Rao et al., 2015]. Note that GHG emissions are also significantly worse at lower powers, particularly concerning NOx gasses and soot Stapersma, 2010.
Current research has, on top of this, only investigated relatively simple power system configurations, consisting of two switchboards with two DGs on either side. Although this concept could work for any diesel-electric configuration, the more engines on a ship, the better the savings of this concept are, as there is a lower load to be distributed from different DGs to the one DG operating at a higher loading. While this concept could be viable for any diesel-electric configuration, more significant fuel savings are likely to be achieved for ships with more and different engines. This is because there is more load to be distributed among DGs.

Moreover, as only an adjustment is required to the PMS, unequal generator loading would be applicable to a variety of existing DP vessels. Such a measure would also be operationally feasible if current operational guidance and the requirements regarding the WCF are evaluated carefully. An increase in safety could lastly be discussed, as a DG operating closer to its intended design point is arguably less likely to fail.
Overall, unequal generator loading will further be considered due to its applicability to a wide range of existing vessels, limited disadvantages, and the relatively little amount of research executed so far.

Load dependent start-stop table optimisation

The objective of load-dependent start table optimisation is to improve DG scheduling based on the loads demanded from the system [Radan et al., 2006].
This solution could help reduce unnecessary (cold) starting procedures of DGs, resulting in reduced GHG emissions and maintenance [Radan et al., 2005]. Although fuel savings vary between papers, reductions of 2 to 8% have been indicated by Radan et al. (2005) and Bø et al. (2013).
As this measure would only require a change in the vessel's PMS, it can easily be applied to a variety of existing diesel-electric vessels. Also, in this case, potential savings could be higher for ships with a more complex power generation system [Radan et al., 2006].
Within current practices, operators override automatic control systems by committing additional DGs. Careful consideration of the operational implementation of load-dependent start table optimisation is therefore required. This could be achieved through operational guidance, as otherwise, the automatic system would be overridden. In order to maintain current safety levels, consideration should furthermore be given to accepting the WCF.
Overall, load-dependent start table optimisation can be applied to a variety of existing vessels, offers several advantages by preventing unnecessary DG start procedures and has no significant drawbacks.

Thruster allocation algorithm improvements

There are several ways a vessel's TA algorithm can be improved. Solutions presented in section A.2.5 range from improved optimisation algorithms to more accurate vessel system modelling, such as considering hydrodynamic effects.

Fuel savings of TA improvements are, however, rarely discussed, with only Kalikatzarakis et al. (2022) discussing reductions of 5% by taking transmission characteristics into account. Nonetheless, implementation costs are likely to be relatively low as only the vessel's control system needs to be adjusted. Implementing such improvements to the TA algorithm does require a trade-off between increased complexity and reduced computation time [Kalikatzarakis et al., 2022, Wu et al., 2016]. If the vessel's computer system cannot handle the complexity of the TA algorithm, solutions and thruster settings may take longer to compute. As a result, this could lead to decreased vessel response time to environmental effects.

In conclusion, although improving the TA algorithm of a vessel could result in GHG reductions, associated fuel or power reductions are often not discussed within the literature. The results, on the other hand, usually focus on improved controllability or controller robustness. Additionally, such knowledge within Boskalis is limited as other companies develop their DP systems. Therefore, this solution will not be considered further.

Load levelling thruster allocation controller

A load levelling TA algorithm is the last solution for decreasing GHG emissions by assisting the power system with reduced load variations. Firstly, this can be achieved by redistributing power from the load-fluctuating consumers to the thrusters. An alternative approach is to allow more significant position deviations so that thrusters require a more consistent power supply.

The degree to which this measure reduces fuel or GHGs is, however, not discussed within current research despite being one of the major arguments for its implementation. On top of that, Radan et al. (2008) and Veksler et al. (2012) warn that power variations and additional position allowances should be carefully selected as they could also reduce efficiency and, with that, increase fuel consumption.
This solution can again relatively easily be implemented for existing vessels by reprogramming their control systems. However, as this solution partially depends on significant power fluctuations from heavy consumers, it will not be relevant for every type of vessel. Crane or cable lay vessels are conceivable vessels with such heavy consumers, though OSVs are likely not.
Another critical remark is that safety will be affected if greater position deviations are allowed. This would especially be problematic for DSVs, which operate with human divers in the water. In that sense, the implementation of an ESD would be a more applicable and safer solution as it will not affect the vessel's position-keeping.

Overall, given the potential safety risks and possible better solutions, load-levelling TA algorithms will not be further considered.

A.4.3. Conclusion

The objective of this literature study is to identify and determine effective solutions for reducing GHG emissions of DP operations from offshore vessels, considering an existing ship design and current industry practices whilst maintaining safety standards. he reflection of section A.4.2 is summarised in Table A.1. Based on the reflection, several solutions will not be considered for the remainder of this study.

As discussed at the start of this chapter, in retrospect, methods for reducing GHG emissions can be divided into three main categories: operational adjustments, technical adjustments, or major overhauls. Given the scope of this research and the corresponding selected assessment criteria, methods regarding operational adjustments were mainly preferred for this literature study. As such, a combination of solutions that align best with this scope was selected. Additionally, technical adjustments or major overhauls will ultimately not present significant fuels if the operational practices are not in order. Moreover, the amount of fuel and power required for efficient operations, among other factors, should be known. As such, solutions regarding operational adjustments were selected.
Additionally, note that there is a clear distinction between ESDs for spinning reserve replacement and ESDs for peak shaving. Although a combination would be possible, a similar distinction was visible and adopted from current research. Lastly, the cost to savings for closed bus-tie configurations could, in reality, be less if adjustments to improved bus-breakers and PMS functions are required.

Table A.1: Summary solution assessments

	GHG reduction	Costs to savings	Technical feasibility	Range of applicability	Operational feasibility	Improvement of safety
Power generation redesign	+	- -	- -	-	+	0
Spinning reserve batteries	+ +	-	-	+	+ +	0
Peak shaving batteries	0	0	+	+ +	+ +	+
Alternative fuels	+ +	- -	- -	0	- -	0
Closed bus-tie configuration	+ +	+ +	+ +	+ +	+	-
DC grids	+	- -	- -	-	+ +	0
Unequal generator loading	0	+ +	+ +	+ +	+	0
Start-stop optimisation	+	+ +	+ +	+	0	0
TA algorithm improvements	0	0	+	+	+	0
Load levelling TA controller	-	0	+ +	-	-	- -

While solutions such as power generation redesign, DC grids or alternative fuels could significantly reduce GHG emissions and fuel consumption, significant costs and efforts are required for their implementation on existing vessels.
Alternatively, TA improvements or load levelling TA algorithms are much more straightforward to implement on existing vessels. However, as there are many possibilities in which TA algorithms can be improved and little information on the respective fuel savings, also this solution will not be further considered in this study.
Lastly, the implementation of spinning reserve batteries will also be left out of scope despite the potential GHG reductions and its great operational feasibility. This is in the end because of a combination of disadvantages, such as disputable the cost to saving proportionality, technical feasibility and effects on current safety standards for existing vessels. As a result, peak shaving batteries, closed bus-tie configurations, unequal generator loading, and load-dependent start-stop table optimisation are the four solutions considered to be effective for the given scope.

From these four, unequal generator loading seems to be the most effective given the assessment criteria. The cost to savings proportionality, technical feasibility and range of applicability first appear to be great.
Operational feasibility is also good, though special attention must be paid to current operational guidances and the operational profile of a vessel during DP. Real-time implementability and fuel savings can otherwise be compromised. The acceptance of the WCF in the event the higher loaded DG fails should especially be kept in mind. Also, methods for handling load variations should be considered.
GHG and fuel reductions appear to be limited within current research to unequal generator loading. However, there also seems to be little consensus between results, and some aspects of current research could be improved, as will be elaborated in section chapter A.5.

Closed bus-tie configurations can additionally be taken into account, as they can easily be combined with unequal generator loading and offer several significant advantages. Although the safety and reliability aspects of bus-tie breakers for preventing blackout propagation are essential, these will be left out of scope. Instead, given some clients oblige contractors to operate with open bus-tie configurations, both types will be taken into account.
Furthermore, unequal generator loading will also affect the star-stop tables of DGs. Considering the advantage this poses, especially in reducing unnecessary DG start procedures, load-dependent start-stop table optimisation could also be taken into account.
A solution that could be promising for handling the load variations with unequal generator loading is the application of peak-shaving batteries. As investigating this solution would require substantially more effort in research, peak shaving batteries are not further considered and will likely be recommended as an addition for further research.

A.5. Gap analysis

Based on the outcomes of chapter A.4, three effective solutions have been identified for the presented objective of this literature study. These are unequal generator loading, closed bus-tie configuration, and load-dependent start-stop optimisation.s.
Several research gaps have been identified during this literature review. This accounts for both general research on DP-improving measures and specific literature on the selected solutions.
Throughout chapter A.5, the identified research gaps are discussed based on three major categories. First, section A.5.1 will discuss research gaps in the operational profile of DP vessels. Next, section A.5.2 presents remarks considering the objective to reduce GHG emissions. Section A.5.3 will lastly elaborate on the currently limited implementation of DP-improving solutions.
Note that most of the aspects mentioned throughout this chapter have been improved and adopted in different sections of the report's Introduction.

A.5.1. Operational profile

The operational profile of a vessel is a critical factor to be considered, particularly for research into power systems. The first aspect to evaluate is the expected power levels the system has to deliver. Many papers assume that all possible load levels are reached during DP operations, therefore considering a power range of 0 to 100% MCR. This is particularly the case for research on unequal generator loading. Considering current practices and the requirement for accepting the WCF, DG loads are, however, not allowed to exceed 50% as elaborated in section A.3.2.
Furthermore, data analysis at Boskalis has shown that generally, for OSVs and DSVs, average DG loads range from 10 to 25% MCR with extremes of 5% to 45%. Looking more closely at current research on unequal generator loading, however, Chai, Sobrayen, et al. (2016) considers for a DSV a minimum load of 20% and an average load of 43 to 63% MCR. Similarly, Chai, Reddy, et al. (2016) considers an operational profile from 25% up to a 100% while both Chauhan et al. (2016) as Rao et al. (2015) do not report results for the average values of 20 and 25%.
The correctness of sfc curves has, on top of that, a significant impact on fuel-saving results, particularly on the characteristics of the curve at lower powers. Nonetheless, Chauhan et al. (2016) maps its sfc curves from 29% MCR onward and Rao et al. (2015) from 18%, indicating that improvements can be made to their results.

A second aspect of the operational profile that should be evaluated is the load variations the power system has to endure because of the poor dynamic behaviour of the DGs. Research on unequal generator loading appears not to consider this at all. The current practice is to share load variations across all DGs. However, it is questionable what the effects are in case power loads on DGs are not equal. It is, for example, interesting to investigate whether the highly loaded DG is able to handle load transients better than the DGs operating at lower loads. Nevertheless, load-dependent start-stop optimisation could prevent such load fluctuations from inducing unnecessary start-up processes of DGs.
Peak shaving battery applications can alternatively be considered for mitigating load fluctuations and could also allow the vessel to operate on fewer DGs. Such a solution may also be effective with the other three proposed solutions.

A.5.2. GHG emissions

Papers proposing measures to improve DP operations often substantiate their research by discussing the potential GHG reductions. Commonly, however, emissions are subsequently left out of scope and not considered further. Accurate mapping of GHG emissions from DP operations, therefore, appears to be a significant research gap in itself.

Moreover, the objective of most studies is to minimise fuel or power consumption. It can be discussed, however, that this does not necessarily lead to a minimisation of GHGs. Although all measures that reduce fuel consumption will inherently reduce CO2 emissions, such is not the case for NOx gasses or particulate matter [Stapersma, 2010].

Firstly, catalysts are much less effective at very low engine loads, therefore increasing NOx emissions [Ihle et al., 2016]. Secondly, there is a greater chance of incomplete combustion with increased particulate matter [Stapersma, 2010]. Emissions furthermore tend to increase, especially during upward load transients, which could especially be a beneficial aspect for peak shaving battery applications [Radan et al., 2008].
Solely focusing on the optimisation of fuel consumption could further result in excessive DG starts and stops. Cold DG start-ups can significantly increase GHG emissions, especially. As discussed, however, such can be reduced through load-dependent start-stop optimisation.

A.5.3. Real-time implementation

As is discussed in the problem statement of section A.1, it currently appears that current practices of DP operations are not well reflected in existing research.
One of the assessment criteria of section A.4.1, therefore, considered the range of applicability of solutions. Although unequal generator loading is considered to be applicable to a wide variety of vessels, current research has only examined this concept for relatively simple power configurations. The four papers that investigated this solution all considered DSVs or OSVs whose power systems consist of two switchboards, each containing two DGs of equal size. Therefore, it could be interesting to investigate potential fuel savings for more complex power systems that contain different DG sizes.

Current research on unequal generator loading furthermore does not appear to take operational regulations and guidelines into account. This is already clear from the fact that only closed bus-tie configurations have been considered. Also, operational guidances are neglected, with Chauhan et al. (2016) and Chai, Reddy, et al. (2016) proposing practices where only one DG is operated, which on top of that exceeds the 50% MCR limits.
From this perspective, it could further be argued that optimisation algorithms are not beneficial for the real-time implementation of solutions. Ultimately, an operator manages the vessels and intervenes if failures or abnormalities occur. As such, they have to be able to safely understand and control the power system settings, which is a factor that is not taken into account by such arbitrary optimisation algorithms. Looking at the proposed control practice of Chauhan et al. (2016) for example, determined by a GA, no clear operating strategy could be applied since power ratios between DGs seem arbitrary. An alternative method that could prevent this is drafting control algorithms with if-else statements. Such would take operator logic and operational practices into account.

A.6. Literature overview

Table A.2: Overview of reviewed literature - Part 1

References	Problem background	Regulations & guidelines	General vessel systems	Power generation redesign	Energy storage devices	Alternative fuels	Closed bus-tie configuration	DC grids	Unequal generator loading	DG start-stop optimisation	TA algorithm improvements	Load levelling TA controller	Current best practices	Operational guidance	Operational profile
ABS (2021b)		x	x				x							x	
Accetta and Pucci (2019)								x							
Adeyemo et al. (2023)					x										
Arditti et al. (2015)											x				
Arditti et al. (2018)											x				
Bergman (2023)						x									
Bø et al. (2013)				x						x					
Bui et al. (2021)					x										
Chai, Reddy, et al. (2016)									x						
Chai, Sobrayen, et al. (2016)								x	x						
Chauhan et al. (2016)								x	x						
Chen et al. (2009)					x										
Clarksons (2023)	x					x							x		
Diggelen et al. (2018)	x												x		
Dinh et al. (2018)					x										
DNV (2023)	x	x													
DNV (n.d.)						x									
Garg et al. (2011)							x								
Godjevac et al. (2017)					x	x									x
Hansen et al. (2011)			x					x							
Hein et al. (2020)					x										
HellenicShippingNews (2023)						x									
IEA (2018)	x														
IEA (2022)	x														
Ihle et al. (2016)	x	x	x										x		
IMCA (2019)		x												x	
IMCA (2020)		x	x												
IMCA (2021a)		x											x	x	x
IMCA (2021b)	x												x		
IMCA (2022a)		x	x				x						x	x	x
IMCA (2022b)		x	x										x	x	x
IMCA DP Conference (2023)	x	x	x		x		x	x					x	x	
IMO (2017)		x	x											x	
IMO (2022)	x	x													

Table A.3: Overview of reviewed literature - Part 2

Reference	Problem background	Regulations & guidelines	General vessel systems	Power generation redesign	Energy storage devices	Alternative fuels	Closed bus-tie configuration	DC grids	Unequal generator loading	DG start-stop optimisation	TA algorithm improvements	Load levelling TA controller	Current best practices	Operational guidance	Operational profile
Kalikatzarakis et al. (2022)											x				
Kambrath et al. (2017)			x					x							
Kulkarni and Santoso (2009)					x										x
Lazarewicz and Rojas (2017)					x										x
Lindstad and Sandaas (2016)			x		x										
Lindstad et al. (2017)			x		x	x									
Lindtjørn et al. (2014)							x								
Lyu (2016)					x	x									
Malikouti (2016)					x										
Montonen et al. (2022)	x		x		x										
Nebb et al. (2012)					x			x							
Oomen (2016)							x	x							
Ørsted (2023)	x														
Osen (2016)				x											
Pestana (2014)						x		x							x
Probst (2022)						x									
Radan et al. (2005)										x					
Radan et al. (2006)										x					
Radan et al. (2008)			x									x			
Rao et al. (2015)								x							
Rekelhof (2016)				x	x										
Ribeiro et al. (2001)					x										
Rozendaal (2021)						x									
Sørensen (2018)			x				x				x				
Stapersma (2010)			x												
Swider and Pedersen (2019)	x		x	x											x
Tufte (2014)			x												x
UNEP (2022)	x														
Vásquez (2016)					x			x							x
Veksler et al. (2012)												x			
Veksler et al. (2014)												x			
Veksler et al. (2016)												x			
Vestas (2022)	x														
Wit (2009)											x				
Woud and Stapersma (2017)			x												
Wu et al. (2016)											x				
Xia et al. (2019)											x				
Zahedi et al. (2013)					x			x							
Zahedi et al. (2014)								x							
Zhao et al. (2010)												x			

B

Appendix II - Case study particulars

B.1. Case vessel particulars

Main Data		
DP Class	2	-
Length overall	115.4	m
Length BPP	107.4	m
Beam	22.2	m
Depth main deck	9	m
Depth shelter deck	11.8	m
Draft	7.035	m @ 0.0 m trim
Displacement	12,565	t @ 0.0 m trim
Deadweight	5,662	t @ 0.0 m trim
Machinery Data		
Main generators (G3 & G4 & G5)	3 x 2,510	kW, 720 rpm
(G2 & G6)	2 x 1,880	kW, 720 rpm
Auxiliary generators (G1 & G7)	2 x 835	kW, 1200 rpm
Emergency generator	1 x 910	kW, 1800 rpm
Bow tunnel thrusters	2 x 1,900	kW
Retractable bow azimuth	1 x 1,500	kW
Stern azimuth	2 x 3,000	kW
Fuel Consumption in DP mode	10 - 12	t MGO/day (weather dep.)

Table B.1: Main particulars of the selected case study vessel

B.2. Main particulars case conditions

General information							
Activities	DP2 Station keeping, Saturation Diving						
Vessel heading	145	deg w.r.t to North					
Fuel consumption	8.3	tons					
Fuel consumption	9.3	m^3					
MGO density	0.892	kg/m^3					
Average Power consumption							
DG no.	DG Power [kW]	Load [%]	Bus				
DG2	282	15%	Port Bus				
DG3	376.5	15%	Port Bus				
DG4	376.5	15%	Stbd. Bus				
DG5	376.5	15%	Stbd. Bus				
DG6	0	0%	Stbd. Bus				
Total	1411.5	12.5%					
Weather conditions							
t	Curr.dir.	V_c [kts]	Wave dir.	H_s [m]	T_m [s]	Wind dir.	V_w [kts]
0h	ESE	0.1	SSE	2	7	SE	25
6h	WSW	0.1	SE	1.5	5	S	15
12h	NE	0.1	SE	1.5	5	SSE	17
18h	SSW	0.2	SE	1.5	6	SE	12
24h	SE	0.2	ESE	1.5	6	ESE	15

Table B.2: Main particulars of the low load test case

General information							
Activities	DP2 Station keeping, ROV & Diving						
Vessel heading	2	deg w.r.t to North					
Fuel consumption	10.7	tons					
Fuel consumption	12	m^3					
MGO density	0.892	kg/m^3					
Average Power consumption							
DG no.	DG Power [kW]	Load [%]	Bus				
DG2	470	25%	Port Bus				
DG3	627.5	25%	Port Bus				
DG4	0	0%	Port Bus				
DG5	502	20%	Stbd. Bus				
DG6	376	20%	Stbd. Bus				
Total	1975.5	17.5%					
Weather conditions							
t	Curr.dir.	V_c [kts]	Wave dir.	H_s [m]	T_m [s]	Wind dir.	V_w [kts]
0h	ESE	0.2	NNE	4	10	N	25
6h	NW	0.3	NNE	4	6	NNW	27
12h	SE	0.3	NNE	3	6	NE	18
18h	WNW	0.3	NNE	3	6	SE	15
24h	ENE	0.2	NNE	3	6	SE	22

Table B.3: Main particulars of the higher load test case

C

Appendix III - Diesel generator loading sequence tables

1. Benchmark condition – Open bus						
		Swb. Port		Swb. Stbd.		
P_tot	%_Load	DG2	DG3	DG4	DG5	DG6
0	0%	0.0%	0.0%	0.0%	0.0%	0.0%
565	5%	5.0%	5.0%	0.0%	7.9%	7.9%
1129	10%	10.0%	10.0%	0.0%	15.7%	15.7%
1694	15%	15.0%	15.0%	0.0%	23.6%	23.6%
2258	20%	20.0%	20.0%	0.0%	31.4%	31.4%
2823	25%	25.0%	25.0%	0.0%	39.3%	39.3%
3387	30%	30.0%	30.0%	0.0%	47.2%	47.2%
3952	35%	35.0%	35.0%	0.0%	55.0%	55.0%
4310	**38.2%**	**38.2%**	**38.2%**	**0.0%**	**60.0%**	**60.0%**
4516	40%	40.0%	40.0%	40.0%	40.0%	40.0%
5081	45%	45.0%	45.0%	45.0%	45.0%	45.0%
5645	50%	50.0%	50.0%	50.0%	50.0%	50.0%
6210	55%	55.0%	55.0%	55.0%	55.0%	55.0%
6774	**60%**	**60.0%**	**60.0%**	**60.0%**	**60.0%**	**60.0%**
7339	65%	65.0%	65.0%	65.0%	65.0%	65.0%
7903	70%	70.0%	70.0%	70.0%	70.0%	70.0%
8468	75%	75.0%	75.0%	75.0%	75.0%	75.0%
9032	80%	80.0%	80.0%	80.0%	80.0%	80.0%
9597	85%	85.0%	85.0%	85.0%	85.0%	85.0%
10161	90%	90.0%	90.0%	90.0%	90.0%	90.0%
10726	95%	95.0%	95.0%	95.0%	95.0%	95.0%
11290	100%	100.0%	100.0%	100.0%	100.0%	100.0%
11855	105%	105.0%	105.0%	105.0%	105.0%	105.0%
12419	110%	110.0%	110.0%	110.0%	110.0%	110.0%

(a) DG loading sequence of strategy 1. Benchmark – Open bus

2. Benchmark condition – Closed bus						
P_tot	%_Load	DG2	DG3	DG4	DG5	DG6
0	0%	0.0%	0.0%	0.0%	0.0%	0.0%
565	5%	8.2%	0.0%	8.2%	8.2%	0.0%
1129	10%	16.4%	0.0%	16.4%	16.4%	0.0%
1694	15%	24.5%	0.0%	24.5%	24.5%	0.0%
2258	20%	32.7%	0.0%	32.7%	32.7%	0.0%
2823	25%	40.9%	0.0%	40.9%	40.9%	0.0%
3387	30%	49.1%	0.0%	49.1%	49.1%	0.0%
3952	35%	57.3%	0.0%	57.3%	57.3%	0.0%
4140	**36.7%**	**60.0%**	**0.0%**	**60.0%**	**60.0%**	**0.0%**
4516	40%	51.4%	0.0%	51.4%	51.4%	51.4%
5081	45%	57.9%	0.0%	57.9%	57.9%	57.9%
5268	**46.7%**	**60.0%**	**0.0%**	**60.0%**	**60.0%**	**60.0%**
5645	50%	50.0%	50.0%	50.0%	50.0%	50.0%
6210	55%	55.0%	55.0%	55.0%	55.0%	55.0%
6774	**60%**	**60.0%**	**60.0%**	**60.0%**	**60.0%**	**60.0%**
7339	65%	65.0%	65.0%	65.0%	65.0%	65.0%
7903	70%	70.0%	70.0%	70.0%	70.0%	70.0%
8468	75%	75.0%	75.0%	75.0%	75.0%	75.0%
9032	80%	80.0%	80.0%	80.0%	80.0%	80.0%
9597	85%	85.0%	85.0%	85.0%	85.0%	85.0%
10161	90%	90.0%	90.0%	90.0%	90.0%	90.0%
10726	95%	95.0%	95.0%	95.0%	95.0%	95.0%
11290	100%	100.0%	100.0%	100.0%	100.0%	100.0%
11855	105%	105.0%	105.0%	105.0%	105.0%	105.0%
12419	110%	110.0%	110.0%	110.0%	110.0%	110.0%

(b) DG loading sequence of strategy 2. Benchmark – Closed bus

Figure C.1: DG loading sequences of benchmark strategies

1.1 Open, 5% - 60%, S>M						
		Swb. Port		Swb. Stbd.		
P_tot	%_Load	DG2	DG3	DG4	DG5	DG6
0	0%	0.0%	0.0%	0.0%	0.0%	0.0%
565	5%	5.0%	5.0%	0.0%	5.0%	11.7%
1129	10%	16.7%	5.0%	0.0%	5.0%	30.0%
1694	15%	28.4%	5.0%	0.0%	5.0%	48.4%
2051	**18.2%**	**35.7%**	**5.0%**	**0.0%**	**5.0%**	**60.0%**
2258	20%	40.0%	5.0%	0.0%	10.0%	60.0%
2823	25%	51.7%	5.0%	0.0%	23.8%	60.0%
3224	**28.6%**	**60.0%**	**5.0%**	**0.0%**	**33.6%**	**60.0%**
3387	30%	60.0%	7.5%	0.0%	37.5%	60.0%
3952	35%	60.0%	16.3%	0.0%	51.3%	60.0%
4310	**38.2%**	**60.0%**	**21.8%**	**0.0%**	**60.0%**	**60.0%**
4516	40%	60.0%	25.0%	5.0%	60.0%	60.0%
5081	45%	60.0%	33.8%	18.8%	60.0%	60.0%
5645	50%	60.0%	42.5%	32.5%	60.0%	60.0%
6210	55%	60.0%	51.3%	46.3%	60.0%	60.0%
6774	**60%**	**60.0%**	**60.0%**	**60.0%**	**60.0%**	**60.0%**
7339	65%	65.0%	65.0%	65.0%	65.0%	65.0%
7903	70%	70.0%	70.0%	70.0%	70.0%	70.0%
8468	75%	75.0%	75.0%	75.0%	75.0%	75.0%
9032	80%	80.0%	80.0%	80.0%	80.0%	80.0%
9597	85%	85.0%	85.0%	85.0%	85.0%	85.0%
10161	90%	90.0%	90.0%	90.0%	90.0%	90.0%
10726	95%	95.0%	95.0%	95.0%	95.0%	95.0%
11290	100%	100.0%	100.0%	100.0%	100.0%	100.0%
11855	105%	105.0%	105.0%	105.0%	105.0%	105.0%
12419	110%	110.0%	110.0%	110.0%	110.0%	110.0%

(a) DG loading sequence of strategy 1.1 Open, 5% - 60%, S>M

1.2 Open, 5% - 60%, M>S						
		Swb. Port		Swb. Stbd.		
P_tot	%_Load	DG2	DG3	DG4	DG5	DG6
0	0%	0.0%	0.0%	0.0%	0.0%	0.0%
565	5%	5.0%	5.0%	0.0%	10.0%	5.0%
1129	10%	5.0%	13.7%	0.0%	23.7%	5.0%
1694	15%	5.0%	22.5%	0.0%	37.5%	5.0%
2258	20%	5.0%	31.2%	0.0%	51.2%	5.0%
2618	**23.2%**	**5.0%**	**36.8%**	**0.0%**	**60.0%**	**5.0%**
2823	25%	5.0%	40.0%	0.0%	60.0%	11.6%
3387	30%	5.0%	48.7%	0.0%	60.0%	30.0%
3952	35%	5.0%	57.5%	0.0%	60.0%	48.4%
4115	**36.4%**	**5.0%**	**60.0%**	**0.0%**	**60.0%**	**53.7%**
4310	**38.2%**	**9.0%**	**60.0%**	**0.0%**	**60.0%**	**60.0%**
4516	40%	13.3%	60.0%	5.0%	60.0%	60.0%
5081	45%	25.0%	60.0%	18.8%	60.0%	60.0%
5645	50%	36.6%	60.0%	32.5%	60.0%	60.0%
6210	55%	48.3%	60.0%	46.3%	60.0%	60.0%
6774	60%	60.0%	60.0%	60.0%	60.0%	60.0%
7339	65%	65.0%	65.0%	65.0%	65.0%	65.0%
7903	70%	70.0%	70.0%	70.0%	70.0%	70.0%
8468	75%	75.0%	75.0%	75.0%	75.0%	75.0%
9032	80%	80.0%	80.0%	80.0%	80.0%	80.0%
9597	85%	85.0%	85.0%	85.0%	85.0%	85.0%
10161	90%	90.0%	90.0%	90.0%	90.0%	90.0%
10726	95%	95.0%	95.0%	95.0%	95.0%	95.0%
11290	100%	100.0%	100.0%	100.0%	100.0%	100.0%
11855	105%	105.0%	105.0%	105.0%	105.0%	105.0%
12419	110%	110.0%	110.0%	110.0%	110.0%	110.0%

(b) DG loading sequence of strategy 1.2 Open, 5% - 60%, M>S

1.3 Open, 5% - 70/75%, S>M						
		Swb. Port		Swb. Stbd.		
P_tot	%_Load	DG2	DG3	DG4	DG5	DG6
0	0%	0.0%	0.0%	0.0%	0.0%	0.0%
565	5%	5.0%	5.0%	0.0%	5.0%	11.7%
1129	10%	16.7%	5.0%	0.0%	5.0%	30.0%
1694	15%	28.4%	5.0%	0.0%	5.0%	48.4%
2258	20%	40.0%	5.0%	0.0%	5.0%	66.7%
2359	**20.9%**	**42.1%**	**5.0%**	**0.0%**	**5.0%**	**70.0%**
2823	25%	51.7%	5.0%	0.0%	16.3%	70.0%
3387	30%	63.4%	5.0%	0.0%	30.0%	70.0%
3707	**32.8%**	**70.0%**	**5.0%**	**0.0%**	**37.8%**	**70.0%**
3952	35%	70.0%	8.8%	0.0%	43.8%	70.0%
4516	40%	70.0%	17.5%	0.0%	57.5%	70.0%
5081	45%	70.0%	26.3%	0.0%	71.3%	70.0%
5233	**46.4%**	**70.0%**	**28.6%**	**0.0%**	**75.0%**	**70.0%**
5645	50%	70.0%	35.0%	10.0%	75.0%	70.0%
6210	55%	70.0%	43.8%	23.8%	75.0%	70.0%
6774	60%	70.0%	52.5%	37.5%	75.0%	70.0%
7339	65%	70.0%	61.3%	51.3%	75.0%	70.0%
7903	70%	70.0%	70.0%	65.0%	75.0%	70.0%
8226	**72.9%**	**70.0%**	**75.0%**	**72.9%**	**75.0%**	**70.0%**
8314	**73.6%**	**71.8%**	**75.0%**	**75.0%**	**75.0%**	**70.0%**
8468	75%	75.0%	75.0%	75.0%	75.0%	75.0%
9032	80%	80.0%	80.0%	80.0%	80.0%	80.0%
9597	85%	85.0%	85.0%	85.0%	85.0%	85.0%
10161	90%	90.0%	90.0%	90.0%	90.0%	90.0%
10726	95%	95.0%	95.0%	95.0%	95.0%	95.0%
11290	100%	100.0%	100.0%	100.0%	100.0%	100.0%
11855	105%	105.0%	105.0%	105.0%	105.0%	105.0%
12419	110%	110.0%	110.0%	110.0%	110.0%	110.0%

(c) DG loading sequence of strategy 1.3 Open, 5% - 70/75%, S>M

1.4 Open, 5% - 70/75%, M>S						
		Swb. Port		Swb. Stbd.		
P_tot	%_Load	DG2	DG3	DG4	DG5	DG6
0	0%	0.0%	0.0%	0.0%	0.0%	0.0%
565	5%	5.0%	5.0%	0.0%	10.0%	5.0%
1129	10%	5.0%	13.7%	0.0%	23.7%	5.0%
1694	15%	5.0%	22.5%	0.0%	37.5%	5.0%
2258	20%	5.0%	31.2%	0.0%	51.2%	5.0%
2823	25%	5.0%	40.0%	0.0%	65.0%	5.0%
3234	**28.6%**	**5.0%**	**46.4%**	**0.0%**	**75.0%**	**5.0%**
3387	30%	5.0%	48.7%	0.0%	75.0%	10.0%
3952	35%	5.0%	57.5%	0.0%	75.0%	28.3%
4516	40%	5.0%	66.2%	0.0%	75.0%	46.7%
5081	45%	5.0%	75.0%	0.0%	75.0%	65.0%
5083	**45.0%**	**5.0%**	**75.0%**	**0.0%**	**75.0%**	**65.1%**
5233	**46.4%**	**8.1%**	**75.0%**	**0.0%**	**75.0%**	**70.0%**
5645	50%	16.6%	75.0%	10.0%	75.0%	70.0%
6210	55%	28.3%	75.0%	23.8%	75.0%	70.0%
6774	60%	40.0%	75.0%	37.5%	75.0%	70.0%
7339	65%	51.6%	75.0%	51.3%	75.0%	70.0%
7903	70%	63.3%	75.0%	65.0%	75.0%	70.0%
8226	**72.9%**	**70.0%**	**75.0%**	**72.9%**	**75.0%**	**70.0%**
8314	**73.6%**	**71.8%**	**75.0%**	**75.0%**	**75.0%**	**70.0%**
8468	75%	75.0%	75.0%	75.0%	75.0%	75.0%
9032	80%	80.0%	80.0%	80.0%	80.0%	80.0%
9597	85%	85.0%	85.0%	85.0%	85.0%	85.0%
10161	90%	90.0%	90.0%	90.0%	90.0%	90.0%
10726	95%	95.0%	95.0%	95.0%	95.0%	95.0%
11290	100%	100.0%	100.0%	100.0%	100.0%	100.0%
11855	105%	105.0%	105.0%	105.0%	105.0%	105.0%
12419	110%	110.0%	110.0%	110.0%	110.0%	110.0%

(d) DG loading sequence of strategy 1.4 Open, 5% - 70/75%, M>S

Figure C.2: DG loading sequences of open bus configurations

2.1 Closed, 5% - 60%, S>M						
P_tot	%_Load	DG2	DG3	DG4	DG5	DG6
0	0%	0.0%	0.0%	0.0%	0.0%	0.0%
565	5%	18.4%	0.0%	5.0%	0.0%	5.0%
1129	10%	48.4%	0.0%	5.0%	0.0%	5.0%
1348	**11.9%**	**60.0%**	**0.0%**	**5.0%**	**0.0%**	**5.0%**
1694	15%	60.0%	0.0%	5.0%	0.0%	23.4%
2258	20%	60.0%	0.0%	5.0%	0.0%	53.4%
2382	**21.1%**	**60.0%**	**0.0%**	**5.0%**	**0.0%**	**60.0%**
2823	25%	60.0%	0.0%	22.6%	0.0%	60.0%
3387	30%	60.0%	0.0%	45.1%	0.0%	60.0%
3762	**33.3%**	**60.0%**	**0.0%**	**60.0%**	**0.0%**	**60.0%**
3952	35%	60.0%	7.5%	60.0%	0.0%	60.0%
4516	40%	60.0%	30.0%	60.0%	0.0%	60.0%
5081	45%	60.0%	52.5%	60.0%	0.0%	60.0%
5268	**46.7%**	**60.0%**	**60.0%**	**60.0%**	**0.0%**	**60.0%**
5645	50%	60.0%	60.0%	60.0%	15.0%	60.0%
6210	55%	60.0%	60.0%	60.0%	37.5%	60.0%
6774	**60%**	**60.0%**	**60.0%**	**60.0%**	**60.0%**	**60.0%**
7339	65%	65.0%	65.0%	65.0%	65.0%	65.0%
7903	70%	70.0%	70.0%	70.0%	70.0%	70.0%
8468	75%	75.0%	75.0%	75.0%	75.0%	75.0%
9032	80%	80.0%	80.0%	80.0%	80.0%	80.0%
9597	85%	85.0%	85.0%	85.0%	85.0%	85.0%
10161	90%	90.0%	90.0%	90.0%	90.0%	90.0%
10726	95%	95.0%	95.0%	95.0%	95.0%	95.0%
11290	100%	100.0%	100.0%	100.0%	100.0%	100.0%
11855	105%	105.0%	105.0%	105.0%	105.0%	105.0%
12419	110%	110.0%	110.0%	110.0%	110.0%	110.0%

(a) DG loading sequence of strategy 2.1 Closed, 5% - 60%, S>M

2.2 Closed, 5% - 60%, M>S						
P_tot	%_Load	DG2	DG3	DG4	DG5	DG6
0	0%	0.0%	0.0%	0.0%	0.0%	0.0%
565	5%	5.0%	0.0%	15.0%	0.0%	5.0%
1129	10%	5.0%	0.0%	37.5%	0.0%	5.0%
1694	15%	5.0%	0.0%	60.0%	0.0%	5.0%
1694	**15.0%**	**5.0%**	**0.0%**	**60.0%**	**0.0%**	**5.0%**
2258	20%	35.0%	0.0%	60.0%	0.0%	5.0%
2728	**24.2%**	**60.0%**	**0.0%**	**60.0%**	**0.0%**	**5.0%**
2823	25%	60.0%	0.0%	60.0%	0.0%	10.1%
3387	30%	60.0%	0.0%	60.0%	0.0%	40.1%
3762	**33.3%**	**60.0%**	**0.0%**	**60.0%**	**0.0%**	**60.0%**
3952	35%	60.0%	7.6%	60.0%	0.0%	60.0%
4516	40%	60.0%	30.1%	60.0%	0.0%	60.0%
5081	45%	60.0%	52.6%	60.0%	0.0%	60.0%
5268	**46.7%**	**60.0%**	**60.0%**	**60.0%**	**0.0%**	**60.0%**
5645	50%	60.0%	60.0%	60.0%	15.1%	60.0%
6210	55%	60.0%	60.0%	60.0%	37.6%	60.0%
6774	**60.0%**	**60.0%**	**60.0%**	**60.0%**	**60.0%**	**60.0%**
7339	65%	65.0%	65.0%	65.0%	65.0%	65.0%
7903	70%	70.0%	70.0%	70.0%	70.0%	70.0%
8468	75%	75.0%	75.0%	75.0%	75.0%	75.0%
9032	80%	80.0%	80.0%	80.0%	80.0%	80.0%
9597	85%	85.0%	85.0%	85.0%	85.0%	85.0%
10161	90%	90.0%	90.0%	90.0%	90.0%	90.0%
10726	95%	95.0%	95.0%	95.0%	95.0%	95.0%
11290	100%	100.0%	100.0%	100.0%	100.0%	100.0%
11855	105%	105.0%	105.0%	105.0%	105.0%	105.0%
12419	110%	110.0%	110.0%	110.0%	110.0%	110.0%

(b) DG loading sequence of strategy 2.2 Closed, 5% - 60%, M>S

2.3 Closed, 5% - 70/75%, S>M						
P_tot	%_Load	DG2	DG3	DG4	DG5	DG6
0	0%	0.0%	0.0%	0.0%	0.0%	0.0%
565	5%	18.4%	0.0%	5.0%	0.0%	5.0%
1129	10%	48.4%	0.0%	5.0%	0.0%	5.0%
1536	**13.6%**	**70.0%**	**0.0%**	**5.0%**	**0.0%**	**5.0%**
1694	15%	70.0%	0.0%	5.0%	0.0%	13.4%
2258	20%	70.0%	0.0%	5.0%	0.0%	43.4%
2758	**24.4%**	**70.0%**	**0.0%**	**5.0%**	**0.0%**	**70.0%**
2823	25%	70.0%	0.0%	7.6%	0.0%	70.0%
3387	30%	70.0%	0.0%	30.1%	0.0%	70.0%
3952	35%	70.0%	0.0%	52.6%	0.0%	70.0%
4515	**40.0%**	**70.0%**	**0.0%**	**75.0%**	**0.0%**	**70.0%**
4516	40%	70.0%	5.0%	70.1%	0.0%	70.0%
5081	45%	70.0%	22.5%	75.0%	0.0%	70.0%
5645	50%	70.0%	45.0%	75.0%	0.0%	70.0%
6210	55%	70.0%	67.5%	75.0%	0.0%	70.0%
6397	**56.7%**	**70.0%**	**75.0%**	**75.0%**	**0.0%**	**70.0%**
6774	60%	70.0%	75.0%	75.0%	15.0%	70.0%
7339	65%	70.0%	75.0%	75.0%	37.5%	70.0%
7903	70%	70.0%	75.0%	75.0%	60.0%	70.0%
8280	**73.3%**	**70.0%**	**75.0%**	**75.0%**	**75.0%**	**70.0%**
8468	75%	75.0%	75.0%	75.0%	75.0%	75.0%
9032	80%	80.0%	80.0%	80.0%	80.0%	80.0%
9597	85%	85.0%	85.0%	85.0%	85.0%	85.0%
10161	90%	90.0%	90.0%	90.0%	90.0%	90.0%
10726	95%	95.0%	95.0%	95.0%	95.0%	95.0%
11290	100%	100.0%	100.0%	100.0%	100.0%	100.0%
11855	105%	105.0%	105.0%	105.0%	105.0%	105.0%
12419	110%	110.0%	110.0%	110.0%	110.0%	110.0%

(c) DG loading sequence of strategy 2.3 Closed, 5% - 70/75%, S>M

2.4 Closed, 5% - 70/75%, M>S						
P_tot	%_Load	DG2	DG3	DG4	DG5	DG6
0	0%	0.0%	0.0%	0.0%	0.0%	0.0%
565	5%	5.0%	0.0%	15.0%	0.0%	5.0%
1129	10%	5.0%	0.0%	37.5%	0.0%	5.0%
1694	15%	5.0%	0.0%	60.0%	0.0%	5.0%
2071	**18.3%**	**5.0%**	**0.0%**	**75.0%**	**0.0%**	**5.0%**
2258	20%	15.0%	0.0%	75.0%	0.0%	5.0%
2823	25%	45.0%	0.0%	75.0%	0.0%	5.0%
3293	**29.2%**	**70.0%**	**0.0%**	**75.0%**	**0.0%**	**5.0%**
3387	30%	70.0%	0.0%	75.0%	0.0%	10.0%
3952	35%	70.0%	0.0%	75.0%	0.0%	40.1%
4515	**40.0%**	**70.0%**	**0.0%**	**75.0%**	**0.0%**	**70.0%**
4516	40%	70.0%	5.0%	75.0%	0.0%	63.4%
5081	45%	70.0%	22.5%	75.0%	0.0%	70.0%
5645	50%	70.0%	45.0%	75.0%	0.0%	70.0%
6210	55%	70.0%	67.5%	75.0%	0.0%	70.0%
6397	**56.7%**	**70.0%**	**75.0%**	**75.0%**	**0.0%**	**70.0%**
6774	60%	70.0%	75.0%	75.0%	15.0%	70.0%
7339	65%	70.0%	75.0%	75.0%	37.5%	70.0%
7903	70%	70.0%	75.0%	75.0%	60.0%	70.0%
8280	**73.3%**	**70.0%**	**75.0%**	**75.0%**	**75.0%**	**70.0%**
8468	75%	75.0%	75.0%	75.0%	75.0%	75.0%
9032	80%	80.0%	80.0%	80.0%	80.0%	80.0%
9597	85%	85.0%	85.0%	85.0%	85.0%	85.0%
10161	90%	90.0%	90.0%	90.0%	90.0%	90.0%
10726	95%	95.0%	95.0%	95.0%	95.0%	95.0%
11290	100%	100.0%	100.0%	100.0%	100.0%	100.0%
11855	105%	105.0%	105.0%	105.0%	105.0%	105.0%
12419	110%	110.0%	110.0%	110.0%	110.0%	110.0%

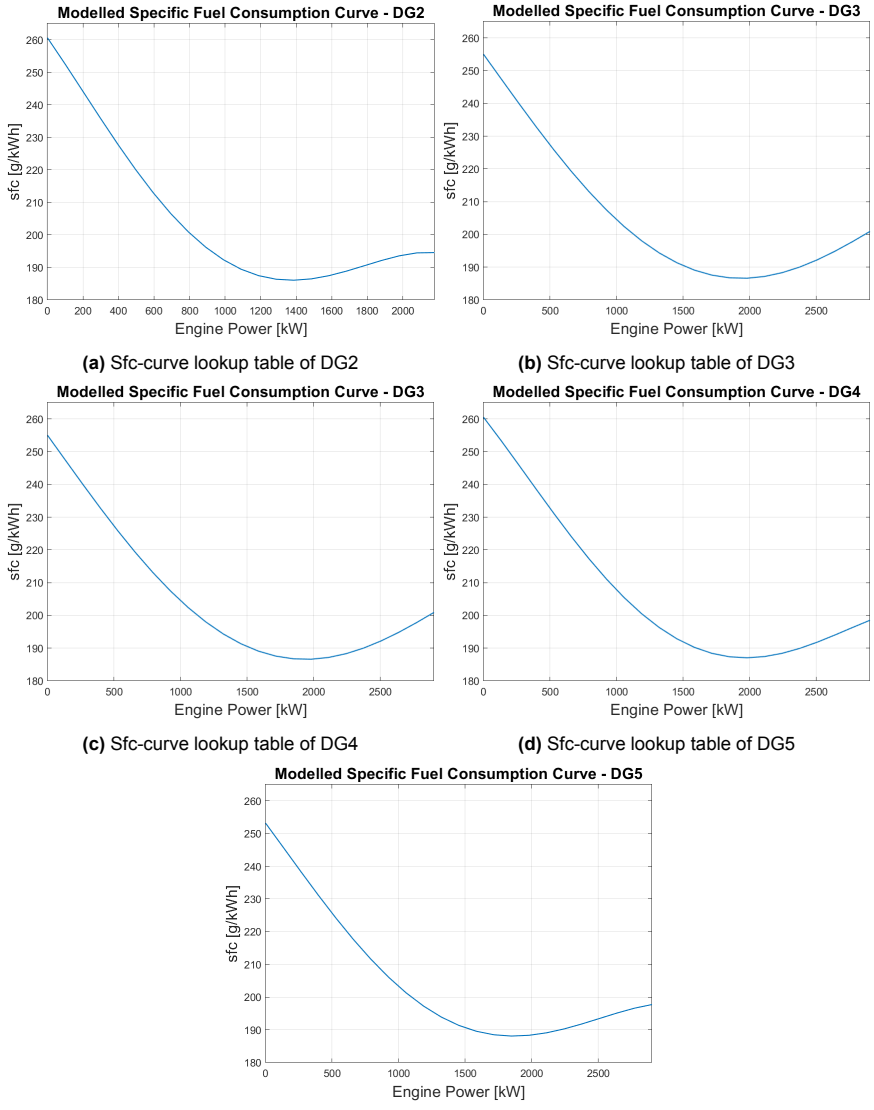
(d) DG loading sequence of strategy 2.4 Closed, 5% - 70/75%, M>S

Figure C.3: DG loading sequences of closed bus configurations

D

Appendix IV - Preliminary analysis

D.1. Specific fuel consumption curve lookup tables



(a) Sfc-curve lookup table of DG2

(b) Sfc-curve lookup table of DG3

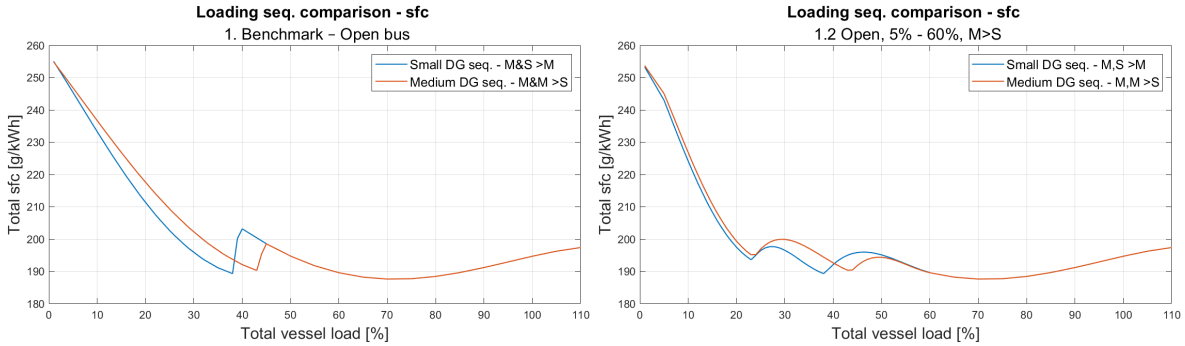
(c) Sfc-curve lookup table of DG4

(d) Sfc-curve lookup table of DG5

(e) Sfc-curve lookup table of DG6

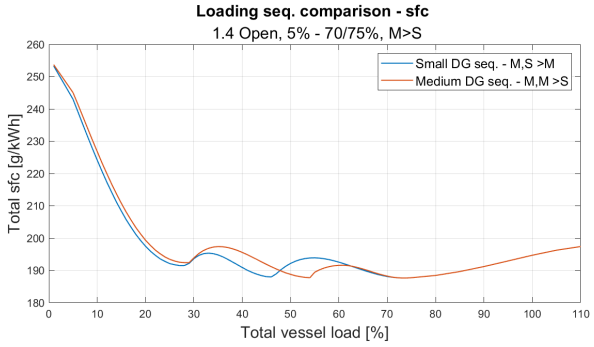
Figure D.1: Sfc-curve lookup tables of all DGs

D.2. Preliminary results - loading sequences

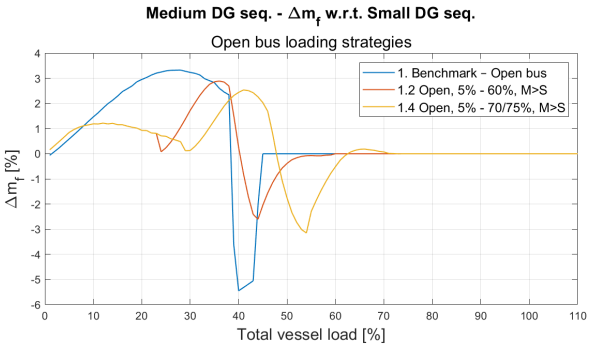


(a) Switchboard sfc-curves of loading strategy 1. sequences

(b) Switchboard sfc-curves of loading strategy 1.2 sequences

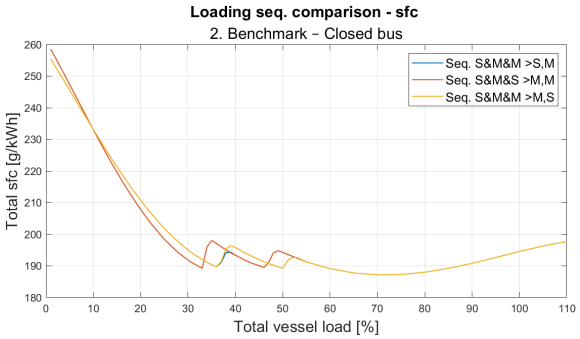


(c) Switchboard sfc-curves of loading strategy 1.4 sequences

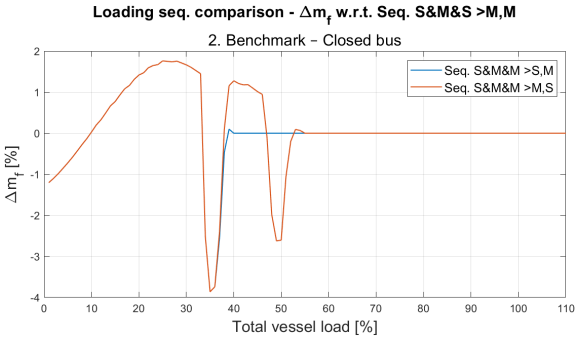


(d) Hourly fuel consumption difference open bus medium DG sequences w.r.t. small DG sequences

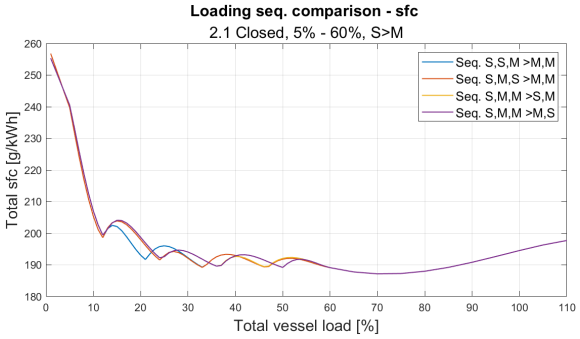
Figure D.2: Preliminary results of open bus DG sequences of strategies 1., 1.2 and 1.4



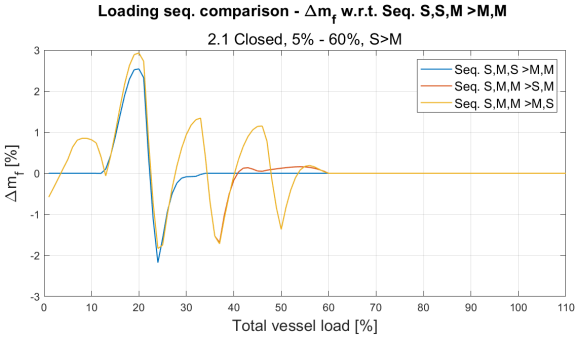
(a) Total system sfc-curves of loading strategy 2. sequences



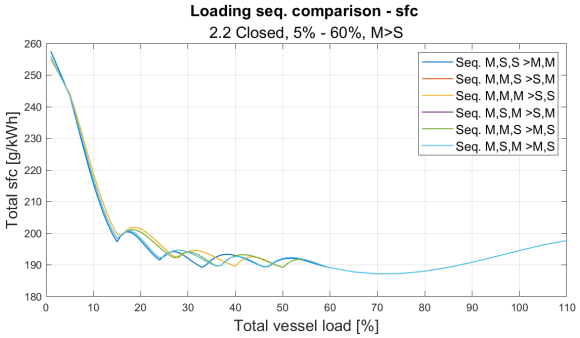
(b) Hourly fuel consumption differences strategy 2. sequences



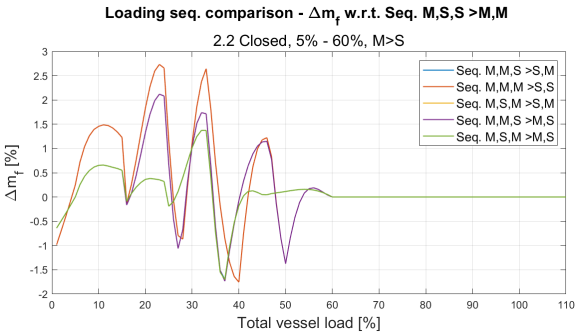
(c) Total system sfc-curves of loading strategy 2.1 sequences



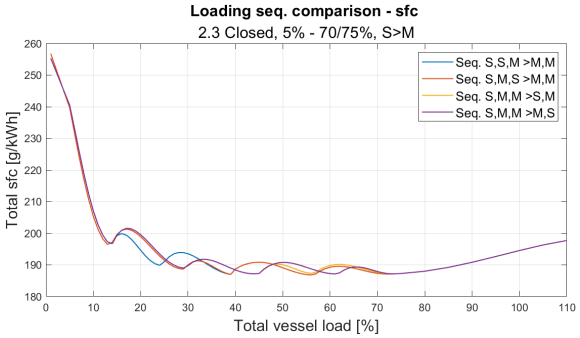
(d) Hourly fuel consumption differences strategy 2.1 sequences



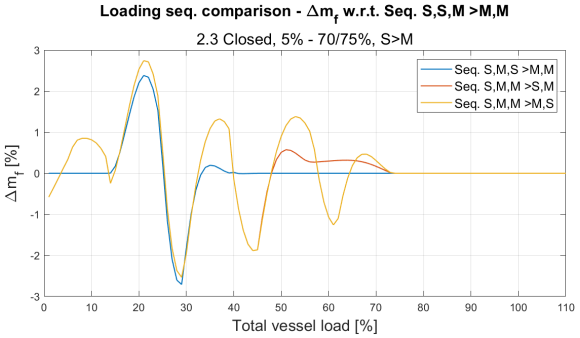
(e) Total system sfc-curves of loading strategy 2.2 sequences



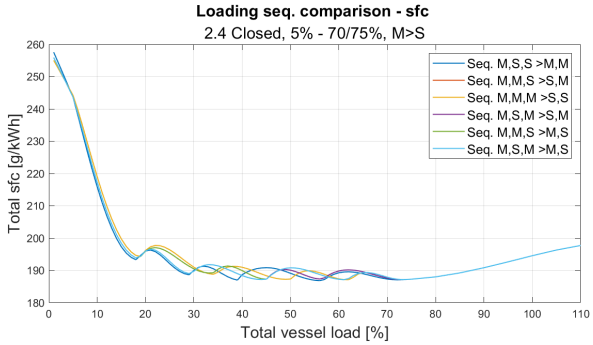
(f) Hourly fuel consumption differences strategy 2.2 sequences



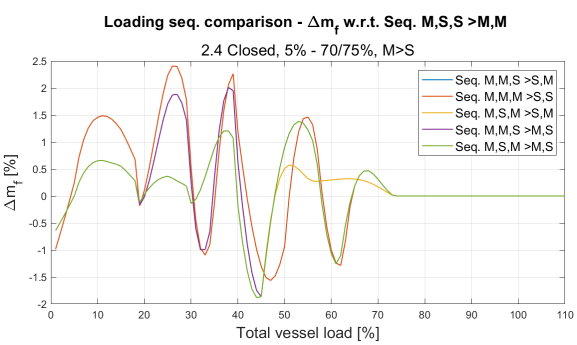
(g) Total system sfc-curves of loading strategy 2.3 sequences



(h) Hourly fuel consumption differences strategy 2.3 sequences



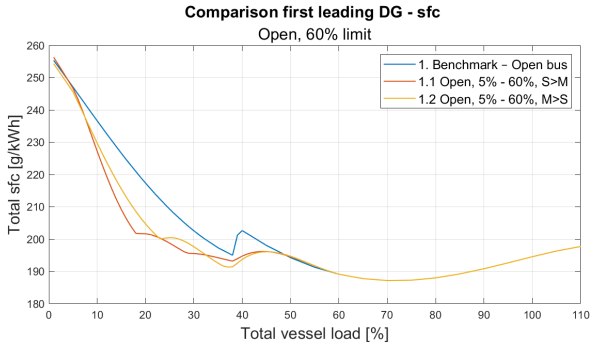
(i) Total system sfc-curves of loading strategy 2.4 sequences



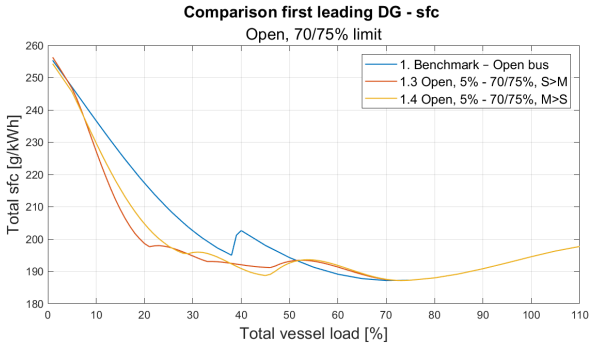
(j) Hourly fuel consumption differences strategy 2.4 sequences

Figure D.3: Preliminary results of all closed bus strategy DG sequences

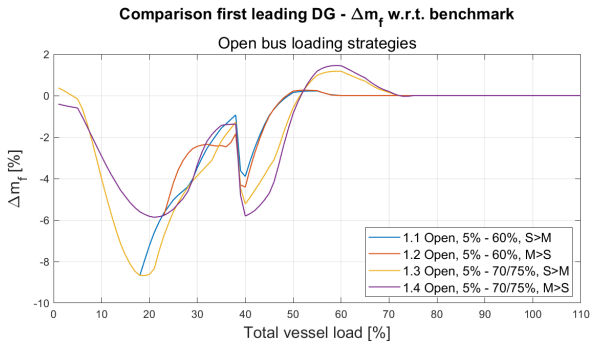
D.3. Preliminary results - selected cases



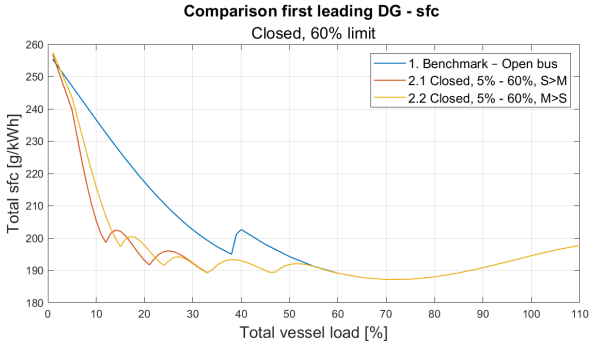
(a) Total system sfc-curves of open bus, 60% limit strategies



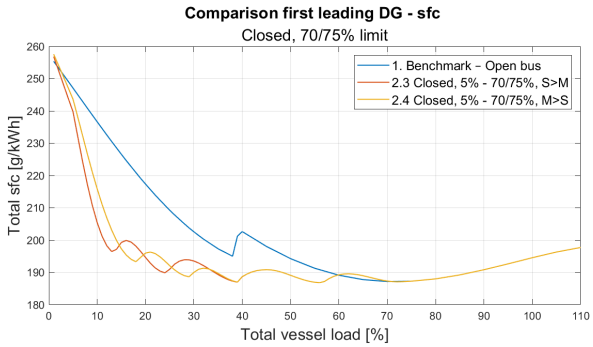
(b) Total system sfc-curves of open bus, 70/75% limit strategies



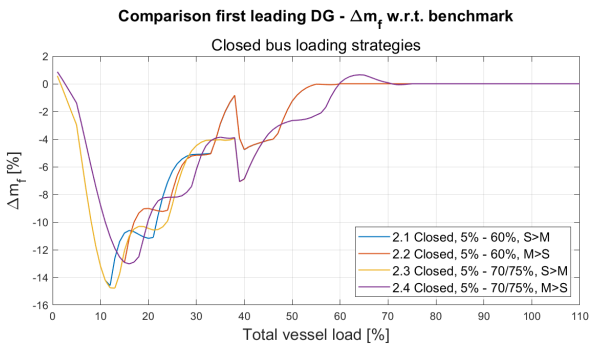
(c) Hourly fuel consumption differences between open bus strategies



(d) Total system sfc-curves of closed bus, 60% limit strategies

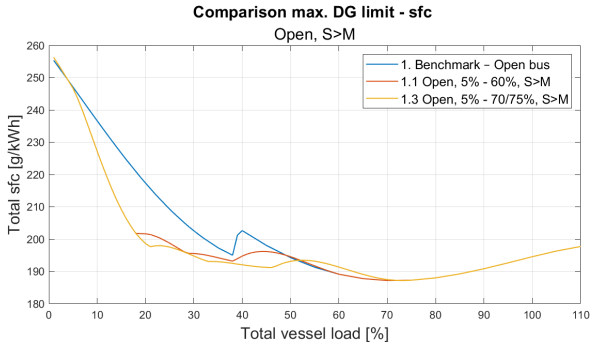


(e) Total system sfc-curves of closed bus, 70/75% limit strategies

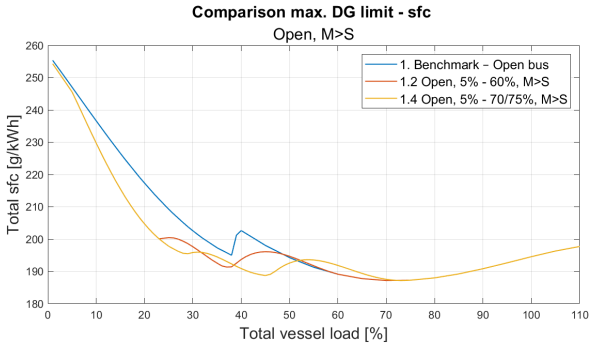


(f) Hourly fuel consumption differences between closed bus strategies

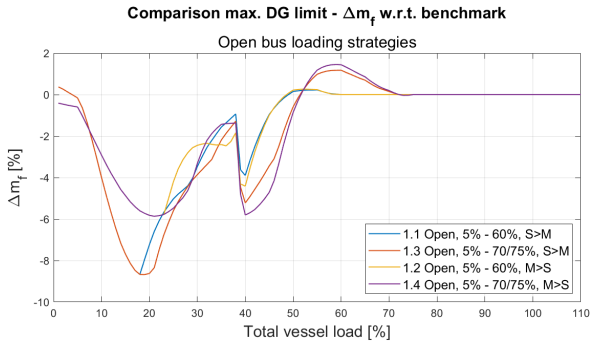
Figure D.4: All preliminary results of first leading DG strategies



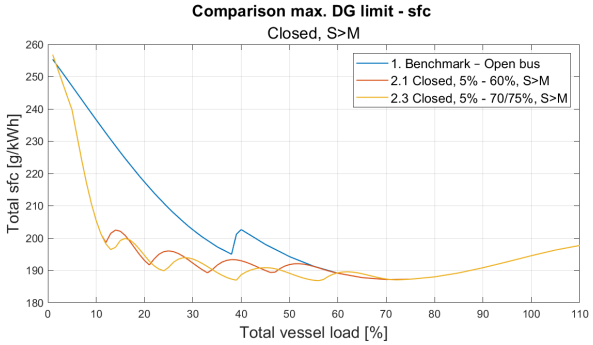
(a) Total system sfc-curves of open, small DG sequence strategies



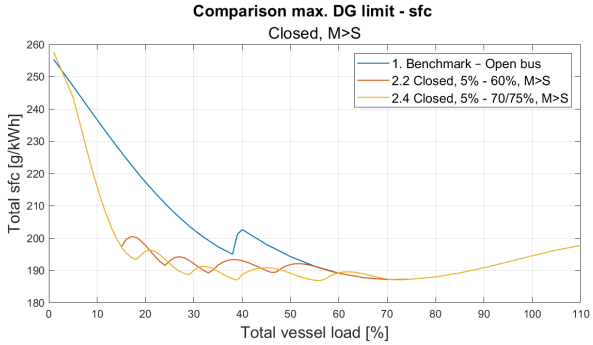
(b) Total system sfc-curves of open, medium DG sequence strategies



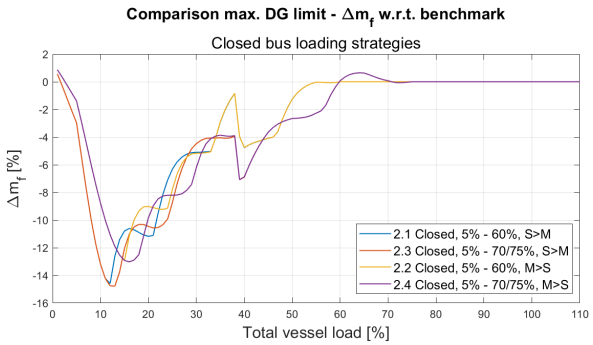
(c) Hourly fuel consumption differences between open bus strategies



(d) Total system sfc-curves of closed, small DG sequence strategies

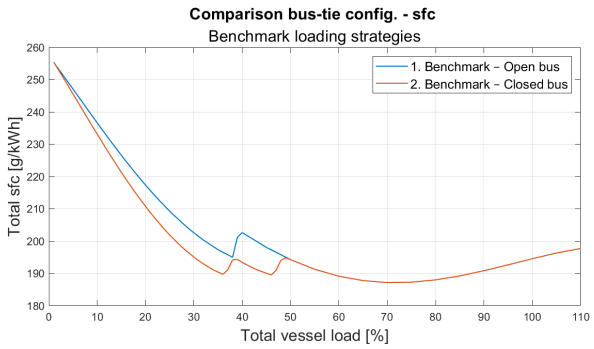


(e) Total system sfc-curves of closed, medium DG sequence strategies

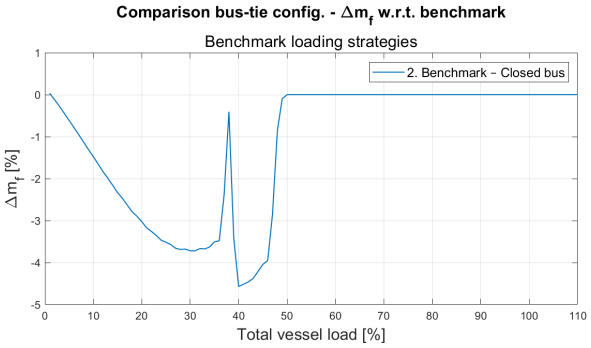


(f) Hourly fuel consumption differences between closed bus strategies

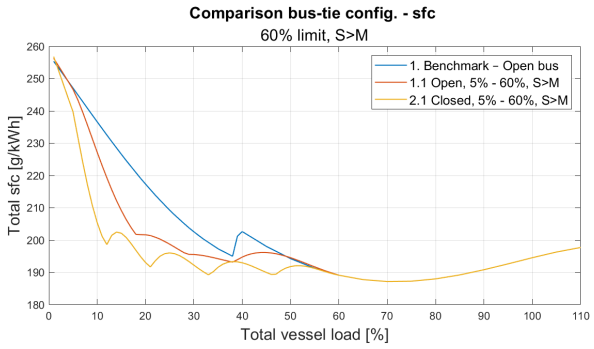
Figure D.5: All preliminary results of maximum DG limit strategies



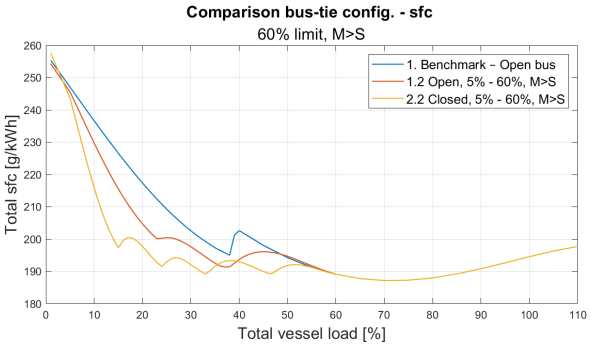
(a) Total system sfc-curves of both benchmark strategies



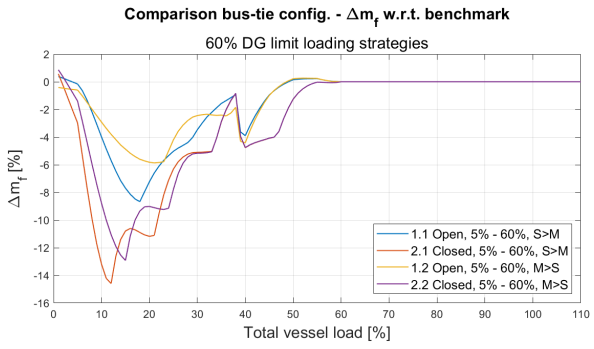
(b) Hourly fuel consumption differences between both benchmark strategies



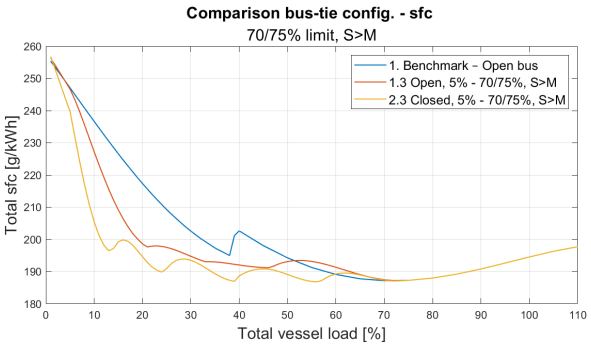
(c) Total system sfc-curves of 60% limit, small DG sequence strategies



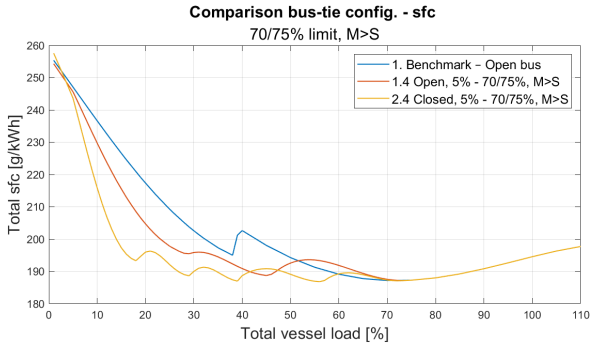
(d) Total system sfc-curves of 60% limit, medium DG sequence strategies



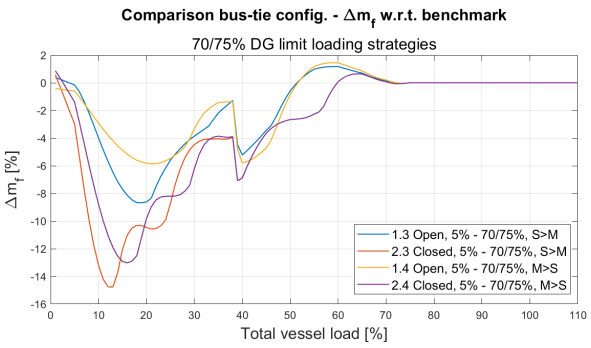
(e) Hourly fuel consumption differences between 60% limit strategies



(f) Total system sfc-curves of 70/75% limit, small DG sequence strategies

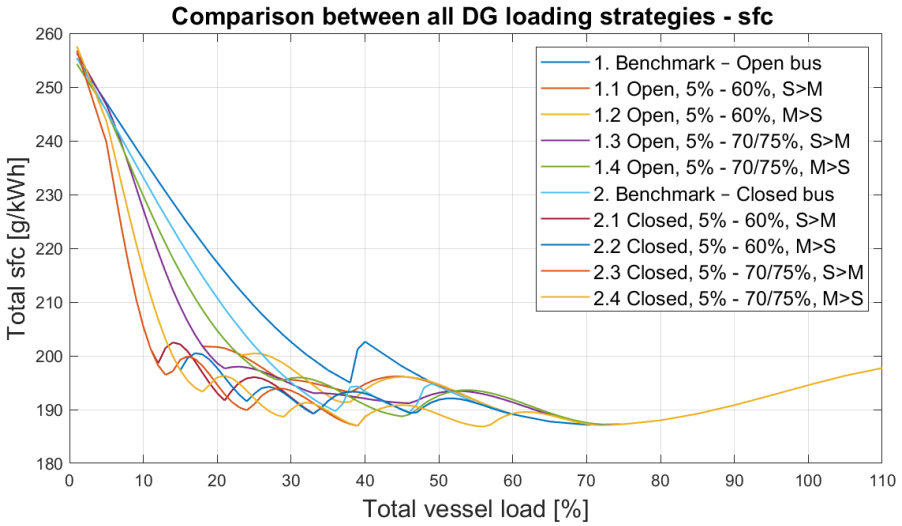


(g) Total system sfc-curves of 70/75% limit, medium DG sequence strategies

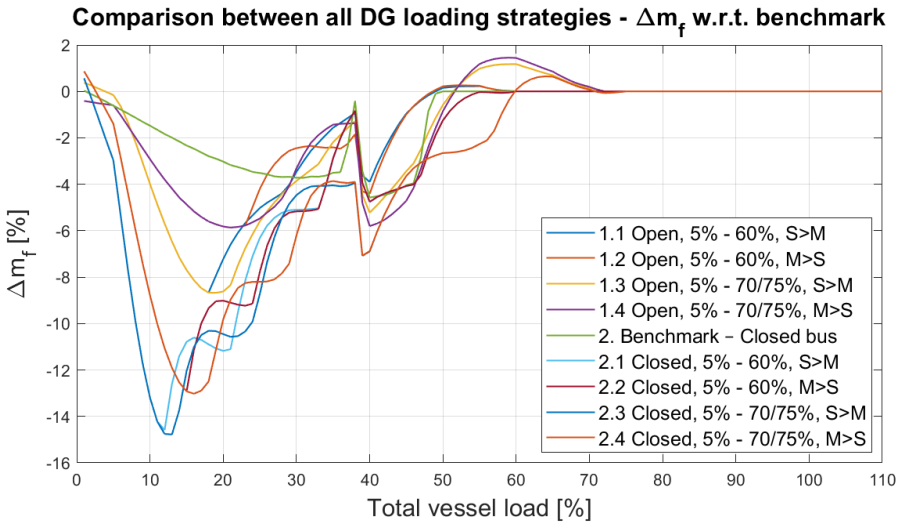


(h) Hourly fuel consumption differences between 70/75% limit strategies

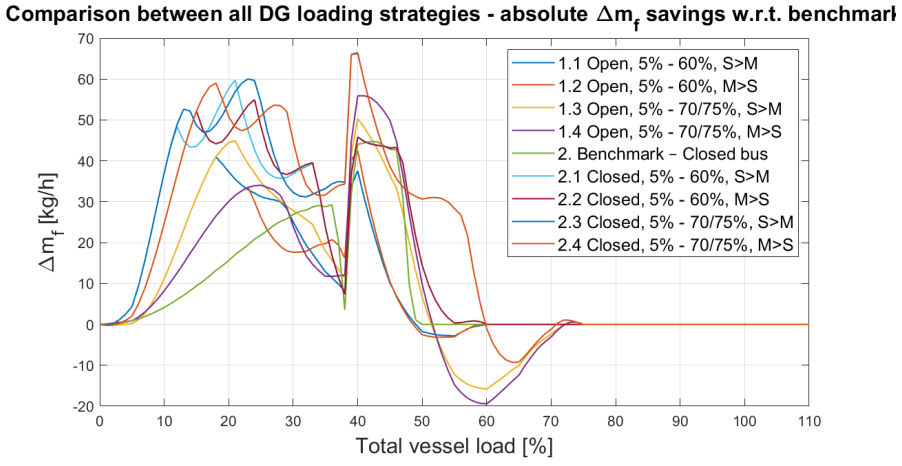
Figure D.6: All preliminary results of open and closed bus strategies comparisons



(a) Total system sfc-curves of all selected load allocation strategies



(b) Fuel mass flow savings of all selected load allocation strategies



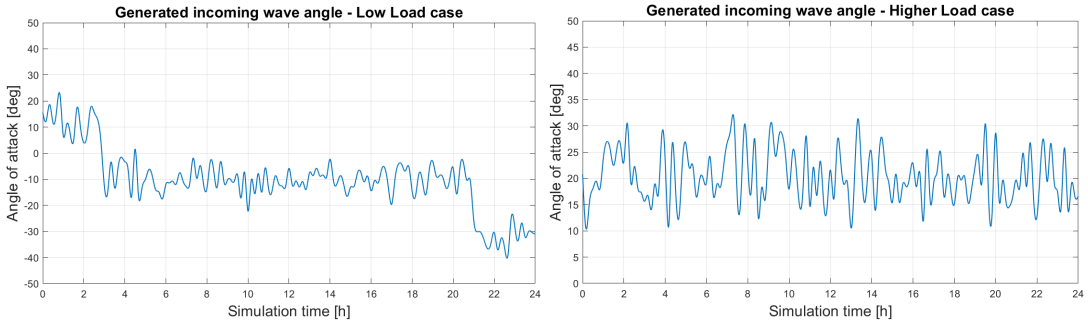
(c) Absolute fuel mass flow results of selected load allocation strategies

Figure D.7: Preliminary results of all selected load allocation strategies

E

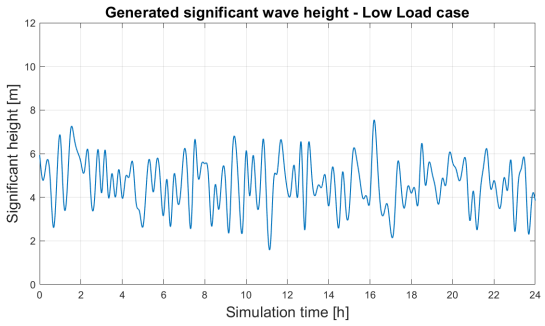
Appendix V - Dynamic Model

E.1. Environmental conditions

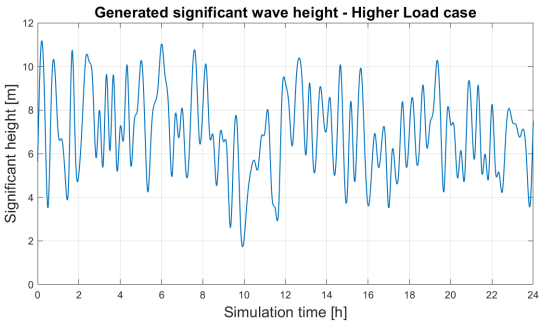


(a) Generated incoming wave angle of the low load case

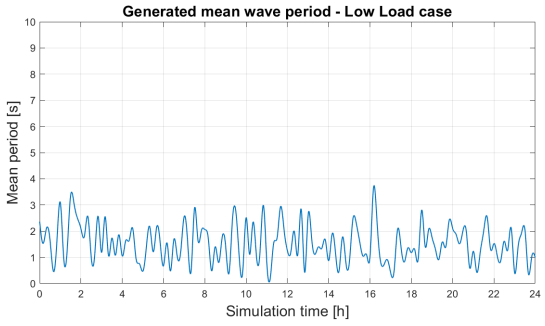
(b) Generated incoming wave angle of the higher load case



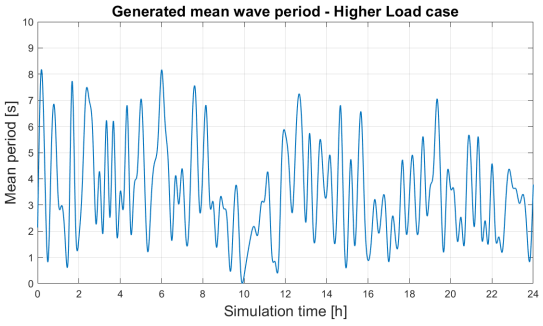
(c) Generated wave height of the low load case



(d) Generated wave height of the higher load case

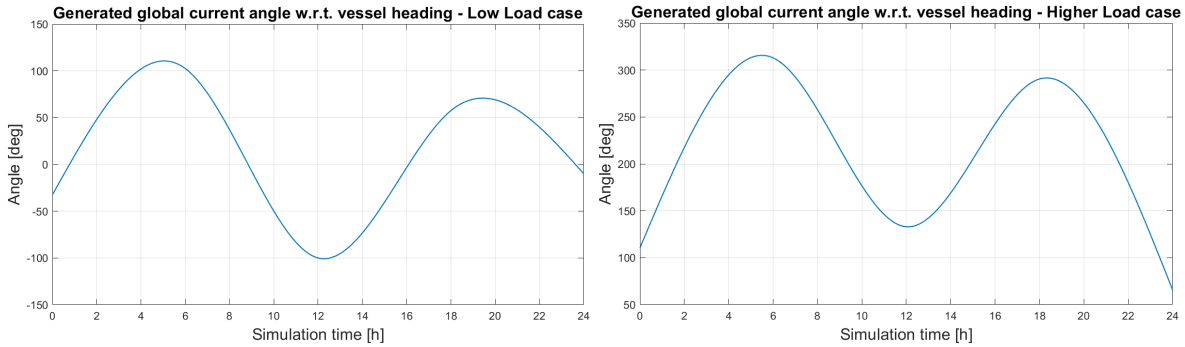


(e) Generated wave period of the low load case



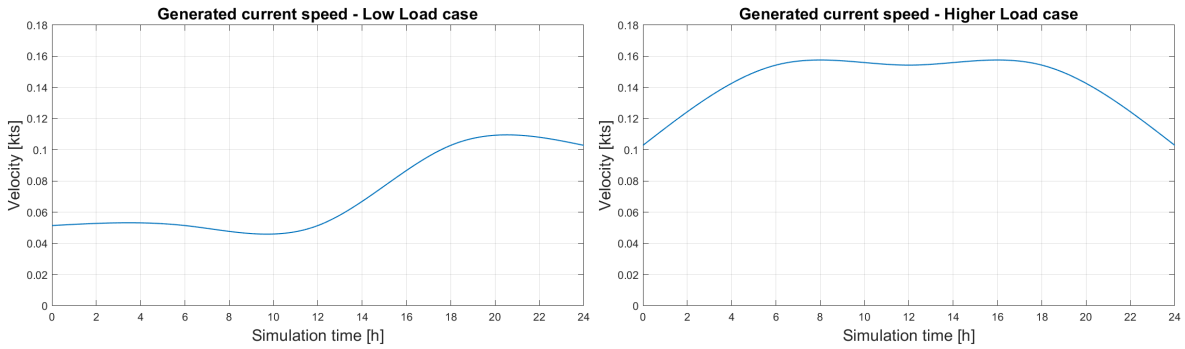
(f) Generated wave period of the higher load case

Figure E.1: Generated wave conditions of both load cases



(a) Generated current angle of the low load case

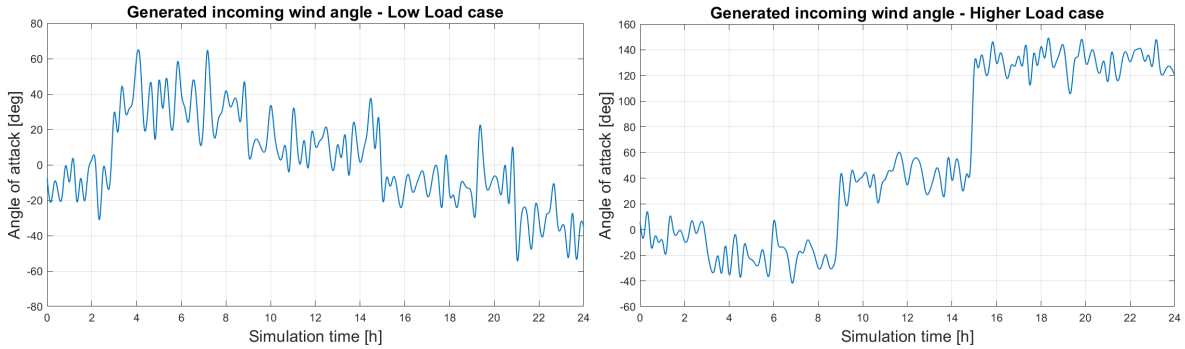
(b) Generated current angle of the higher load case



(c) Generated current speed of the low load case

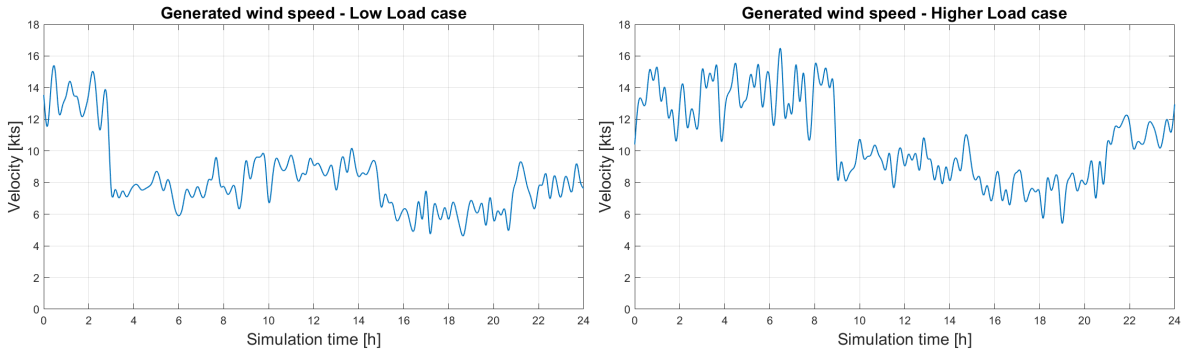
(d) Generated current speed of the higher load case

Figure E.2: Generated current conditions of both load cases



(a) Generated incoming wind angle of the low load case

(b) Generated incoming wind angle of the higher load case

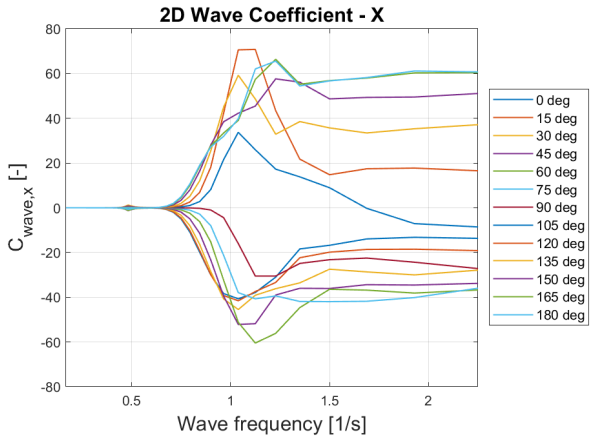


(c) Generated incoming wind speed of the low load case

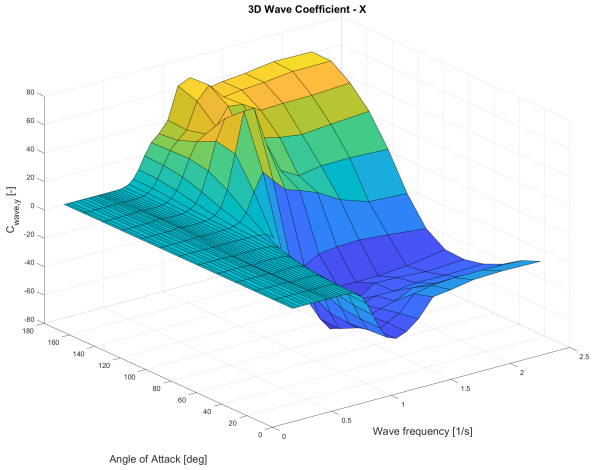
(d) Generated incoming wind speed of the higher load case

Figure E.3: Generated wind conditions of both load cases

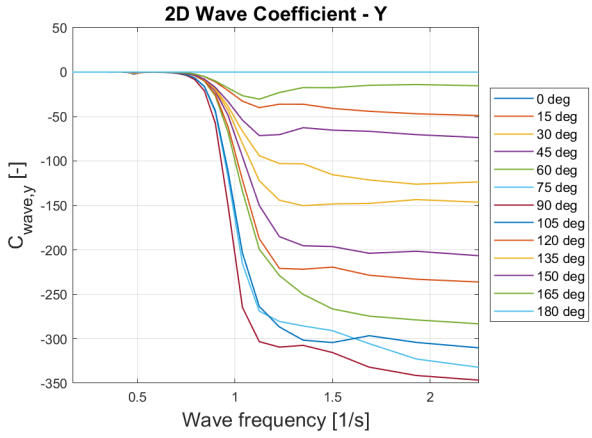
E.2. Environmental coefficients



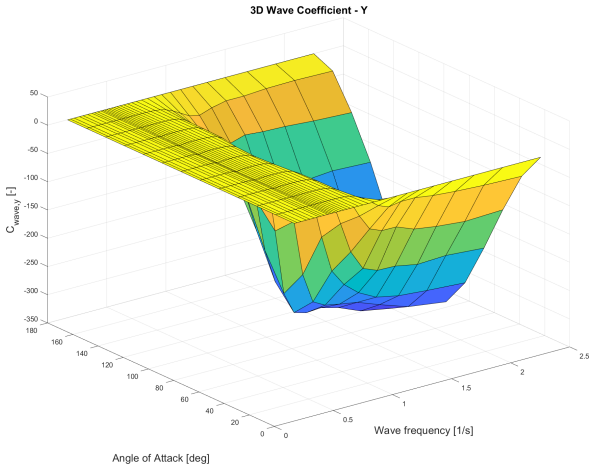
(a) 2D lookup table for wave coefficients in surge



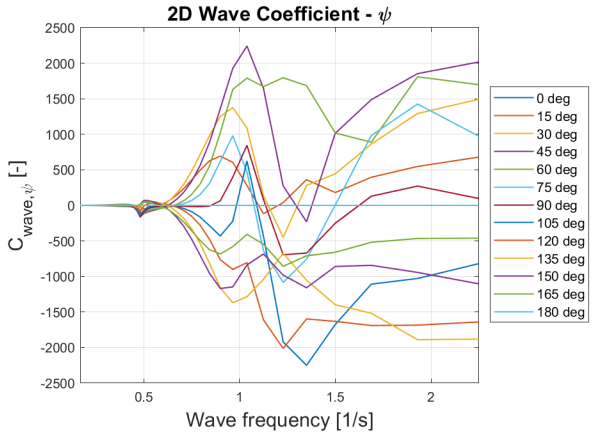
(b) 3D lookup table for wave coefficients in surge



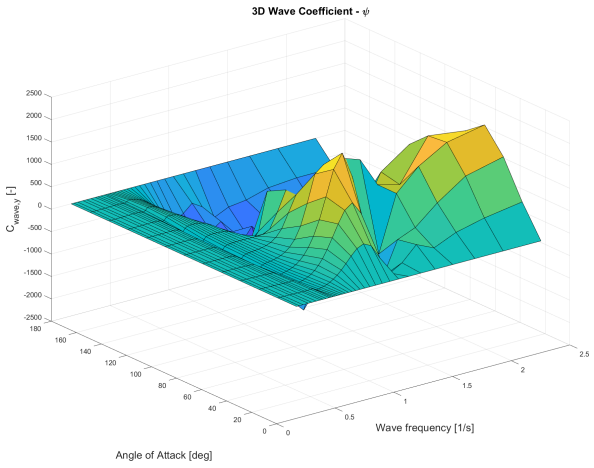
(c) 2D lookup table for wave coefficients in sway



(d) 3D lookup table for wave coefficients in sway

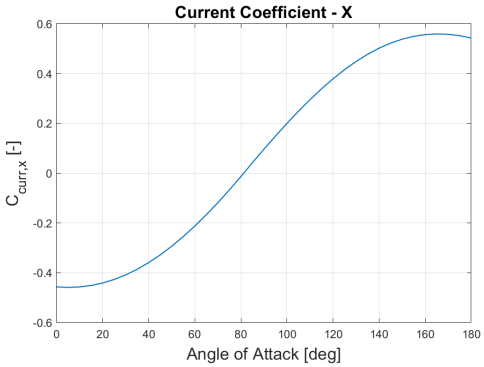


(e) 2D lookup table for wave coefficients in yaw

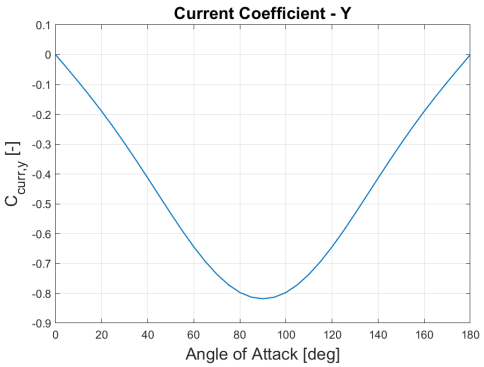


(f) 3D lookup table for wave coefficients in yaw

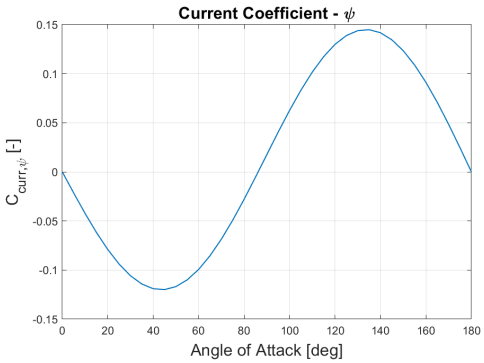
Figure E.4: Wave coefficient lookup tables



(a) Lookup table for current coefficients in surge

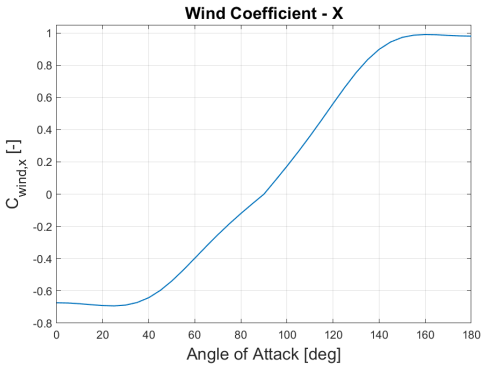


(b) Lookup table for current coefficients in sway

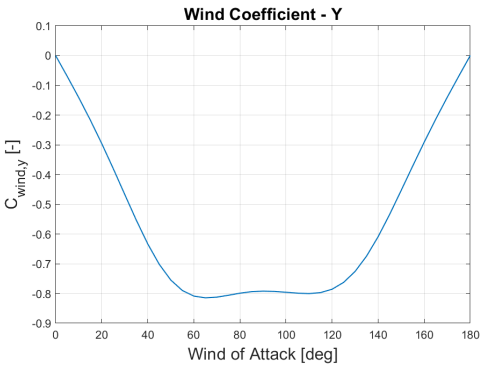


(c) Lookup table for current coefficients in yaw

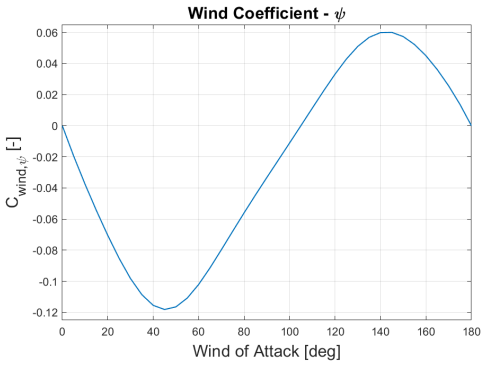
Figure E.5: Current coefficient lookup tables



(a) Lookup table for wind coefficients in surge



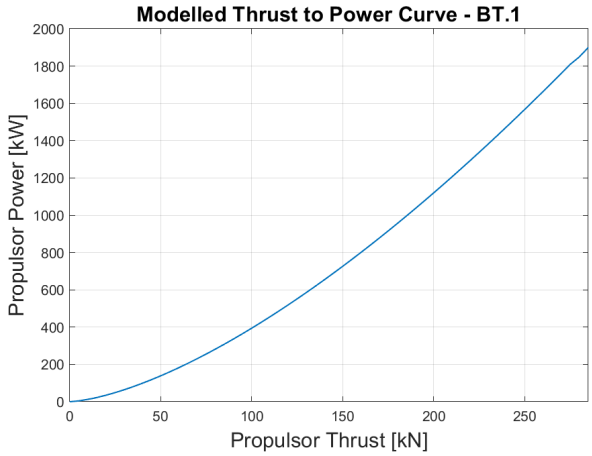
(b) Lookup table for wind coefficients in sway



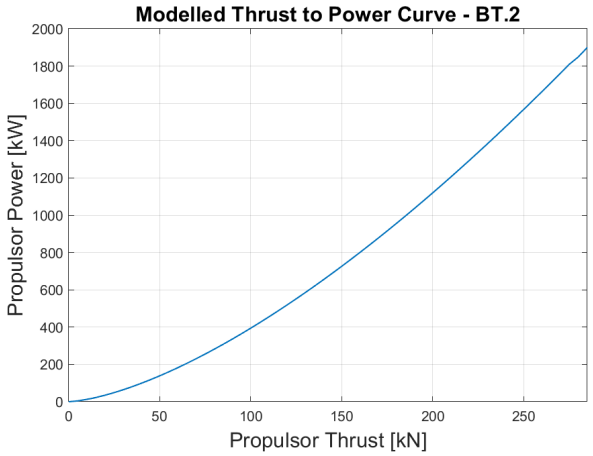
(c) Lookup table for wind coefficients in yaw

Figure E.6: Wind coefficient lookup tables

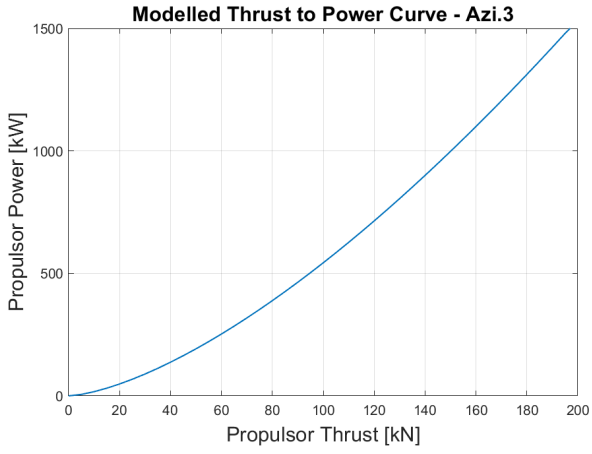
E.3. Thrust to shaft power lookup table



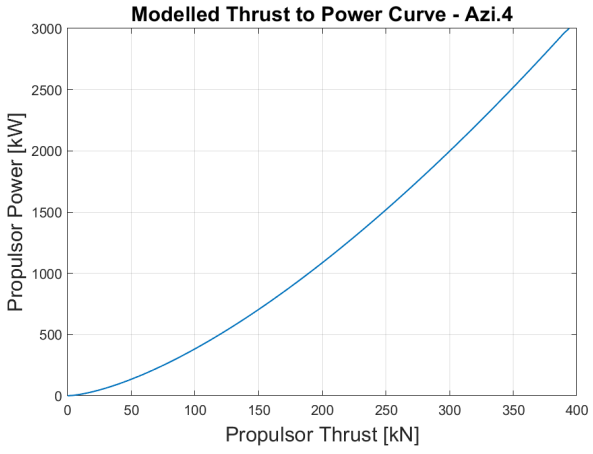
(a) Thrust to shaft power lookup table of Bow thruster 1



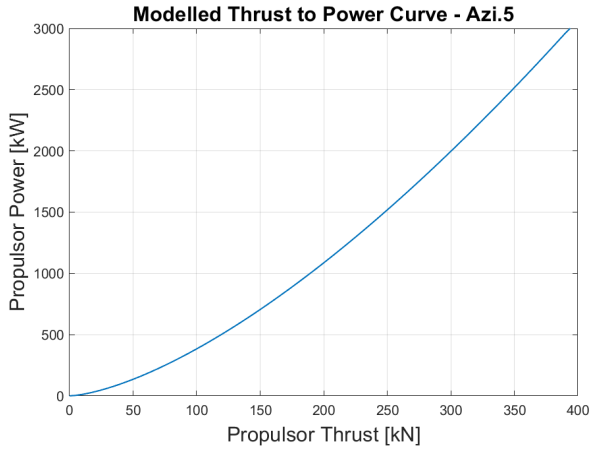
(b) Thrust to shaft power lookup table of Bow thruster 2



(c) Thrust to shaft power lookup table of Bow azimuth 3



(d) Thrust to shaft power lookup table of Azimuth 4



(e) Thrust to shaft power lookup table of Azimuth 5

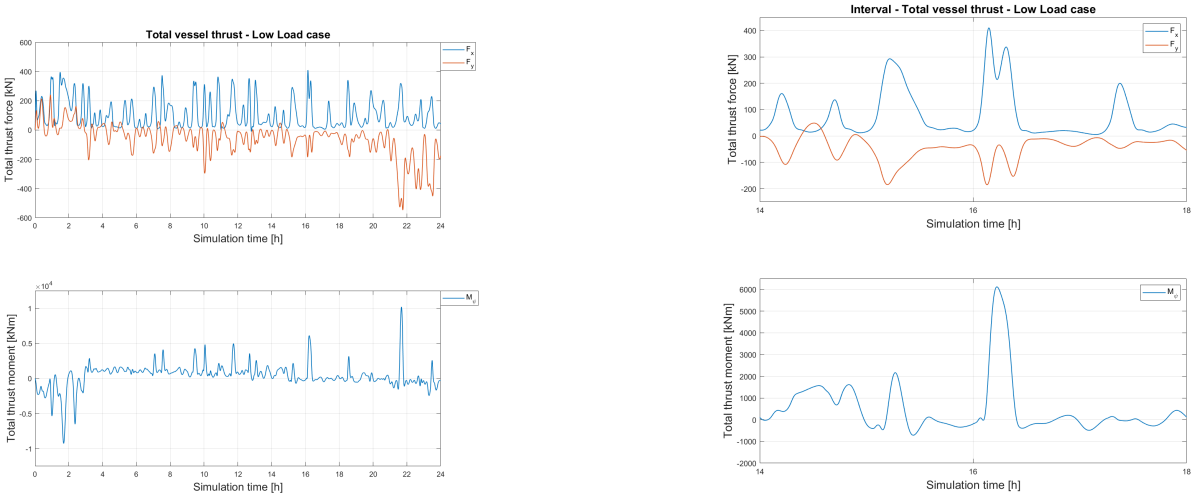
Figure E.7: Thrust to shaft power lookup tables of all propulsors

F

Appendix VI - Results

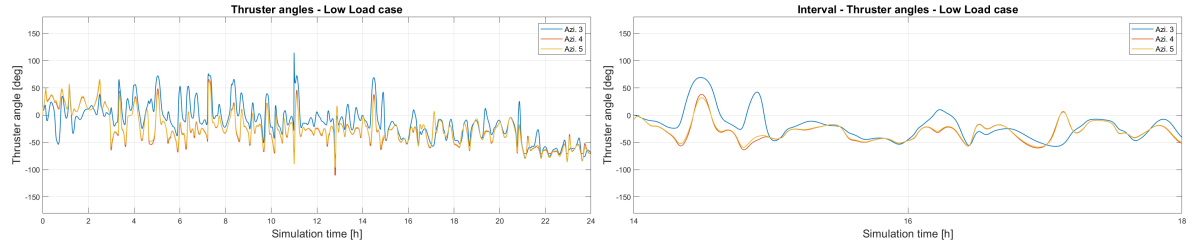
F.1. Low load case results

F.1.1. Vessel behaviour low load case



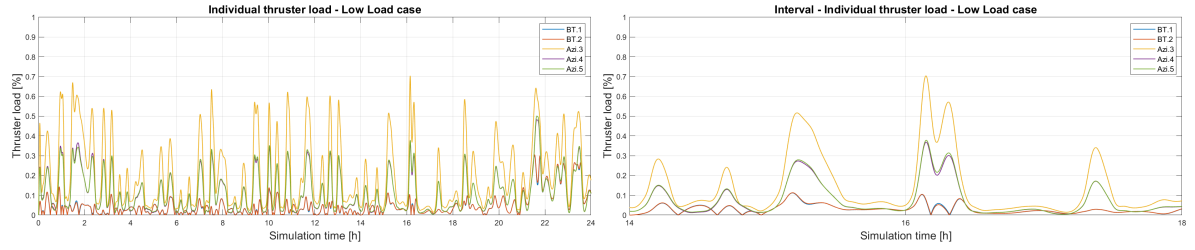
(a) Total thr. forces for the low load case

(b) Total thr. forces for the low load case interval



(c) Ind. thr. angles for the low load case

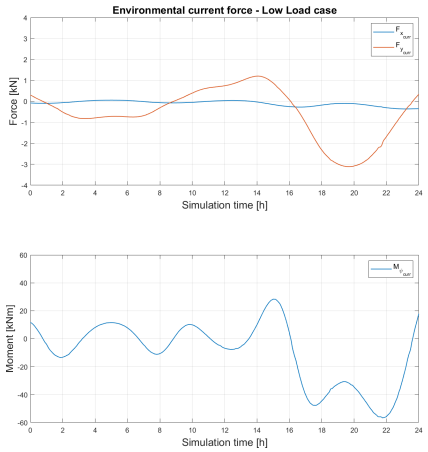
(d) Ind. thr. angles for the low load case interval



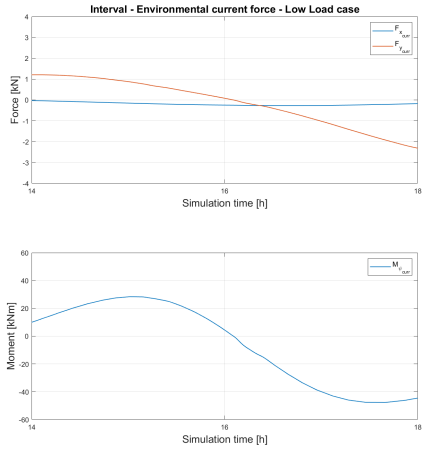
(e) Ind. thr. loads for the low load case

(f) Ind. thr. loads for the low load case interval

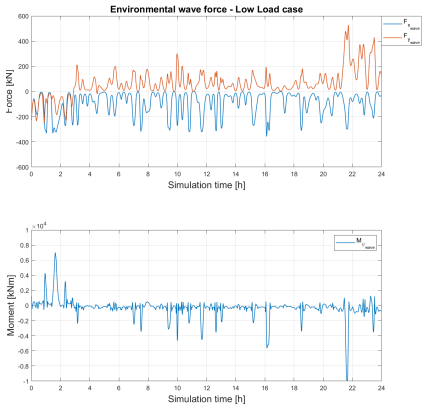
Figure F.1: Thruster characteristics for the low load case



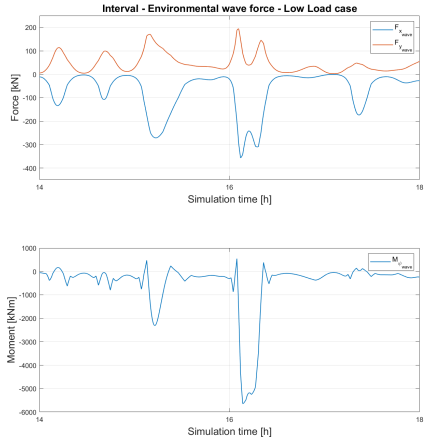
(a) Env. curr. forces for the low load case



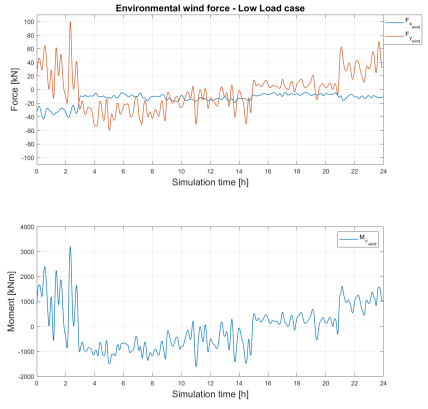
(b) Env. curr. forces for the low load case interval



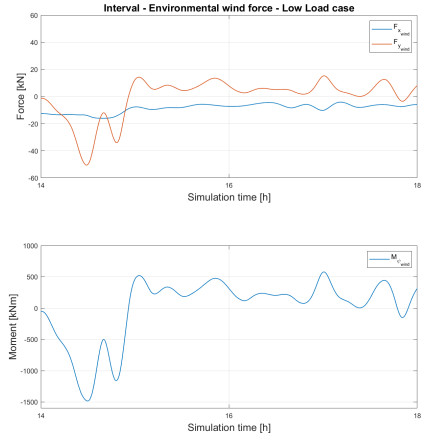
(c) Env. wave forces for the low load case



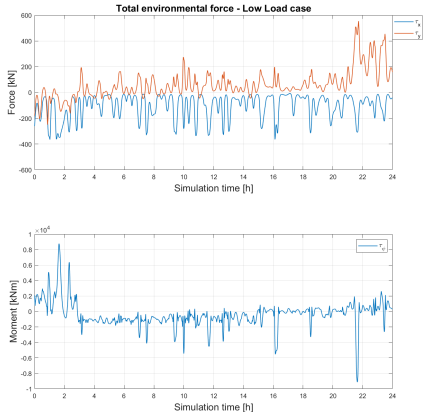
(d) Env. wave forces for the low load case interval



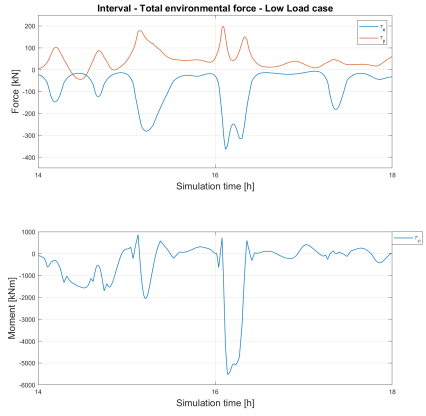
(e) Env. wind forces for the low load case



(f) Env. wind forces for the low load case interval

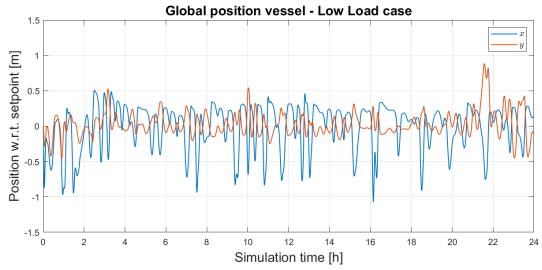


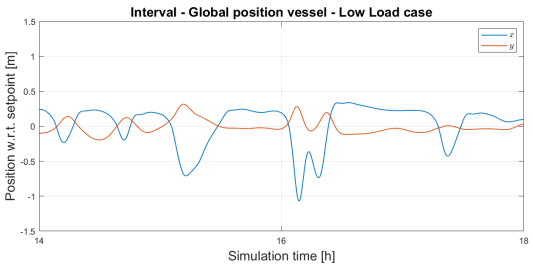
(g) Total Env. forces for the low load case

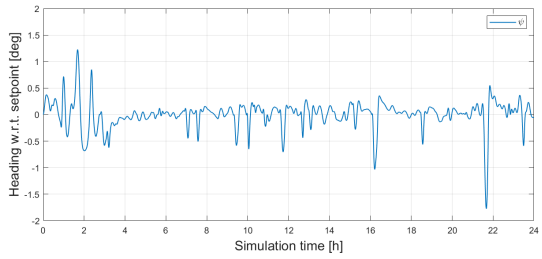


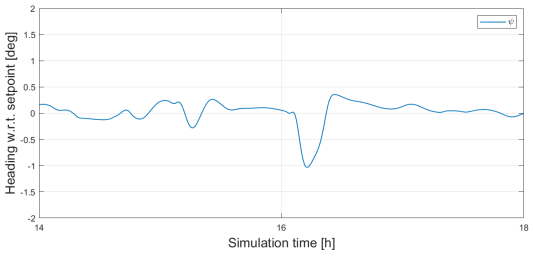
(h) Total Env. forces for the low load case interval

Figure F.2: Environmental forces for the low load case



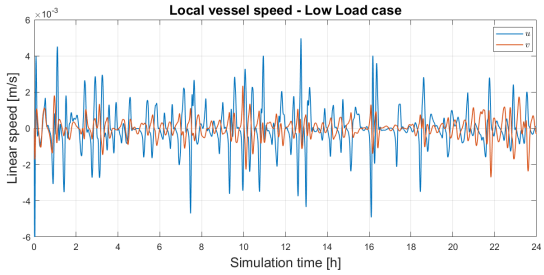


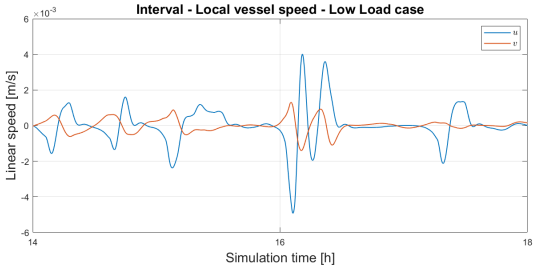


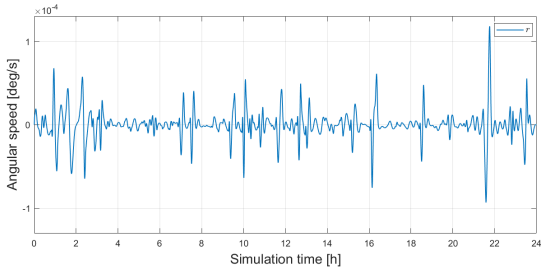


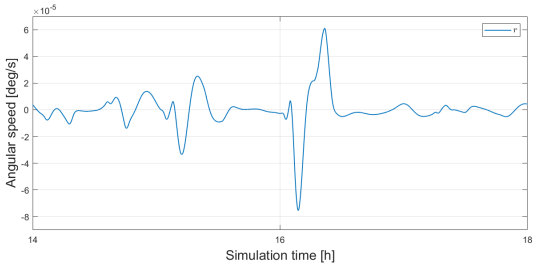
(a) global pos. for the low load case

(b) global pos. for the low load case interval



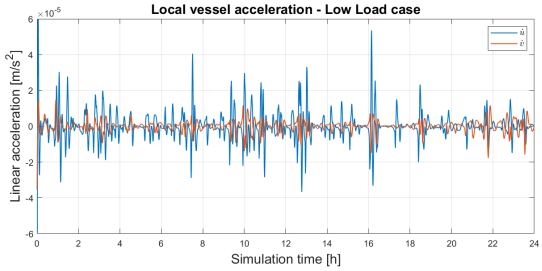


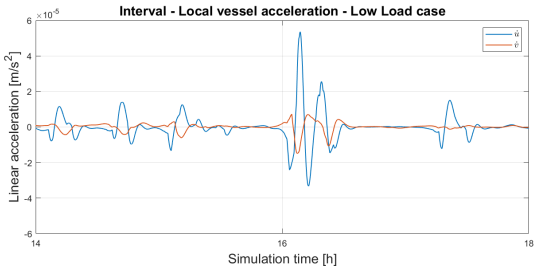


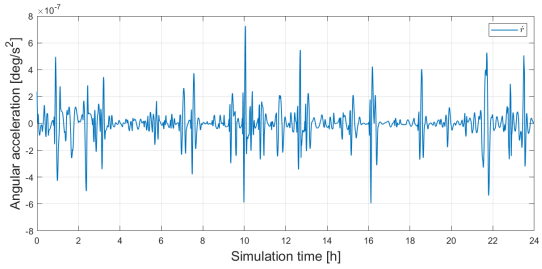


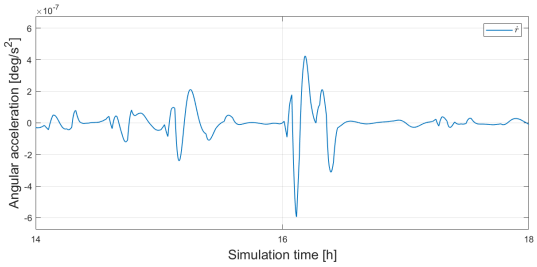
(c) Local speed for the low load case

(d) Local speed for the low load case interval







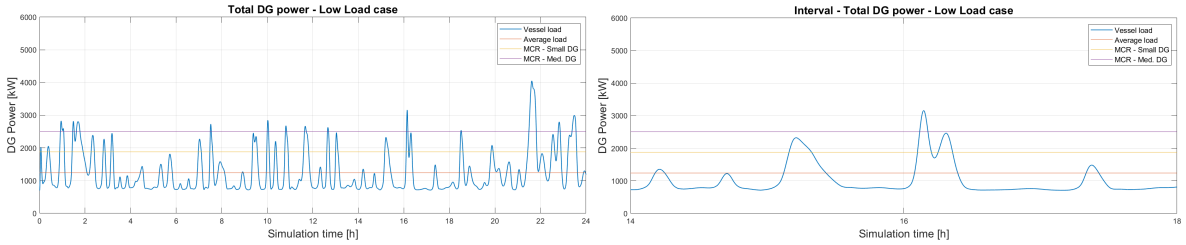


(e) Local accel. for the low load case

(f) Local accel. for the low load case interval

Figure F.3: Vessel dynamics for the low load case

F.1.2. DG load profiles low load case

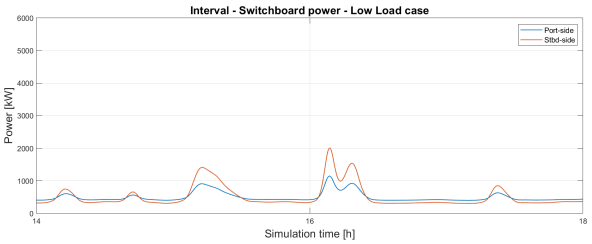


(a) Power system load for the low load case

(b) Power system load for the low load case interval

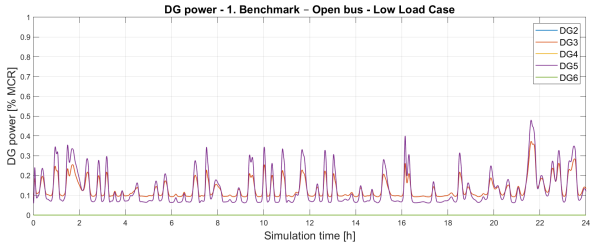


(c) Swb. load for the low load case

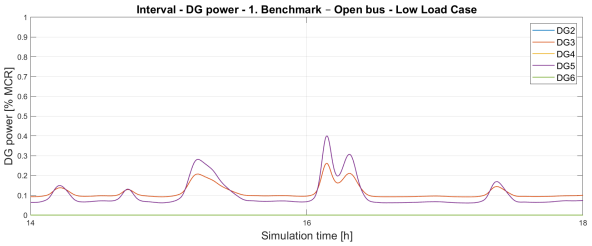


(d) Swb. load for the low load case interval

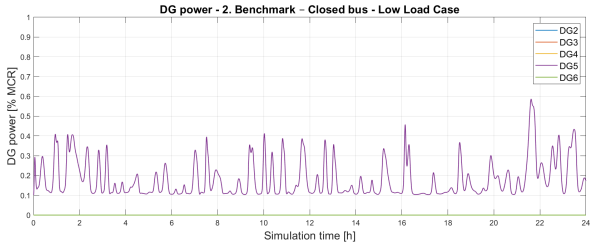
Figure F.4: Total load profile for the low load case



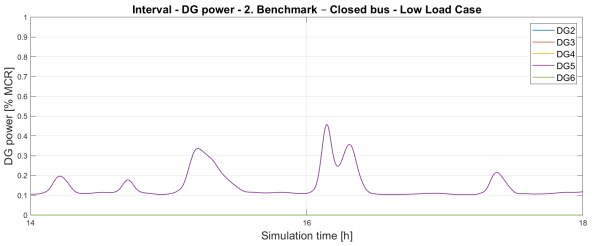
(a) Load profile of strategy 1. for the low load case



(b) Load profile of strategy 1. for the low load case interval

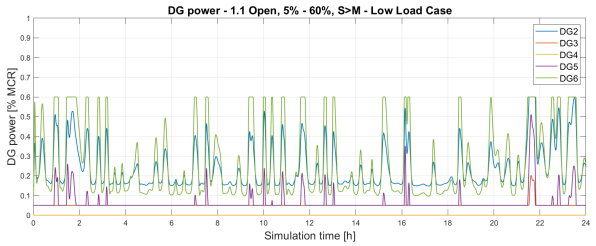


(c) Load profile of strategy 2. for the low load case

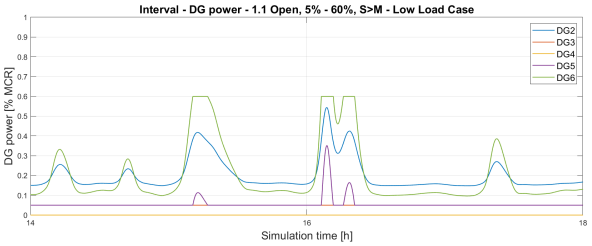


(d) Load profile of strategy 2. for the low load case interval

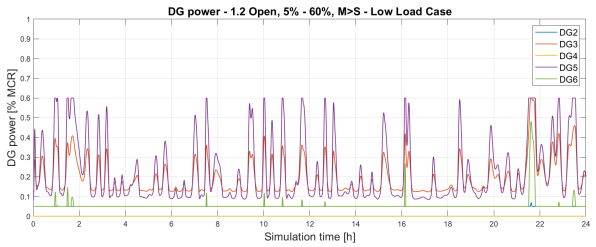
Figure F.5: DG loads of benchmark strategies for the low load case



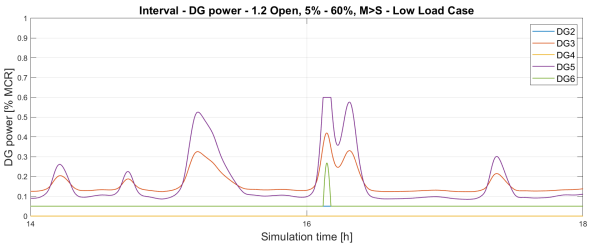
(a) Load profile of strategy 1.1 for the low load case



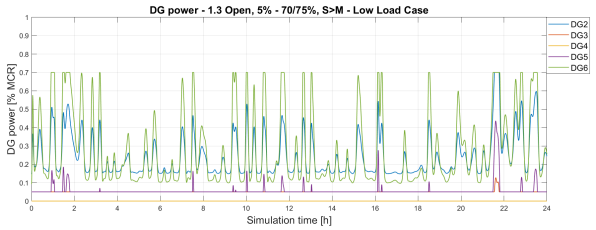
(b) Load profile of strategy 1.1 for the low load case interval



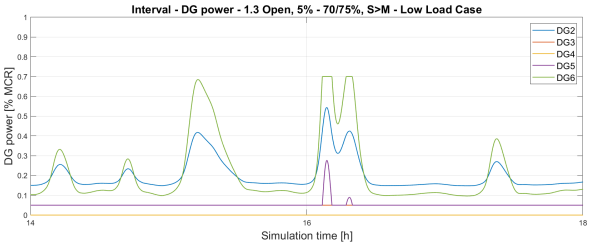
(c) Load profile of strategy 1.2 for the low load case



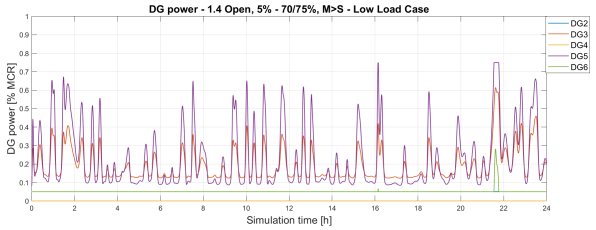
(d) Load profile of strategy 1.2 for the low load case interval



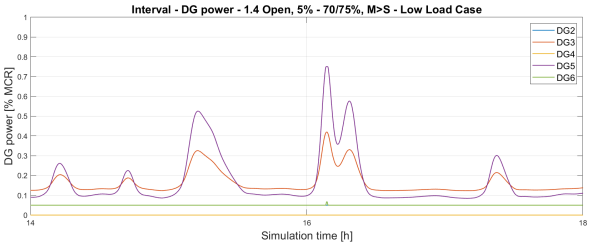
(e) Load profile of strategy 1.3 for the low load case



(f) Load profile of strategy 1.3 for the low load case interval

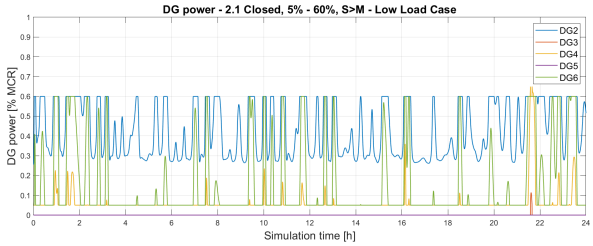


(g) Load profile of strategy 1.4 for the low load case

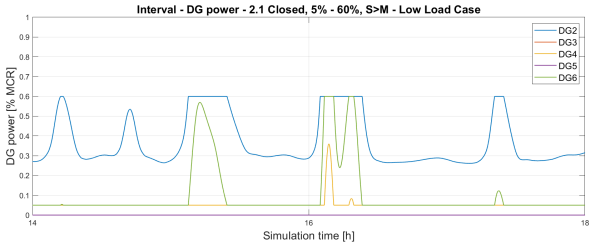


(h) Load profile of strategy 1.4 for the low load case interval

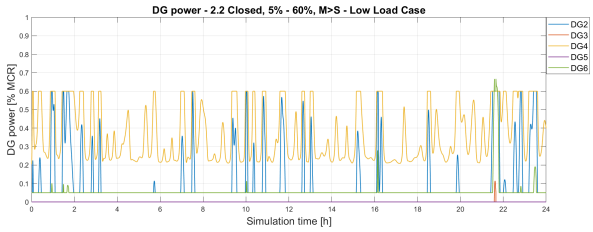
Figure F.6: DG loads of open bus strategies for the low load case



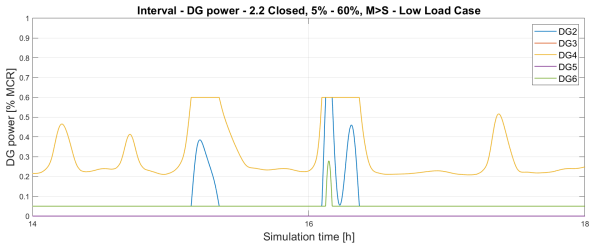
(a) Load profile of strategy 2.1 for the low load case



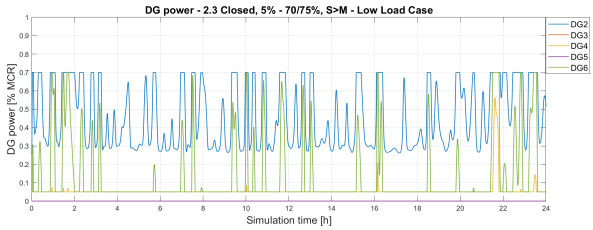
(b) Load profile of strategy 2.1 for the low load case interval



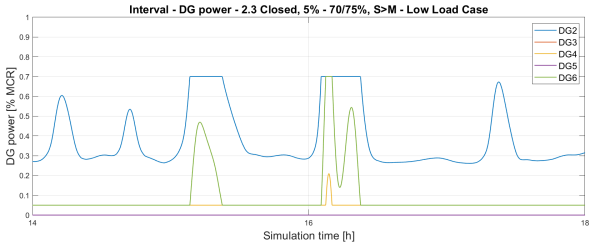
(c) Load profile of strategy 2.2 for the low load case



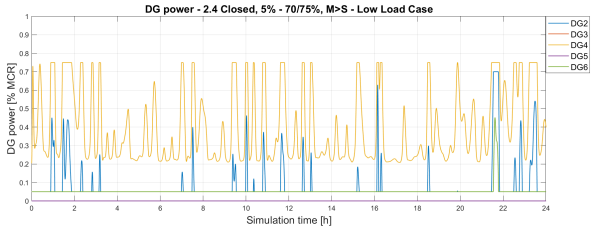
(d) Load profile of strategy 2.2 for the low load case interval



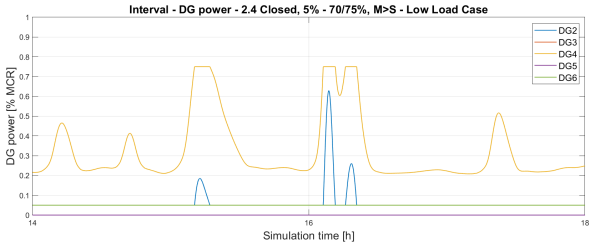
(e) Load profile of strategy 2.3 for the low load case



(f) Load profile of strategy 2.3 for the low load case interval



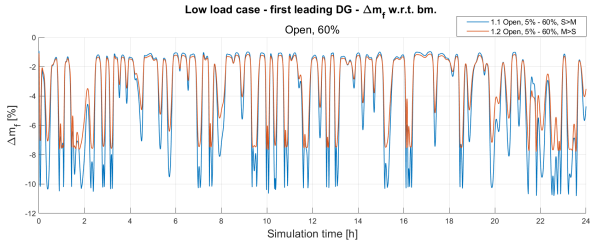
(g) Load profile of strategy 2.4 for the low load case



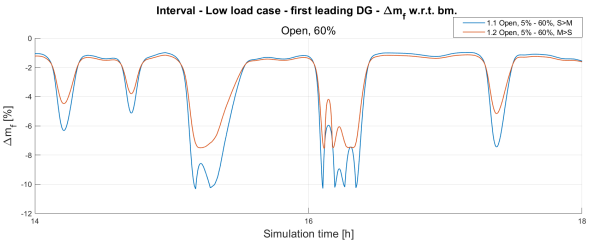
(h) Load profile of strategy 2.4 for the low load case interval

Figure F.7: DG loads of closed bus strategies for the low load case

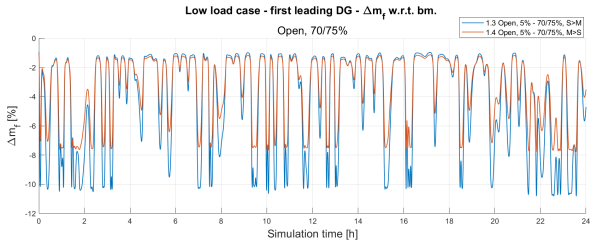
F.1.3. Fuel consumption results of low load case



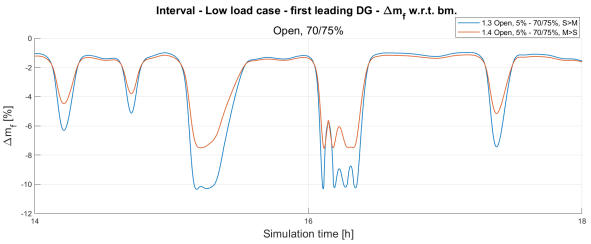
(a) Fuel savings of 1.1 vs 1.2 for the low load case



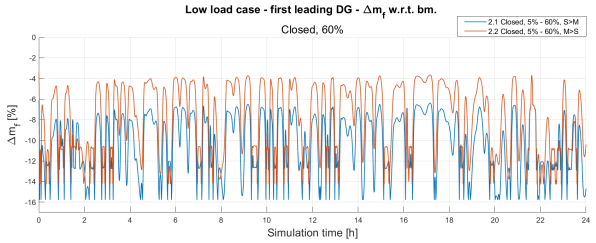
(b) Fuel savings of 1.1 vs 1.2 for the low load case interval



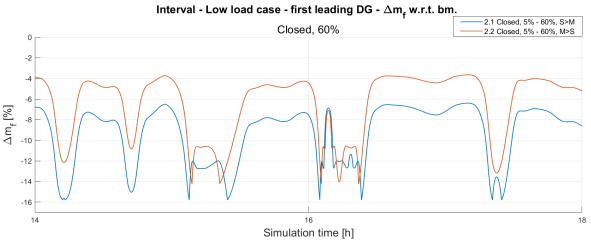
(c) Fuel savings of 1.3 vs 1.4 for the low load case



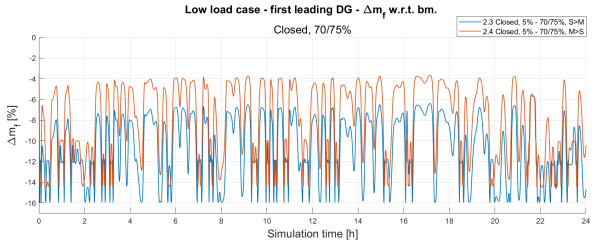
(d) Fuel savings of 1.3 vs 1.4 for the low load case interval



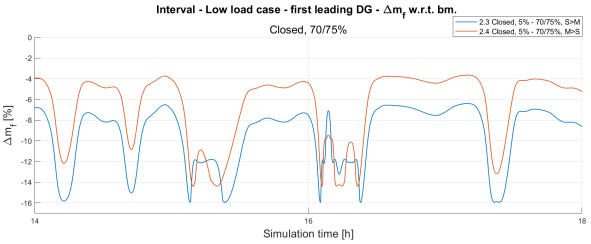
(e) Fuel savings of 2.1 vs 2.2 for the low load case



(f) Fuel savings of 2.1 vs 2.2 for the low load case interval

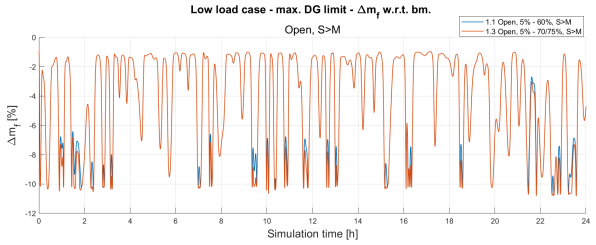


(g) Fuel savings of 2.3 vs 2.4 for the low load case

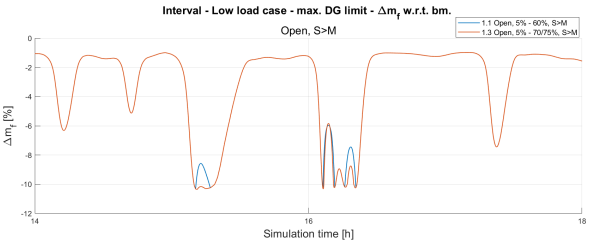


(h) Fuel savings of 2.3 vs 2.4 for the low load case interval

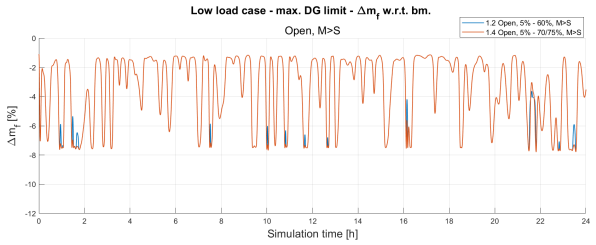
Figure F.8: Hourly fuel-saving results of the dynamic model, w.r.t. the open bus benchmark strategy, for first leading DG strategies for the low load case



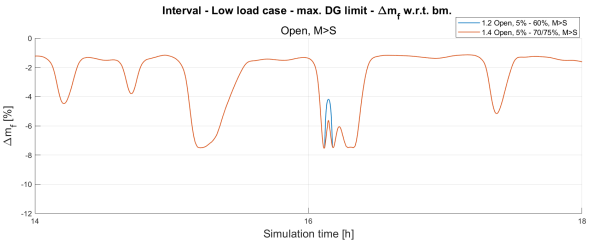
(a) Fuel savings of 1.1 vs 1.3 for the low load case



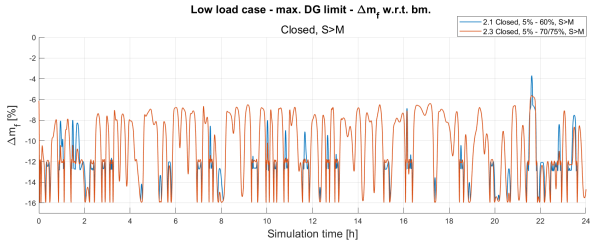
(b) Fuel savings of 1.1 vs 1.3 for the low load case intervals



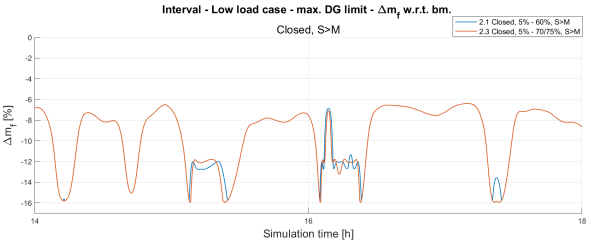
(c) Fuel savings of 1.2 vs 1.4 for the low load case



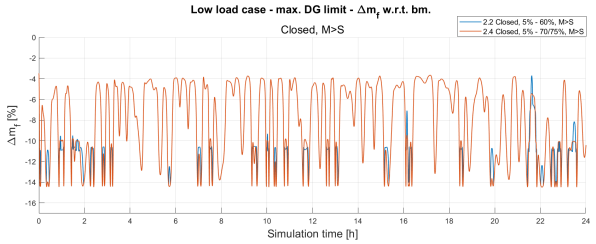
(d) Fuel savings of 1.2 vs 1.4 for the low load case intervals



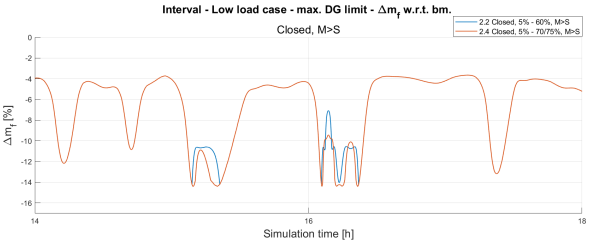
(e) Fuel savings of 2.1 vs 2.3 for the low load case



(f) Fuel savings of 2.1 vs 2.3 for the low load case intervals

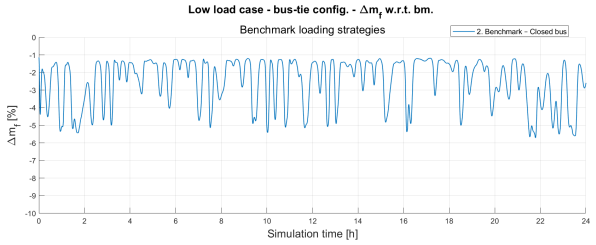


(g) Fuel savings of 2.2 vs 2.4 for the low load case

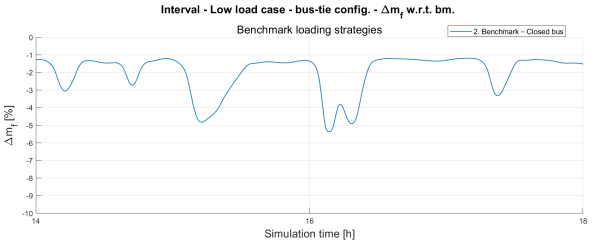


(h) Fuel savings of 2.2 vs 2.4 for the low load case intervals

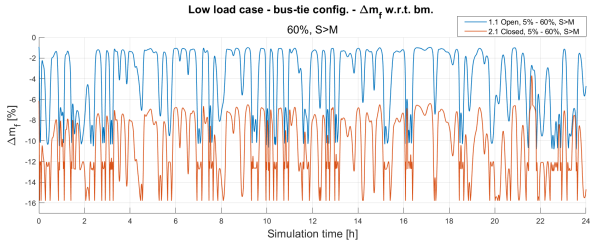
Figure F.9: Hourly fuel-saving results of the dynamic model, w.r.t. the open bus benchmark strategy, for max. DG limit strategies for the low load case



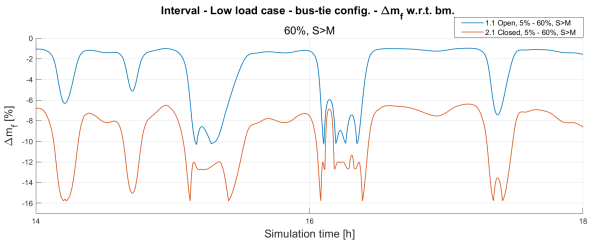
(a) Fuel savings of 2. for the low load case



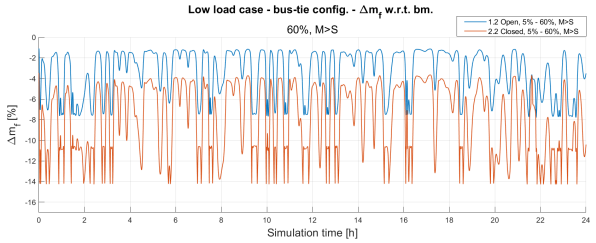
(b) Fuel savings of 2. for the low load case intervals



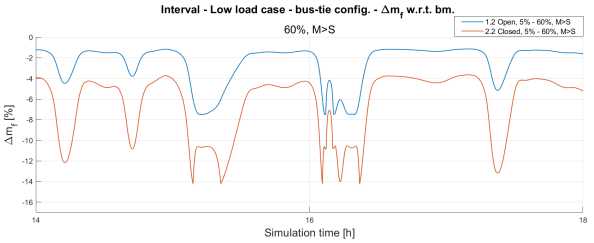
(c) Fuel savings of 1.1 vs 2.1 for the low load case



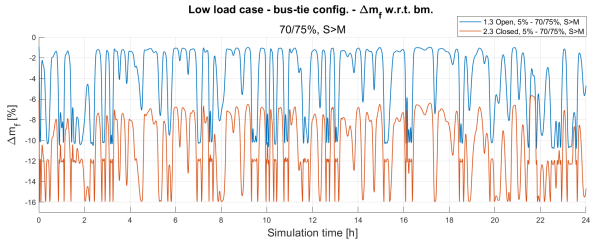
(d) Fuel savings of 1.1 vs 2.1 for the low load case intervals



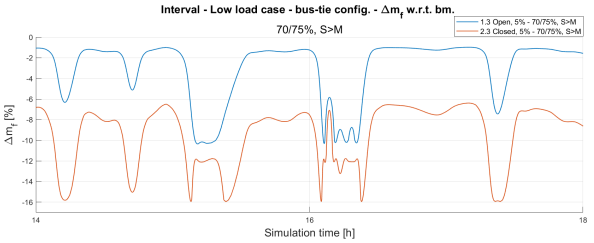
(e) Fuel savings of 1.2 vs 2.2 for the low load case



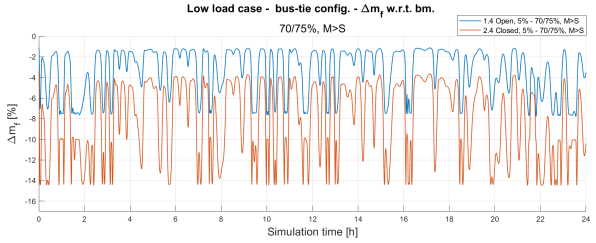
(f) Fuel savings of 1.2 vs 2.2 for the low load case intervals



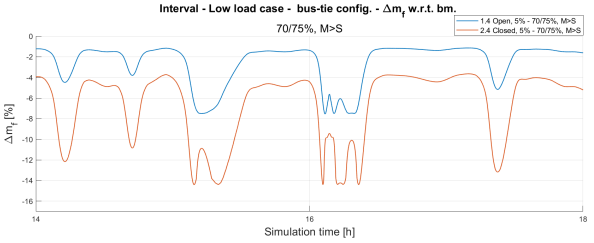
(g) Fuel savings of 1.3 vs 2.3 for the low load case



(h) Fuel savings of 1.3 vs 2.3 for the low load case intervals



(i) Fuel savings of 1.4 vs 2.4 for the low load case

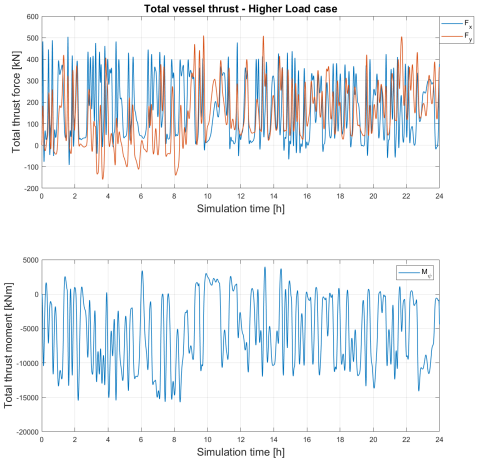


(j) Fuel savings of 1.4 vs 2.4 for the low load case intervals

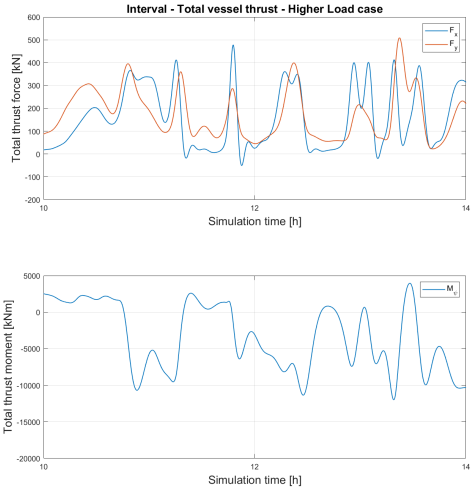
Figure F.10: Hourly fuel-saving results of the dynamic model, w.r.t. the open bus benchmark strategy, for open and closed strategies for the low load case

F.2. Higher load case results

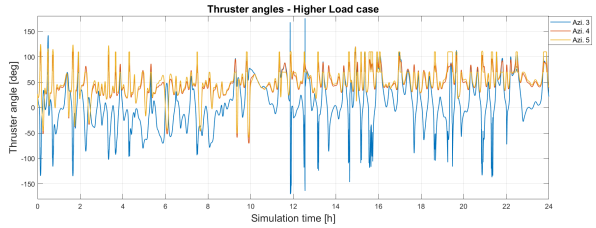
F.2.1. Vessel behaviour higher load case



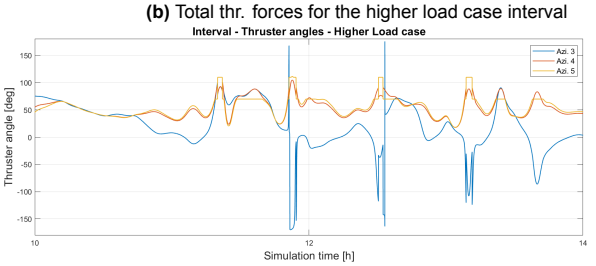
(a) Total thr. forces for the higher load case



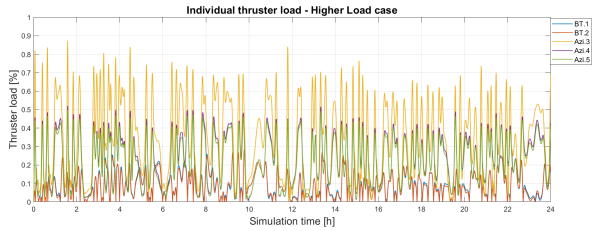
(b) Total thr. forces for the higher load case interval



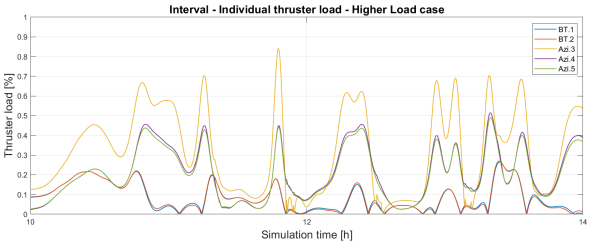
(c) Ind. thr. angles for the higher load case



(d) Ind. thr. angles for the higher load case interval

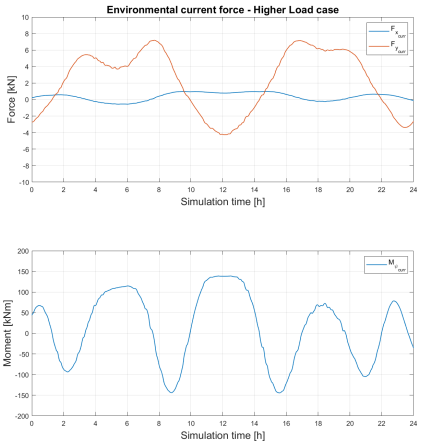


(e) Ind. thr. loads for the higher load case

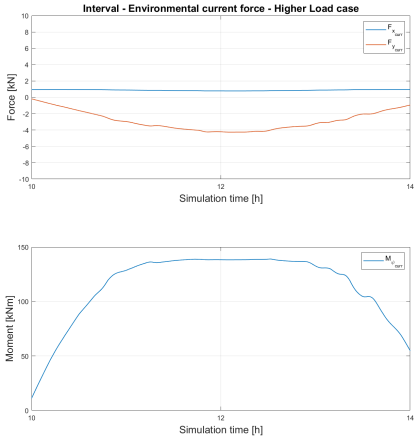


(f) Ind. thr. loads for the higher load case interval

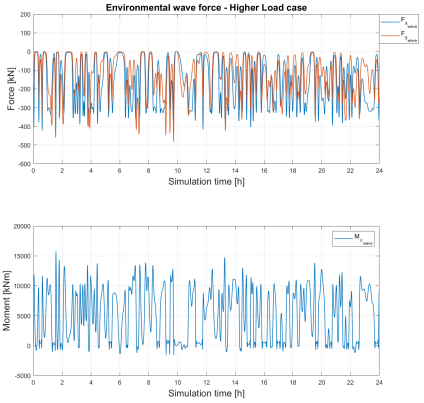
Figure F.11: Thruster characteristics for the higher load case



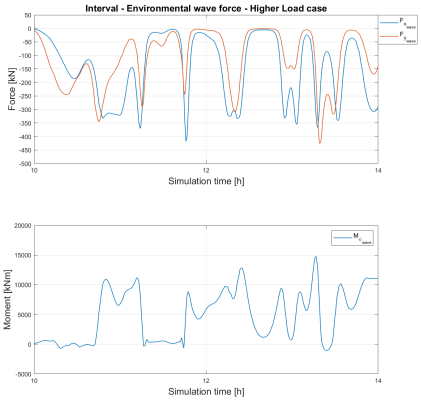
(a) Env. curr. forces for the higher load case



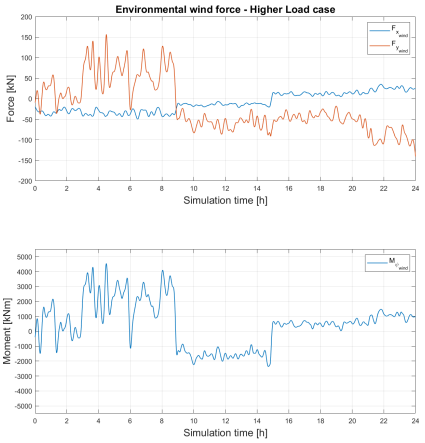
(b) Env. curr. forces for the higher load case interval



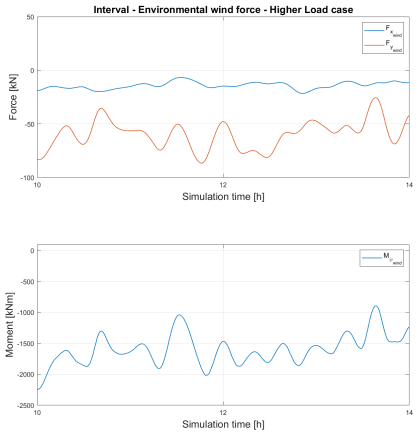
(c) Env. wave forces for the higher load case



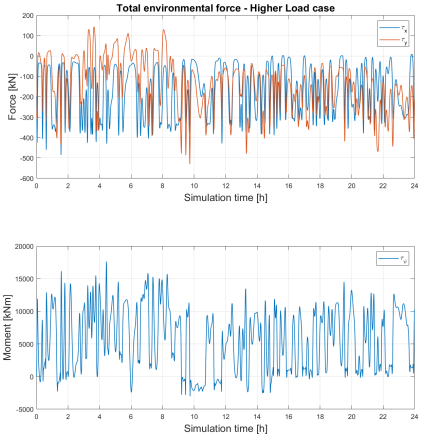
(d) Env. wave forces for the higher load case interval



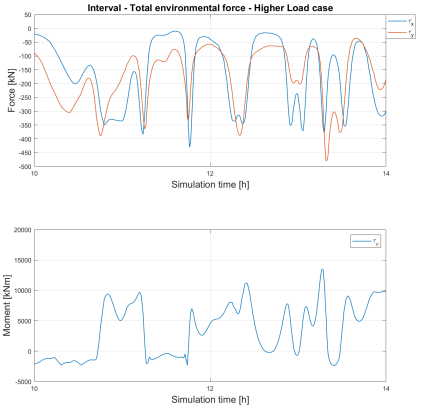
(e) Env. wind forces for the higher load case



(f) Env. wind forces for the higher load case interval

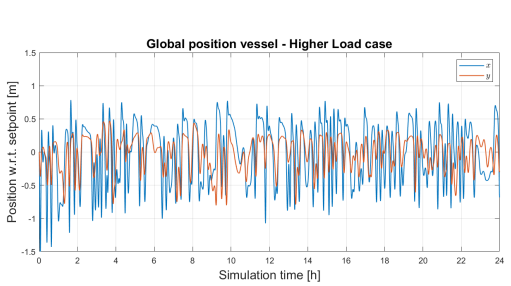


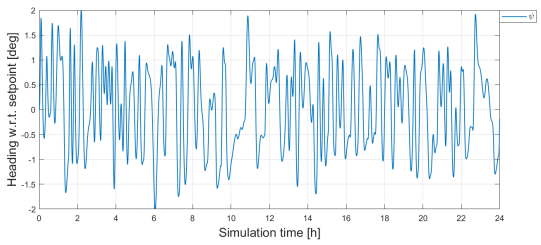
(g) Total Env. forces for the higher load case



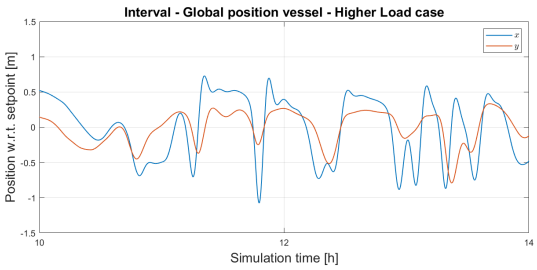
(h) Total Env. forces for the higher load case interval

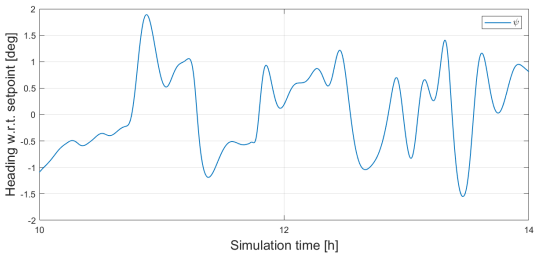
Figure F.12: Environmental forces for the higher load case



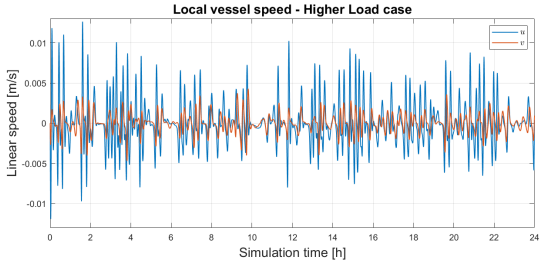


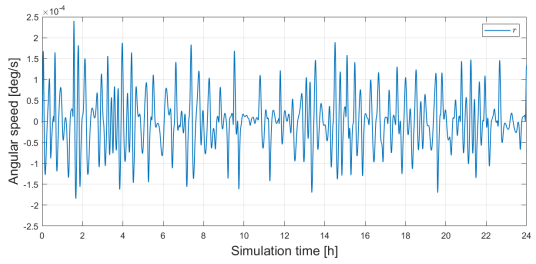
(a) global pos. for the higher load case



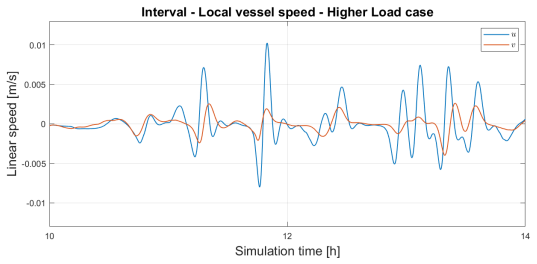


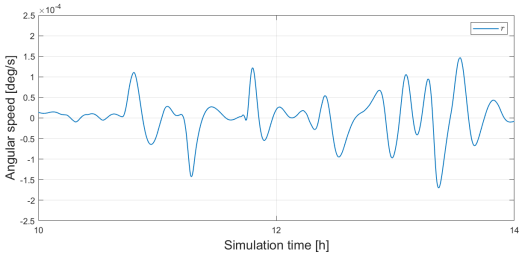
(b) global pos. for the higher load case interval



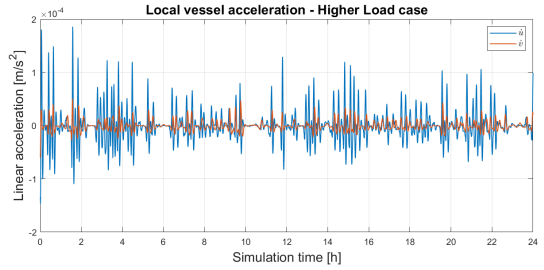


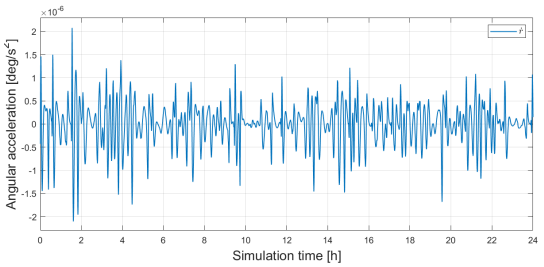
(c) Local speed for the higher load case



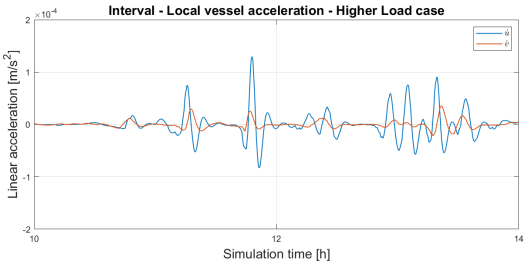


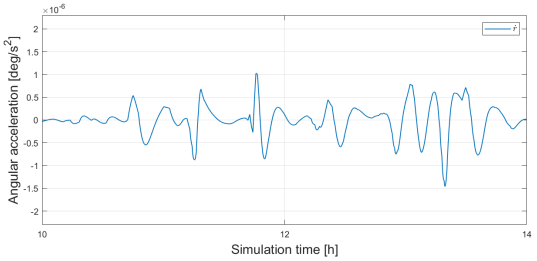
(d) Local speed for the higher load case interval





(e) Local accel. for the higher load case

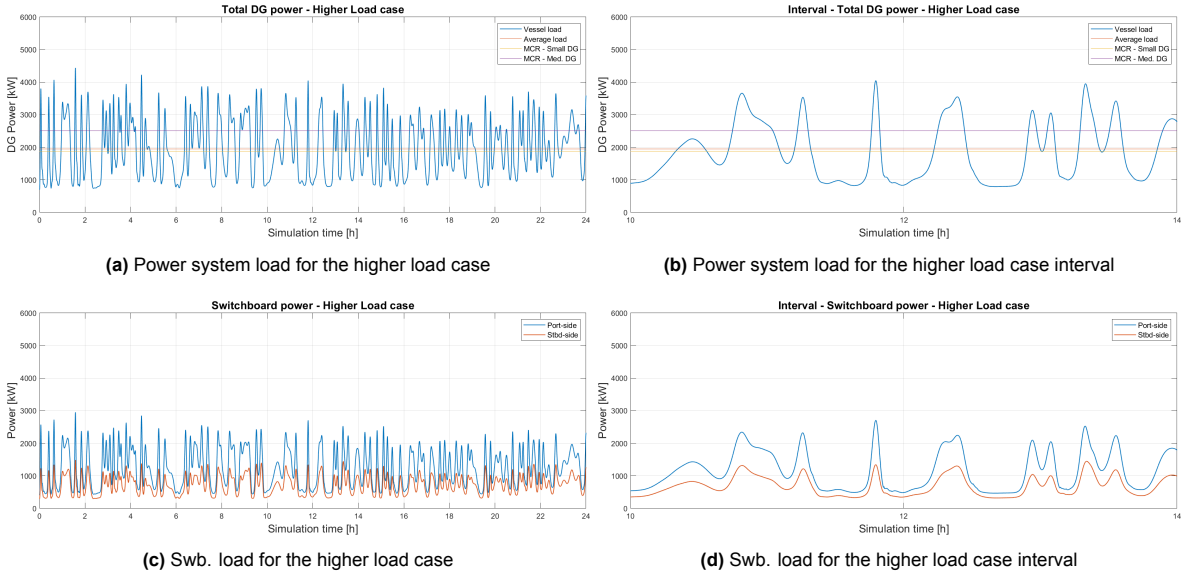




(f) Local accel. for the higher load case interval

Figure F.13: Vessel dynamics for the higher load case

F.2.2. DG load profiles higher load case



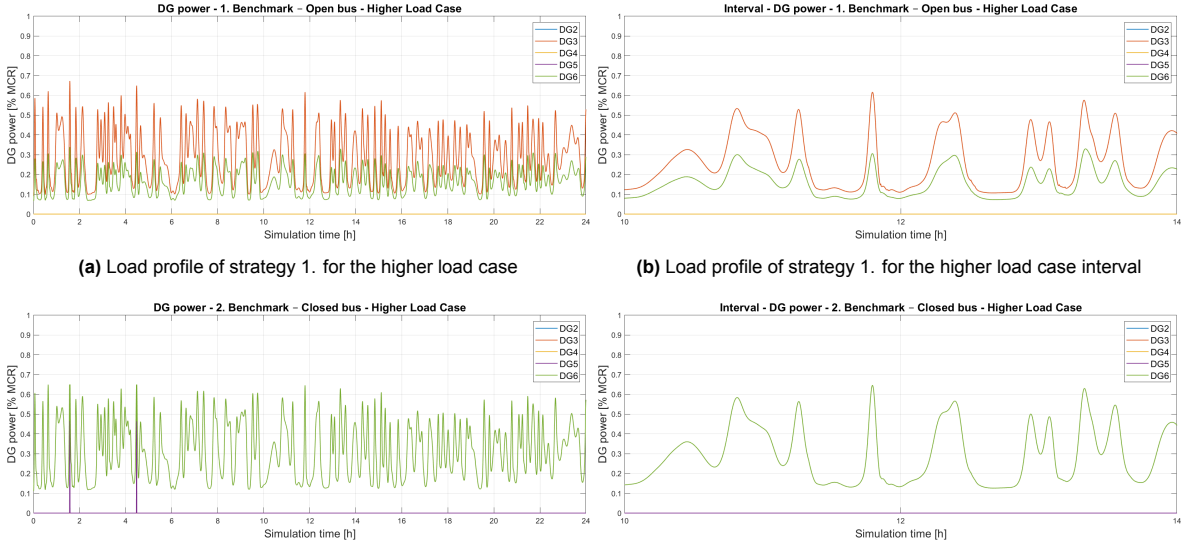
(a) Power system load for the higher load case

(b) Power system load for the higher load case interval

(c) Swb. load for the higher load case

(d) Swb. load for the higher load case interval

Figure F.14: Total load profile for the higher load case



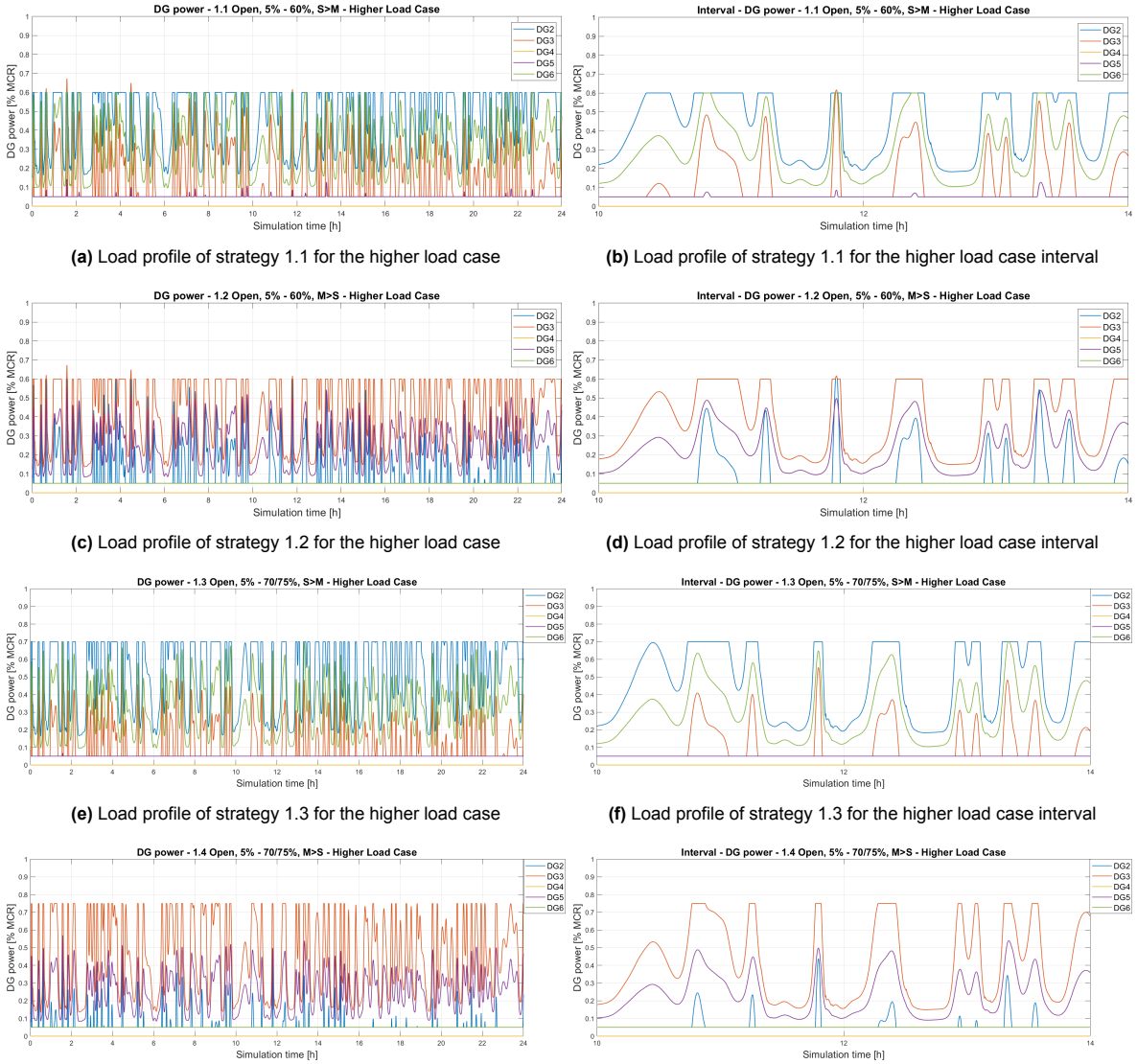
(a) Load profile of strategy 1. for the higher load case

(b) Load profile of strategy 1. for the higher load case interval

(c) Load profile of strategy 2. for the higher load case

(d) Load profile of strategy 2. for the higher load case interval

Figure F.15: DG loads of benchmark strategies for the higher load case



(a) Load profile of strategy 1.1 for the higher load case

(b) Load profile of strategy 1.1 for the higher load case interval

(c) Load profile of strategy 1.2 for the higher load case

(d) Load profile of strategy 1.2 for the higher load case interval

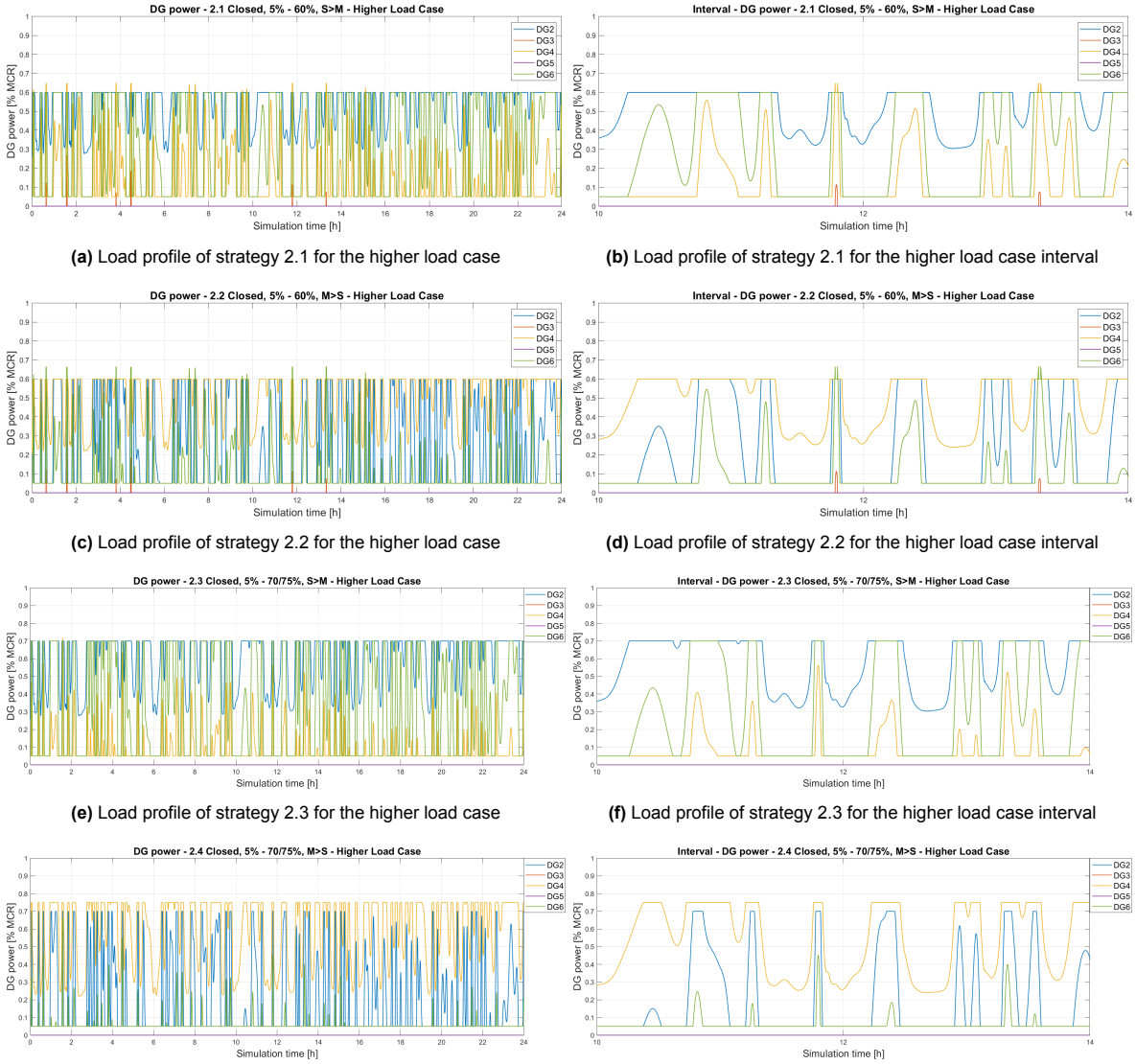
(e) Load profile of strategy 1.3 for the higher load case

(f) Load profile of strategy 1.3 for the higher load case interval

(g) Load profile of strategy 1.4 for the higher load case

(h) Load profile of strategy 1.4 for the higher load case interval

Figure F.16: DG loads of open bus strategies for the higher load case



(a) Load profile of strategy 2.1 for the higher load case

(b) Load profile of strategy 2.1 for the higher load case interval

(c) Load profile of strategy 2.2 for the higher load case

(d) Load profile of strategy 2.2 for the higher load case interval

(e) Load profile of strategy 2.3 for the higher load case

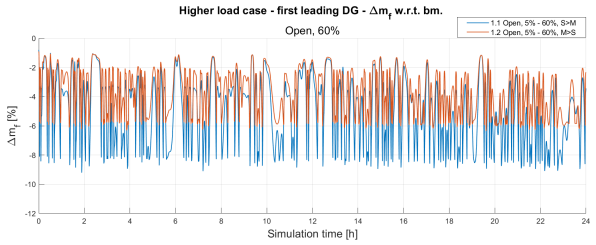
(f) Load profile of strategy 2.3 for the higher load case interval

(g) Load profile of strategy 2.4 for the higher load case

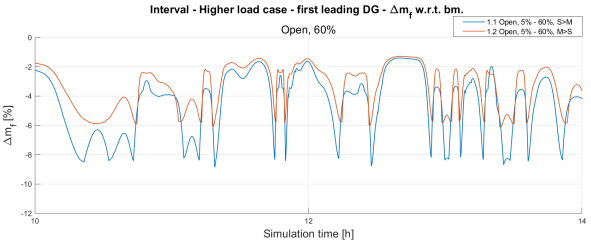
(h) Load profile of strategy 2.4 for the higher load case interval

Figure F.17: DG loads of closed bus strategies for the higher load case

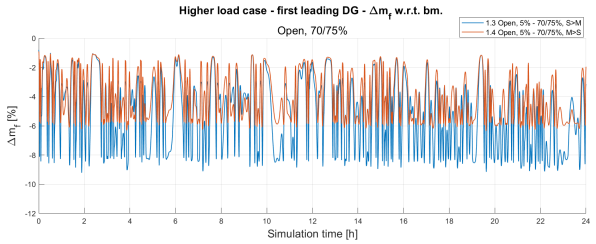
F.2.3. Fuel consumption results of higher load case



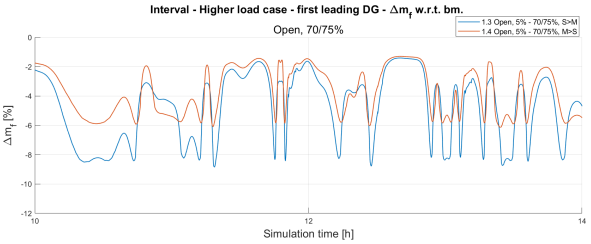
(a) Fuel savings of 1.1 vs 1.2 for the higher load case



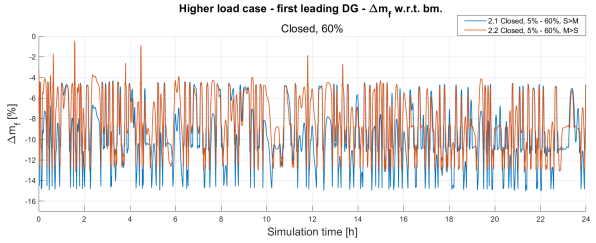
(b) Fuel savings of 1.1 vs 1.2 for the higher load case interval



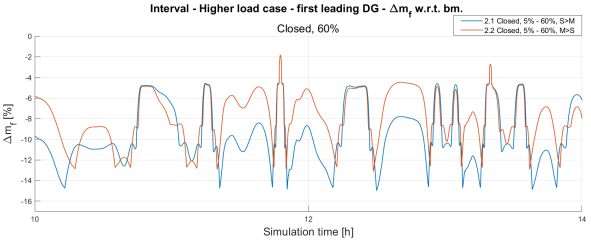
(c) Fuel savings of 1.3 vs 1.4 for the higher load case



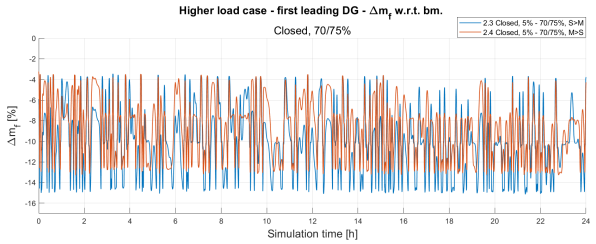
(d) Fuel savings of 1.3 vs 1.4 for the higher load case interval



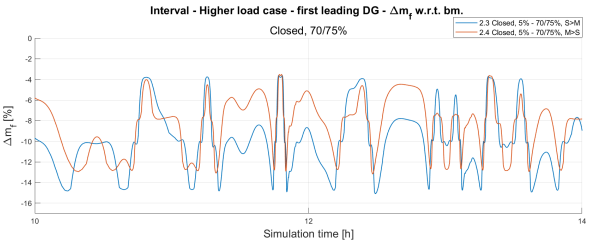
(e) Fuel savings of 2.1 vs 2.2 for the higher load case



(f) Fuel savings of 2.1 vs 2.2 for the higher load case interval

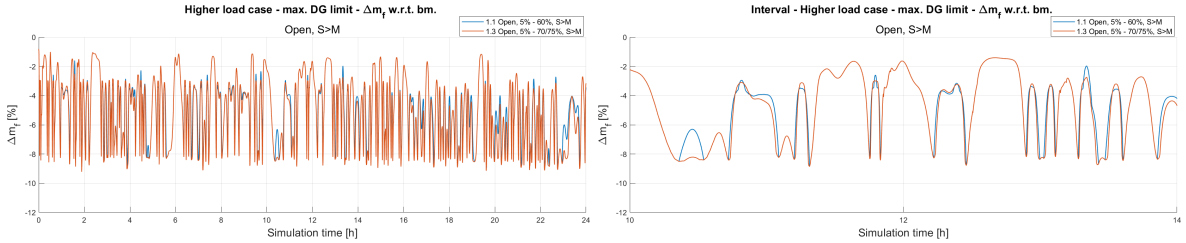


(g) Fuel savings of 2.3 vs 2.4 for the higher load case



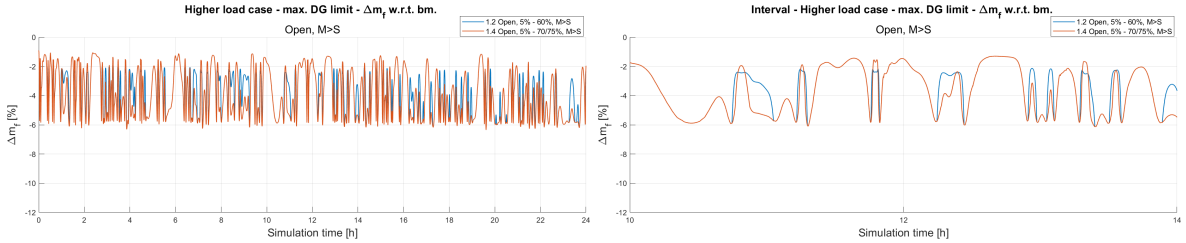
(h) Fuel savings of 2.3 vs 2.4 for the higher load case interval

Figure F.18: Hourly fuel-saving results of the dynamic model, w.r.t. the open bus benchmark strategy, for first leading DG strategies for the higher load case



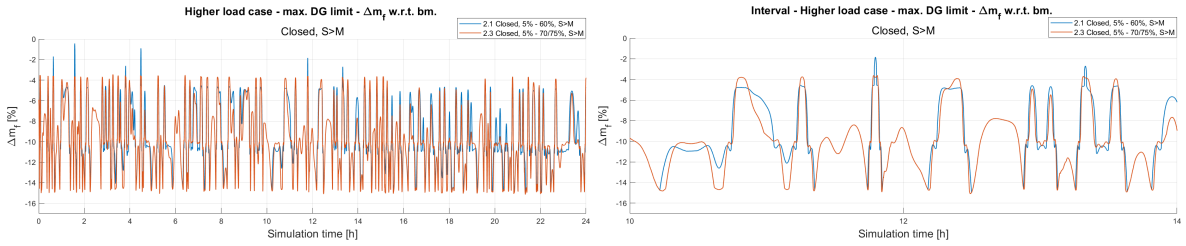
(a) Fuel savings of 1.1 vs 1.3 for the higher load case

(b) Fuel savings of 1.1 vs 1.3 for the higher load case intervals



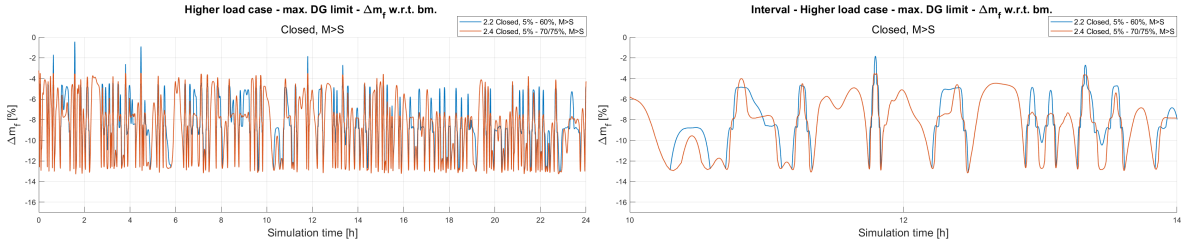
(c) Fuel savings of 1.2 vs 1.4 for the higher load case

(d) Fuel savings of 1.2 vs 1.4 for the higher load case intervals



(e) Fuel savings of 2.1 vs 2.3 for the higher load case

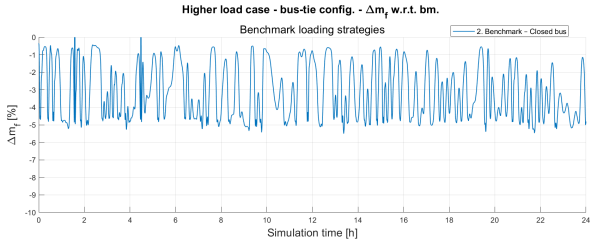
(f) Fuel savings of 2.1 vs 2.3 for the higher load case intervals



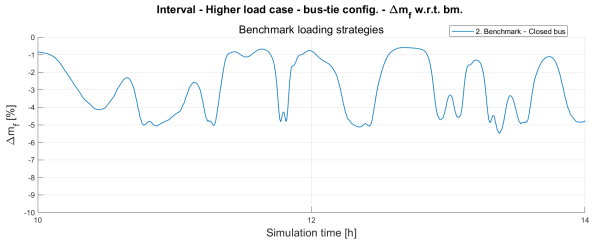
(g) Fuel savings of 2.2 vs 2.4 for the higher load case

(h) Fuel savings of 2.2 vs 2.4 for the higher load case intervals

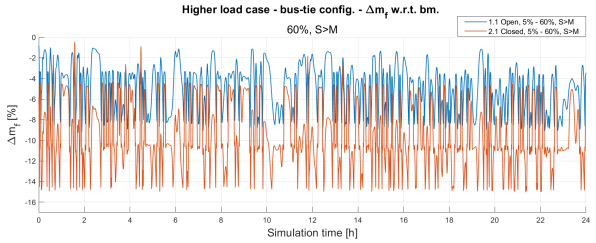
Figure F.19: Hourly fuel-saving results of the dynamic model, w.r.t. the open bus benchmark strategy, for max. DG limit strategies for the higher load case



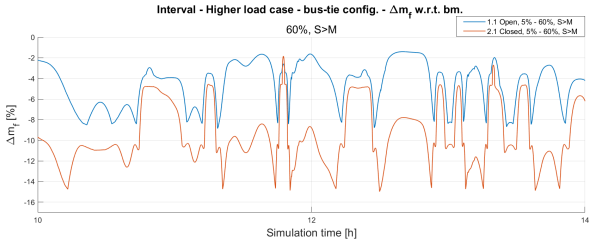
(a) Fuel savings of 2. for the higher load case



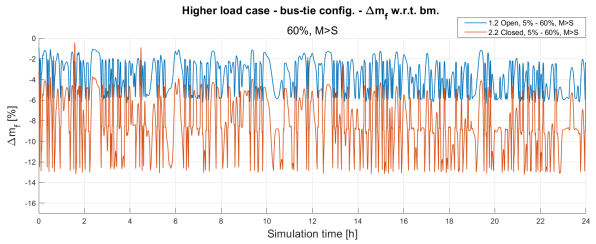
(b) Fuel savings of 2. for the higher load case intervals



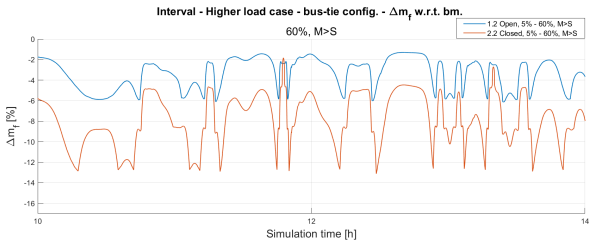
(c) Fuel savings of 1.1 vs 2.1 for the higher load case



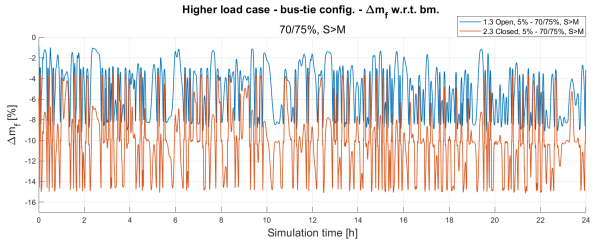
(d) Fuel savings of 1.1 vs 2.1 for the higher load case intervals



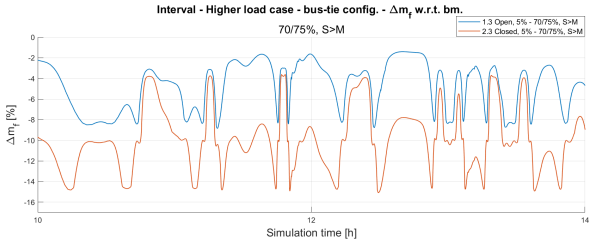
(e) Fuel savings of 1.2 vs 2.2 for the higher load case



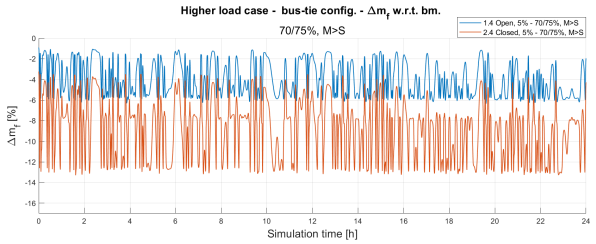
(f) Fuel savings of 1.2 vs 2.2 for the higher load case intervals



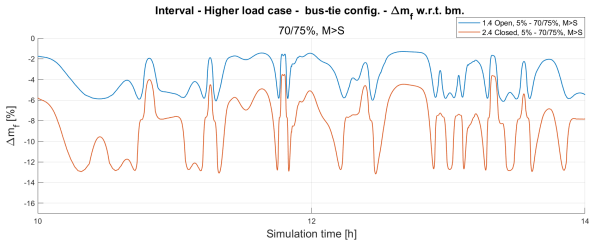
(g) Fuel savings of 1.3 vs 2.3 for the higher load case



(h) Fuel savings of 1.3 vs 2.3 for the higher load case intervals



(i) Fuel savings of 1.4 vs 2.4 for the higher load case



(j) Fuel savings of 1.4 vs 2.4 for the higher load case intervals

Figure F.20: Hourly fuel-saving results of the dynamic model, w.r.t. the open bus benchmark strategy, for open and closed strategies for the higher load case